MycoKeys 58: 1–26 (2019)
doi: 10.3897/mycokeys.58.36723
http://mycokeys.pensoft.net

RESEARCH ARTICLE

A peer-reviewed open-access journal
MycoKeys
Launched to accelerate biodiversity research

Rubroshiraia gen. nov., a second hypocrellin-producing genus in Shiraiaceae (Pleosporales)

Dong-Qin Dai[1], Nalin N. Wijayawardene[1], Li-Zhou Tang[1,2], Chao Liu[1], Li-Hong Han[1], Hong-Long Chu[1], Hai-Bo Wang[1], Chun-Fang Liao[1], Er-Fu Yang[1], Rui-Fang Xu[1], Yun-Min Li[1], Kevin D. Hyde[3], D. Jayarama Bhat[4], Paul F. Cannon[5]

1 *Center for Yunnan Plateau Biological Resources Protection and Utilization, College of Biological Resource and Food Engineering, Qujing Normal University, Qujing, Yunnan 655011, China* **2** *State Key Laboratory of Genetic Resources and Evolution, Kunming Institute of Zoology, Chinese Academy of Sciences, Kunming, Yunnan 650223, China* **3** *Centre of Excellence in Fungal Research, Mae Fah Luang University, Chiang Rai 57100, Thailand* **4** *No. 128/1-J, Azad Housing Society, Curca, P.O. Goa Velha 403108, India* **5** *Royal Botanic Gardens, Kew, Surrey TW9 3AB, UK*

Corresponding author: *Li-Zhou Tang* (biologytang@163.com); *Chao Liu* (liuchao_80@163.com)

Academic editor: *Pedro Crous* | Received 3 June 2019 | Accepted 13 August2019 | Published 28 August 2019

Citation: Dai D-Q, Wijayawardene NN, Tang L-Z, Liu C, Han L-H, Chu H-L, Wang H-B, Liao C-F, Yang E-F, Xu R-F, Li Y-M, Hyde KD, Bhat DJ, Cannon PF (2019) *Rubroshiraia* gen. nov., a second hypocrellin-producing genus in Shiraiaceae (Pleosporales). MycoKeys 58: 1–26. https://doi.org/10.3897/mycokeys.58.36723

Abstract

Shiraiaceae is an important family in Pleosporales (Dothideomycetes), which includes medical fungi and plant pathogens. Two hypocrellin-producing taxa, *Shiraia bambusicola* and a novel genus *Rubroshiraia* **gen. nov.**, typified by *Rubroshiraia bambusae* are treated in this article. Maximum likelihood analysis, generated via RAxML (GTR+G model), using a combined SSU, LSU, TEF1 and RPB2 sequence dataset, shows that *Rubroshiraia* is close to *Shiraia* and belongs to the family Shiraiaceae. Descriptions, illustrations and a taxonomic key are provided for the genera in Shiraiaceae. *Rubroshiraia* morphologically differs from *Shiraia* in having small and dark ascostromata and filiform ascospores. Production of the ascostromatal metabolites, hypocrellin A and B, were examined by HPLC and spectrophotometer. The content of hypocrellin A and B of specimen HKAS 102255 (*R. bambusae*) is twice that produced by HKAS 102253 (*S. bambusicola*). To clarify the relationship between *R. bambusae* and *Hypocrella bambusae*, type material of the latter was examined and provided the illustration.

Keywords

HPLC, metabolite, new genus, phylogeny, taxonomy

Introduction

Liu et al. (2013) introduced the family Shiraiaceae Y.X. Liu, Zi Y. Liu & K.D. Hyde which is typified by *Shiraia* Henn. and placed the family in Pleosporales Luttr. ex M.E. Barr. Ariyawansa et al. (2013) accommodated *Grandigallia* M.E. Barr, Hanlin, Cedeño, Parra & R. Hern. in Shiraiaceae since it morphologically resembles *Shiraia*. Subsequent publications by Wijayawardene et al. (2014, 2017, 2018) agreed with this placement and, thus, the family currently comprises two genera.

Shiraia is typified by *S. bambusicola* Henn. (Hennings 1900), which is parasitic on living bamboo culms and has conspicuous large, pinkish, fleshy ascostromata with multi-locules located near the periphery, fissitunicate asci and hyaline, muriform ascospores (Liu et al. 2013). *S. bambusicola* has been reported from temperate regions of Asia, such as China and Japan (Table 1) (Hino 1961; Li et al. 2009; Liu et al. 2013).

Shiraia has previously been placed in several families, depending on the opinions of authors. Hennings (1900) considered *Shiraia* to have unitunicate asci and treated as a member in the family Nectriaceae Tul. & C. Tul. (Hypocreales, Sordariomycetes) when he established the genus. Based on its large and fleshy fruiting bodies, *Shiraia* was transferred to Hypocreaceae De Not by Saccardo (1902). Amano (1980) re-examined the type specimen and regarded *Shiraia* as having bitunicate asci and, hence, placed the genus in Pleosporaceae Nitschke (Pleosporales, Dothideomycetes). However, it was subsequently transferred to Dothideales, genera *incertae sedis* by Kirk et al. (2001).

Earlier classifications of *Shiraia* were based on morphological characters. The first attempt of DNA-based taxonomy (Cheng et al. 2004) confirmed that *Shiraia* belongs in Pleosporales and was phylogenetically close to species of Phaeosphaeriaceae M.E. Barr. Thus, Cheng et al. (2004) considered *Shiraia* as a member in Phaeosphaeriaceae. Liu et al. (2013) carried out significant studies on *Shiraia* taxonomy by re-examining the holotype and carrying out phylogenetic analysis, based on LSU sequence data. Liu et al. (2013) also designated an epitype of both sexual and asexual morphs and introduced Shiraiaceae in the Pleosporales.

Shiraia bambusicola has been reported as a pathogen on various bamboo species (Table 2) or as endophyte of bamboo culms (Morakotkarn et al. 2007, 2008). The bamboo genus *Brachystachyum* Keng is significantly affected by *S. bambusicola* (Table 2; Lai and Fu 2000). The holotype of *S. bambusicola* was recorded from a *Bambusa* sp. (Liu et al. 2013). *Shiraia bambusicola* has also been recorded on several common bamboo genera, including *Fargesia* Franch., *Phyllostachys* Sieb. et Zucc., *Pleioblastus* Nakai and *Indosasa* Mcclure (Lai and Fu 2000; Li et al. 2009). However, these hosts need to be further verified.

Shiraia bambusicola produces hypocrellins. Four hypocrellins have been extracted from the fungal stromata (Wan and Chen 1981; Kishi et al. 1991; Chen and Chen 2009). Endophytes, named as *Shiraia* spp., were also shown to produce hypocrellins on media (Lu et al. 2004; Morakotkarn et al. 2008; Liang et al. 2009; Zhang et al. 2014; Tong et al. 2017). The fruiting body of "Zhuhongjun" also contains hypocrellins

Table 1. Distribution of *Shiraia bambusicola*.

Distribution		References
Country	Province	
China	Anhui	Li et al. (2009), Lai and Fu (2000)
	Guangxi	Li et al. (2009)
	Guizhou	Li et al. (2009)
	Henan	Li et al. (2009)
	Hubei	Li et al. (2009)
	Hunan	Li et al. (2009)
	Jiangsu	Zhao and Liang (2005), Li et al. (2009)
	Jiangxi	Li et al. (2009)
	Sichuan	Chen and Chen (2009), Li et al. (2009)
	Yunan	Fang et al. (2006), Chen et al. (2010)
	Zhejiang	Li et al. (2009), Liu et al. (2013)
Japan	Tokyo	Hino (1961), Liu et al. (2013)
	Osaka	Morakotkarn et al. (2007)

Table 2. List of bamboo hosts of *Shiraia bambusicola*.

Bamboo host	References
Brachystachyum densiflorum (Rendle) Keng	Lai and Fu (2000)
Brachystachyum albostriatum G.H. Lai	Li et al. (2009)
Brachystachyum ensiflorum (Pendle) Keng	Li et al. (2009)
*Brachystachyum yixingens*e	Li et al. (2009)
Phyllostachys nidularia Munro	GenBank
Phyllostachys praecox f. *prevernalis* S.Y. Chen & C.Y. Yao	GenBank
Pleioblastus amarus (Keng) Keng f.	GenBank

(Hudson et al. 1994; Huang et al. 2001). Hypocrellin seems to be an important feature when clarifying the taxa of Shiraiaceae.

A Chinese medical fungus named "Zhuhongjun" in Chinese, was identified as *Hypocrella bambusae* (Berk. & Broome) Sacc. by Liu (1978), based on its conspicuous and fleshy fruiting body. However, according to our knowledge, Zhuhongjun is similar to *S. bambusicola* and unrelated to *Hypocrella*. Therefore, the taxonomic status of this taxon needs to be clarified.

The monotypic genus *Grandigallia*, collected on *Polylepis sericea* Wedd. (*Rosaceae*), was introduced by Barr et al. (1987) with *G. dictyospora* M.E. Barr et al. as the type species. *Grandigallia dictyospora* was reported from Venezuela in a locality above 3,400 m and the fungus was found to produce large ascostromata (3–14 cm in diam.), with bitunicate asci and dictyospores (Barr et al. 1987).

In this study, ten specimens of *S. bambusicola* and a hypocrellin producing taxon ("Zhuhongjun" in Chinese) were collected from Yunnan Province in China. Morphological and phylogenetic studies were carried out to determine the taxonomic status of these taxa. Sequences from endophytic strains, named as *Shiraia* spp., were also downloaded from GenBank and included in the phylogenetic analyses. The metabolite content of hypocrellin extracted from the specimens was determined by HPLC (Chem 2012). Based on the morphology and phylogenetic analyses, the hypocrellin producing taxon "Zhuhongjun" is treated as a new genus in Shiraiaceae.

Material and methods

Collecting and examination of specimens

Bamboo culms with large, reddish to pale yellow ascostromata were collected from Yunnan, China and brought to the laboratory in 2017. Samples were examined following the methods described in Dai et al. (2017). Micro-morphological characters were examined and photographed by differential interference contrast (DIC), using a Leica DM2500 compound microscope with a Leica DMC4500 camera. Fruiting bodies were observed by stereomicroscopy using a Leica S8AP0 and photographed by HDMI 200C. Measurements were made using Tarosoft (R) Image Frame Work software. Specimens have been deposited at the herbarium of Kunming Institute of Botany, Chinese Academy of Sciences (**KUN**) and Herbarium Mycologicum, Academiae Sinicae (**HMAS**) in Beijing. Facesoffungi (Jayasiri et al. 2015) and Index Fungorum (Index Fungorum 2019) numbers were provided for new taxa. Type material of *H. bambusae* was loaned and examined from the Royal Botanic Gardens, Kew.

DNA extraction, PCR amplification and sequencing

The surface of fungal fruiting bodies was sterilised by 75% alcohol and rinsed three times in sterile water. The internal tissue with locules was cut into pieces and ground in a mortar into powder with liquid nitrogen. The powder was used to directly extract DNA with an OMEGA E.Z.N.A. Forensic DNA Kit, following the manufacturer's instructions.

ITS5 and ITS4, NS1 and NS4 (White et al. 1990) and LROR and LR5 (Vilgalys and Hester 1990) primers were used for the amplification of internal transcribed spacers (ITS), small subunit rDNA (SSU) and large subunit rDNA (LSU), respectively. Translation elongation factor 1-α gene region (TEF 1-alpha) and RNA polymerase II second largest subunit (RPB2) genes were amplified by using EF1-983F and EF1-2218R (Rehner 2001), fRPB2-5f and fRPB2-7cr primers (Liu et al. 1999), respectively.

The final volume of the polymerase chain reaction (PCR) was prepared following Dai et al. (2017). The PCR thermal cycle programme of ITS, SSU, LSU, RPB2 and TEF 1-alpha genes amplifications were run under the same conditions as described in Dai et al. (2017). The quality of PCR products was checked by 1% Biowest agarose gel electrophoresis. Amplified PCR fragments were sequenced at Shanghai Majorbio Bio-Pharm Technology Co., Ltd. and BGI Tech Solutions Co., Ltd. (BGI-Tech), P.R. China. Generated new sequences of ITS, LSU, SSU, Rpb2 and TEF1 regions are deposited in GenBank (Table 4).

Table 3. HPLC condition used in this study.

Instrument	Condition
Reverse phase-column	CAPCELL PAK C18 (4.6 mm × 25 cm, 5 μm)
Oven temp. (°C)	35
Flow rate (ml/min)	1
Mobile phase (%)	38% solvent A: H2O + 0.5% formic acid; 62% solvent B: acetonitrile
UV Absorbance (nm)	265
Gradient elution	isocratic elution
Run time (min)	30–40

Table 4. List of newly generated sequences with their culture collection numbers and GenBank accession numbers.

Organism	Specimen voucher	GenBank accession numbers				
		ITS	LSU	SSU	TEF	RPB2
Shiraia bambusicola	HKAS102253	MK804668	MK804648	MK804694	MK819208	MK819228
	HKAS102254	MK804669	MK804649	MK804695	MK819209	MK819229
	HKAS102257	MK804670	MK804650	MK804696	MK819210	MK819230
	HKAS102261	MK804671	MK804651	MK804697	MK819211	MK819231
	HKAS102262	MK804672	MK804652	MK804698	MK819212	MK819232
	HKAS102263	MK804673	MK804653	MK804699	MK819213	MK819233
	HKAS102264	MK804674	MK804654	MK804700	MK819214	MK819234
	HKAS102265	MK804675	MK804655	MK804701	MK819215	MK819235
	HKAS102266	MK804676	MK804656	MK804702	MK819216	MK819236
	HKAS102267	MK804677	MK804657	MK804703	MK819217	MK819237
Rubroshiraia bambusae	**HKAS102255**	**MK804678**	**MK804658**	**MK804704**	**MK819218**	
	HKAS102256	MK804679	MK804659	MK804705	MK819219	
	HKAS102260	MK804680	MK804660	MK804706	MK819220	
	HKAS102268	MK804681	MK804661	MK804707	MK819221	
	HKAS102269	MK804682	MK804662	MK804708	MK819222	
	HKAS102270	MK804683	MK804663	MK804709	MK819223	
	HKAS102271	MK804684	MK804664	MK804710	MK819224	
	HKAS102272	MK804685	MK804665	MK804711	MK819225	
	HKAS102273	MK804686	MK804666	MK804712	MK819226	
	HKAS102274	MK804687	MK804667	MK804713	MK819227	

The holotype specimen is highlighted in bold. Abbreviations: HKAS: herbarium of Kunming Institute of Botany, Chinese Academy of Sciences.

Phylogenetic analysis

The BLAST searches in GenBank, using LSU and ITS sequence data were carried out to obtain the close strains. Additional sequences were downloaded from GenBank based on recent publications (Liu et al. 2017).

Single gene sequence alignments were carried out with MAFFT v. 7.215 (Katoh and Standley 2013, http://mafft.cbrc.jp/alignment/server/index.html) and edited manually when necessary in BioEdit v. 7.0 (Hall 2004). The alignments of LSU, SSU, Rpb2 and TEF1 regions were combined in MEGA6 version 6.0 (Tamura et al. 2013).

Maximum-likelihood (ML) analyses, including 1000 bootstrap replicates, were run using RAxMLGUI v.1.0. (Stamatakis 2006; Silvestro and Michalak 2011). Align-

ments in PHYLIP format were exchanged and loaded from the website (http://sing.ei.uvigo.es/ALTER/). The online tool Findmodel (http://www.hiv.lanl.gov/content/sequence/findmodel/findmodel.html) was used to determine the best nucleotide substitution model for each partition data.

Maximum-parsimony (MP) analyses were carried out in PAUP v. 4.0b10 (Swofford 2002) with 1000 replications. Maxtrees were set to 1000, branches of zero length were collapsed and all multiple equally most parsimonious trees were saved. The robustness of the most parsimonious trees was evaluated from 1000 bootstrap replications (Phillips et al. 2013).

Bayesian analyses were performed using MrBayes v. 3.0b4 (Ronquist and Huelsenbeck 2003). The model of evolution was performed using MrModeltest v. 2.2 (Nylander 2004). Posterior Probabilities (PP) (Rannala and Yang 1996; Zhaxybayeva and Gogarten 2002) were determined by Markov Chain Monte Carlo sampling (MCMC) in MrBayes v. 3.0b4 (Huelsenbeck and Ronquist 2001). Six simultaneous Markov chains were run for 1,000,000 generations and trees were sampled every 100th generation. The burn-in was set to 0.25 and the run was automatically stopped when the average standard deviation of split frequencies reached below 0.01 (Maharachchikumbura et al. 2015).

Trees were visualised with TreeView (Page 1996) or FigTree v. 1.4.0 (http://tree.bio.ed.ac.uk/software/figtree/) and, additionally, layouts were done with Adobe Illustrator CS v. 5. Maximum-likelihood bootstrap values (MLBP) and Maximum-parsimony bootstrap values (MPBP) equal to or greater than 50% are given for each tree. Bayesian posterior probabilities (BYPP) > 0.90 are indicated as thickened lines. The sequences used in this study are listed in Table 1. The combined alignment and phylogenetic tree were submitted at TreeBASE (http://purl.org/phylo/treebase/phylows/study/TB2:S24345).

HPLC profiling

Standards of hypocrellin A and hypocrellin B were purchased from Shanghai Tauto Biotech CO., Ltd. (http://www.tautobiotech.com) and used as received. Their purity is ≥ 98% (HPLC) and their structures are redrawn based on references (Wan and Chen 1981; Morakotkarn et al. 2008) and shown in Figure 1. The dry powder of ascostromata of *S. bambusicola* (HKAS102266) and "Zhuhongjun" (HKAS102270) was extracted followed the methods described by Stadler et al. (2001) and accurately weighed to 0.5 g and added to 25 ml of methanol and sonicated for 30 min. Semi-preparative HPLC was performed on an Agilent 1260 apparatus equipped with a UV detector and a CAPCELL PAK C18 (Agilent, 4.6 mm × 25 cm, 5 μm) column, with 38% solvent A: H_2O + 0.5% formic acid; 62% solvent B: acetonitrile, isocratic elution, UV/Vis the detection in the range of 265 nm (Table 3). The UV-Vis spectra were recorded at room temperature on a Perkin-Elmer Lambda 900 spectrophotometer (Fig. 5).

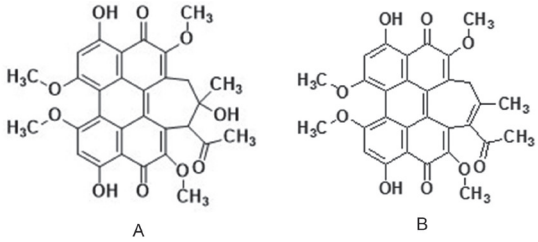

Figure 1. Chemical structures of hypocrellin A and hypocrellin B. **A** hypocrellin A **B** hypocrellin B.

Results

Phylogeny

To clarify the family placement of newly established taxa, maximum likelihood phylogenetic analysis was generated from RAxML (GTR+G model), based on combined SSU, LSU, TEF1 and RPB2 sequences data (Fig. 2). The combined alignment comprised 4025 characters including gaps for 127 ingroup taxa and one outgroup taxon *Dothidea insculpta* (CBS 189.58). Based on the phylogenetic tree in Fig. 2, the new collections cluster within family Shiraiaceae with high bootstrap support (96/1.00 MLBS/BSPP) and emerge as two groups, which are *S. bambusicola* lineage and a new clade named as *R. bambusae* in this paper. *Shiraia* and *Rubroshiraia* have more or less similar ascostromata and both of them can produce the metabolite hypocrellins. However, they can be phylogenetically distinguished with high bootstrap support (100/1.00 MLBS/BSPP) (Fig. 2). *Grandigallia* has not been included in phylogenetic analysis as it is lacking sequences in the GenBank. However, the new taxa can be morphologically distinguished from it. Shiraiaceae is phylogenetically close with family Phaeosphaeriaceae in Pleosporales and this has been confirmed by Liu et al. (2013).

To clarify the relationship between endophytic strains named as shiraia-like (*Shiraia* spp.) and Shiraiaceae, a phylogenetic tree was constructed (RAxML (GTR+G model), based on combined LSU and ITS sequences data and compared. The combined alignment comprises 1442 characters including gaps for 57 ingroup taxa and one outgroup taxon *Pleospora herbarum* (CBS 191.86). Of the 1442 characters of the combined matrix, 1116 were constant and 220 were parsimony informative. The endophytic strains separated into two lineages (Group A and group B) forming at the base clade of Shiraiaceae (Fig. 3). Several strains in group A ca. JP7, JP93, JP232, JP256, SUPER-H168, A8 and ML-2004, isolated from bamboo tissue can produce hypocrellins in media (Lu et al. 2004; Morakotkarn et al. 2008; Liang et al. 2009; Cai et al. 2011; Zhang et al. 2014). However, no hypocrellins were detected from Group B, which included three Japanese strains viz. JP119, JP151 and JP185 (Morakotkarn et al. 2008).

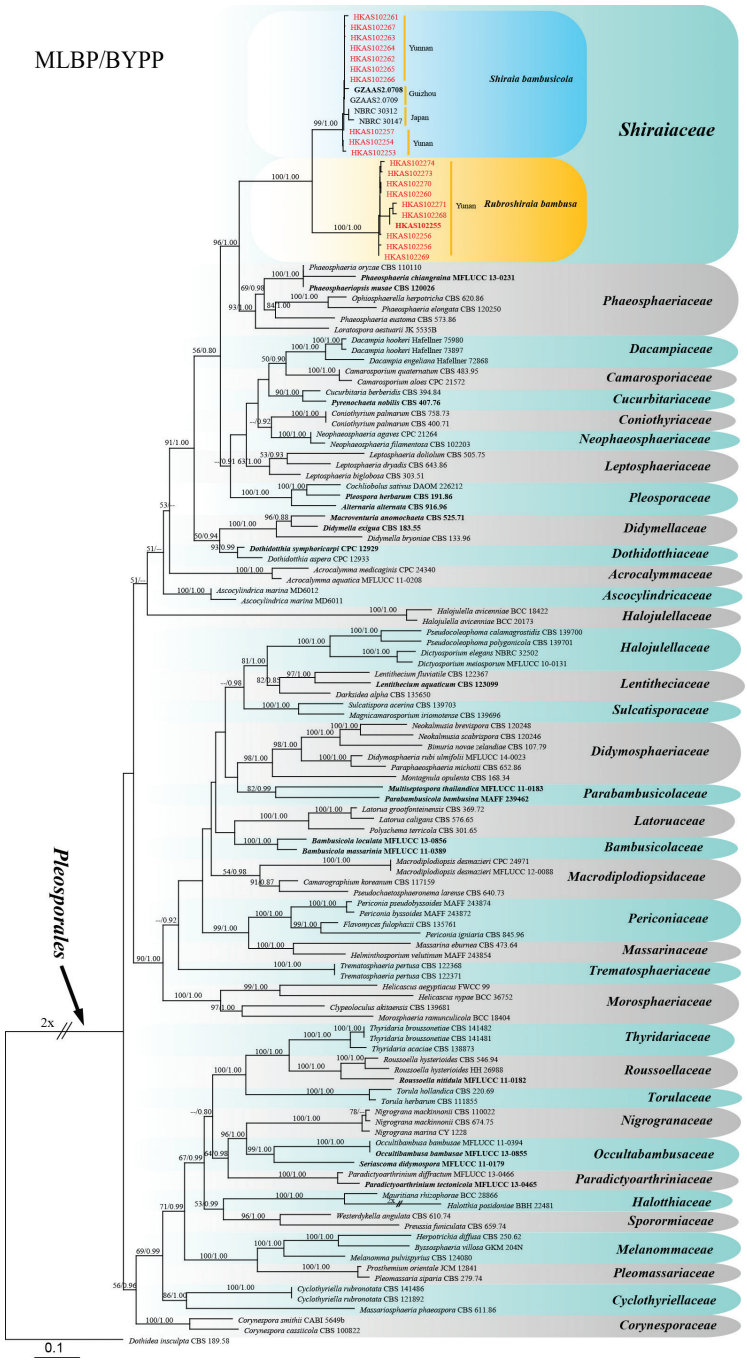

Figure 2. Maximum likelihood phylogenetic tree generated from RAxML (GTR+G model), based on combined LSU, SSU, TEF1 and RPB2 sequences data. ML values (MLBP) (> 50%), resulting from 1000 bootstrap replicates and Bayesian posterior probabilities (BYPP) greater than 0.90, are given at the nodes. The original isolate numbers' codes are noted after the species names. The tree is rooted to *Dothidea insculpta* (CBS 189.58). Ex-type or ex-epitype strains are in bold. Newly generated strains are in *red* and the new genus is in yellow background.

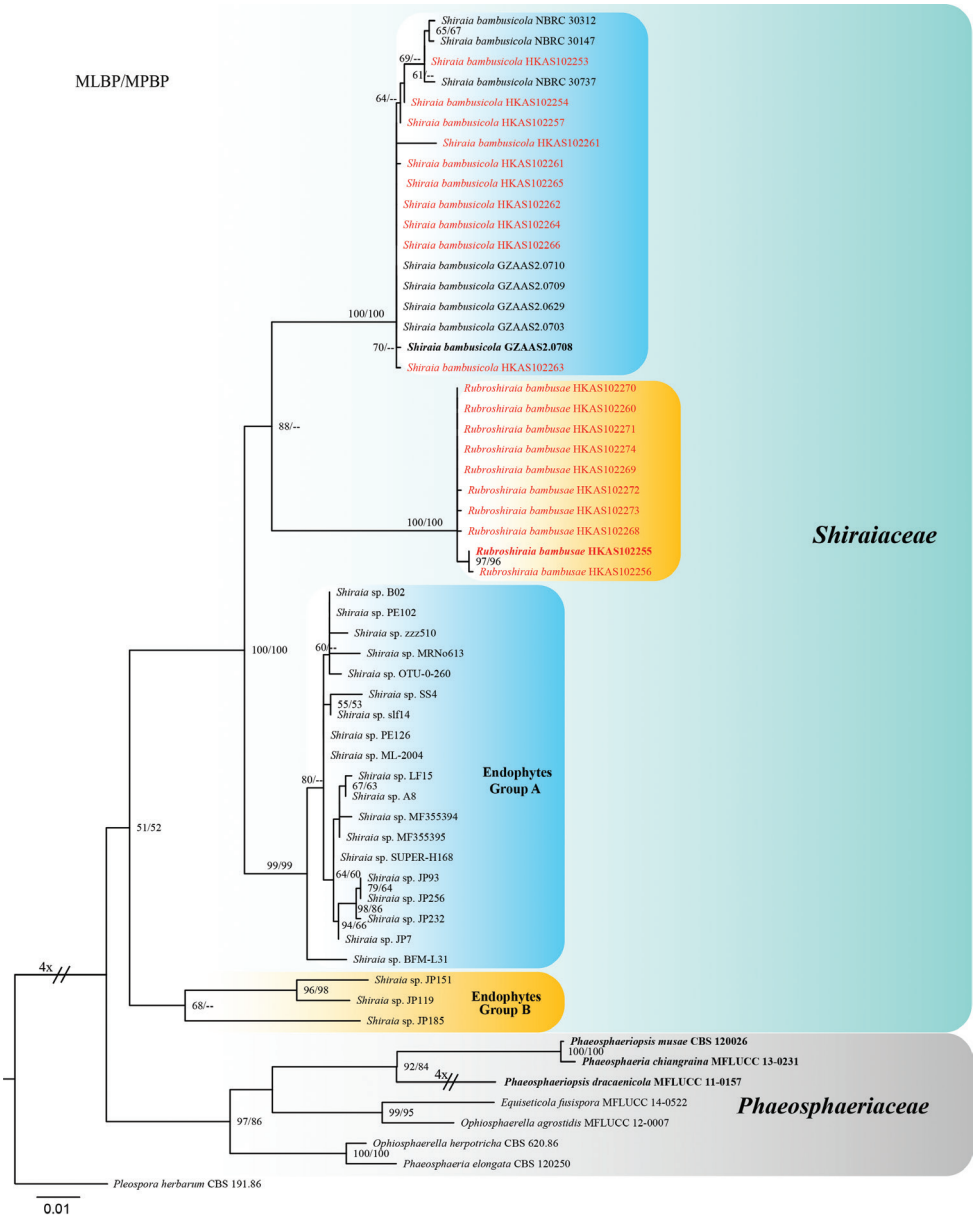

Figure 3. Maximum likelihood phylogenetic tree generated from RAxML (GTR+G model), based on combined LSU and ITS sequences data. ML and MP values (MLBP/MPBP) (> 50%), resulting from 1000 bootstrap replicates, are given at the nodes. The original isolate numbers' codes are noted after the species names. The tree is rooted to *Pleospora herbarum* (CBS 191.86). Ex-type or ex-epitype strains are in bold. Newly generated strains are in red.

Metabolites production

Stromatal extracts from specimens of *S. bambusicola* (HKAS102266) and *R. bambusae* (HKAS102270) contained high quantities of hypocrellin A (304.03 ng/ul and 790.86 ng/ul, respectively). Stromatal extracts from specimens of *S. bambusicola* contained 42.55 ng/ul hypocrellin B, whereas *R. bambusae* produces a higher quantity (204.60 ng/ul). The HPLC profiles of *S. bambusicola* and *R. bambusae* are depicted in Figure 4. The UV spectrum of the standards and of hypocrellin A and B from the samples (*S. bambusicola* HKAS 102253 and *R. bambusae* HKAS 102255) were recorded in alcohol and shown in Figure 5.

Taxonomy

Shiraiaceae Y.X. Liu, Zi Y. Liu & K.D. Hyde, Phytotaxa 103(1): 53 (2013)
Index Fungorum number: IF803884
Facesoffungi number: FoF 06202

Notes. The family Shiraiaceae was introduced by Liu et al. (2013) with a single genus and later *Grandigallia* was added to this family by Ariyawansa et al. (2013). In previous studies, Shiraiaceae was closely related with Phaeosphaeriaceae and their distinction was questionable (Cheng et al. 2004, Liu et al. 2013). However, our multi-gene analyses (Fig. 2) clearly indicate that Shiraiaceae and Phaeosphaeriaceae are distinct. Evidence is also borne out by the fact the Phaeosphaeriaceae have single ascostromata (Phookamsak et al. 2014), while in Shiraiaceae, ascostromata have multiple ascomata. Moreover, Shiraiaceae produces a high quantity of hypocrellins and no such metabolites, secreted by Phaeosphaeriaceae, were reported as far as we know (Phookamsak et al. 2014). In this study, the third genus (i.e. *Rubroshiraia*) is introduced to the family and produces hypocrellins. The endophytic strains in the phylogenetic tree in Figure (2) probably can be named as new genera, once the types are selected. Thus, currently three genera are placed in Shiraiaceae.

Type genus. *Shiraia* Henn., Bot. Jb. 28(3): 274 (1900).

Type species. *S. bambusicola* Henn., Bot. Jb. 28(3): 274 (1900).

***Shiraia bambusicola* Henn., Bot. Jb. 28(3): 274 (1900)**
Fig. 6
Index Fungorum number: IF158454
Facesoffungi number: FoF 06203

Description. Parasitic on living branches of bamboo. **Sexual morph**: ***Ascostromata*** 1–6 cm long × 1–4 cm wide, solitary, superficial, subglobose, long ellipsoid to irregular, tuberculate, fleshy, white to pinkish, with locules lining the periphery,

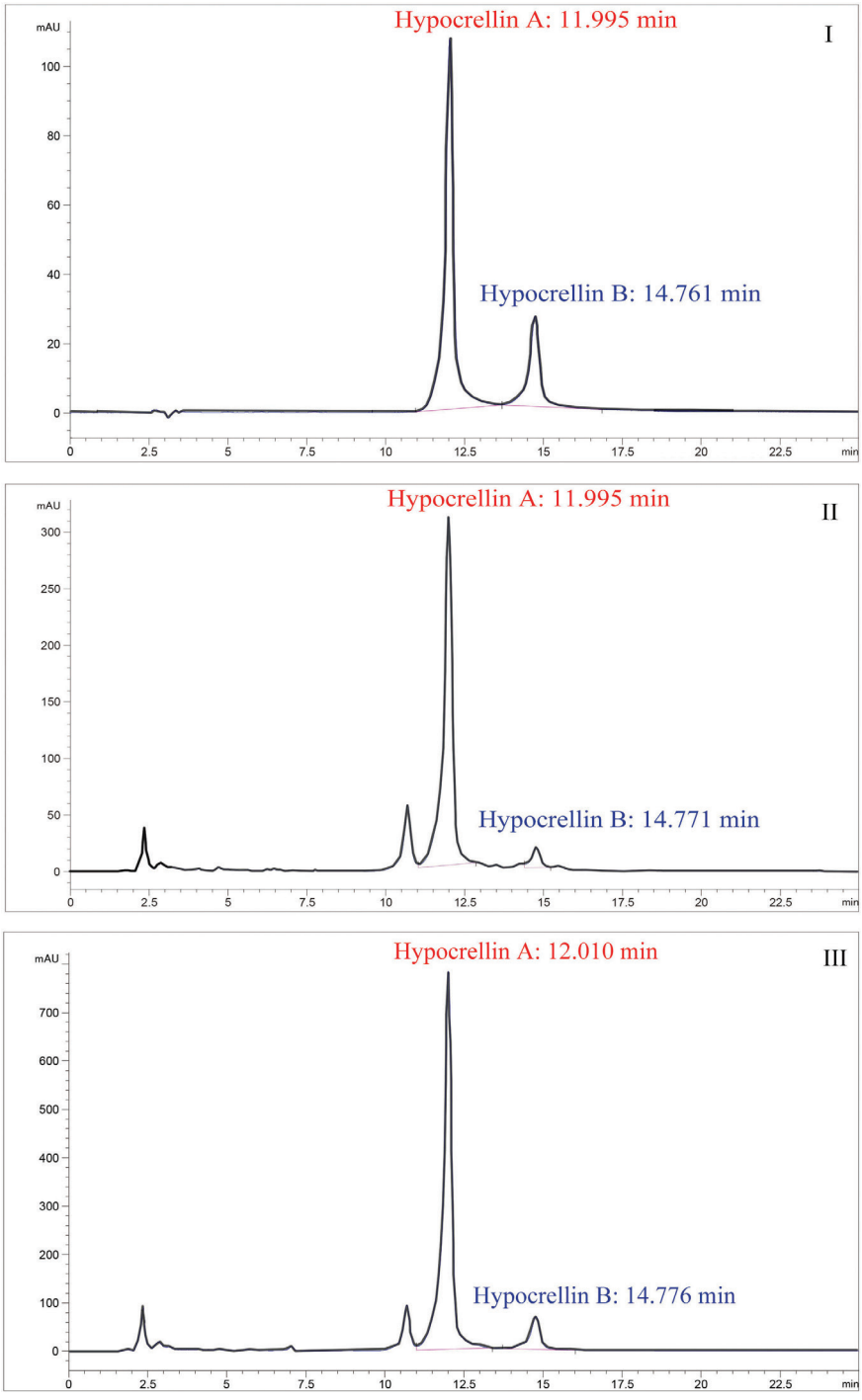

Figure 4. Hypocrellin A and hypocrellin B HPLC-UV profiles (265 nm) of standards and stromatal HPLC-UV profiles (265 nm) of specimens of *Shiraia bambusicola* (HKAS 102253) (II) and *Rubroshiraia bambusae* (HKAS 102255) (III) and DAD spectra of major metabolites.

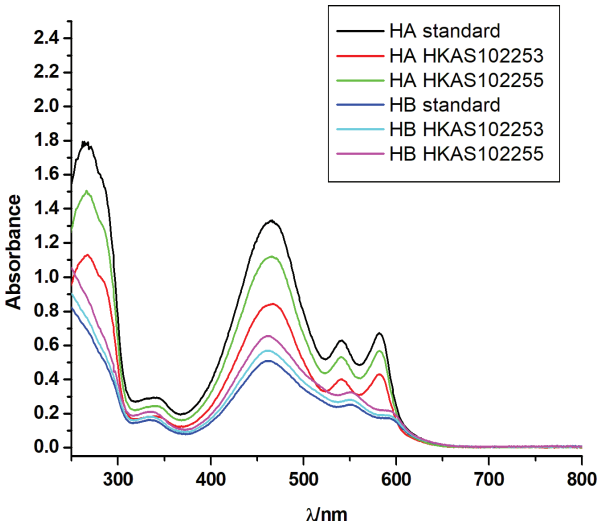

Figure 5. The UV spectrum of the standards and of hypocrellin A and B from the samples (*Shiraia bambusicola* HKAS 102253 and *Rubroshiraia bambusae* HKAS 102255) were recorded in alcohol at room temperature. HA: hypocrellin A, HB: hypocrellin B.

with dark ostiolate points appearing on surface. ***Ascostromatic tissue*** thick, pinkish, composed of wide, woven hyphae of textura intricata. ***Locules*** in vertical section 370–700 µm high × 370–700 µm diam. ($\bar{x}$ = 541 × 513 µm, n = 20), globose to subglobose, immersed in the peripheral layer of ascostromata, with 100–200 µm wide ostioles. ***Peridium*** 20–45 µm thick, composed of several layers of hyaline to light brown, small cells of textura angularis to textura intricata. ***Hamathecium*** composed of interthecial, hyaline septate, branched pseudoparaphyses, 1–2.5 µm wide. ***Asci*** 200–370 × 20–35 µm ($\bar{x}$ = 291.6 × 26.6 µm, n = 20), 4–6-spored, thick-walled, bitunicate, fissitunicate, cylindrical, short-pedicellate, with an ocular chamber. ***Ascospores*** 50–77 × 15–24 µm ($\bar{x}$ = 62.3 × 18.1 µm, n = 20), 1-seriate, overlapped, fusiform, muriform, hyaline, with 7 transverse septa, constricted at the septum, smooth-walled. **Asexual morph**: ***Conidiomata*** 200–500 µm high, 300–400 µm wide, loculate, forming within ascostromata, globose to subglobose or irregular. ***Wall of locules*** 20–40 µm thick, composed of several layers of hyaline to light brown, small cells of textura intricata. ***Conidiophores*** reduced to conidiogenous cells. ***Conidiogenous cells*** 3–6 × 2–3 µm ($\bar{x}$ = 4.7 × 2.1 µm, n = 10), blastic, cylindrical, hyaline, smooth-walled. ***Conidia*** 60–80 × 19–25 µm ($\bar{x}$ = 75.4 × 23.1 µm, n = 20), fusiform, muriform, hyaline, with irregularly transverse and longitudinal septa, straight to curved, smooth-walled.

Culture characters. Colonies growing slowly, attaining 30 mm diam. after 2 weeks at 27 °C under dark, circular, with even margin, floccose at the centre, drift white at margin, light greenish at centre, dark from below.

Material examined. CHINA, Yunnan province, Lijiang, on living branches of *Brachystachyum densiflorum* (Rendle) Keng, 3 May 2017, Dong-Qin Dai, DDQ00409

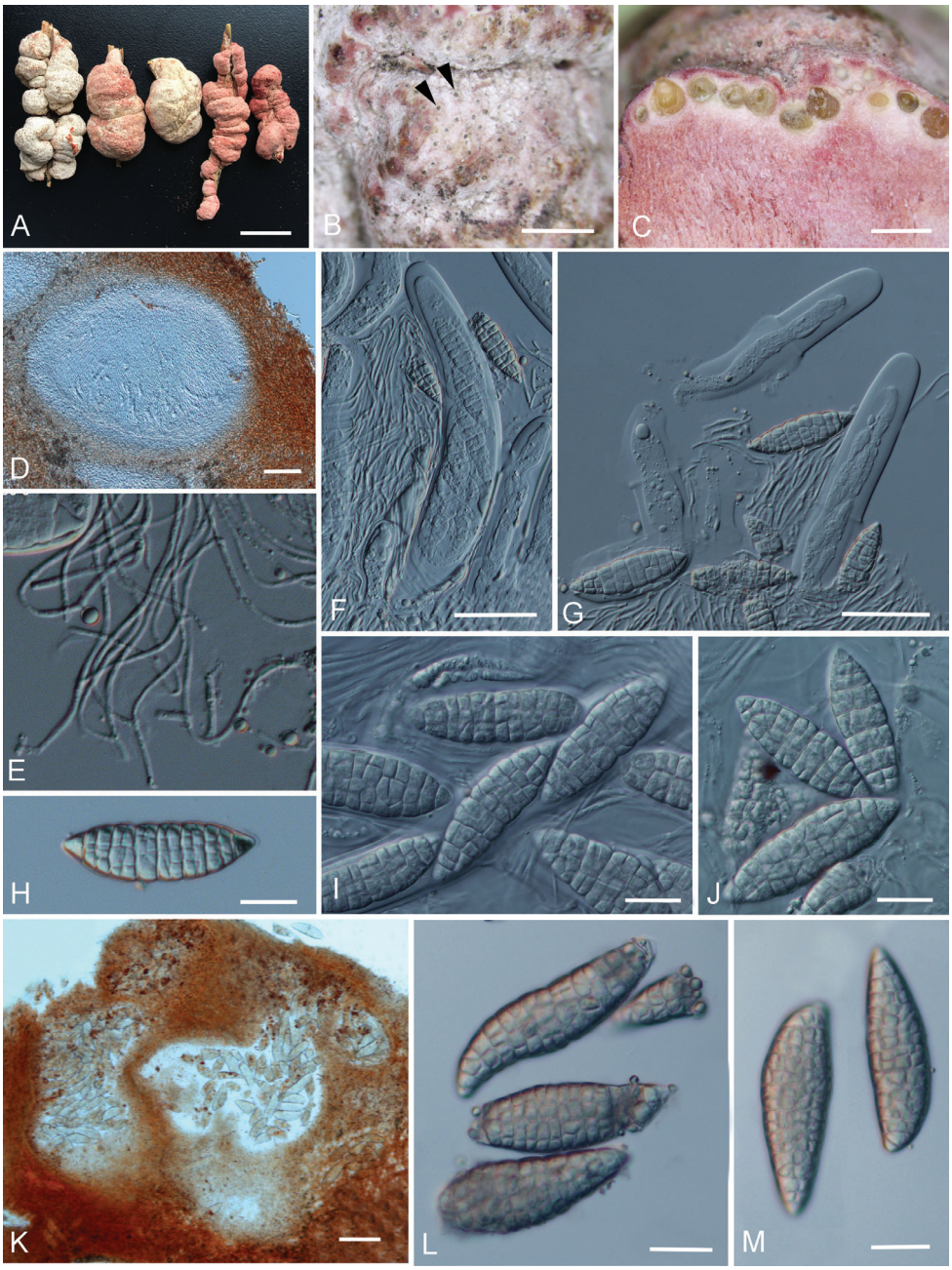

Figure 6. *Shiraia bambusicola* **A–J** sexual morph **A** fruiting bodies (HKAS102253, HKAS102254, HKAS102257, HKAS102261, HKAS102262) **B–J** photographs from material HKAS102253 **B** Surface of ascostromata showing the dark openings of ostiole **C** vertical section of ascostromata **D** vertical section of locule **E** pseudoparaphyses **F, G** asci (**G** Showing the fissitunicate asci) **H–J** ascospores **K–M** asexual morph **K** vertical section of asexual locules **L–M** conidia. Scale bars: 2 cm (**A**), 5 mm (**B**), 1 mm (**C**), 100 μm (**D, K**), 50 μm (**F, G**), 20 μm (**H–J, L, M**).

(HKAS102253), *Ibid*. (duplicate specimen deposited in HMAS 290446), *Ibid*. DDQ00410 (HKAS102254), *Ibid*. DDQ00413 (HKAS102257), *Ibid*. 10 June 2017, Dong-Qin Dai, DDQ00418 (HKAS102261), *Ibid*. DDQ00419 (HKAS102262), *Ibid*. DDQ00420 (HKAS102263), *Ibid*. DDQ00421 (HKAS102264), *Ibid*. DDQ00422 (HKAS102265), *Ibid*. DDQ00423 (HKAS102266), *Ibid*. DDQ00424 (HKAS102267).

Notes. *Shiraia bambusicola* was erected by Hennings (1900), based on a collection from Japan. Liu et al. (2013) re-examined the holotype with 1–2.5 cm wide ascostromata, which is smaller than the new collections (1–4 cm wide in ascostromata) in China. The holotype has large ascospores compared with the new specimens in this study (75–125 × 23–47 μm vs. 50–77 × 15–24 μm). The epitype designated by Liu et al. (2013) which has similar-sized (50–77 × 15–24 μm) ascospores and similar ITS sequence, as in our new collections.

Other genera included

Grandigallia **M.E. Barr et al., Mycotaxon 29: 196. 1987.**
Index Fungorum number: IF12090
Facesoffungi number: FoF 06204

Description. See Ariyawansa et al. (2013).

Type species. *Grandigallia dictyospora* M.E. Barr et al., Mycotaxon 29: 196 (1987)

Notes. The monotypic genus *Grandigallia* was introduced by Barr (1987) and is typified by *G. dictyospora*. The fungus infects branches of *Polylepis sericea* Wedd. (*Rosaceae*) and produces conspicuous (3–14 cm in diam.) and black ascostromata. *Grandigallia* closely resembles *Shiraia* in having muriform ascospores, however, it differs by its black and larger ascostromata. Kirk et al. (2008) and Lumbsch and Huhndorf (2010) placed *Grandigallia* in Dothideomycetes, genera *incertae sedis.* Ariyawansa et al. (2013) re-examined the type material and transferred it to Shiraiaceae in Pleosporales. Wijayawardene et al. (2014, 2017, 2018) accepted this placement.

Rubroshiraia **D.Q. Dai & K.D. Hyde, gen. nov.**
Index Fungorum number: IF556564
Facesoffungi number: FoF 06205

Etymology. The epithet "*Rubro*" means red colour referring to reddish ascotromata similar to the genus *Shiraia*.

Description. Parasitic on living branches of bamboo. **Sexual morph**: ***Ascostromata*** solitary, superficial, globose to subglobose, fleshy, reddish, with locules lining the periphery, with dark ostiolate tips appearing on surface. ***Ascostromatic tissue*** thick,

pinkish, composed of wider woven hyphae of textura intricata. ***Locules*** globose to subglobose, immersed in the peripheral layer of ascostromata, with narrow ostiolate openings. ***Peridium*** composed of several layers of hyaline to dark brown, small cells of textura angularis to textura intricata. ***Hamathecium*** of interthecial, hyaline, septate, branched pseudoparaphyses above asci. ***Asci*** 8-spored, thick-walled, bitunicate, fissitunicate, cylindrical, short-pedicellate, with an ocular chamber. ***Ascospores*** spirally arranged in asci, filiform, hyaline, with transverse septa, smooth-walled. **Asexual morph**: Undetermined.

Type species. *R. bambusae* D.Q. Dai & K.D. Hyde.

Notes. The hypocrellin-producing fungus *R. bambusae* is a well-known taxon used in Chinese traditional medicine which is called "Zhuhongjun" or "Zhuxiaorouzhuojun" in Chinese. However, without molecular data, it was wrongly named as *H. bambusae* (Liu 1978).

Hypocrella bambusae was combined by Saccardo (1878), based on its linear asci and filiform ascospores. Index Fungorum (2019) lists its basionym as *Hypocrea bambusae* Berk. & Broome, which was collected on the inflorescences of bamboo in Sir Lanka and had linear asci and filiform ascospores (Berkeley and Broome 1875). Liu (1978) recorded a well-known Chinese medicinal ascomycete, producing 0.7–1.5 mm diam., hemispheric and reddish stromata with multi-locules, cylindrical asci and filiform ascospores which are spirally arranged and more than 250 μm long on bamboo culms. Liu (1978) identified this fungus as *H. bambusae*, probably based on its cylindrical asci and filiform ascospores. In addition, species of *Hypocrella* usually produce perithecial ascomata (Saccardo 1878). To our knowledge, no fungal records or herbal medicine like that described in Liu (1978) occur in Sir Lanka. Moreover, based on the examination of type material of *Hypocrea bambusae*, it has smaller (0.1 cm vs. 0.7–1.5 mm in diam.) and black stromata, unitunicate asci and ascospores are in a single fascicle but not significantly helically coiled (Fig. 7). Hence, we conclude that Liu (1978) made a wrong identification.

New collections of "Zhuhongjun" were collected and sequenced. The phylogenetic analyses showed it belongs to Shiraiaceae and is separate from *Shiraia* with high bootstrap support (100/1.00 MLBS/BSPP) (Fig. 2). *Grandigallia* has not been included in the phylogenetic tree as it is lacking gene sequences in the GenBank (retrieved date: 13 May 2019). However, *Grandigallia* can be morphologically distinguished from the new taxon in having black ascostromata and muriform ascospores (Barr 1987; Ariyawansa et al. 2013). Thus, this fungus is introduced as *R. bambusae* gen. et sp. nov in this study.

Rubroshiraia bambusae is often confused with *S. bambusicola* by Chinese traditional folk residents, probably because of the similarity of their ascostromata, parasitism on bamboo host and similar efficacy of medical treatment. However, it differs from *S. bambusicola* by its smaller sized ascostromata (0.7–1.2 cm long × 0.7–1 cm wide vs. 1–6 cm long × 1–4 cm wide) and distinct ascospores (filiform ascospores vs. fusiform and muriform ones). Both of the above species can produce the metabolites hypocrellin A and B, whereas *R. bambusae* contains almost double the content compared to *S. bambusicola* (Fig. 4).

Rubroshiraia bambusae **D.Q. Dai & K.D. Hyde, sp. nov.**
Fig. 7
Index Fungorum number: IF556564
Facesoffungi number: FoF 06206

Etymology. Refers the bamboo host.

Holotype. HKAS102255.

Description. Parasitic on living branches of bamboo. **Sexual morph**: ***Ascostromata*** 0.7–1.5 cm long × 0.7–1.3 cm wide, solitary, superficial, globose to subglobose, fleshy, reddish, with locules lining the periphery, with dark ostiolate points appearing on the surface. ***Ascostromatic tissue*** thick, pinkish, composed of wider woven hyphae of textura intricata. ***Locules*** in vertical section 800–1800 μm high × 1000–2000 μm diam. ($\bar{x}$ = 1289.4 ×1368.8 μm, n = 20), globose to subglobose, immersed in the periphery layer of ascostromata, with 250–500 μm wide × 450–550 μm high ostioles. ***Peridium*** 20–35 μm thick, composed of several layers of hyaline to dark brown, small cells of textura angularis to textura intricata. ***Hamathecium*** of interthecial, hyaline septate, branched pseudoparaphyses, 1–3 μm wide. ***Asci*** 660–800 × 45–55 μm ($\bar{x}$ = 751.6 × 49.5 μm, n = 20), 8-spored, thick-walled, bitunicate, fissitunicate, cylindrical, short-pedicellate, with an ocular chamber. ***Ascospores*** 600–750 × 5.5–11 μm ($\bar{x}$ = 728.8 × 9.1 μm, n = 20), spirally arranged in asci, filiform, hyaline, with 15–18 transverse septa, smooth-walled. **Asexual morph**: Undetermined.

Material examined. CHINA, Yunnan, Dali, on living branches of *Fargesia spathacea* Franch, 13 May 2017, Dong-Qin Dai, DDQ00411 (HKAS102255, **holotype**), *Ibid*. (HMAS 290447, **isotype**), *Ibid*. DDQ00412 (HKAS102256), *Ibid*. DDQ00416 (HKAS102260), *Ibid*. 20 June 2017, Dong-Qin Dai, DDQ00425 (HKAS102268), *Ibid*. DDQ00426 (HKAS102269), *Ibid*. DDQ00427 (HKAS102270), *Ibid*. DDQ00428 (HKAS102271), *Ibid*. DDQ00429 (HKAS102272), *Ibid*. DDQ00430 (HKAS102273), *Ibid*. DDQ00431 (HKAS102274).

Key for distinguishing genera in Shiraiaceae

1	Parasitising bamboo branches, ascostromata are white to reddish	**2**
–	Parasitising Rosaceae branches, ascostromata are black	***Grandigallia***
2	Ascospores muriform	***Shiraia***
–	Ascospores filiform	***Rubroshiraia***

Since the familial placement of *H. bambusae* is controversial in different studies (Berkeley and Broome 1875, Saccardo 1878, Liu 1978), we re-studied the isotype. Based on morphology, we conclude that it has unitunicate asci thus related to Sordariomycetes.

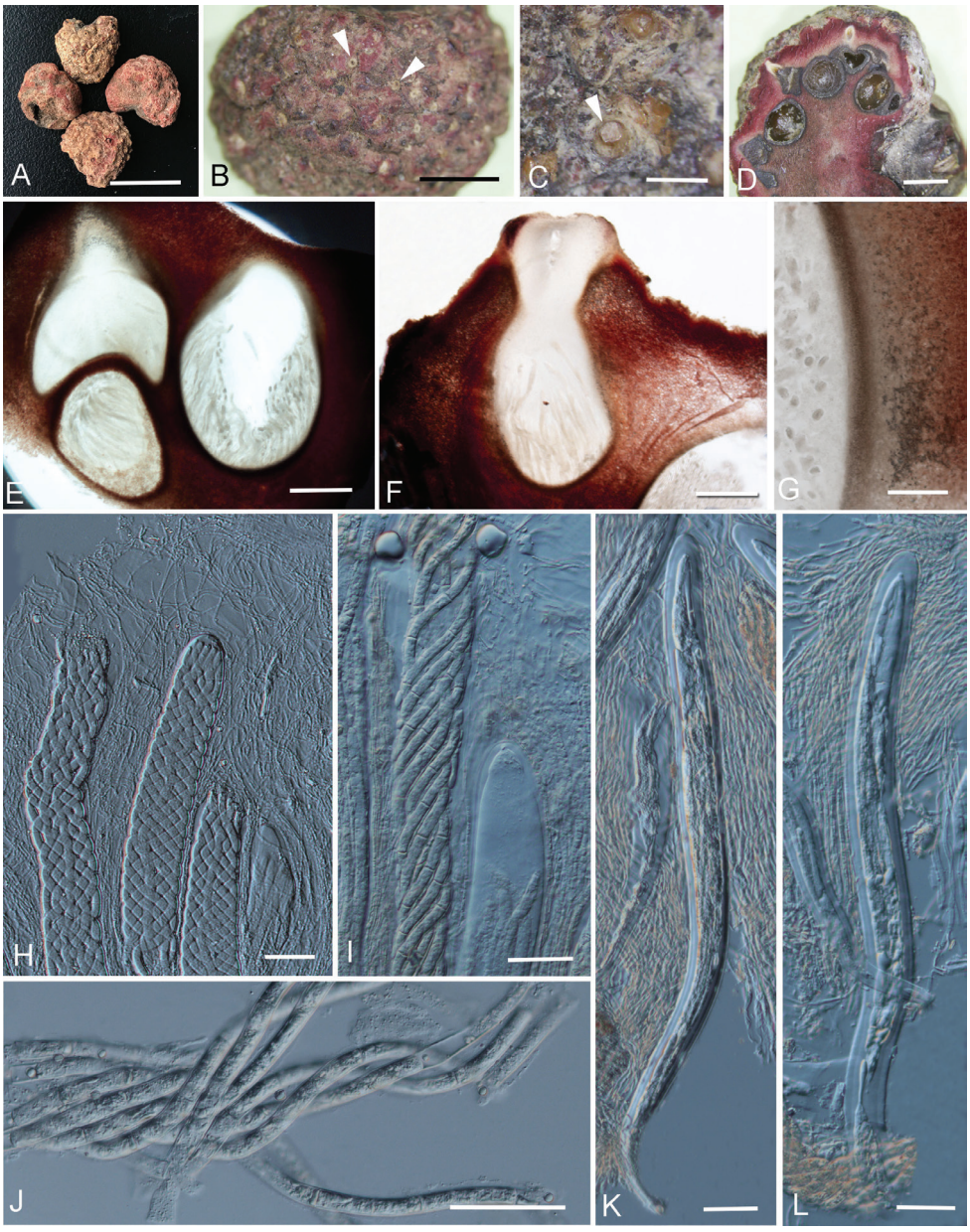

Figure 7. *Rubroshiraia bambusae* (HKAS102255, holotype) **A** fruiting bodies **B, C** surface of ascostromata showing the openings of ostiole **D** vertical section of ascostromata **E, F** vertical section of locule **G** peridium of locule **H** asci and pseudoparaphyses **I** asci and asci ocular chamber **J** ascospores **K, L** immature asci. Scale bars: 1 cm (**A**), 25 mm (**B**), 2 mm (**C, D**), 500 μm (**E, F**), 200 μm (**G**), 50 μm (**H–L**).

***Hypocrella bambusae* (Berk. & Broome) Sacc. 1878**
Fig. 8
Index Fungorum number: IF160297

Basionym. *Hypocrea bambusae* Berk. & Broome, 1873

Description. Parasitic on living inflorescence of bamboo. **Sexual morph**: ***Stromata*** around 0.14 cm diam., 0.06 cm high, solitary, superficial, subglobose, fleshy to coriaceous, black, with around 20 perithecia lining the periphery, with ostioles slightly raised above stroma surface. ***Stromatic tissue*** thick, brown to dark brown. ***Perithecia*** in vertical section around 100 μm diam., 200 μm high, pyriform, immersed in the periphery layer of stromata. ***Asci*** more than 220 μm long, 5–6 μm diam., 8-spored, unitunicate, cylindrical, with a glassy refractive cap around 3 μm from apex to base. ***Ascospores*** around 180 μm long, 1–1.5 μm diam., in a single fascicle but not significantly helically coiled, filiform, hyaline, with 9–10 transverse septa, with rounded ends, smooth-walled. **Asexual morph**: Undetermined.

Material examined. SRI LANKA, on inflorescence of bamboo, January 1855, G.H.K. Thwaites s.n. (ex herb. M.J. Berkeley), K(M)52469, **isotype**.

Notes. This taxon has typical morphology of the *Clavicipitaceae*, which is pyriform perithecia with a gradually tapering upper part and cylindrical asci with a glassy refractive cap. New collections are required and need to be sequenced to clarify its placement.

Discussion

Members of the family Shiraiaceae are distributed from Asia to South America but so far reported only from three countries, viz. China, Japan and Venezuela (Barr et al. 1987; Liu et al. 2013). The family comprises three genera, i.e. *Grandigallia*, *Rubroshiraia* and *Shiraia* wherein the former genus is lacking DNA sequences and, thus in here, we did not include it in the molecular analyses (Figs 2 and 3). These genera show the typical characters of Shiraiaceae, viz. conspicuous large, tuberculate, fleshy and multi-loculate ascostromata producing bitunicate asci. *Shiraia bambusicola* has various types of ascostromata, such as subglobose to tuberculate with white to pinkish colours (Fig. 6). However, the phylogenetic analysis shows these specimens with different types of ascostromata belong to same species (Figs 2 and 3). Thus, we assume that the different shapes of ascostromata are because of the host and different environment conditions.

Stromatal methanol extracts of *Rubroshiraia* and *Shiraia* contain Hypocrellins (Fig. 4). However, so far no extracts have been reported from *Grandigallia*. Fresh material of *Grandigallia* is essential to determine the metabolites. *Rubroshiraia* has darker reddish ascostromata compared with *Shiraia*, probably because its stromatal methanol extracts contain larger quantity of hypocrellins. Some endophytes, named as Shiraia-like fungi, are known to produce hypocrellins on media. They were isolated from different parts of bamboo, such as seeds, nods and internodes (Lu et al. 2004; Mora-

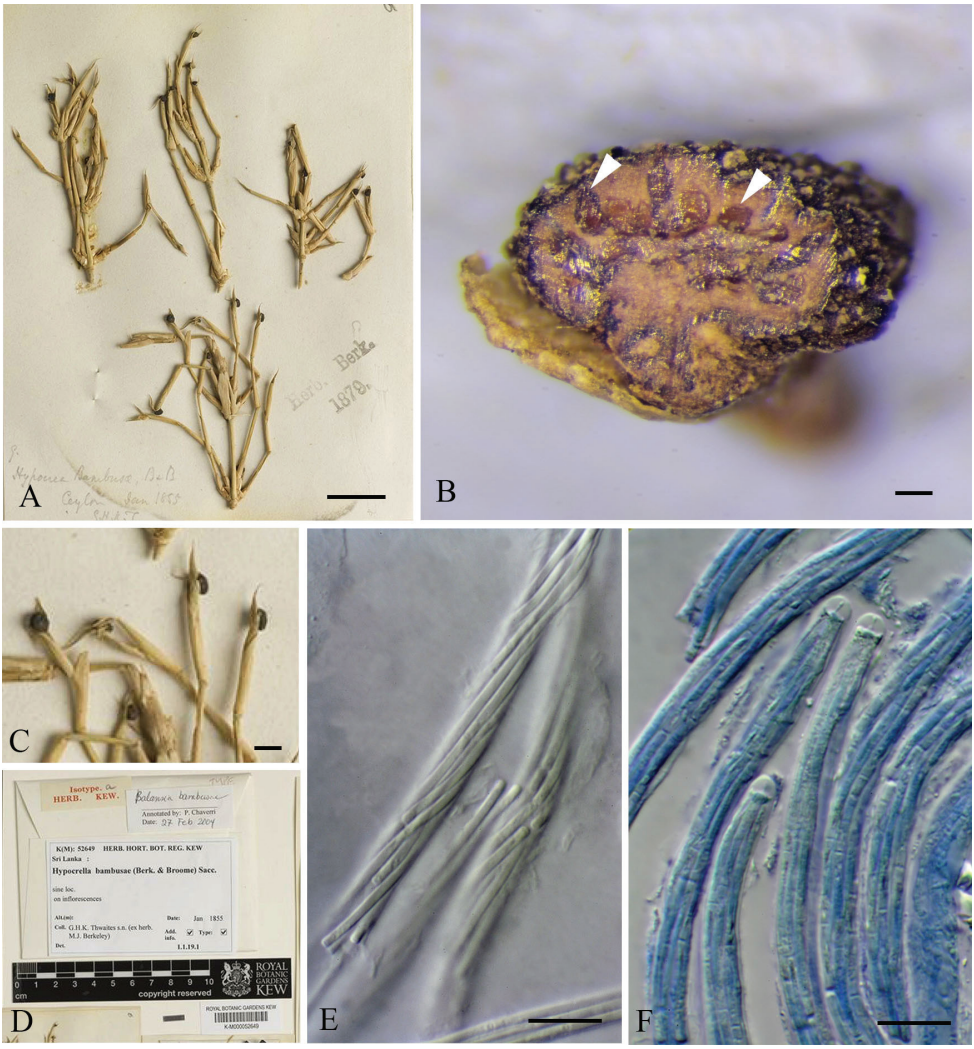

Figure 8. *Hypocrella bambusae* (K(M)52469, isotype, images are accredited to the Royal Botanic Gardens, Kew) **A, C** fruiting bodies on inflorescence of bamboo **B** vertical section of stromata showing the perithecia locating **D** herbarium envelope **E** filiform ascospores **F** asci with caps (Staining by cotton blue). Scale bars: 5 mm (**A**), 200 µm (**B**), 2 mm (**C**), 20 µm (**E, F**).

kotkarn et al. 2008; Liang et al. 2009; Cai et al. 2011; Zhang et al. 2014). Other Shiraia-like endophytes, isolated from the rhizome of *Gastrodia*, leaves of *Huperzia serrata* and from *Triticum aestivum*, phylogenetically cluster within the former group (Fig. 3). However, no hypocrellins were produced from their mycelium (Zhu et al. 2010; Wang et al. 2011, 2016). The bamboo tissue may be providing the needful substances for fungi to produce hypocrellins. The endophytic Shiraia-like taxa (Fig. 3) appear as a distinct genus in Shiraiaceae. The nomination will be made once the type material is available.

Shiraia bambusicola has been used as a Chinese traditional folk-medicine, in curing rheumatoid arthritis, infantile convulsion and pertussis etc. for more than 400 years, because of its stromatal metabolites (Huang et al. 2001; Shen et al. 2002). Japanese scientists first obtained three perylenequinones from air-dried ascostromata of *S. bambusicola* and named them as hypocrellin A, B and C (Kishi et al. 1991). However, hypocrellin A was originally discovered by Wan and Chen (1981) from a different fungus on bamboo which was called as "Zhuhongjun" in Chinese and was erroneously identified as *H. bambusae* (Liu 1978). Later the fourth hypocrellin analogue (hypocrellin D) was named by Fang et al. (2006). Therefore, in total, four hypocrellins have so far been named. Hypocrellins are types of biologically active compounds and naturally occurring perylenequinones with photodynamic activity (Wan and Chen 1981; Kishi et al. 1991; Chowdhury et al. 2002; Liang et al. 2009; Liu et al. 2013). These secondary metabolites have gained much attention owing to their light-induced anti-tumour, anti-fungal and anti-viral activities (Wan and Chen 1981; Liang et al. 2009; Li et al. 2000a, b). In clinical trials, hypocrellin shows promising treatment for various skin diseases, such as skin cancer and white lesions of the vulva (Wan and Chen 1981; Li et al. 2000b). In China, a costly medicinal unguent named Bamboo Parasitic Fungus Ointment is made of hypocrellin B (Dai et al. 2018). Interestingly, it was proved that hypocrellin has bactericidal activities which inhibit various bacteria, such as *Bacillus subtilis* Ehrenberg and *Micrococcus luteus* Schroeter (Chen et al. 2010). In addition, hypocrellin A has an antiviral activity against human immunodeficiency virus (HIV-1) (Hudson et al. 1994) and is promising as a new-fashioned photoelectric conversion material (Li et al. 2000a).

Hypocrellin has wide application prospects, but it was earlier only found existing in ascostromata of *S. bambusicola* and "Zhuhongjun" (*R. bambusae* in this paper) (Wan and Chen 1981; Kishi et al. 1991). For gaining a high yield of Hypocrellin, scientists devoted themselves to looking for strains that can produce hypocrellin through fermentation production (Liang et al. 2009). Numerous endophytes, isolated from bamboo tissue such as culms, leaves, nodes and seeds, were published (Lu et al. 2004; Morakotkarn et al. 2007, 2008; Liang et al. 2009; Cai et al. 2011; Shen et al. 2012, 2014; Zhang et al. 2014), several of which had the potential for hypocrellin production (Lu et al. 2004; Morakotkarn et al. 2008; Liang et al. 2009; Zhang et al. 2014; Tong et al. 2017). However, the strains with promising industrial fermentation were identified as *Shiraia* sp. based on the blast search in GenBank by ITS sequences. More endophytes producing biologically active compounds, such as huperzine, isolated from the plant *Huperzia serrata* (Thunb. ex Murray) Trev., were also named as *Shiraia* sp. (Wang et al. 2011, 2016; Zhu et al. 2010). These strains usually have around 80%–90% ITS similarity with *S. bambusicola*, which also shows that they are phylogenetically close with members of Shiraiaceae. In this study, these endophytes are placed in Shiraiaceae, based on the phylogenetic analyses (Fig. 3).

According to Deng et al. (2017), polyketide synthase (*SbaPKS*) is involved in hypocrellin biosynthesis, based on the methods of CRISPR/Cas9 genome editing. It provides evidence for decoding the hypocrellin pathway (Deng et al. 2017). This pathway has the potential for producing high quality hypocrellins.

Acknowledgements

This work was supported by the Key Laboratory of Yunnan Province Universities of the Diversity and Ecological Adaptive Evolution for Animals and plants on Yun-Gui Plateau, the National Natural Science Foundation of China (No. NSFC 31760013, 31950410558, 31260087, 31460561, 31860005, 31460179 and 31860057) and the Scientific Research Foundation of Yunnan Provincial Department of Education (2017ZZX186). Dong-Qin Dai would like to thank Yunnan Province Universities of the Science and Technology Innovation Team for the exploitation and utilisation of endophytes and the Thousand Talents Plan, Youth Project of Yunnan Provinces for support. Chao Liu thanks the Yunnan Local Colleges Applied Basic Research Projects (2017FH001-034). Dong-Qin Dai would like to thank Xiu Gao (Qujing Normal University) for the help with drawing chemical structures of hypocrellins and is grateful to Dr. Joanne E. Taylor for the help of the loaned herbarium.

References

Amano N (1980) Studies on the Japanese Loculoascomycetes. II. Taxonomic position of the genus *Shiraia*. Bulletin of the National Science Museum 6: 55–60.

Ariyawansa HA, Kang JC, Alias SA, Chukeatirote E, Hyde KD (2013) Towards a natural classification of Dothideomycetes: The genera *Dermatodothella*, *Dothideopsella*, *Grandigallia*, *Hysteropeltella* and *Gloeodiscus* (Dothideomycetes *incertae sedis*). Phytotaxa 147: 35–47. https://doi.org/10.11646/phytotaxa.147.2.1

Barr ME, Boise JR, Hanlin RT (1987) A spectacular Loculoascomycete from Venezuela. Mycotaxon 29: 195–198.

Berkeley MJ, Broome CE (1875) Enumeration of the fungi of Ceylon. Part II. Botanical Journal of the Linnean Society 14: 29–141. https://doi.org/10.1111/j.1095-8339.1873.tb00301.x

Cai Y, Liao X, Liang X, Ding Y, Sun J, Zhang D (2011) Induction of hypocrellin production by Triton X-100 under submerged fermentation with *Shiraia* sp. SUPER-H168. New Biotechnology 28: 588–592. https://doi.org/10.1016/j.nbt.2011.02.001

Chem A (2012) Practical HPLC method development. Carbohydrate Polymers 16: 338–338. https://doi.org/10.1016/0144-8617(91)90119-W

Chen H, Chen WQ (2009) The analysis and comparison of bioactive ingredients in *Shiraia bambusicola* from different regions. Journal of Zhejiang Shuren University 9: 17–19.

Chen YJ, Zhong WW, Yang SY (2010) Study on the Antibacterial Activity of *Shiraia bambusicola* Henn. Journal of Yunnan University of Nationalities (Natural Sciences Edition) 19: 154–156.

Cheng TF, Jia XM, Ma XH, Lin HP, Zhao YH (2004) Phylogenetic study on *Shiraia bambusicola* by rDNA sequence analyses. Journal of Basic Microbiology 44: 339–350. https://doi.org/10.1002/jobm.200410434

Chowdhury PK, Das K, Datta A, Liu WZ, Zhang HY, Petrich JW (2002) A comparison of the excited-state processes of nearly symmetrical perylene quinones: hypocrellin A and hypomycin B. Journal of Photochemistry & Photobiology A: Chemistry 154: 107–116. https://doi.org/10.1016/S1010-6030(02)00309-X

Dai DQ, Phookamsak R, Wijayawardene NN, Li WJ, Bhat DJ, Mortimer PE, Xu JC, Taylor JE, Hyde KD, Chukeatirote E (2017) Bambusicolous fungi. Fungal Diversity 82: 1–105. https://doi.org/10.1007/s13225-016-0367-8

Dai DQ, Tang LZ, Wang HB (2018) Review of bambusicolous ascomycetes. Bamboo: Current and Future Prospects 2018: 165. https://doi.org/10.5772/intechopen.76463

Deng HX, Gao RJ, Liao, XG, Cai YJ (2017) Genome editing in *Shiraia bambusicola* using CRISPR-Cas9 system. Journal of Biotechnology 259: 228–234. https://doi.org/10.1016/j.jbiotec.2017.06.1204

Fang LZ, Qing C, Shao HJ, Yang YD, Dong ZJ, Wang F, Zhao W, Yang WQ, Liu JK (2006) Hypocrellin D, a cytotoxic fungal pigment from fruiting bodies of the ascomycete *Shiraia bambusicola*. Journal of Antibiotics 59: 351–354. https://doi.org/10.1038/ja.2006.49

Hall T (2004) BioEdit. Ibis Therapeutics, Carlsbad. http://www.mbio.ncsu.edu/BioEdit/bioedit.html [18 Mar 2005]

Hennings P (1900) Fungi Japonici. Botanische Jahrbücher für Systematik, Pflanzengeschichte und Pflanzengeographie 28: 259–280.

Hino I (1961) Icones fungorum bambusicolorum japonicorum. The Fuji Bamboo Garden, Kobe.

Huang TK, Ding ZZ, Zhao SX, Yan YQ, Xu GJ, Chen L, Yu CL, Gao XL, Zhang ZD (2001) Xian Dai Ben Cao Gang Mu. China Medical Science Press, Beijing. [In Chinese]

Hudson JB, Zhou J, Chen J, Harris L, Towers GH (1994) Hypocrellin, from *Hypocrella bambusae*, is phototoxic to human immunodeficiency virus. Photochem Photobiol 60: 253–255. https://doi.org/10.1111/j.1751-1097.1994.tb05100.x

Huelsenbeck JP, Ronquist F (2001) MRBAYES: Bayesian inference of phylogenetic trees. Bioinformatics 17: 754–755. https://doi.org/10.1093/bioinformatics/17.8.754

Index Fungorum (2019) Index Fungorum. http://www.indexfungorum.org/names/Names.asp

Jayasiri SC, Hyde KD, Ariyawansa HA, Bhat DJ, Buyck B, Cai L, Dai YC, Abd-Elsalam KA, Ertz D, Hidayat I, Jeewon R, Jones EBG, Bahkali AH, Karunarathna SC, Liu JK, Luangsa-ard JJ, Lumbsch HT, Maharachchikumbura SSN, McKenzie EHC, Moncalvo JM, Ghobad-Nejhad M, Nilsson H, Pang KL, Pereira OL, Phillips AJL, Raspé O, Rollins AW, Romero AI, Etayo J, Selçuk F, Stephenson SL, Suetrong S, Taylor JE, Tsui CKM, Vizzini A, Abdel-Wahab MA, Wen TC, Boonmee S, Dai DQ, Daranagama DA, Dissanayake AJ, Ekanayaka AH, Fryar SC, Hongsanan S, Jayawardena RS, Li WJ, Perera RH, Phookamsak R, de Silva NI, Thambugala KM, Tian Q, Wijayawardene NN, Zhao RL, Zhao Q, Kang JC, Promputtha I (2015) The Faces of Fungi database: fungal names linked with morphology, phylogeny and human impacts. Fungal Diversity 74: 3–18. https://doi.org/10.1007/s13225-015-0351-8

Katoh K, Standley DM (2013) MAFFT multiple sequence alignment software version 7: improvements in performance and usability. Molecular Biology and Evolution 30: 772–780. https://doi.org/10.1093/molbev/mst010

Kirk PM, Cannon PF, David JC, Stalpers JA (2001) Ainsworth and Bisby's Dictionary of the Fungi (9th edn). CAB International, Wallingford, 655 pp.

Kirk PM, Cannon PF, Minter DW, Stalpers JA (2008) Dictionary of the Fungi (10th edn). CABI, Wallingford, 784 pp.

Kishi T, Tahara S, Taniguchi N, Tsuda M, Tanaka C, Takahashi S (1991) New perylenequinones from *Shiraia bambusicola*. Planta Medica 57: 376–379. https://doi.org/10.1055/s-2006-960121

Lai GH, Fu LY (2000) Study on main host plants of *Shiraia bambusicola*. Chinese Wild Plant Resources 1: 8–11. [In Chinese]

Li C, Chen YT, Lin NY, Wang HQ, Liu WZ, Xie JL (2000a) Analysis on the chemical components of a fungus producing perylenequinones photosensitive compounds. Mycosystema 19: 122–127.

Li C, Wang HQ, Xie JL, Lin NY, Dai WH, Chen YT (2000b) Analysis and comparisons of compounds among three medical fungi of Hypocreaceae. Chinese Traditional and Herbal Drugs 31: 250–251.

Li XM, Gao J, Yue YD, Hou CL (2009) Studies on Systematics, Biology and Bioactive Substance of *Shiraia bambusicola*. Forest Research 22: 279–284.

Liang XH, Cai YJ, Liao XR, Wu K, Wang L, Zhang DB, Meng Q (2009) Isolation and identification of a new hypocrellin A-producing strain *Shiraia* sp. SUPER-H168. Microbiological Research 164: 9–17. https://doi.org/10.1016/j.micres.2008.08.004

Liu B (1978) Chinese medicinal fungi (2nd edn). Shanxi people's publishing house, Taiyuan. [In Chinese]

Liu YJ, Whelen S, Hall BD (1999) Phylogenetic relationships among ascomycetes: evidence from an RNA polymerse II subunit. Molecular Biology and Evolution 16: 1799–1808. https://doi.org/10.1093/oxfordjournals.molbev.a026092

Liu YX, Hyde KD, Ariyawansa HA, Li WJ, Zhou DQ, Yang YL, Chen YM, Liu ZY (2013) Shiraiaceae, new family of Pleosporales (Dothideomycetes, Ascomycota). Phytotaxa 103: 51–60. https://doi.org/10.11646/phytotaxa.103.1.4

Liu JK, Hyde KD, Jeewon R, Phillips AL, Maharachchikumbura SSN, Ryberg M, Liu ZY, Zhao Q (2017) Ranking higher taxa using divergence times: a case study in Dothideomycetes. Fungal Diversity 84:75–99. https://doi.org/10.1007/s13225-017-0385-1

Lu MF, Huang YB, Zhang HY, Wang HN, Zhang YJ (2004) Cloning and sequencing of the ITS in rDNA Gene of a Fungus Producing Perylenequinones Deriveration. Journal of Sichuan Agricultural University 22: 138–141. https://doi.org/10.1300/J064v24n01_09

Lumbsch HT, Huhndorf SM (2010) Myconet Volume 14. Part one. Outline of Ascomycota-2009. Part Two. Notes on Ascomycete Systematics. Nos. 4751–5113. Fieldiana Life and Earth Sciences 1: 1–64. https://doi.org/10.3158/1557.1

Maharachchikumbura SS, Hyde KD, Jones EBG, McKenzie EHC, Huang SK, Abdel-Wahab MA, Daranagama DA, Dayarathne M, D'souza MJ, Goonasekara ID, Hongsanan S, Jayawardena RS, Kirk PM, Konta S, Liu JK, Liu ZY, Norphanphoun C, Pang KL, Perera RH, Senanayake IC, Shang Q, Shenoy BD, Xiao YP, Bahkali AH, Kang JC, Somrothipol S, Suetrong S, Wen TC, Xu JC (2015) Towards a natural classification and backbone tree for Sordariomycetes. Fungal Diversity 72: 199–301. https://doi.org/10.1007/s13225-015-0331-z

Morakotkarn D, Kawasaki H, Seki T (2007) Molecular diversity of bamboo-associated fungi isolated from Japan. FEMS Microbiology Letters 266: 10–19. https://doi.org/10.1111/j.1574-6968.2006.00489.x

Morakotkarn D, Kawasaki H, Tanaka K, Okane I, Seki T (2008) Taxonomic characterization of Shiraia-like fungi isolated from bamboos in Japan. Mycoscience 49: 258–265. https://doi.org/10.1007/S10267-008-0419-3

Nylander JAA (2004) MrModeltest 2.0. Program distributed by the author. Evolutionary Biology Centre, Uppsala University

Page RDM (1996) TreeView: an application to display phylogenetic trees on personal computers. Computer Applications in the Biosciences 12: 357–358. https://doi.org/10.1093/bioinformatics/12.4.357

Phillips AJL, Alves A, Abdollahzadeh J, Slippers B, Wingfield MJ, Groenewald JZ, Crous PW (2013) The *Botryosphaeriaceae*: genera and species known from culture. Studies in Mycology 76: 51–167. https://doi.org/10.3114/sim0021

Phookamsak R, Liu JK, McKenzie EHC, Manamgoda DS, Ariyawansa H, Thambugala KM, Dai DQ, Camporesi E, Chukeatirote E, Wijayawardene NN, Bahkali AH, Mortimer PE, Xu JC, Hyde KD (2014) Revision of Phaeosphaeriaceae. Fungal Diversity 68: 159–238. https://doi.org/10.1007/s13225-014-0308-3

Rannala B, Yang Z (1996) Probability distribution of molecular evolutionary trees: a new method of phylogenetic inference. Journal of molecular evolution 43: 304–311. https://doi.org/10.1007/BF02338839

Rehner S (2001) Primers for elongation factor 1-α (EF1-α). http://ocid.NACSE.ORG/research/deephyphae/EF1primer.pdf

Ronquist F, Huelsenbeck JP (2003) MrBayes 3: Bayesian phylogenetic inference under mixed models. Bioinformatics 19: 1572–1574. https://doi.org/10.1093/bioinformatics/btg180

Saccardo PA (1878) Enumeratio pyrenomycetum Hpocreaceorum hucusque cognitorum systemate carpologico dispositorum. Michelia 1: 277–325.

Saccardo PA (1902) Sylloge Fungorum. Omnium hucosque cognitorum. Supplementum universale XVI: 421

Shen YX, Rong XG, Gao ZH (2002) Studies on the chemical constituents of *Shiraia bambusicola*. China Journal of Chinese Materia Medica 27: 674–677.

Shen X, Zheng D, Gao J, Hou CL (2012) Isolation and evaluation of endophytic fungi with antimicrobial ability from *Phyllostachys edulis*. Bangladesh Journal of Pharmacology 7: 249–257. https://doi.org/10.3329/bjp.v7i4.12068

Shen XY, Cheng YL, Cai CJ, Fan L, Gao J, Hou CL (2014) Diversity and Antimicrobial Activity of Culturable Endophytic Fungi Isolated from Moso Bamboo Seeds. PloS one 9: e95838. https://doi.org/10.1371/journal.pone.0095838

Silvestro D, Michalak I (2011) raxmlGUI: a graphical front-end for RAxML. Organisms Diversity & Evolution 12: 335–337. https://doi.org/10.1093/bioinformatics/btg180

Stadler M, Wollweber H, Mühlbauer A, Henkel T, Asakawa Y, Hashimoto T, Rogers JD, Ju YM, Wetzstein HG, Tichy HV (2001) Secondary metabolite profiles, genetic fingerprints and taxonomy of *Daldinia* and allies. Mycotaxon 77: 379–429.

Stamatakis A (2006) RAxML-VI-HPC: maximum likelihood-based phylogenetic analyses with thousands of taxa and mixed models. Bioinformatics 22: 2688–2690. https://doi.org/10.1093/bioinformatics/btl446

Swofford DL (2002) PAUP: phylogenetic analysis using parsimony, version 4.0 b10. Sinauer Associates, Sunderland. https://doi.org/10.1002/0471650129.dob0522

Tamura K, Stecher G, Peterson D, Filipski A, Kumar S (2013) MEGA6: molecular evolutionary genetics analysis version 6.0. Molecular Biology and Evolution 30: 2725–2729. https://doi.org/10.1093/molbev/mst197

Tong ZW, Mao L, Liang H, Zhang Z, Wang Y, Yan R, Zhu D (2017) Simultaneous Determination of Six Perylenequinones in *Shiraiaia* sp. Slf14 by HPLC. Journal of Liquid Chromatography & Related Technologies 40: 536–540. https://doi.org/10.1080/10826076.2017.1331172

Vilgalys R, Hester M (1990) Rapid genetic identification and mapping of enzymatically amplified ribosomal DNA from several Cryptococcus species. Journal of Bacteriology 172: 4238–4246. https://doi.org/10.1128/jb.172.8.4238-4246.1990

Wan XY, Chen YT (1981) Hypocrellin A-A new drug for photochemotherapy. Chinese Science Bulletin 26: 1040–1042.

Wang Y, Zeng QG, Zhang ZB, Yan RM, Wang LY, Zhu D (2011) Isolation and characterization of endophytic huperzine A-producing fungi from *Huperzia serrata*. Journal of Industrial Microbiology & Biotechnology 38: 1267–1278. https://doi.org/10.1007/s10295-010-0905-4

Wang Y, Zheng L, Li XX, Yan RM, Zhang ZB, Yang HL, Zhu D (2016) Isolation, diversity and acetylcholinesterase inhibitory activity of the culturable endophytic fungi harboured in *Huperzia serrata* from Jinggang Mountain, China. World Journal of Microbiology & Biotechnology 32: 1–23. https://doi.org/10.1007/s11274-015-1966-3

White TJ, Bruns T, Lee S, Taylor J (1990) Amplification and direct sequencing of fungal ribosomal RNA genes for phylogenetics. In: Innis MA, Gelfand DH, Sninsky JJ, White TJ (Eds) PCR protocols: a guide to methods and applications, Academic, San Diego, 315–322. https://doi.org/10.1016/B978-0-12-372180-8.50042-1

Wijayawardene NN, Crous PW, Kirk PM, Hawksworth DL, Boonmee S, Braun U, Chomnunti P, Dai DQ, D'souza MJ, Diederich P, Dissanayake A, Doilom M, Hongsanan S, Jones EBG, Groenewald JZ, Jayawardena R, Lawrey JD, Liu JK, Lücking R, Madrid H, Manamgoda DS, Muggia L, Nelsen MP, Phookamsak R, Suetrong S, Tanaka K, Thambugala KM, Wikee S, Zhang Y, Aptroot A, Ariyawansa HA, Bahkali AH, Bhat JD, Gueidan C, De Hoog GS, Knudsen K, McKenzie EHC, Miller AN, Mortimer PE, Wanasinghe DN, Phillips AJL, Raja HA, Slippers B, Shivas RS, Taylor JE, Wang Y, Woudenberg JHC, Piątek M, Cai L, Jaklitsch WM, Hyde KD (2014) Naming and outline of Dothideomycetes. (2014) including proposals for the protection or suppression of generic names. Fungal Diversity 69: 1–55. https://doi.org/10.1007/s13225-014-0309-2

Wijayawardene NN, Papizadeh M, Phillips AJL, Wanasinghe DN, Bhat DJ, Weerahewa HLD, Shenoy BD, Wang Y, Huang YQ (2017) Mycosphere Essays 19: Recent advances and future challenges in taxonomy of coelomycetous fungi. Mycosphere 8: 934–950. https://doi.org/10.5943/mycosphere/8/7/9

Wijayawardene NN, Hyde KD, Lumbsch HT, Liu JK, Maharachchikumbura SSN, Ekanayaka AH, Tian Q, Phookamsak R (2018) Outline of Ascomycota: 2017. Fungal Diversity 88: 167–263. https://doi.org/10.1007/s13225-018-0394-8

Zhang M, Pang W, Wang J (2014) Effect of oxidative stress on hypocrellin A yield in submerged cultures of endophytic *Shiraia* sp. A8. Planta Med 80: P1N2. https://doi.org/10.1055/s-0034-1394593

Zhaxybayeva O, Gogarten JP (2002) Bootstrap, Bayesian probability and maximum likelihood mapping: exploring new tools for comparative genome analyses. BMC Genomics 3: 4. https://doi.org/10.1186/1471-2164-3-4

Zhao D, Liang ZQ (2005) Reviews of Studies on Isolation and Culture of *Shiraia bambusicola* Henn. Journal of Fungal Research 3: 53–57.

Zhu D, Wang JX, Zeng QG, Zhang ZB, Yan RM (2010) A novel endophytic huperzine A-producing fungus, *Shiraia* sp. Slf14, isolated from *Huperzia serrata*. Journal of Applied Microbiology 109: 1469–1478. https://doi.org/10.1111/j.1365-2672.2010.04777.x

MycoKeys 58: 27–45 (2019)
doi: 10.3897/mycokeys.58.36557
http://mycokeys.pensoft.net

RESEARCH ARTICLE

A peer-reviewed open-access journal
MycoKeys
Launched to accelerate biodiversity research

Microsatellite based genetic diversity of the widespread epiphytic lichen *Usnea subfloridana* (Parmeliaceae, Ascomycota) in Estonia: comparison of populations from the mainland and an island

Polina Degtjarenko[1,2], Inga Jüriado[2], Tiina Mandel[1,2], Tiiu Tõrra[1,2], Andres Saag[2], Christoph Scheidegger[1], Tiina Randlane[2]

1 *Biodiversity and Conservation Biology, Swiss Federal Research Institute WSL, Zürcherstrasse 111, 8903, Birmensdorf, Switzerland* **2** *Department of Botany, University of Tartu, Lai 40, 51005, Tartu, Estonia*

Corresponding author: *Polina Degtjarenko* (polina.degtjarenko@ut.ee)

Academic editor: *T. Lumbsch* | Received 27 May 2019 | Accepted 11 July 2019 | Published 30 August 2019

Citation: Degtjarenko P, Jüriado I, Mandel T, Tõrra T, Saag A, Scheidegger C, Randlane T (2019) Microsatellite based genetic diversity of the widespread epiphytic lichen *Usnea subfloridana* (Parmeliaceae, Ascomycota) in Estonia: comparison of populations from the mainland and an island. Title. MycoKeys 58: 27–45. https://doi.org/10.3897/mycokeys.58.36557

Abstract

Understanding the distribution of genetic patterns and structure is an essential target in population genetics and, thereby, important for conservation genetics. The main aim of our study was to investigate the population genetics of *Usnea subfloridana*, a widespread lichenised fungus, focusing on a comparison of genetic variation of its populations amongst three geographically remote and disconnected regions, in order to determine relationships amongst environmental data, variation in lichen secondary chemistry and microsatellite data in genotyped populations. In all, 928 *Usnea* thalli from 17 populations were genotyped using seven specific fungal microsatellite markers. Different measures of genetic diversity (allelic richness, private allelic richness, Nei's unbiased genetic diversity and clonal diversity) were calculated and compared between lichen populations. Our results revealed a low genetic differentiation of *U. subfloridana* populations amongst three distant areas in Estonia and also a high level of gene flow. The results support suggestion of the long-range vegetative dispersal of subpendulous *U. subfloridana* via symbiotic propagules (soralia, isidia or fragments of thalli). Our study has also provided evidence that environmental variables, including mean annual temperature and geographical longitude, shape the genetic structure of *U. subfloridana* populations in Estonia. Additionally, a weak but statistically significant correlation between lichen chemotypes and microsatellite allele distribution was found in genotyped specimens.

Keywords

Chemotypes, genetic diversity, environmental factors, lichenised fungi, microsatellites

Introduction

The disentangling processes which shape genetic patterns and structure of natural populations is of great importance in understanding basic questions concerning evolution, ecology and conservation biology of species. The distribution of genetic diversity, which is a significant part of overall biodiversity, could indicate patterns of gene flow, genetic drift and potential for local adaptation (Frankham et al. 2010). The vast majority of previous studies about microsatellite diversity of lichenised fungi have used threatened, regionally rare or narrowly distributed lichens (e.g. Nadyeina et al. 2014; Jones et al. 2015; Prieto et al. 2015). However, the genetic diversity of common taxa could also be of particular interest since common species could be similarly susceptible to genetic consequences of habitat fragmentation as rare species (Honnay and Jacquemyn 2007). To date, only a few investigations have studied the genetic diversity of common and widespread lichenised fungi and genetic differentiation of their populations using microsatellite markers (e.g. Mansournia et al. 2012; Degtjarenko et al. 2018).

The epiphytic fruticose lichen *Usnea subfloridana* Stirt. has a wide distribution across Eurasia, Macaronesia and North America (Nash et al. 2007; Randlane et al. 2009; Smith et al. 2009). This is one of the commonest *Usnea* species in Estonia (Northern Europe) being frequently found on Norway spruce (*Picea abies*), Scots pine (*Pinus sylvestris*) and Silver birch (*Betula pendula*), as well as other deciduous trees and lignum (Tõrra and Randlane 2007; Randlane et al. 2011). Recent microsatellite studies of *U. subfloridana* populations indicated that unconstrained gene flow and exchange of multilocus genotypes existed between two geographically remote regions (the maximum distance between the two regions was 184 km) within the mainland of Estonia or had occurred at least in the past (Degtjarenko et al. 2018). Moreover, the natural habitat characteristics, such as stand age and mean circumference of the host tree, did not reveal any significant influence on measures of genetic diversity of *U. subfloridana* populations (Degtjarenko et al. 2016, 2018). However, some negative impact caused by alkaline dust pollution has been recorded on the genetic variation of this species (Degtjarenko et al. 2016).

Microsatellites or simple sequence repeats (SSR) are highly variable DNA sequences of short tandem repeats of 1–6 bp with co-dominant inheritance and appear as widely used markers for studying genetic variation and structure of natural populations (Goldstein and Schlötterer 1999; Ellegren 2004). The microsatellites are highly polymorphic and species-specific markers, considered as a most promising tool for investigating genetic diversity of highly clonal and complex organisms such as lichens (Werth 2010). The microsatellites were usually assumed to be neutral markers, occurring mainly in non-coding DNA (Ellegren 2004). Recent studies, however, have questioned this assumption, since microsatellites are also found in coding regions (e.g. Gemayel et al. 2012; Gao et al. 2013), playing a role in species adaptation and phenotypic plasticity within and across generations (Vieira et al. 2016).

Lichens produce a great number of extracellular secondary metabolites; these are synthesised by the mycobiont, although the carbon which is necessary for these substances is provided by the photobiont and subsequently transported to the fungus (Elix and Stocker-Wörgötter 2008). The production of polyketides, the most studied class of secondary metabolites in lichens, is regulated by polyketide synthases (PKS), the genes for which have been found in clusters (Shen 2003). Secondary metabolites of lichen-forming fungi are considered to have a distinct function, such as protecting the thalli against herbivores, pathogens or UV-radiation (Molnár and Farkas 2010). The presence or absence of specific secondary substances or their replacements by another substance has played an important role in identification and classification of these organisms when correlated with morphological or geographical differences (Elix and Stocker-Wörgötter 2008). Hence, variation of secondary compounds in lichens is probably not selectively neutral (Werth 2010). In *U. subfloridana*, three chemotypes have been reported (Halonen et al. 1998, 1999) while, in Estonia, two of them are known: (i) with thamnolic acid and (ii) with squamatic acid as the main substance in the medulla (Tõrra and Randlane 2007).

In the present research, we studied the population genetics of *U. subfloridana*, a widespread lichenised fungus, concentrating on a comparison of genetic variation of populations amongst three geographically remote and disconnected (by sea) regions. The main aims of our research were: (i) to study the genetic differentiation of *U. subfloridana* populations, growing in the south-eastern and northern regions of mainland and on a western island in Estonia, Northern Europe; (ii) to compare the measures of genetic diversity of *U. subfloridana* populations amongst the three study areas; (iii) to find whether allele frequencies in studied populations correlate with environmental variables; and (iv) to check if there were correlations between lichen chemotypes and microsatellite allele distribution in genotyped data.

Material and methods

Study area

The study area is located in Northern Europe, in three geographically separate parts of Estonia: Lääne-Viru County, the northern region of mainland (hereafter N), Põlva County, the south-eastern region of mainland (hereafter SE) and Hiiumaa County, the second largest western island (hereafter W) of Estonia, located in the Baltic Sea (Fig. 1). According to climate norms from 1981 to 2010, N has a mean annual temperature of 5.7 °C, a mean annual precipitation of 587 mm, a mean wind speed of 3.9 m/s and a mean relative humidity of 80%, W has a mean annual temperature of 6.8 °C, a mean annual precipitation of 639 mm, a mean wind speed of 3.9 m/s and a mean relative humidity of 82% and SE has a mean annual temperature of 5.8 °C, a mean annual precipitation is 680 mm, a mean wind speed of 3.2 m/s and a

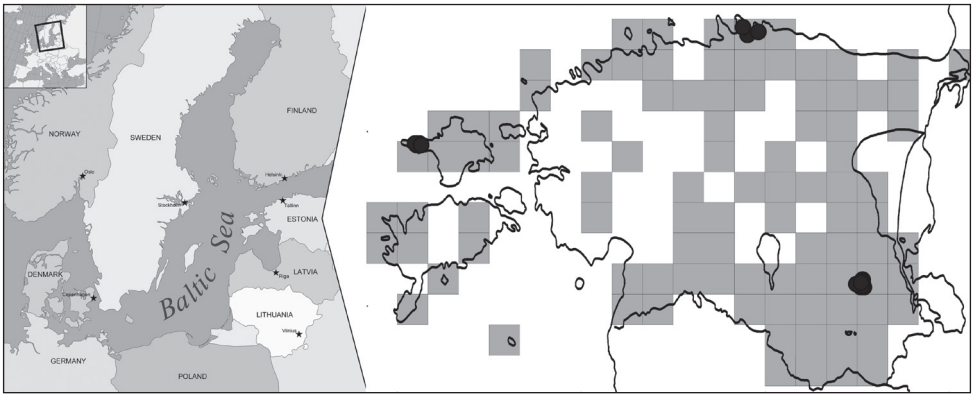

Figure 1. Distribution map of *Usnea subfloridana* in Estonia (light grey squares) and study populations (black circles) on Hiiumaa island in the western region (W), in the south-eastern region (SE) and in the northern region of Estonia; the map of Scandinavia was taken from free map resource http://d-maps.com/carte.php?num_car=5977&lang=en.

mean relative humidity of 80% (Estonian Weather Service 2019). The vegetation of Estonia belongs to the hemiboreal forest zone, lying in the transitional area, where the southern taiga forest subzone changes into the spruce-hardwood subzone (Ahti et al. 1968; Laasimer and Masing 1995). The study sites from both geographical regions were situated in *Pinus sylvestris*-dominated boreal forests, being classified as the *Oxalis-Vaccinium myrtillus*, the *Vaccinium myrtillus*, the *Calamagrostio-Pinetum* and the *Vaccinium vitis-idaea* forest site types. These forest types are also widely distributed in other Baltic states (Kairiūkštis 1966; Bušs 1997), in Fennoscandia (Dierßen 1996) and in northwest Russia (Fedorchuk et al. 2005).

Data collection

Fieldwork was carried out during the summer of 2011 (in SE), the autumn of 2014 (in N) and the autumn of 2016 (in W). The potential study sites for sampling were selected from forest survey maps using comparable forest characteristics (stand age and site type) from their forest survey (Forest Public Registry 2017). *Usnea subfloridana* populations, sampled from 17 study sites, three in N, eight in SE and six in W (Fig. 1; Table 1), were defined according to the boundaries of forest sites sharing the same values of forest survey data (forest site type, age of trees and proportion of trees in forest stand), according to the Forest Public Registry (2017). In each lichen population, an average of three *Usnea* thalli were collected from each Norway spruce tree, up to 6 m from the ground using a tree pruner. In total, 10–21 trees were surveyed and 30–66 thalli were randomly collected from each lichen population (Table 1). The tree circumference (BHC) was recorded for each sampled tree at breast height (1.3 m). The stand age was taken from the Forest Public Registry (2017).

Table 1. Characteristics of the studied *Usnea subfloridana* populations from the northern region (1–3), the southeastern region (4–11) and Hiiumaa island (12–17) of Estonia: sample size, geographical coordinates, tree variables, and measurements of genetic variation. Populations, the number of population; Specimens, the number of collected thalli per population; Trees, the number of host trees from which thalli were collected in each population; Latitude, latitudinal coordinates of the centre of forest site; Longitude, longitudinal coordinates of the centre of forest site; Age, the stand age (based on the oldest trees in the stands); BHC, mean circumference (cm) of the host tree per population (measured from each sampled tree at breast height 1.3 m); Squamatic acid, the number of collected thalli containing squamatic acid; Thamnolic acid, the number of collected thalli containing thamnolic acid; H, Nei's unbiased genetic diversity per population; A, standardized allelic richness per population; G, the number of multilocus genotypes per population; M, clonal diversity per population; P, private allelic richness per population.

Variables	Region	Northern (N)			Southeastern (SE)					
	Population	1	2	3	4	5	6	7	8	9
Sample size	Specimens	46	30	36	52	60	60	58	60	57
	Trees	11	10	11	21	21	21	21	21	21
Coordinates	Latitude N	59°33'9.1"	59°35'54.6"	59°34'31.1"	58°6'13.5"	58°6'28.2"	58°7'13.2"	58°7'23.8"	58°7'23.0"	58°8'51.8"
	Longitude E	25°48'4.1"	25°45'23.8"	25°55'47.7"	22°4'28.9"	22°2'50.4"	27°3'2.8"	26°59'6.0"	26°59'20.3"	27°3'16.2"
Tree variables	Age	97	146	131	164	164	99	92	162	94
	BHC	93	119	90	125	117	136	77	119	84
Chemotypes	Squamatic acid	23	18	16	28	39	35	34	27	33
	Thamnolic acid	23	12	21	27	21	25	24	33	24
Genetic variation	H	0.58	0.60	0.63	0.65	0.62	0.65	0.62	0.62	0.63
	A	5.33	4.86	5.26	5.94	5.10	5.71	5.61	5.28	5.92
	G	38	27	31	42	50	46	45	50	45
	M	0.83	0.90	0.86	0.81	0.83	0.77	0.78	0.83	0.79
	P	0.13	0.04	0	0.28	0	0.11	0.03	0	0.05
Variables	**Region**	**Southeastern (SE)**			**Hiiumaa (W)**					**Total**
	Population	**10**	**11**	**12**	**13**	**14**	**15**	**16**	**17**	**17**
Sample size	Specimens	55	50	60	59	59	62	58	66	928
	Trees	20	20	20	20	21	21	21	21	322
Coordinates	Latitude N	58°8'29.3"	58°7'54.7"	58°55'45.7"	58°55'17.3"	58°55'55.5"	58°55'36.3"	58°55'52.2"	58°55'19.5"	
	Longitude E	27°3'2.3"	27°2'28.3"	22°14'58.6"	22°14'39.3"	22°12'50.8"	22°12'07.4"	22°11'55.5"	22°15'10.6"	
Tree variables	Age	94	174	96	167	167	157	96	96	
	BHC	119	107	74	130	110	135	86	80	
Chemotypes	Squamatic acid	26	22	27	36	31	28	29	25	477
	Thamnolic acid	29	28	33	23	28	34	29	41	455
Genetic variation	H	0.61	0.65	0.64	0.66	0.65	0.67	0.67	0.66	
	A	5.38	5.57	5.07	5.32	5.63	5.38	5.41	5.59	
	G	48	43	41	37	39	39	53	51	
	M	0.87	0.86	0.68	0.63	0.66	0.63	0.91	0.77	
	P	0.14	0	0.02	0	0.11	0.02	0	0.15	

Chemical and molecular analyses

All collected *Usnea* thalli were air dried, cleaned to remove other lichen specimens and examined under a stereomicroscope. Thin layer chromatography (TLC) with solvent A (Orange et al. 2001) was used to confirm the identification of collected *Usnea* species. Then, 50 mg of each specimen was maintained in 1.5 ml microtubes at –20 °C until molecular analyses. The total genomic DNA was extracted using PowerPlant Pro DNA Isolation Kit and DNeasy Plant Mini Kit (MO BIO Laboratories, Inc., Qiagen, USA), according to the manufacturer's protocol. Seven fungal microsatellite loci (*Us02*, *Us03*, *Us04*, *Us05*, *Us06*, *Us08* and *Us09*) were amplified in two multiplex PCR using QIAGEN Multiplex PCR Kit, following the instructions described in Tõrra et al. (2014) and Degtjarenko et al. (2016). Fragment lengths of PCR products were determined on a 3730xl DNA Analyzer (Applied Biosystems) with LIZ-500 as the internal size standard. The alleles were sized and genotyped using GeneMapper Software ver 5 (Applied Biosystems).

Statistical analyses

The basic measurements of population genetics (the total number of alleles, mean number of alleles per locus, Nei's unbiased genetic diversity (H) and allelic richness (A)) for *U. subfloridana* populations were calculated in the Microsatellite Analyzer ver 2.65 (MSA) (Dieringer and Schlötterer 2003). The measures of A were standardised using the rarefaction procedure implemented in the software MSA (Dieringer and Schlötterer 2003). The allelic richness of private alleles (P) per population was calculated using software HP-Rare (Kalinowski 2005). The number of multilocus genotypes (G), the percentage of multilocus genotypes, i.e. clonal diversity or genotypic diversity (M; the proportion of different genotypes in the population, G/N) and total number of multilocus genotypes from all populations were calculated in the software R (R Core Team 2013), using the R script by Werth et al. (2006). One-way analysis (ANOVA, type III) in the TIBCO Statistica ver 13.3 (TIBCO Software Inc.) was used to compare the different measurements of genetic diversity (A, H, P and M) amongst the three regions, N, SE and W.

The number of shared multilocus genotypes between populations was calculated in the software ARLEQUIN ver 3.5 (Excoffier and Lischer 2010). Clone correction of the genotyped dataset was performed in the software R (R Core Team 2013) using the R package 'poppr' (Kamvar et al. 2014; 2015). Hierarchical analyses of molecular variance (AMOVA) with 1023 permutations to estimate genetic differentiation were performed using ARLEQUIN ver 3.5 (Excoffier and Lischer 2010). The first, second and third AMOVA were performed at the tree level; genotyped individuals (364 multilocus genotypes and 124 trees) from populations of W, genotyped individuals (112 multilocus genotypes and 32 trees) from populations of N and genotypes individuals (452 multilocus genotypes and 166 trees) from populations of SE were analysed separately

where each tree was treated as a distinct population. The fourth AMOVA was undertaken using all genotyped individuals (928 multilocus genotypes) and the fifth without identical multilocus genotypes or clone corrected dataset (403 multilocus genotypes). The rate of gene flow (Nm) across seven loci amongst 17 populations was estimated using GenAlex ver 6.5 (Peakall and Smouse 2012). Index of Association (Ia) was calculated to measure the extent of linkage equilibrium within a dataset by quantifying the amount of recombination amongst a set of sequences and observing association between alleles at different loci (Smith et al. 1993). The Ia was measured in the software R (R Core Team 2013) using the R package 'poppr' (Kamvar et al. 2014; 2015).

To assess the variation in data of *U. subfloridana* multilocus genotypes, the principal component analysis (PCA) was performed, implemented with the programme package Canoco 5.0 (Šmilauer and Lepš 2014). The data matrix of alleles in seven loci from 928 sample specimens was used. Variable 'Lichen substance' (squamatic or thamnolic acid) was used to group the samples. Subsequently, the redundancy analysis (RDA) (Šmilauer and Lepš 2014) was performed and nine explanatory variables were used to assess the correlation with accounted multilocus genotypes. The explanatory variables used in RDA were 'Lichen substance' and environmental variables as Latitude, Longitude, Stand Age, a mean BHC of sample trees per population, a mean annual temperature, a mean annual precipitation, a mean wind speed and a mean relative humidity for populations in the region.

To assess the significance of the associations between allele frequency in the populations and environmental variables, the second RDA was implemented in the same programme package. The data matrix of frequency of 62 alleles in 17 populations was used. The number of records of each allele in each population was counted and log-transformed for data analyses. The same environmental variables as in the first RDA were used as the explanatory variables. In both RDA models, the interactive forward selection procedure with randomisation tests was employed to select the most important environmental variables influencing variation in response data, retaining variables with an independent significant contribution at the $p < 0.05$ level. Subsequently, variation partitioning analysis (VPA) in the same programme was employed. The unique effects of statistically significant explanatory variables and the shared proportion of variation, explaining the distribution of multilocus genotypes (the first RDA) or allele frequency in populations (the second RDA), was calculated. The statistically significant contribution of variables was tested by the permutation test (Monte-Carlo permutation test, 4999 unrestricted permutations).

Results

In total, 62 alleles at seven microsatellite loci, all polymorphic (Table 1), in 928 specimens from 17 *U. subfloridana* populations were recorded. The minimum number of alleles was four in locus *Us04* and the maximum was 15 in locus *Us03* and, on average, 2.8–9.1 were detected per locus across 17 populations. The mean number of alleles per

population varied from 5.3 to 6.1 in populations on the western island in Estonia (W), from 5.3 to 6.2 in populations in the south-eastern region of mainland (SE) and from 4.9 to 5.4 in populations in the northern region of the mainland (N). There were 403 different multilocus genotypes across 928 genotyped specimens in 17 lichen populations. Allelic richness (A) varied from 4.86 to 5.94 across all lichen populations and Nei's unbiased genetic diversity (H) ranged from 0.58 to 0.67 (Table 1). Other detailed measurements of genetic diversity per population are given in Table 1. The mean gene flow (Nm) for all populations across seven loci was 7.29.

The results of ANOVA showed that Nei's unbiased genetic diversity (H) depended significantly on the region (F (2, 12) = 10.74, p = 0.001); H was higher in populations from W and lower in populations from N. The clonal diversity (M) also depended significantly on the region (F (2, 14) = 5.62, p = 0.02); M was higher in populations from N and lower in populations from W. The allelic richness (A; F (2, 14) = 2.83, p = 0.09) and private allelic richness (P; F (2, 14) = 0.18, p = 0.83 did not differ amongst the three regions (N, SE and W).

The analyses for checking shared haplotypes amongst populations in the software ARLEQUIN ver 3.5 indicated that all *Usnea* populations shared the identical multilocus genotypes with other populations, as well as amongst three regions, N, W and SE (Fig. 2; Suppl. material 1). The Index of Association (Ia) differs significantly from zero which means that *Usnea* multilocus genotypes are likely undergoing clonal reproduction in study populations (Kamvar et al. 2014; 2015). The first, second and third AMOVA results showed that most of the total genetic variation (96.1% in W, 97.5% in SE and 95.1% in N) was due to the differences amongst individuals within study tree and 0.5%, 0.3% and 0.7% of genetic variation (for W, SE and N, respectively) was found amongst populations (Table 2). The fourth AMOVA results (928 genotypes) revealed that most of the total genetic variation (97.7%) was due to the differences amongst individuals within studied *Usnea* populations; a low proportion (1.8%) of genetic variation was attributed to regional differences (Table 2). The results from the fifth AMOVA (clone corrected, 403 genotypes) showed that most of the total genetic variation (98.7%) was also due to differences amongst individuals within studied *Usnea* populations and 1.2% of genetic variation was found between the regions (Table 2).

In the PCA ordination of multilocus genotypes of *U. subfloridana*, the first ordination axis accounted for 34.5% and the second axis for 20.5% of variation in the sample data. The sampled specimens constituted a rather homogenous cluster in the PCA ordination plot and only a minor distinction, according to the presence of thamnolic or squamatic acid, was visible (Fig. 3). In the RDA analyses with nine explanatory variables, the model accounted for 5.7% of variation in the response data. According to the results of the interactive forward selection of explanatory variables, the variables 'Lichen substance' and 'Temperature' contributed significantly to the explanation of variation in the response data (Fig. 4). The other environmental variables did not make a significant contribution to the model and were left out during the interactive forward selection of variables ($p \geq 0.05$). The results of variation partitioning analysis (VPA) showed that two variables, 'Lichen substance' and 'Temperature', represent 5.5% of

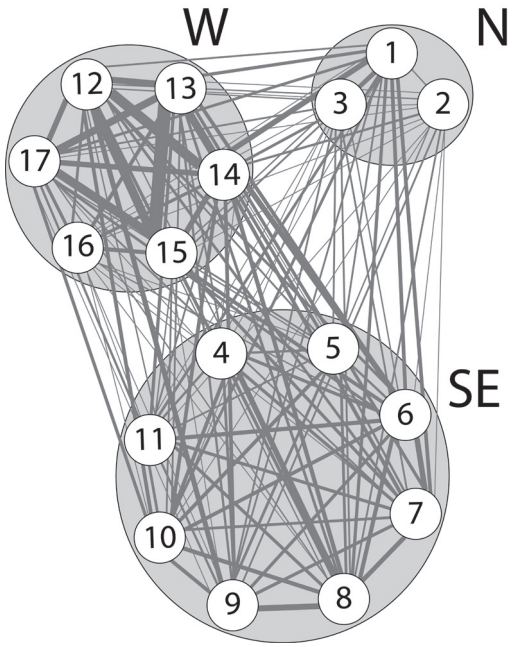

Figure 2. Total number of shared haplotypes between populations of *Usnea subfloridana* in the south-eastern (SE), the western (W) and northern (N) regions of Estonia; the thickness of lines reflects the number of shared haplotypes between populations.

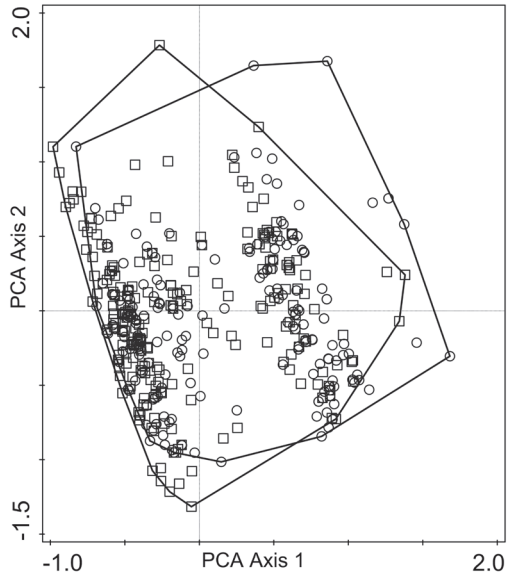

Figure 3. *Usnea subfloridana* multilocus genotypes in the principal component analysis (PCA) ordination plot of the first and second axes. Samples are grouped according to the presence of lichen substance: samples containing thamnolic (square) or squamatic acid (circle).

Table 2. Results of hierarchical analyses of molecular variance (AMOVA) for 17 populations of *Usnea subfloridana* according to seven microsatellite loci with 364 multilocus genotypes from populations on the western island in Estonia (W), with 452 multilocus genotypes from populations in the south-eastern region of the mainland (SE), with 112 multilocus genotypes from populations in the northern region of the mainland (N), with all multilocus genotypes (928 specimens) and clone corrected dataset (403 specimens). Values of P, in bold, represent a significant effect; d.f., the number of degrees of freedom.

Source of variation	d.f.	Sum of squares	Variance	Percentage %	P
I AMOVA (364 multilocus genotypes and 124 trees)					
Amongst regions (i.e. populations)	5	15.9	0.01	0.5%	**0.005**
Amongst populations within regions (i.e. amongst trees)	118	292.8	0.08	3.4%	**0.008**
Within populations (i.e. trees)	240	539.0	2.25	96.1%	**0.08**
Total	363	847.7	2.3		
II AMOVA (452 multilocus genotypes and 166 trees)					
Amongst regions (i.e. populations)	7	18.8	0.007	0.3%	**0.02**
Amongst populations within regions (i.e. amongst trees)	158	365.5	0.05	2.3%	**0.04**
Within populations (i.e. trees)	286	622.5	2.2	97.5%	0.1
Total	451	1006.9	2.2		
III AMOVA (112 multilocus genotypes and 32 trees)					
Amongst regions	2	6.04	0.02	0.7%	**0.02**
Amongst populations within regions	29	68.3	0.09	4.2%	**0.04**
Within populations	80	163.9	2.05	95.1%	0.13
Total	111	238.2	2.2		
IV AMOVA (928 genotypes)					
Amongst regions	2	28.1	0.04	1.8%	**<0.001**
Amongst populations within regions	14	40.7	0.01	0.5%	**0.001**
Within populations	911	2052.6	2.5	97.7%	**<0.001**
Total	927	2121.5	2.3		
V AMOVA (403 genotypes)					
Amongst regions	2	11.5	0.03	1.2%	**0.007**
Amongst populations within regions	14	33.6	0.002	0.03%	0.389
Within populations	386	906.6	2.3	98.7%	**<0.001**
Total	402	951.7	2.4		

the variation of *U. subfloridana* multilocus genotypes (adjusted variation), the former being 4.1% and the latter 1.3% of the total variation, while the co-effect of both variables was less than 0.1% ($p = 0.0005$).

The model of the second RDA with allele frequency data in studied populations accounted for 36.1% of variation in the response data. According to the results of the interactive forward selection of explanatory variables, the variables 'Temperature' and 'Longitude' contributed significantly to the explanation of variation in the response data (Fig. 5), the other explanatory variables not making a significant contribution to the model and were left out during the interactive forward selection of variables ($p \geq 0.05$). The results of variation partitioning analysis (VPA) showed that the two explanatory variables, 'Temperature' and 'Longitude', represent 27.0% of the variation of allele frequency data (adjusted variation), the former being 8.2% and the latter 7.6% of the total variation, while the co-effect of both variables was 11.2% ($p = 0.0005$). Alleles, occurring only (e.g. 326 and 346 (*Us05*), 201(*Us08*, coded as 8201)) or being more frequent (e.g. 322 and 330 (*Us05*), 195(*Us08*), 345 (*Us09*)) in populations of western Estonia with an average higher air temperature, are located in the positive side of the

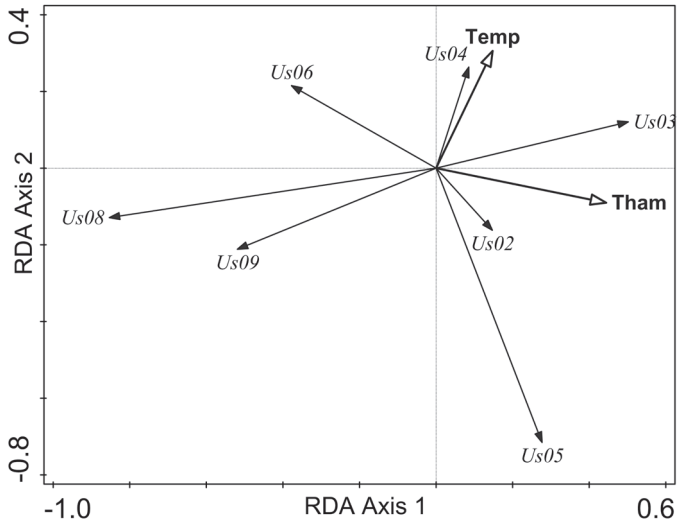

Figure 4. *Usnea subfloridana* multilocus genotypes (Us02, Us03, Us04, Us05, Us06, Us08, Us09) and explanatory variables mean annual air temperature ('Temp') and the presence of thamnolic acid ('Tham') in a lichen sample in the bi-plot of the redundancy analysis (RDA) of the first and second axes.

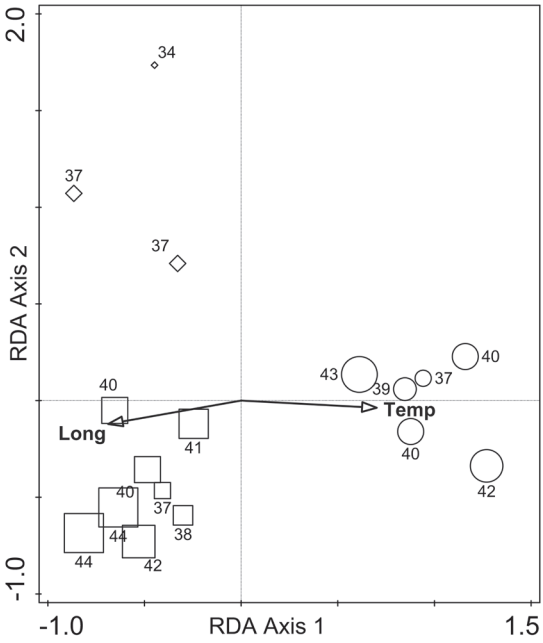

Figure 5. Sample populations of *Usnea subfloridana* and explanatory variables mean annual air temperature ('Temp') and geographical longitude of populations ('Long') in the bi-plot of the redundancy analysis (RDA) of the first and second axes. The shape of symbols indicates the geographical location of studied populations (square – south-eastern region of mainland, circle - western island and diamond – north-eastern region) and the size of symbols indicates the number of different alleles found in the studied populations.

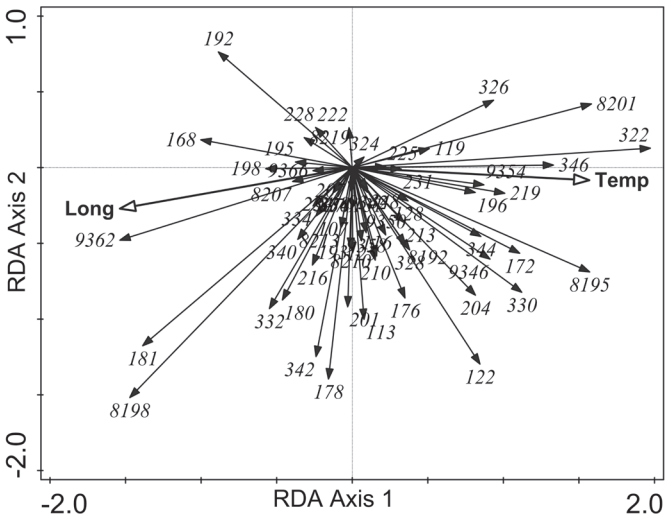

Figure 6. Alleles of *Usnea subfloridana* and explanatory variables mean annual air temperature ('Temp') and geographical longitude of populations ('Long') in the bi-plot of the redundancy analysis (RDA) of the first and second axes. Labels of alleles prefixed by '8' or '9' indicate that these alleles belong to loci *Us08* or *Us09,* respectively; for example, 8201 means that allele 201 is from *Us08*

ordination plot. The alleles, occurring only (e.g. 362 (*Us09*)) or being more frequent (e.g. 168 and 180 (*Us02*), 181 (*Us04*), 332 (*Us05*), 198 (*Us08*)) in populations of south-eastern Estonia, are located on the negative side of the ordination plot (Fig. 6).

Discussion

Lichen-forming fungi, reproducing purely sexually, are assumed to have a longer dispersal distance and exhibit less genetic structure than clonally reproducing species via isidia/soredia or fragments of thalli (Werth 2010; Singh et al. 2015; Alors et al. 2017). However, our study showed that *Usnea subfloridana,* which usually reproduces asexually by symbiotic propagules, exhibited a very long dispersal range and a negligible level of genetic differentiation in populations from three geographically remote areas, namely the south-eastern (SE) and northern (N) regions of the Estonian mainland and Hiiumaa (W), an island in the Baltic Sea (Fig. 1; Table 2). Small-scale AMOVA also exhibited similar results; a negligible level of genetic differentiation was found amongst populations in three study regions (Table 2). Using highly variable microsatellite markers, our study also showed high levels of gene flow (Nm = 7.29) or genetic similarity amongst all studied *U. subfloridana* populations. Moreover, our results demonstrated that *Usnea* population shared common identical multilocus genotypes amongst all studied populations and also amongst the three regions (Fig. 2; Suppl. material 1). Our previous study also recorded a very low genetic differentiation of *U. subfloridana* populations between two distant areas in Estonia, suggesting spatially unrestricted

dispersal of individuals and unconstrained gene flow in *U. subfloridana* populations (Degtjarenko et al. 2018). However, the genetic variation, attributed to regional differences, was slightly higher in the current study (1.8% and 1.2%; Table 2) than in the previous microsatellite study (0.5%) concerning *U. subfloridana* populations in Estonia (Degtjarenko et al. 2018). A possible explanation for this is that the maximum distance amongst the populations was longer (viz. the maximum distance was 295 km in the current and 184 km in the previous study) and, in addition, one region (W) with six populations was relatively isolated, i.e. an island. Similar levels of genetic differentiation at local scales have been indicated in previous studies; for example, for populations of *Lobaria pulmonaria* L., a lichen-forming fungus that also reproduces predominantly asexually (e.g. Walser 2004; Scheidegger et al. 2012). According to the test of Index of Association (Ia), our study found that multilocus genotypes of *U. subfloridana* in our localities most likely originated from asexual reproduction (Suppl. material 2). Therefore, it appears that the long-range dispersal of subpendulous *U. subfloridana* occurred via symbiotic propagules (soralia, isidia or fragments of thalli) that had to travel several kilometres over the sea.

The genetic diversity of natural populations is shaped by cumulative synergy of historical and present-day processes (Hewitt 2000; Frankham et al. 2010). Previous studies have shown that the climatic and habitat heterogeneity could be important in explaining the levels of genetic diversity of lichen populations; for example, annual precipitation had an effect on genetic diversity of *Lobaria pulmonaria* populations in the Iberian Peninsula (Otálora et al. 2015). Nadyeina et al. (2014) demonstrated that the microclimatic factors (air humidity and temperature) influenced the distribution of gene pools of *L. pulmonaria* in the Carpathian Mountains. The genetic diversity of *L. pindarensis* Räsänen was significantly influenced by altitude, revealing higher levels of genetic diversity at a high elevation in the Himalayas (Devkota et al. submitted). Belinchón et al. (2018) showed that *Nephroma parile* (Ach.) Ach. and *N. laevigatum* Ach. were also related to measured environmental and habitat variables, indicating micro-evolutionary responses to the environment. Our studies showed that genetic diversity (H) of *Usnea subfloridana* populations was higher on Hiiumaa island while clonal diversity (M) was higher in the northern region (N) of Estonia. This is contrary to our *a priori* assumption that relatively isolated populations, occurring on islands, will exhibit a lower genetic diversity and higher levels of clonal diversity. Moreover, the allele distribution in studied populations correlated with a mean annual temperature and geographical longitude (Fig. 5). These findings suggest (in our study – average annual temperature and longitude) are important factors for shaping the genetic structure and patterns of *U. subfloridana* populations in Estonia and indicating local adaptation to landscape conditions. The results of the redundancy analysis (RDA) indicated that, for example, several alleles occurring only or being more frequent are found in the populations of western Estonia with a higher average air temperature while other alleles, occurring only or being more frequent in populations of south-eastern Estonia, are related to a lower average air temperature (Fig. 6). Habitat quality measured as age of stand or host tree could be important in explaining the distribution of genetic

diversity of lichen populations (Jüriado et al. 2011; Otálora et al. 2011; Scheidegger et al. 2012). However, RDA showed that the age of forest stands and circumference of host trees did not have a significant effect on the distribution of allele frequencies in the studied populations. This also accords with our earlier observations, which showed that stand age or tree circumference were not of great importance in explaining the genetic patterns of *U. subfloridana* populations (Degtjarenko et al. 2016, 2018). Overall, our results reveal that, despite extensive gene flow and low genetic differentiation amongst the distant areas, geographical longitude and temperature heterogeneity might promote the current levels of genetic diversity of *U. subfloridana* populations amongst these three remote regions in Estonia.

Recent studies highlighted that microsatellites could be found in coding regions and be linked with adaptation and phenotypic consequences (e.g. Gemayel et al. 2012; Gao et al. 2013). In our study, for the first time any probable correlations between the chemotypes of a lichen-forming fungus, *U. subfloridana* and its microsatellite allele distribution in genotyped data were checked. Both chemotypes of *U. subfloridana* are common in Estonia (Tõrra and Randlane 2007) and nearly evenly represented in study regions (Table 1). The results of this study showed that only a minute difference, according to the presence of thamnolic or squamatic acid, was visible (Fig. 3) in sampled specimens, representing a rather homogenous cluster in the PCA ordination plot (Fig. 3). Recently, Lagostina et al. (2018) showed that chemotypes were not correlated with any of the genetic clusters of the two morphotypes, *U. antarctica* Du Rietz and *U. aurantiacoatra* (Jacq.) Bory, in the study delimiting species within the genus *Usnea* subgenus *Neuropogon*. However, the chemical variation across these species was not randomly distributed between the two morphotypes nor amongst the genetic clusters (Lagostina et al. 2018). The presence of particular secondary compounds is also known to be specific to a certain habitat or ecoregion and to respond to the environmental gradients (e.g. Nash and Zavada 1977; Culberson et al. 1977; Zhou et al. 2006). We speculate that the correlation between particular microsatellite alleles and secondary metabolite could be relevant to the adaptation of populations to a certain geographical region and contribute thus to the minute isolation by geographical distance.

Conclusion

We studied the population genetics of *U. subfloridana*, a widespread lichenised fungus, concentrating on a comparison of genetic variation of populations amongst three geographically remote and disconnected (by sea) regions in Estonia. We recorded a very low genetic differentiation of *U. subfloridana* populations amongst three distant areas, suggesting spatially unrestricted dispersal of individuals and unconstrained gene flow in *U. subfloridana* populations. Furthermore, geographical longitude and the mean annual temperature might play an important role in forming genetic variation in *U. subfloridana* populations in Estonia. This work contributes to the existing knowledge of population genetics of highly clonal and complex organisms, such as lichens.

Acknowledgements

This research was supported by the Estonian Research Council (grant PUT1017 to TR, grant MOBTP66 to IJ and grant IUT20-30) and by a fellowship to TT (Sciex project 10.005). We are also grateful to the Genetic Diversity Centre (ETH Zurich, Switzerland) for technical assistance, to Liis Marmor for help during fieldwork, to Ants Kaasik (University of Tartu, Estonia) for advice in the statistical analyses, to Rasmus Puusepp (University of Tartu, Estonia) and Carolina Cornejo (WSL, Switzerland) for help with laboratory work, to Tuuli Reisberg and Lauri Saag (University of Tartu, Estonia) for support with microsatellite genotyping, to Kristiina Kübarsepp for help with TLC, to Prof. Mark Seaward (University of Bradford, UK) for linguistic support and to Silke Werth (LMU München, Germany) for helpful discussions of this paper.

References

Ahti T, Hämet-Ahti L, Jalas J (1968) Vegetation zones and their sections in northwestern Europe. Annales Botanici Fennici: 169–211.

Alors D, Dal Grande F, Cubas P, Crespo A, Schmitt I, Molina MC, Divakar PK (2017) Panmixia and dispersal from the Mediterranean Basin to Macaronesian Islands of a macrolichen species. Scientific Reports 7: 40879. https://doi.org/10.1038/srep40879

Belinchón R, Ellis CJ, Yahr R (2018) Climate-woodland effects on population genetics for two congeneric lichens with contrasting reproductive strategies. FEMS Microbiology Ecology 94: fiy159. https://doi.org/10.1093/femsec/fiy159

Bušs K (1997) Forest ecosystem classification in Latvia. Proceedings of the Latvian Academy of Sciences 51: 204–218.

Culberson WL, Culberson CF, Johnson A (1977) Correlations between secondary-product chemistry and ecogeography in the *Ramalina siliquosa* group (lichens). Plant Systematics and Evolution 127: 191–200. https://doi.org/10.1007/BF00984149

Degtjarenko P, Marmor L, Tõrra T, Lerch M, Saag A, Randlane T, Scheidegger C (2016) Impact of alkaline dust pollution on genetic variation of *Usnea subfloridana* populations. Fungal Biology 120: 1165–1174. https://doi.org/10.1016/j.funbio.2016.05.010

Degtjarenko P, Tõrra T, Mandel T, Marmor L, Saag A, Scheidegger C, Randlane T (2018) Unconstrained gene flow between populations of a widespread epiphytic lichen *Usnea subfloridana* (Parmeliaceae, Ascomycota) in Estonia. Fungal Biology 122: 731–737. https://doi.org/10.1016/j.funbio.2018.03.013

Dieringer D, Schlötterer C (2003) Microsatellite analyser (MSA): a platform independent analysis tool for large microsatellite data sets. Molecular Ecology Notes 3: 167–169. https://doi.org/10.1046/j.1471-8286.2003.00351.x

Dierßen K (1996) Vegetation Nordeuropas. Ulmer, 1–838.

Elix JA, Stocker-Wörgötter E (2008). Biochemistry and secondary metabolites. In: Nash TH (Ed.) Lichen biology (2nd edn). Cambridge University Press, Cambridge, 106–135. https://doi.org/10.1017/CBO9780511790478.008

Ellegren H (2004) Microsatellites: simple sequences with complex evolution. Nature Reviews Genetics 5: 435–445. https://doi.org/10.1038/nrg1348

Estonian Weather Service (2019) Estonian Weather online Service. http://www.ilmateenistus.ee/?lang=en [Accessed 16 May 2019]

Excoffier L, Lischer HEL (2010) Arlequin suite ver 3.5: A new series of programs to perform population genetics analyses under Linux and Windows. Molecular Ecology Resources 10: 564–567. https://doi.org/10.1111/j.1755-0998.2010.02847.x

Fedorchuk VN, Neshatayev VY, Kuznetsova ML (2005) Forest Ecosystems of the North-Western Regions of Russia: Typology, Dynamics, Forest Management Features. Forestry Scientific Research Institute, 382 pp.

Forest Public Registry (2017) Forestry Public Registry Web Service. http://register.metsad.ee/avalik [Accessed 14 August 2017]

Frankham R, Ballou JD, Briscoe DA (2010) Introduction to Conservation Genetics. Cambridge University Press, 642 pp. https://doi.org/10.1017/CBO9780511809002

Gao C, Ren X, Mason AS, Li J, Wang W, Xiao M, Fu D (2013) Revisiting an important component of plant genomes: microsatellites. Functional Plant Biology 40: 645–645. https://doi.org/10.1071/FP12325

Gemayel R, Cho J, Boeynaems S, Verstrepen KJ (2012) Beyond Junk-Variable Tandem repeats as facilitators of rapid evolution of regulatory and coding sequences. Genes 3: 461–480. https://doi.org/10.3390/genes3030461

Goldstein DB, Schlötterer C (1999) Microsatellites: Evolution and applications. Oxford University Press, 368 pp.

Halonen P, Clerc P, Goward T, Brodo IM, Wulff K (1998) Synopsis of the genus *Usnea* (lichenized Ascomycetes) in British Columbia, Canada. Bryologist 101: 36–60. https://doi.org/10.2307/3244073

Halonen P, Myllys L, Ahti T, Petrova OV (1999) The lichen genus *Usnea* in East Fennoscandia. III. The shrubby species. Annales Botanici Fennici 36: 235–256.

Hewitt GM (2000) The genetic legacy of quaternary ice ages. Nature 405: 907–913. https://doi.org/10.1038/35016000

Honnay O, Jacquemyn H (2007) Susceptibility of common and rare plant species to the genetic consequences of habitat fragmentation. Conservation Biology 21: 823–831. https://doi.org/10.1111/j.1523-1739.2006.00646.x

Jones TC, Hogg ID, Wilkins RJ, Green TGA (2015) Microsatellite analyses of the Antarctic endemic lichen *Buellia frigida* Darb. (Physciaceae) suggest limited dispersal and the presence of glacial refugia in the Ross Sea region. Polar Biology 38: 941–949. https://doi.org/10.1007/s00300-015-1652-9

Jüriado I, Liira J, Csencsics D, Widmer I, Adolf C, Kohv K, Scheidegger C (2011) Dispersal ecology of the endangered woodland lichen *Lobaria pulmonaria* in managed hemiboreal forest landscape. Biodiversity and Conservation 20: 1803–1819. https://doi.org/10.1007/s10531-011-0062-8

Kairiūkštis LA (1966) Forests of the Lithuanian S.S.R. In: Žhukov AB (Ed.) Forests of the SSSR, Vol. 2 – The subzone of southern taiga and mixed forests. Nauka, Moscow, 93–130.

Kalinowski ST (2005) HP-Rare: a computer program for performing rarefaction on measures of allelic diversity. Molecular Ecology Notes 5: 187–189. https://doi.org/10.1111/j.1471-8286.2004.00845.x

Kamvar ZN, Tabima JF, Grünwald NJ. (2014) Poppr: an R package for genetic analysis of populations with clonal, partially clonal, and/or sexual reproduction. Peer J 2:e281. https://doi.org/10.7717/peerj.281

Kamvar ZN, Brooks JC, Grünwald NJ (2015) Novel R tools for analysis of genome-wide population genetic data with emphasis on clonality. Frontiers of Genetics 6: 208. https://doi.org/10.3389/fgene.2015.00208

Laasimer L, Masing V (1995) Flora and plant cover. In: Raukas A (Ed.) Estonian nature. Valgus and Eesti entsüklopeediakirjastus, Tallinn, 364–401.

Lagostina E, Dal Grande F, Andreev M, Printzen C (2018) The use of microsatellite markers for species delimitation in Antarctic *Usnea* subgenus *Neuropogon*. Mycologia 110: 1047–1057. https://doi.org/10.1080/00275514.2018.1512304

Mansournia MR, Wu B, Matsushita N, Hogetsu T (2012) Genotypic analysis of the foliose lichen *Parmotrema tinctorum* using microsatellite markers: association of mycobiont and photobiont, and their reproductive modes. Lichenologist 44: 419–440. https://doi.org/10.1017/S0024282911000909

Molnár K, Farkas E (2010) Current results on biological activities of lichen secondary metabolites. A review. Zeitschrift für Naturforschung C 65: 3–4. https://doi.org/10.1515/znc-2010-3-401

Nadyeina O, Dymytrova L, Naumovych A, Postoyalkin S, Werth S, Cheenacharoen S, Scheidegger C (2014) Microclimatic differentiation of gene pools in the *Lobaria pulmonaria* symbiosis in a primeval forest landscape. Molecular Ecology 23: 5164–5178. https://doi.org/10.1111/mec.12928

Nash TH, Ryan BD, Gries C, Bungartz F (2007) Lichen Flora of the Greater Sonoran Desert Region, vol. 3. Arizona State University Lichen Herbarium, 567 pp.

Nash TH, Zavada M (1977) Population studies among Sonoran desert species of *Parmelia* subg. *Xanthoparmelia* (Parmeliaceae). American Journal of Botany 64: 664–669. https://doi.org/10.2307/2441718

Orange A, James PW, White FJ (2001) Microchemical methods for the identification of lichens. British Lichen Society, 101 pp.

Otálora MG, Martinez I, Belinchon R, Widmer I, Aragon G, Escudero A, Scheidegger C (2011) Remnants fragments preserve genetic diversity of the old forest lichen *Lobaria pulmonaria* in a fragmented Mediterranean mountain forest. Biodiversity and Conservation 20: 1239–1254. https://doi.org/10.1007/s10531-011-0025-0

Otálora MG, Belinchón R, Prieto M, Aragón G, Izquierdo P, Martínez I (2015) The threatened epiphytic lichen *Lobaria pulmonaria* in the Iberian Peninsula: Genetic diversity and structure across a latitudinal gradient. Fungal Biology 119: 802–811. https://doi.org/10.1016/j.funbio.2015.05.004

Peakall R, Smouse PE (2012) GenAlEx 6.5: genetic analysis in Excel. Population genetic software for teaching and research – an update. Bioinformatics 28: 2537–2539. https://doi.org/10.1093/bioinformatics/bts460

Prieto M, Romera L, Merinero S, Aragon G, Martínez I (2015) Development and characterization of fungal specific microsatellite markers in the lichen *Lobarina scrobiculata* (Lobariaceae, Ascomycota). Lichenologist 47: 183–186. https://doi.org/10.1017/S0024282915000109

R Core Team (2013) R: A language and environment for statistical computing. R Foundation for Statistical Computing, 201 pp.

Randlane T, Tõrra T, Saag A, Saag L (2009) Key to European *Usnea* species. Bibliotheca Lichenologica 100: 433–478.

Randlane T, Saag A, Martin L, Timdal E, Nimis PL (2011) Epiphytic Macrolichens of Estonia. University of Tartu, 326 pp.

Scheidegger C, Bilovitz P, Werth S, Widmer I, Mayrhofer H (2012) Hitchhiking with forests: population genetics of the epiphytic lichen *Lobaria pulmonaria* in primeval and managed forests in southeastern Europe. Ecology and Evolution 2: 2223–2240. https://doi.org/10.1002/ece3.341

Shen B (2003) Polyketide biosynthesis beyond the type I, II and III polyketide synthase paradigms. Current Opinion in Chemical Biology 7: 285–295. https://doi.org/10.1016/S1367-5931(03)00020-6

Singh G, Dal Grande F, Werth S, Scheidegger C (2015) Long-term consequences of disturbances on reproductive strategies of the rare epiphytic lichen *Lobaria pulmonaria*: clonality a gift and a curse. FEMS Microbiology Ecology 91: 1–11. https://doi.org/10.1093/femsec/fiu009

Smith CW, Aptroot A, Coppins BJ, Fletcher A, Gilbert OL, James PW, Wolseley PA (2009) The Lichens of Great Britain and Ireland. British Lichen Society, 1046 pp.

Smith JM, Smith NH, O'Rourke M, Spratt BG (1993) How clonal are bacteria? Proceedings of the National Academy of Sciences of the United States of America 90: 4384–4388. https://doi.org/10.1073/pnas.90.10.4384

Šmilauer P, Lepš J (2014) Multivariate analysis of ecological data using Canoco 5. Cambridge University Press, 1–376. https://doi.org/10.1017/CBO9781139627061

Tõrra T, Cornejo C, Cheenacharoen S, Dal Grande F, Marmor L, Scheidegger C (2014) Characterization of Fungus-Specific Microsatellite Markers in the Lichen Fungus *Usnea subfloridana* (Parmeliaceae). Applications in Plant Sciences 2: apps.1400034. https://doi.org/10.3732/apps.1400034

Tõrra T, Randlane T (2007) The lichen genus *Usnea* (lichenized Ascomycetes, *Parmeliaceae*) in Estonia with a key to the species in the Baltic countries. Lichenologist 39: 415–438. https://doi.org/10.1017/S0024282907007220

Vieira MLC, Santini L, Diniz AL, Munhoz CF (2016). Microsatellite markers: what they mean and why they are so useful. Genetics and Molecular Biology 39: 312–328. https://doi.org/10.1590/1678-4685-GMB-2016-0027

Walser JC (2004) Molecular evidence for limited dispersal of vegetative propagules in the epiphytic lichen *Lobaria pulmonaria*. American Journal of Botany 91: 1273–1276. https://doi.org/10.3732/ajb.91.8.1273

Werth S, Wagner HH, Holderegger R, Kalwij JM, Scheidegger C (2006) Effect of disturbances on the genetic diversity of an old-growth forest associated lichen. Molecular Ecology 15: 911–921. https://doi.org/10.1111/j.1365-294X.2006.02838.x

Werth S (2010) Population genetics of lichen-forming fungi – a review. Lichenologist 42: 499–519. https://doi.org/10.1017/S0024282910000125

Zhou OM, Guo SY, Huang MR, Wei JC (2006) A study of the genetic variability of *Rhizoplaca chrysoleuca* using DNA sequences and secondary metabolic substances. Mycologia 98: 57–67. https://doi.org/10.1080/15572536.2006.11832713

Supplementary material 1

Authors: Polina Degtjarenko, Inga Jüriado, Tiina Mandel, Tiiu Tõrra, Andres Saag, Christoph Scheidegger, Tiina Randlane

Link: https://doi.org/10.3897/mycokeys.58.36557.suppl1

Supplementary material 2

Authors: Polina Degtjarenko, Inga Jüriado, Tiina Mandel, Tiiu Tõrra, Andres Saag, Christoph Scheidegger, Tiina Randlane

Link: https://doi.org/10.3897/mycokeys.58.36557.suppl2

MycoKeys 58: 47–68 (2019)
doi: 10.3897/mycokeys.58.35764
http://mycokeys.pensoft.net

RESEARCH ARTICLE

A peer-reviewed open-access journal
MycoKeys
Launched to accelerate biodiversity research

Phylogeny and species delimitations in the entomopathogenic genus *Beauveria* (Hypocreales, Ascomycota), including the description of *B. peruviensis* sp. nov.

Danilo E. Bustamante[1,2], Manuel Oliva[1], Santos Leiva[1], Jani E. Mendoza[1,2], Leidy Bobadilla[1], Geysen Angulo[1], Martha S. Calderon[1,2]

1 *Instituto de Investigación para el Desarrollo Sustentable de Ceja de Selva (INDES-CES), Universidad Nacional Toribio Rodríguez de Mendoza, Chachapoyas, Amazonas, Peru* **2** *Laboratorio de Biología Molecular, Universidad Nacional Toribio Rodríguez de Mendoza, Chachapoyas, Amazonas, Peru*

Corresponding author: *Danilo E. Bustamante* (danilo.bustamante@untrm.edu.pe); *Martha S. Calderon* (martha.calderon@untrm.edu.pe)

Academic editor: *P. Chaverri* | Received 25 April 2019 | Accepted 28 August 2019 | Published 9 September 2019

Citation: Bustamante DE, Oliva M, Leiva S, Mendoza JE, Bobadilla L, Angulo G, Calderon MS (2019) Phylogeny and species delimitations in the entomopathogenic genus *Beauveria* (Hypocreales, Ascomycota), including the description of *B. peruviensis* sp. nov. MycoKeys 58: 47–68. https://doi.org/10.3897/mycokeys.58.35764

Abstract

The genus *Beauveria* is considered a cosmopolitan anamorphic and teleomorphic genus of soilborne necrotrophic arthropod-pathogenic fungi that includes ecologically and economically important species. Species identification in *Beauveria* is difficult because of its structural simplicity and the lack of distinctive phenotypic variation. Therefore, the use of multi-locus sequence data is essential to establish robust species boundaries in addition to DNA-based species delimitation methods using genetic distance, coalescent, and genealogical concordance approaches (polyphasic approaches). In this regard, our study used multilocus phylogeny and five DNA-based methods to delimit species in *Beauveria* using three molecular makers. These polyphasic analyses allowed for the delimitation of 20–28 species in *Beauveria*, confirming cryptic diversity in five species (i.e. *B. amorpha*, *B. bassiana*, *B. diapheromeriphila*, and *B. pseudobassiana*) and supporting the description of *B. peruviensis* as a new taxon from northeastern Peru. The other five species were not evaluated as they did not have enough data (i.e. *B. araneola*, *B. gryllotalpidicola*, *B. loeiensis*, *B. medogensis*, and *B. rudraprayagi*). Our results demonstrate that the congruence among different methods in a polyphasic approach (e.g. genetic distance and coalescence methods) is more likely to show reliably supported species boundaries. Among the methods applied in this study, genetic distance, coalescent approaches, and multilocus phylogeny are crucial when establishing species boundaries in *Beauveria*.

Keywords
Beauveria, fungal diversity, multi-locus phylogeny, Peru, polyphasic approaches, species delimitation

Introduction

Around 1800, a silkworm disease called "calcine", "real del segno" or "muscardine" was causing great trouble in Italy and France (Redaelli and Visocchi 1940). Experiments developed by Agostino Bassi in Mariago, Italy showed that a parasitic fungus produced this disease (Redaelli and Visocchi 1940). Balsamo (1835) confirmed this discovery and concluded that the incrustation and white efflorescence, which covered the body of a dead silkworm, were a fungus of the genus *Botrytis*. He first named this species *Botrytis paradoxa* Balsamo and later *Botrytis bassiana* Balsamo (Balsamo 1835). Then, this species was transferred to its own genus and *Beauveria* Vuillemin was established on the basis of *B. bassiana* Vuillemin as the type species (Vuillemin 1912).

The genus *Beauveria* is considered a cosmopolitan genus of soilborne necrotrophic arthropod-pathogenic fungi that includes ecologically and economically important species (Rehner et al. 2011, Kepler et al. 2017, Chen et al. 2018). Morphologically, *Beauveria* genus have been characterized asexually by having conidiogenous cells arising from short, often one-celled, more or less swollen stalk cells, often in dense clusters, or scattered or in whorls from undifferentiated hyphae; they consist of a globose to fusiform basal part, and a geniculate, denticulate rachis. Conidia one-celled, hyaline, smooth, thin-walled, globose to ellipsoidal (de Hoog 1972). The sexual morphs form stromata solitary, paired or gregarious, unbranched, fleshy texture, fertile area apical, cylindrical to clavate, yellowish to orange; perithecia partially immersed, in longitudinal section oval to ovoid; and asci hyaline with cylindrical and filiform ascospores (Kepler et al. 2017).

Based on the end of dual nomenclature for different morphs of the same fungus in 2011 (McNeill et al. 2012), Kepler et al. (2017) phylogenetically established the genetic boundaries in *Cordycipitaceae* regardless of life-stage or the associated morphological differences. One of the most significant changes was the recognition of *Beauveria* as a genus separate from *Cordyceps*. Although direct links between species of *Beauveria* and cordyceps-like sexual morphs have been demonstrated from molecular data and culture-based experiments (Shimazu et al. 1988, Li et al. 2001, Huang et al. 2002, Shrestha et al. 2014), their respective type species are not congeneric (Kepler et al. 2017). Thereby, the clade composed of *Beauveria* currently includes the traditional species known from asexual morphs, as well as several taxa previously described for sexual morphs in *Cordyceps* (Sanjuan et al. 2014, Kepler et al. 2017).

Initially, *Beauveria* was delimitated based on diagnostic features, and three species were recognized, i.e., *B. bassiana*, *B. brongniartii* and *B. alba* (Limber) Saccas (de Hoog, 1972). New additions were included by de Hoog and Rao (1975), Samson and Evans (1982), Bissett and Widden (1986) and Rehner et al. (2006). Molecular analyses confirmed the monophyly and placement of seven species of *Beauveria* within Cordycipitaceae (Rehner and Buckley 2005, Sung et al. 2007). More recent molecular studies based on multilocus phylogenetic analysis that included the *Bloc* nuclear intergenic region, internal

transcribed spacer (ITS), translation elongation factor-1α (*TEF*), and RNA polymerase II largest subunit (*RPB*1) and second largest subunit (*RPB*2) demonstrated that *Beauveria* is composed of 26 species (Rehner et al. 2011, Sanjuan et al. 2014, Kepler et al. 2017, Chen et al. 2018). These phylogenetic studies also revealed that the most commonly reported species, namely, *B. bassiana* and *B. brongniartii*, encompass cryptic lineages with worldwide distributions (Rehner et al. 2006, 2011, Ghikas et al. 2010). Although morphologically distinctive as a genus, species identification in *Beauveria*, especially in the conidiogenic state, is difficult because of its structural simplicity and lack of distinctive phenotypic variation. Thus, numerous registered mycoinsecticide formulations based on *B. bassiana* and *B. brongniartii* that are extensively used for the control of insect pests worldwide (Faria and Wraight 2007) are not likely based on these species (Rehner et al. 2006).

In the Amazonian region, a total of five species have been reported (Rehner et al. 2011, Sanjuan et al. 2014). Two of these species *B. acridophila* (T. Sanjuan & Franco-Mol.) T. Sanjuan, B. Shrestha, Kepler & Spatafora and *B. diapheromeriphila* (T. Sanjuan & S. Restrepo) T. Sanjuan, B. Shrestha, Kepler & Spatafora, and a lectotype, namely, *B. locustiphila* (Henn.) B. Shrestha, Kepler & Spatafora were recently described on the basis of molecular data and their sexual stages were characterized (Sanjuan et al. 2014). Additionally, two species of *Beauveria* were reported from Peru: *B. amorpha* Samson & Evans and *B. bassiana*, but only the former has been confirmed by molecular analysis while the latter is extensively used in coffee rust programs to control the expansion of the coffee borer (Rehner et al. 2011).

Given the problems with species delimitation in fungi using morphology, molecular data are becoming the standard for delimiting species and testing their traditional boundaries (Rehner et al. 2011). The recognition of distinct clades in gene trees as species is likely to be misleading in understanding the evolutionary history of taxa (Lu et al. 2016). Therefore, the use of multi-locus sequence data is essential to establish robust species boundaries (Lumbsch and Leavitt 2011). Most researchers, however, did not carefully examine the species boundaries but simply recognized distinct clades in single-gene trees as separate species (Stewart et al. 2014). Estimating the species tree and species delimitation using genetic distance (e.g. automated barcode gap discovery algorithm, ABGD; and statistical parsimony, SPN), coalescent (e.g. generalized mixed Yule coalescent, GMYC; and Bayesian phylogenetics and phylogeography, BPP), and genealogical concordance (genealogical concordance phylogenetic species recognition, GCPSR) methods have proven very useful and have been used for a range of animal and plant taxa (Liu et al. 2016). These methods have otherwise not been used much in fungi, especially in studies of pathogenic fungi (Millanes et al. 2014, Liu et al. 2015). Therefore, the use of several methodologies and data sets to delimit species is recommended, and subsequently, the achievement of congruent results across the methods is likely to prove most useful for framing reliably supported species boundaries (Carstens et al. 2013).

In this study, we analyzed species of the newly circumscribed genus *Beauveria*, including an unreported species isolated from coffee farms in northeastern Peru, based on morphological observations, phylogenetic inferences, and DNA-species delimitation meth-

ods. Three nuclear molecular markers (*Bloc*, *rpb*1, and *tef*1) were used to examine their phylogenetic relationships and to assess species boundaries within the genus *Beauveria*.

Materials and methods

Collection of specimens and isolation

Fungal strains were isolated from infected coffee borers (*Hypothenemus hampei*) obtained from infected coffee berries according to Gerónimo-Torres et al. (2016). They were collected during July and August 2017 from three districts in the province of Rodriguez de Mendoza, Amazonas, Peru (Fig. 1). Briefly, infected coffee berries were preserved at 5 °C until coffee borers were recovered from them. The coffee borers with signs of fungal infection were cleaned superficially in 0.5% sodium hypochlorite solution and rinsed with sterile distilled water. Then, insects were placed in a humid chamber (90% RH and 25 °C) for 8 days to allow the growth of the entomopathogenic fungus. Once visible mycelia appeared on the borers under observations with a stereo microscope (Nikon SMZ18, Tokyo, Japan), these were transferred to a Petri-dish containing potato dextrose agar (PDA; Merck, Darmstadt, Germany).

Identification of isolates

Fifty-five fungal strains were incubated as monosporic cultures on PDA at 25 °C for 15 days. Morphological characterization of the fungus was performed as described by Rehner and Buckley (2005). Microscope observations were made from fungal mycelia and other structures stained with methylene blue (0.1–0.5%). Photomicrographs were taken under an inverted microscope (IX83; Olympus, Tokyo, Japan) with an integrated camera (Nikon D810, Tokyo, Japan). Fungal strains were deposited as semisolid and dry material in the herbarium of Toribio Rodriguez de Mendoza National University (UT), Peru.

Molecular phylogenetic analyses

Genomic DNA was extracted from semisolid PDA cultures using the NucleoSpin Plant II Kit (Macherey-Nagel, Düren, Germany), following the manufacturer's instructions. Three genes were sequenced, i.e., *Bloc*, *rpb1*, and *tef1*. Each gene was amplified using polymerase chain reaction (PCR) with MasterMix (Promega, Wisconsin, USA) in the following reaction mixture: 10 ng of DNA and 0.25–0.5 pmol of forward and reverse primers for a total volume of 10 µl. The PCR protocols and primer combinations for *Bloc* (B5.1F, B5.4F, B3.1R, B3.3R), *rpb1*(RPB1A, RPB1A_VH6R, RPB1B_VH6Fa, RPB1B_G2R), and *tef1* (983F, 1567RintB) followed Rehner et al. (2011). The se-

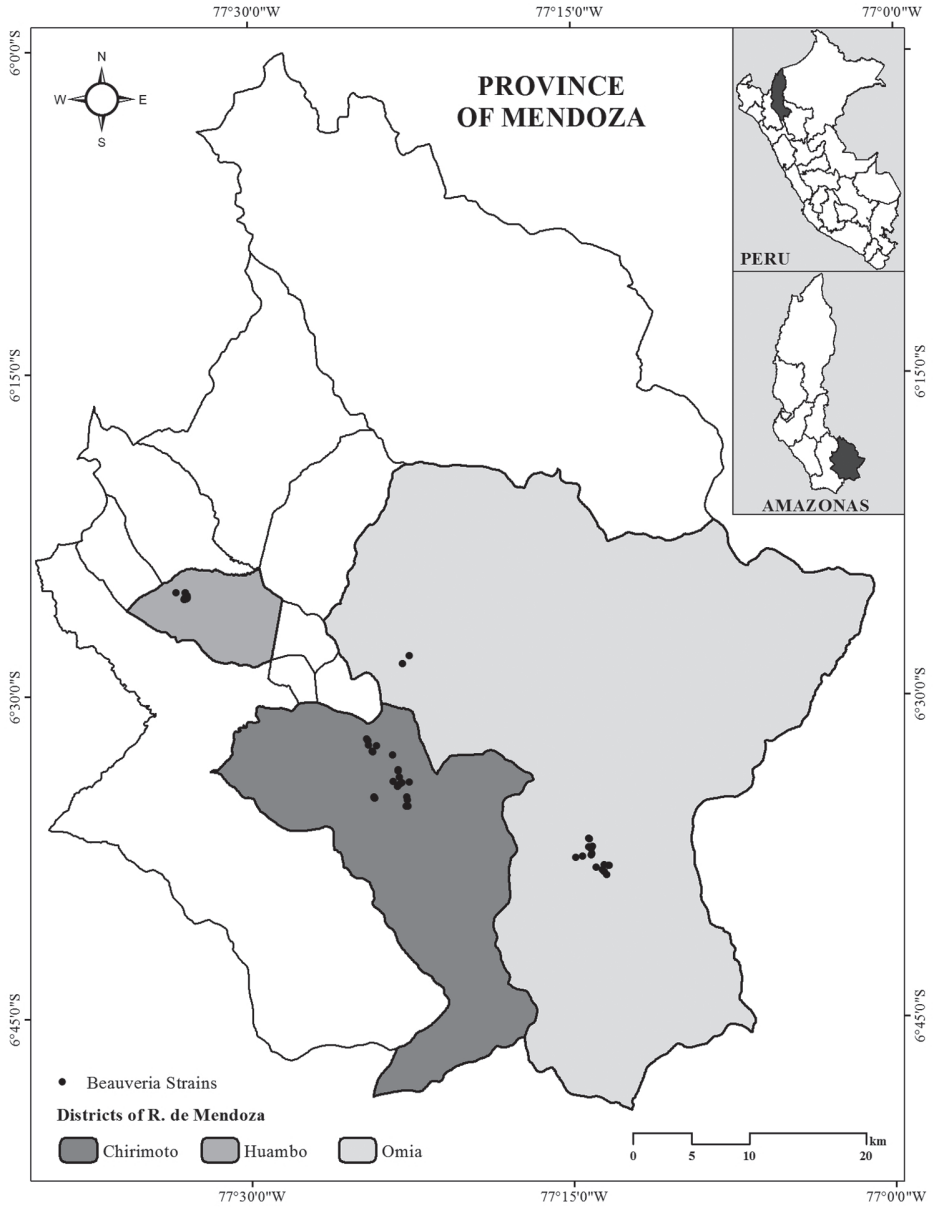

Figure 1. Collections of the 55 strains of *B. amazonensis* sp. nov. from the Rodriguez de Mendoza Province.

quences of the forward and reverse strands were determined commercially by Macrogen Inc. (Macrogen, Seoul, Korea). New *Bloc*, *rpb1*, and *tef1* sequences were deposited in GenBank (Table 1). These sequences and others obtained from GenBank were initially aligned with Muscle algorithms (Thompson et al. 1994) and were adjusted manually with MEGA6 software (Tamura et al. 2013).

Table 1. List of species used in the molecular analyses.

Species	Country	Strain	*Bloc*	*RPB1*	*tef1*
B. acridophila	Colombia	HUA 179219	–	JX003857	JQ958613
	Colombia	HUA 179221	–	JX003853	JQ958615
	Colombia	HUA 179220	–	JX003852	JQ958614
	Colombia	MCA 1181	–	MF416628	–
B. amorpha	Australia	ARSEF4149	HQ880735	HQ880876	HQ881006
	USA, Colorado	ARSEF7542	HQ880736	HQ880877	HQ881007
	Chile	B518a	HQ880737	HQ880878	HQ881008
	Peru	ARSEF1969	HQ880738	HQ880879	AY531907
	Brazil	ARSEF2641	HQ880739	HQ880880	AY531917
B. asiatica	China	ARSEF4384	HQ880716	HQ880857	AY531935
	China	ARSEF4474	HQ880717	HQ880858	AY531936
	Korea	ARSEF4850	HQ880718	HQ880859	AY531937
B. australis	Australia	ARSEF4580	HQ880719	HQ880860	HQ880994
	Australia	ARSEF4622	HQ880721	HQ880862	HQ880996
	Australia	WCN2015	KT961698	HQ880861	HQ880995
B. bassiana	Japan	ARSEF1040	HQ880689	HQ880830	AY531881
	Australia	ARSEF300	HQ880690	HQ880831	AY531924
	Italy	ARSEF1564	HQ880692	HQ880833	HQ880974
	Japan	ARSEF7518	HQ880693	HQ880834	HQ880975
	Vietnam	ARSEF751	HQ880694	HQ880831	AY531954
	Brazil	ARSEF1478	HQ880695	HQ880836	AY531890
	Morocco	ARSEF1811	HQ880696	HQ880837	AY531901
B. brongniartii	Japan	ARSEF7516	HQ880697	HQ880838	HQ880976
	USA, Oregon	ARSEF10278	HQ880700	HQ880841	HQ880979
	Korea	ARSEF7268	HQ880703	HQ880844	HQ880982
	USA, New York	ARSEF6213	HQ880706	HQ880847	HQ880985
	Japan	ARSEF4363	HQ880707	HQ880848	HQ880986
	Japan	ARSEF4362	HQ880708	HQ880849	HQ880980
	USA, Kentucky	ARSEF2271	HQ880710	HQ880851	HQ880988
	USA, Oregon	ARSEF10277	HQ880711	HQ880852	HQ880989
	France	ARSEF979	HQ880714	HQ880855	HQ880992
B. caledonica	Switzerland	ARSEF1567	HQ880747	HQ880888	AY531894
	Scotland	ARSEF2567	HQ880748	HQ880889	AY531915
	Denmark	ARSEF8024	HQ880749	HQ880890	HQ881012
	Brazil	ARSEF2251	HQ880750	HQ880891	AY531912
	USA, Georgia	ARSEF7117	HQ880751	HQ880892	HQ881013
	Australia	ARSEF4302	HQ880752	HQ880893	HQ881014
B. diapheromeriphila	Ecuador	QCNE 186272	–	JX003848	JQ958610
	Ecuador	QCNE 186714	–	MF416648	MF416491
	Ecuador	MCA 1557	–	JX003848	JQ958610
B. hoplocheli	Reunion	Bt116	KM453967	KM453957	KC339703
	Reunion	Bt121	KM453968	KM453956	KC339704
	Reunion	Bt124	KM453969	KM453955	KC339699
	Reunion	Bt125	KM453970	KM453953	KC339701
	Reunion	Bt128	KM453972	KM453952	KC339705
	Reunion	Bt129	KM453973	KM453951	KC339706
	Madagascar	Bt96	KM453974	KM453950	KC339709
	Reunion	Bt99	KM453975	KM453949	KC339710

Species	Country	Strain	*Bloc*	*RPB1*	*tef1*
B. kipukae	USA, Hawaii	ARSEF7032	HQ880734	HQ880875	HQ881005
B. lii	China	RCEF5500	JN689373	JN689374	JN689371
B. malawiensis	China	GZU12142	MG052638	MG052645	MG052641
	China	GZU12141	MG052639	MG052644	MG052640
	Australia	ARSEF4755	HQ880754	HQ880895	HQ881015
	Australia	BCC17613	HQ880755	HQ880896	HQ881016
	Malawi	ARSEF7760	HQ880756	HQ880897	DQ376246
B. peruviensis	Peru	UTRF21	MN094752	MN100113	MN094767
	Peru	UTRF24	MN094753	MN100119	MN094768
	Peru	UTRF25	MN094754	MN100114	MN094769
	Peru	UTRF26	MN094758	MN100120	MN094770
	Peru	UTRF35	MN094755	MN100115	MN094771
	Peru	UTRF37	MN094756	MN100116	MN094772
	Peru	UTRF38	MN094759	MN100121	MN094773
	Peru	UTRF40	MN094760	MN100122	MN094774
	Peru	UTRF42	MN094761	MN100123	MN094775
	Peru	UTRF58	MN094762	MN100124	MN094776
	Peru	UTRP6	MN094763	MN100125	MN094777
	Peru	UTRP7	MN094764	MN100127	MN094778
	Peru	UTRP13	MN094765	MN100126	MN094779
	Peru	UTRP17	MN094766	MN100117	MN094780
	Peru	UTRP19	MN094757	MN100118	MN094781
B. pseudobassiana	Portugal	ARSEF3220	HQ880722	HQ880863	AY531928
	USA, Kentucky	ARSEF3405	HQ880723	HQ880864	AY531931
	USA, Wisconsin	ARSEF3216	HQ880725	HQ880866	AY531927
	USA, Maryland	ARSEF3529	HQ880726	HQ880867	HQ880998
	France	ARSEF4933	HQ880726	HQ880870	AY531938
	Canada	ARSEF1855	HQ880727	HQ880868	HQ880999
	Canada	ARSEF2997	HQ880728	HQ880869	HQ881000
	China	ARSEF6229	HQ880730	HQ880871	HQ881001
	Korea	ARSEF7242	HQ880730	HQ880865	HQ880997
B. scarabaeicola	Korea	ARSEF5689	–	DQ522380	DQ522335
	Japan	ARSEF1685	HQ880740	HQ880881	AY531899
	Korea	ARSEF5689	HQ880741	HQ880882	AY531939
	Korea	ARSEF7043	HQ880742	HQ880883	AY531948
	Korea	ARSEF7044	HQ880743	HQ880884	AY531949
	Korea	ARSEF7279	HQ880743	HQ880885	HQ881009
	Korea	ARSEF7280	HQ880744	HQ880886	HQ881010
	Korea	ARSEF7281	HQ880746	HQ880887	HQ881011
B. sinensis	China	RCEF3903	–	JX524283	HQ270151
B. staphylinidicola	Korea	ARSEF5718	–	EF468881	EF468776
B. varroae	France	ARSEF8259	HQ880732	HQ880873	HQ881003
	Switzerland	ARSEF2694	HQ880733	HQ880874	HQ881004
	France	ARSEF8257	HQ880733	HQ880872	HQ881002
B. vermiconia	Chile	ARSEF2922	HQ880753	HQ880894	AY531920
Cordyceps cicadae	Korea	ARSEF7260	HQ880757	HQ880898	HQ881017
Blackwiella cardinalis	USA	OSC93610	–	EF469088	EF469059
Ascopolyporus polychrous	–	PC546	–	DQ127236	DQ118745

The phylogeny was based on concatenated data combining *Bloc*, *rpb1*, and *tef1* (101 sequences, Table 1). Selection of the best-fitting nucleotide substitution model was conducted using the program PartitionFinder (Lanfear et al. 2012) with three partitions (*Bloc*, *rpb1*, and *tef1*). The best partition strategy and model of sequence evolution were selected based on the Bayesian Information Criterion (BIC). The general time reversible nucleotide substitution model with a gamma distribution and a proportion of invariable sites (GTR + Γ + I) was selected for all partitions. Maximum likelihood (ML) analyses were conducted with the RAxML HPC-AVX program (Stamatakis 2014) implemented in the raxmlGUI 1.3.1 interface (Silvestro and Michalak 2012) using a GTRGAMMAI model with 1000 bootstrap replications. Bayesian inference (BI) was performed with MrBayes v. 3.2.6 software (Ronquist et al. 2012) using Metropolis-coupled MCMC and the GTR + Γ + I model. We conducted two runs each with four chains (three hot and one cold) for 10,000,000 generations, sampling trees every 1,000 generations. We plotted likelihood vs. generation using the Tracer Version v. 1.6 program (Rambaut et al. 2014) to reach a likelihood plateau and set the burn-in value.

DNA-based species delimitation

Although 26 species have been molecularly confirmed in *Beauveria* (Rehner et al. 2011, Kepler et al. 2017, Chen et al. 2018), only 21 of these species and *Beauveria* sp. from Peru were used in the DNA-based delimitation methods. *Beauveria araneola* W.H. Chen, Y.F. Han, Z.Q. Liang & D.C. Jin, *B. gryllotalpidicola* Luangsa-ard, Ridkaew & Tasanathai, *B. loeiensis* Luangsa-ard, Ridkaew & Tasanathai, *B. medogensis* Imoulan & Y.J. Yao, and *B. rudraprayagi* Y. Agrawal, P. Mual & B.D. Shenoy were not used due to abundant missing data and short sequences for the three markers (e.g. ~731 bp for *rpb1* and ~720 bp for *tef1*).

We explored five different DNA-based delimitation methods using *Bloc*, *rpb1*, and *tef1* data sets to assess species boundaries in *Beauveria*. Although *B. acridophila*, *B. blattidicola* M. Chen, Aime, T.W. Henkel & Spatafora, *B. diapheromeriphila*, *B. locustiphila*, and *B. staphylinidicola* (Kobayasi & Shimizu) B. Shrestha, Kepler & Spatafora lack *Bloc* sequences, these species were used in the analysis to evaluate its status in the new circumscribed *Beauveria.* Two of these DNA-based delimitation methods are based on genetic distance [statistical parsimony network analysis (SPN) (Hart and Sunday 2007) and automatic barcoding gap detection (ABGD) (Puillandre et al. 2012)], two in coalescence [generalized mixed Yule coalescent method (GMYC) (Pons et al. 2006) and Bayesian phylogenetics and phylogeography (BPP) (Rannala and Yang 2003)], and one in genealogical concordance [genealogical concordance phylogenetic species recognition (GCPSR) (Quaedvlieg et al. 2014)]. For the SPN analyses of *Bloc*, *rpb1*, and *tef1*, data sets were generated in TCS 1.21 (Clement et al. 2000) with a maximum connection probability set at 95% statistical confidence. The ABGD method was tested via a web interface (ABGD web, http://wwwabi.snv.jussieu.fr/public/abgd/abgdweb.html). Before analysis, the model criteria were set as follows: variability (P) between 0.001 (Pmin) and 0.1 (Pmax), minimum gap width (X) of 0.1, Kimura-2-parameters and 50 screening steps.

To perform the GMYC delimitation method, an ultrametric tree was constructed in BEAST v.2.0.2 (Drummond et al. 2012), relying on the uncorrelated lognormal relaxed clock, the GTR + Γ + I model, and a coalescent tree prior. Bayesian Markov chain Monte Carlo was run for 50 million generations, and trees and parameters were sampled every 1000 generations. Log files were visualized in Tracer v.1.6 (Rambaut et al. 2014) for assessing the stationary state of parameters on the basis of the value of estimate-effective sample size (ESS). After removing 25% of trees as burn-in, the remaining trees were used to generate a single summarized tree in TreeAnnotator v.2.0.2 (part of the BEAST v.2.0.2 package) as an input file for GMYC analyses. The GMYC analyses with a single threshold model were performed in R (R Development Core Team, http://www.R-project.org) under the 'splits' package using the 'gmyc' function (R-Forge, http://r-forge.r-project.org/projects/splits/).

To validate the outcomes of single locus species delimitation, a multilocus BPP was applied using the program BP&P v.2.0 (Rannala and Yang 2003, Yang and Rannala 2010, Liu et al. 2015). The three-gene data (*Bloc*, *rpb1*, and *tef1*) were used as input for BPP under the A11 model (A11: species delimitation = 1, species tree = 1). Specimens were *a priori* assigned to species based only on the minimum number of species from the results of the phylogenetic analysis. The guide tree derived from the three-gene ML analysis was used. Five variables (ε1~ε5) were automatically fine-tuned following the instructions of BP&P (Rannala and Yang 2003, Yang and Rannala 2010). The prior distribution of θ and τ could have influenced the posterior probabilities for different models (Yang and Rannala 2010). Analyses were run with three different prior combinations (Leaché and Fujita 2010). Each analysis was run three times to confirm consistency between runs. Two independent MCMC analyses were run for 100,000 generations with the 'burn-in' = 20,000.

GCPSR was implemented by identifying independent evolutionary lineages (IELs) and by exhaustive subdivision of strains into phylogenetic species. The criteria used to identify IELs and exhaustive subdivision were the same as those used by Brankovics et al. (2018). These were implemented using Perl scripts developed by Brankovics et al. (2018) and available at GitHub (https://github.com/b-brankovics/GCPSR).

Results

Molecular phylogeny

In the phylogeny of *Beauveria* species, the analyzed data matrix included 1592 base pairs (bp) for *Bloc*, 2890 bp *rpb1*, and 1181 bp for *tef1* of 101 individuals. Phylogenetic trees obtained from ML and BI analyses confirmed the robustly supported monophyly of the genus *Beauveria* (Fig. 2). The tree topologies for the individual genes (*tef1*, *Bloc*, and *rpb1*) did not show congruence (Suppl. material 1: Figs S1–S3). These trees showed topological differences, especially in the clades composed of *B. asiatica* / *B. majiangensis* and by *B. bassiana* / *B. staphylinidicola* / *Beauveria* sp. from Peru. Although the individual gene trees did not show congruence with the combined data, the latter resolved these clades, suggesting conspecificity in the first clade and sister relationship

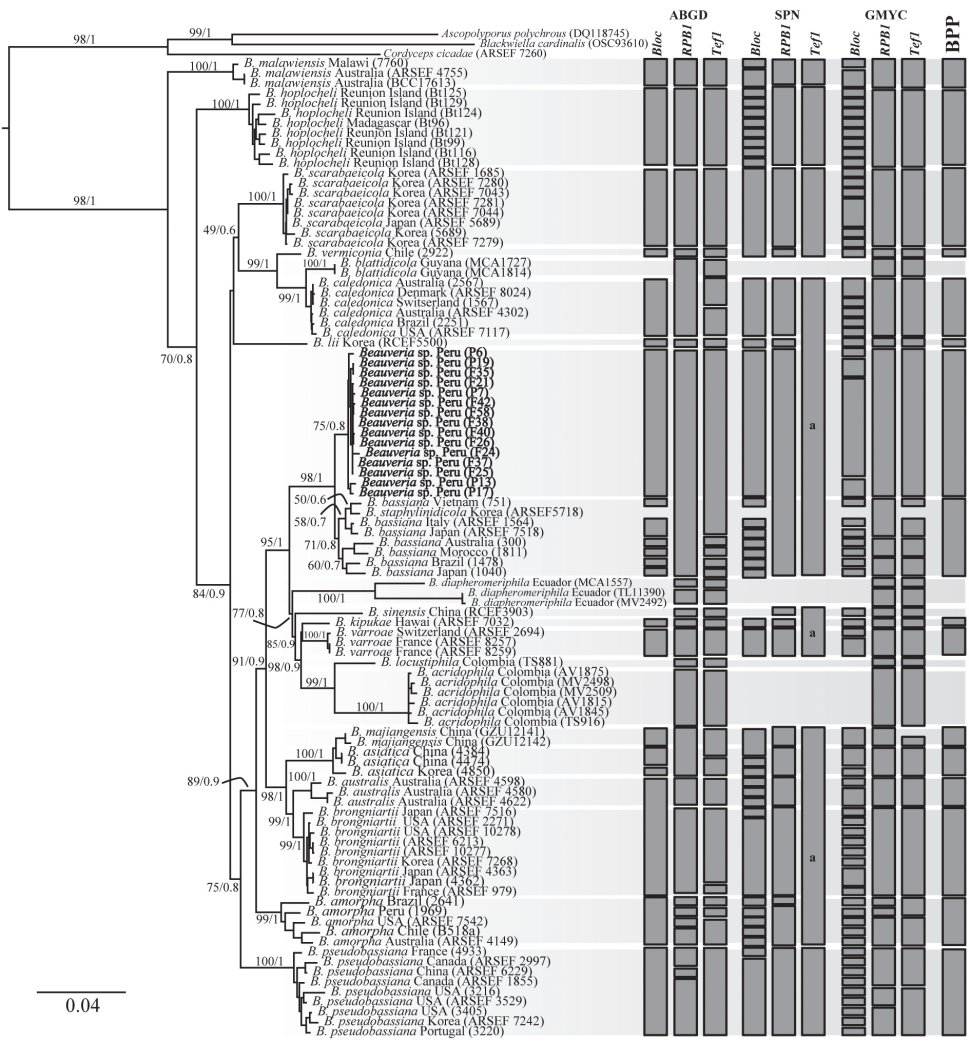

Figure 2. Phylogenetic tree based on maximum likelihood inference of combined *Bloc*, *RPB*1, *Tef*1 data. Value above branches = Maximum likelihood bootstrap values (BS) / Bayesian posterior probabilities. Grey bars represent species delimitation results from ABGD-, SPN-, GMYC- and BPP based algorithmic methods based on *Bloc*, *RPB*1, and *Tef*1 sequences. Scale bar indicates the number of nucleotide substitution per site. a: delimited as the same species. *B. araneola*, *B. gryllotalpidicola*, *B. loeiensis*, *B. medogensis*, and *B. rudraprayagi* were not delimited by any DNA-based algorithm due to abundant missing data in their sequences.

in the second. Moreover, the multilocus phylogeny showed well-supported clades in both the ML and BI analyses except in *B. lii*, *B. majiangensis*, and *B. staphylinidicola*. The genetic divergence comparisons showed that the minimum threshold (p-distance) to distinguish genetic species in *Beauveria* was 1.3%, 0.4%, and 0.2% for *Bloc*, *rpb1*, and *tef1*, respectively, as occurred between *B. australis* and *B. asiatica*.(Table 2).

Table 2. Genetic distance (p-distances) in percentage for species of *Beauveria* for three markers.

Taxa	Markers		
	Bloc	***RPB*1**	***tef1***
B. australis – B. asiatica	1.3	0.4	0.2
B. bassiana – B. staphylinidicola	3.1	0.5	0.2
B. bassiana – B. peruviensis	3.5–4.1	0.3–0.5	0.2–0.4
B. peruviensis – B. staphylinidicola	4.1–4.7	0.7–1.1	0.2

Table 3. Species number in *Beauveria* identified under DNA-based species-delimitations methods and phylogeny.

Taxa	Genetic distance						Coalescence				Genealogical concordance	Phylogeny
	ABGD			SPN			GMYC			BPP	GCPSR	
	Bloc	***RPB*1**	***Tef1***	***Bloc***	***RPB*1**	***Tef1***	***Bloc***	***RPB*1**	***Tef1***			
B. acridophila	–	1	1	–	x	x	–	1	1	–		1
B. amorpha	1	4	3	5	2	x	5	3	2	1		1
B. asiatica	2	x	1	2	1	x	2	1	1	1		1
B. australis	x	1	1	3	1	x	2	1	1	1		1
B. bassiana	6	x	5	6	x	x	6	3	3	1		1
B. blattidicola	–	x	1	–	x	x	–	1	1	–		1
B. brongniartii	x	1	2	2	1	x	8	1	1	1		1
B. caledonica	1	1	2	1	1	x	6	1	1	1		1
B. diapheromeriphila	–	2	2	–	x	x	–	2	2	–		1
B. hoplocheli	1	1	1	8	1	1	8	1	1	1		1
B. kipukae	1	1	1	1	1	x	1	1	1	1		1
B. lii	1	1	1	1	1	x	1	1	1	1	1	1
B. locustiphila	–	1	1	–	x	x	–	1	1	–		1
B. majiangensis	1	x	x	x	1	x	1	1	1	1		1
B. malawiensis	1	1	1	2	1	1	2	1	1	1		1
B. pseudobassiana	1	3	1	2	1	1	9	3	2	1		1
B. scarabaeicola	1	1	1	x	1	x	6	1	1	1		1
B. sinensis	–	1	1	–	1	x	1	1	1	–		1
B. staphylinidicola	–	x	x	–	x	x	–	x	x	–		1
B. varroae	1	1	1	1	1	x	2	1	1	1		1
B. vermiconia	1	1	1	x	1	x	1	1	1	1		1
B. peruviensis	1	x	x	1	x	x	2	1	1	1		1
Total	20	22	28	35	16	3	63	28***	26***	16*	1	22

x = non recognized as species, - = not evaluated, * = posterior probabilities higher or equal than 0.53, *** =highly significant

Species delimitation

The species-delimitation methods based on genetic distance (ABGD, SPN), coalescence (GMYC, BPP), and genealogical concordance (GCPSR) showed incongruent results for the three genes (Fig. 2, Table 3). Among these methods, the highest number of species was delimited in the GMYC analysis for the *Bloc* gene, whereas conservative results were observed in BPP. The species delimitations by SPN and GCPSR have inadequate and contradictory results. The genetic distance method based on the barcode gap (ABGD) found similar species numbers for *Bloc*, *rpb1*, and *tef1*, differing

only in the species recognized in the clades *B. asiatica* / *B. majiangensis* and *B. bassiana* / *B. staphylinidicola* / *Beauveria* sp. from Peru. In the former clade, there were 3, 1 and 2 species for *Bloc*, *rpb1*, and *tef1*; whereas in the latter clade, there were 7, 1, and 5 species for *Bloc*, *rpb1*, and *tef1*. The GMYC identified relatively conserved results in *RPB*1 (28) and *tef1* (26) and plenty of species in the *Bloc* data set (63). This high number of species for the *Bloc* data set is a consequence of the splitting of the main clades into different species but lacking significance (Suppl. material 1: Table S1, Fig. S4). Regarding the multi-locus coalescent species validation (BPP), the highest posterior probabilities for *Bloc*, *rpb1*, and *tef1* were found by recognizing 16 species based on the results from the phylogenetic analysis and single species delimitation methods (Suppl. material 1: Table S2). Conversely, the BPP analyses with the maximum number of species (39 and 62) were not used based on the inadequate results from SPN and GCPSR. Although there were incongruent results among different methods, the conservative results from species delimitation methods (ABGD and GMYC) and phylogenetic analysis suggest that *Beauveria* is composed of 20–28 and 26 species, respectively. These results also suggest that the clade composed of *B. asiatica* / *B. majiangensis*, *B. diapheromeriphila*, and *B. bassiana* / *B. staphylinidicola* / *Beauveria* sp. from Peru were genetically composed of more than one species. Our analysis also revealed that *Beauveria* sp. from Peru was supported as a distinct species by ABGD (*Bloc* gene), GMYC, BPP, and phylogeny. Thereby, the description of *Beauveria* sp. as a new species is proposed.

Morphological observations

Beauveria peruviensis **D.E.Bustamante, M.S.Calderon, M.Oliva, S.Leiva, sp. nov.**
MycoBank No: 829032
Fig. 3

Diagnosis. Species very similar morphologically to *Beauveria bassiana*, but differing in the sister phylogenetic relationship with this species (Fig. 2). The sequence divergence between *B. peruviensis* and *B. bassiana* is 3.5–4.1% for *Bloc*, 0.3–0.5% for *rpb1*, and 0.2–0.4% for *tef1*. *B. peruviensis* is occurring in coffee plantations located in the middle altitudes of the Amazon region of Peru.

Type. PERU. Amazonas: Prov. Rodríguez de Mendoza, Dist. Huambo, latitude -6.469, longitude -77.376, elev. 1642 m, entomopathogenic, 08 Nov. 2017, G. Ángulo, UTRP19 (holotype: UFV5609; isotype: ARSEF14196).

Description. Colony growth on PDA, 15–38 mm diam. after 15 d at 25 C, 1.4–1.9 daily rate of radial growth, velutinous and closely appressed to agar surface, up to 3.5 mm thick, white, changing to yellowish white in older sections of the colony. Conidia aggregated as ca. 0.1 mm spherical clusters and white in mass. Colony reverse colorless or yellowish white to grayish white. Odor indistinct. Vegetative hyphae septate, branched, hyaline, smooth-walled, 1–1.5 µm wide. Conidiogenous cells, phialidic, solitary or occurring in dense lateral clusters, base subsphaerical, 3–6

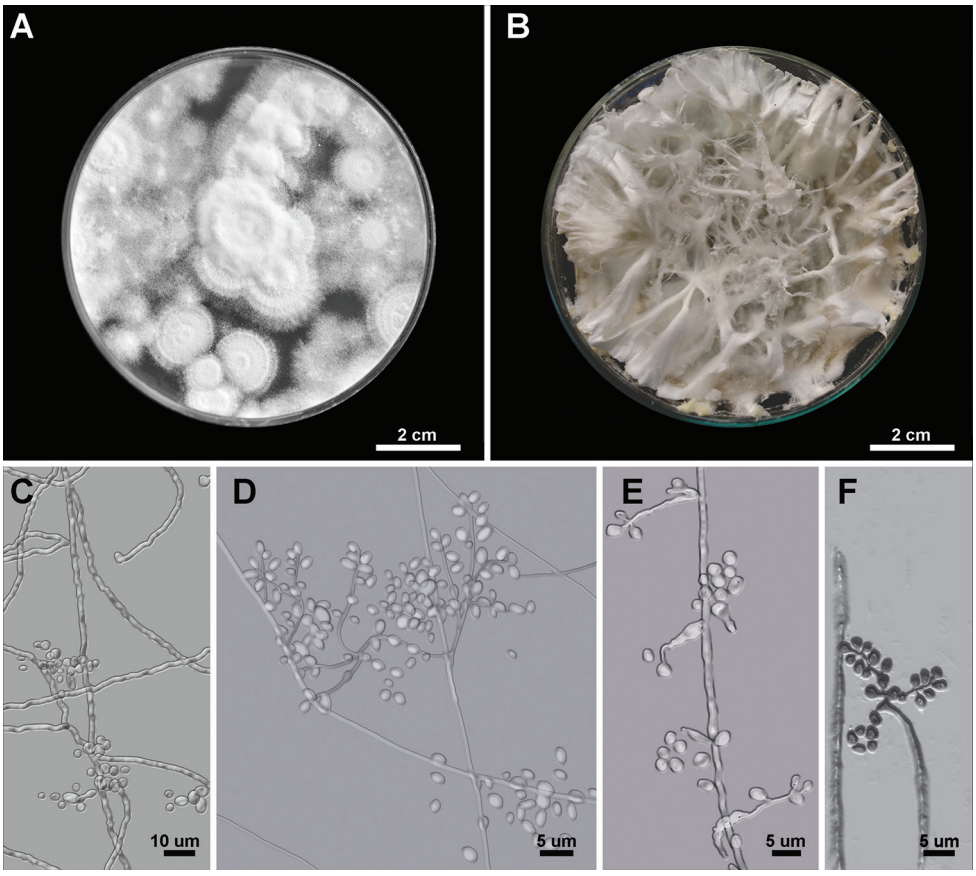

Figure 3. Morphology of *Beauveria amazonensis*. **A, B** Colony growth on PDA showing the habit **C–F** conidiogenous cells and conidia.

µm wide, sympodially branched neck tapering into a long slender denticulate rachis, geniculate or irregularly bent, 2.0–3.5 × 1.5–2.5 µm. Conidia, 2–3 × 1–3 µm, Q = 1.0–1.8 (L^m = 2.5 µm, W^m = 2.2 µm, Q^m = 1.6), mainly globose, slightly ellipsoid, oblong or cylindrical, hyaline, aseptate, walls smooth and thin. Mycelium on the host is granular-pulverulent, sometimes funiculose or rarely producing synnemata, white, rarely yellowish. Hyphae of the aerial mycelium bearing a conidial apparatus as described above. Basal parts of the conidiogenous cells globose, subglobose or somewhat flask-shaped.

Distribution. This species is widely spread on coffee plantations in the middle altitudes of the Amazon region in northeastern Peru.

Ecology. *B. peruviensis* was isolated from coffee borers (*Hypothenemus hampei*) obtained from coffee grains. Only the asexual stage was found.

Etymology. The specific epithet '*peruviensis*' is derived from the country where the samples were collected.

Additional specimens examined. PERU. Amazonas: Prov. Rodríguez de Mendoza, Dist. Chirimoto, Achamal, latitude -6.535, longitude -77.408, 1351 m alt., 26 Jul. 2017, G. Angulo UTRF21 (UTR) ; latitude -6.534, longitude -77.409, 1345 m alt., 26 Jul. 2017, G. Angulo UTRF22 (UTR) ; latitude -6.544, longitude -77.404, 1435 m alt., 26 Jul. 2017, G. Angulo UTRF23 (UTR); latitude -6.539, longitude -77.401, 1374 m alt., 26 Jul. 2017, G. Angulo UTRF24 (UTR); latitude -6.539, longitude -77.407, 1386 m alt., 26 Jul. 2017, G. Angulo UTRF25 (UTR); latitude -6.543, longitude -77.405, 1428 m alt., 26 Jul. 2017, G. Angulo UTRF26 (UTR); Paraiso, latitude -6.569, longitude -77.383, 1218 m alt., 26 Jul. 2017, G. Angulo UTRF37 (UTR); latitude -6.568, longitude -77.382, 1197 m alt., 26 Jul. 2017, G. Angulo UTRF38 (UTR); latitude -6.567, longitude -77.389, 1387 m alt., 26 Jul. 2017, G. Angulo UTRF39 (UTR); latitude -6.571, longitude -77.385, 1250 m alt., 26 Jul. 2017, G. Angulo UTRF40 (UTR); latitude -6.579, longitude -77.403, 1427 m alt., 10 Aug. 2017, G. Angulo UTRP12 (UTR); latitude -6.58, longitude -77.403, 1444 m alt., 10 Aug. 2017, G. Angulo UTRP13 (UTR); latitude -6.579, longitude -77.404, 1439 m alt., 10 Aug. 2017, G. Angulo UTRP14 (UTR); Trancapata, latitude -6.546, longitude -77.389, 1255 m alt., 26 Jul. 2017, G. Angulo UTRF31 (UTR); latitude -6.564, longitude -77.384, 1161 m alt., 26 Jul. 2017, G. Angulo UTRF34 (UTR); Virgen del Carmen, latitude -6.586, longitude -77.379, 1313 m alt., 26 Jul. 2017, G. Angulo UTRF42 (UTR); latitude -6.586, longitude -77.378, 1271 m alt., 26 Jul. 2017, G. Angulo UTRF43 (UTR); latitude -6.586, longitude -77.377, 1256 m alt., 26 Jul. 2017, G. Angulo UTRF44 (UTR); latitude -6.581, longitude -77.377, 1138 m alt., 26 Jul. 2017, G. Angulo UTRF46 (UTR); Zarumilla, latitude -6.568, longitude -77.376, 1118 m alt., 26 Jul. 2017, G. Angulo UTRF35 (UTR); latitude -6.58, longitude -77.403, 1461 m alt., 10 Aug. 2017, G. Angulo UTRP15 (UTR); latitude -6.58, longitude -77.403, 1149 m alt., 10 Aug. 2017, G. Angulo UTRP16 (UTR); latitude -6.559, longitude -77.385, 1160 m alt., 10 Aug. 2017, G. Angulo UTRP17 (UTR); latitude -6.558, longitude -77.385, 1160 m alt., 10 Aug. 2017, G. Angulo UTRP18 (UTR); Huambo, Chontapamapa, latitude -6.419, longitude -77.557, 1637 m alt., 27 Jul. 2017, G. Angulo UTRF66 (UTR); Dos Cruces, latitude -6.579, longitude -77.378, 1624 m alt., 27 Jul. 2017, G. Angulo UTRF53 (UTR); latitude -6.424, longitude -77.548, 1668 m alt., 27 Jul. 2017, G. Angulo UTRF58 (UTR); latitude -6.425, longitude -77.55, 1642 m alt., 11 Aug. 2017, G. Angulo UTRP19 (UTR); latitude -6.425, longitude -77.55, 1629 m alt., 11 Aug. 2017, G. Angulo UTRP20 (UTR); latitude -6.424, longitude -77.549, 1661 m alt., 11 Aug. 2017, G. Angulo UTRP21 (UTR); latitude -6.425, longitude -77.548, 1671 m alt., 11 Aug. 2017, G. Angulo UTRP22 (UTR); latitude -6.424, longitude -77.548, 1681 m alt., 11 Aug. 2017, G. Angulo UTRP23 (UTR); latitude -6.423, longitude -77.548, 1682 m alt., 11 Aug. 2017, G. Angulo UTRP24 (UTR); latitude -6.422, longitude -77.548, 1671 m alt., 11 Aug. 2017, G. Angulo UTRP25 (UTR); Escobar, latitude -6.42, longitude -77.549, 1666 m alt., 27 Jul. 2017, G. Angulo UTRF59 (UTR); latitude -6.42, longitude -77.549, 1674 m alt., 27 Jul. 2017, G. Angulo UTRF60 (UTR); Omia, El Tingo, latitude -6.469, longitude -77.376, 1431 m alt., 25 Jul. 2017, G. Angulo UTRF19

(UTR); latitude -6.475, longitude -77.381, 1349 m alt., 25 Jul. 2017, G. Angulo UTRF20 (UTR); La Primavera, latitude -6.634, longitude -77.231, 1283 m alt., 25 Jul. 2017, G. Angulo UTRF5 (UTR); latitude -6.64, longitude -77.224, 1362 m alt., 25 Jul. 2017, G. Angulo UTRF7 (UTR); latitude -6.632, longitude -77.222, 1205 m alt., 3 Aug. 2017, G. Angulo UTRP4 (UTR); latitude -6.632, longitude -77.222, 1209 m alt., 3 Aug. 2017, G. Angulo UTRP5 (UTR); latitude -6.638, longitude -77.225, 1280 m alt., 3 Aug. 2017, G. Angulo UTRP6 (UTR); latitude -6.637, longitude -77.225, 1275 m alt., 3 Aug. 2017, G. Angulo UTRP7 (UTR); latitude -6.636, longitude -77.227, 1255 m alt., 25 Jul. 2017, G. Angulo UTRP8 (UTR); latitude -6.632, longitude -77.225, 1238 m alt., 4 Aug. 2017, G. Angulo UTRP9 (UTR); Libano, latitude -6.623, longitude -77.235, 1174 m alt., 24 Jul. 2017, G. Angulo UTRF2 (UTR); latitude -6.611, longitude -77.237, 1330 m alt., 24 Jul. 2017, G. Angulo UTRF3 (UTR); latitude -6.625, longitude -77.242, 1235 m alt., 24 Jul. 2017, G. Angulo UTRF4 (UTR); latitude -6.612, longitude -77.237, 1307 m alt., 3 Aug. 2017, G. Angulo UTRP1 (UTR); latitude -6.618, longitude -77.234, 1242 m alt., 3 Aug. 2017, G. Angulo UTRP2 (UTR); latitude -6.626, longitude -77.247, 1284 m alt., 3 Aug. 2017, G. Angulo UTRP3 (UTR); latitude -6.62, longitude -77.235, 1226 m alt., 3 Aug. 2017, G. Angulo UTRP10 (UTR); latitude -6.618, longitude -77.237, 1236 m alt., 4 Aug. 2017, G. Angulo UTRP11 (UTR).

Notes. *Beauveria peruviensis* is practically indistinguishable in morphology to other *Beauveria* species. The shape and size of the conidia and the colony color of *B. peruviensis* among other morphological features have been observed in *B. bassiana*, *B. kipukae*, *B. pseudobassiana*, and *B. varroae* (Rehner et al. 2011). The lack of diagnostic morphological features to distinguish *Beauveria peruviensis* was overcome by delimiting this species with DNA-based methodologies.

Discussion

Accurate species identification within the entomopathogenic fungi *Beauveria* is crucial for disease control and prevention (Lu et al. 2016). This genus has recently been circumscribed, and its taxonomy has been updated with new combinations and the description of new species based mainly on multi-locus phylogenies in the absence of diagnostic features that delimit species (Sanjuan et al. 2014, Shrestha et al. 2014, Kepler et al. 2017, Chen et al. 2017, 2018). In addition to phylogenies, other methodologies and data sets to delimit species are recommended to establish well-supported boundaries among species (Carstens et al. 2013) because most researchers simply recognize distinct clades in either single- or multi-locus trees as species (Stewart et al. 2014). In this regard, our study used phylogeny and five DNA-based methods to delimit species in *Beauveria* using three molecular makers. Although incongruence among some of these methods was observed in our analyses, a genetic distance (ABGD), a coalescence method (BPP), and the multilocus phylogeny strongly supported 20–28 different species, including the new species *B. peruviensis* from Peru.

The use of multi-locus sequence data is essential to establish robust species boundaries (Lumbsch and Levitt 2011), and our results for *Beauveria* showed well-supported clades, although it resulted in incongruence to the single locus phylogenies (Suppl. material 1: Figs S1–S3). This conflict can be a result of incomplete lineage sorting, horizontal gene transfer, gene duplication and loss, hybridization, or recombination (Degnan and Rosenberg 2009). This study cannot determine which of these scenarios are occurring in *Beauveria*; nevertheless, it serves as a baseline for investigating causes of gene tree discordance that can be identified by further analyses at the genomic level (Patterson et al. 2006, Lu et al. 2016). According to our multilocus phylogeny, 22 of the 26 molecularly confirmed species in *Beauveria* were recognized. Previous studies have delimited *B. araneola*, *B. gryllotalpidicola*, *B. loeiensis*, *B. medogensis*, and *B. rudraprayagi* as valid species on the basis of their phylogenies (Agrawal et al. 2014, Imoulan et al. 2016, Chen et al. 2017); however, our study did not include these sequences because they have abundant missing data, and thus, their status was not evaluated. These species would require further revision to be recognized as supported lineage within the genus *Beauveria*.

Regarding the genetic distance methods, the ABGD showed similar results when delimiting *Beauveria* species to those from the multilocus phylogeny. The additional putative species in ABGD is mainly due to the split of *B. bassiana*. This confirms that *B. bassiana* encompasses cryptic lineages as proposed initially by Rehner et al. (2011). Therefore, the original *B. bassiana* should be the clade that includes the specimen from the type locality, namely, Italy (Vuillemin 1912). Additionally, these results delimited *B. majiangensis* and *B. asiatica* as different lineages, although the multilocus analysis showed low support. *B. majiangensis* needs further analysis with additional and longer sequences to confirm its status because one or only a few individuals often fail to represent the species as a whole (Davis and Nixon 1992, Walsh 2000). On the other hand, the SPN method showed conflicting results among the *Bloc*, *RPB*1, and *tef1* loci, leading to incorrect inferences. The number of species inferred by SPN greatly matched the number of Linnaean species in mitochondrial markers (e.g., COI) (Hart and Sunday 2007). Therefore, our nuclear markers due to indels might generate many reticulations that allow inadequate species delimitation in our data (Paradis 2018).

In the coalescence methods, although 6 species were not included in the BPP analysis due to the lack of their *Bloc* sequences, this method supports the conservative results obtained from the multilocus phylogeny. BPP supported the status of 16 species (posterior probabilities higher than 0.52), which are not high supportive, but these probabilities are not supportive at all when splitting or merging species in the BPP analysis (Suppl. material 1: Table S2). Zhang et al. (2011) found that the correct species model was inferred with a high posterior probability with only one or two loci when 5 or 10 sequences were sampled from each population or with 50 loci when only one sequence was sampled, and they also demonstrated that the migration rate might affect these results. This suggests that further analysis might need to increase the number of sequences per locus among different populations of species of *Beauveria* and assess their migration rate to obtain supportive delimitations. Moreover, the highly

significant results obtained from the GMYC method for the *tef1* and *rpb1* loci partially support the ABGD and multilocus analyses. The additional number of putative species in the GMYC analyses, as occurred with the ABGD, is due to the presence of more than one lineage in *B. amorpha*, *B. bassiana*, *B. diapheromeriphila*, and *B. pseudobassiana* confirming cryptic diversity (Rehner et al. 2011). The performance in empirical studies of the ABGD and GMYC tends to under- and oversplit species, respectively (Luo et al. 2018). However, our results suggest that GMYC and ABGD are appropriate for determining cryptic diversity in *Beauveria* by splitting well-supported clades from the multi-locus phylogeny.

Regarding *B. peruviensis*, ABGD (*Bloc*), SPN (*Bloc*), GMYC, BPP, and the phylogenetic analyses support this species as a different lineage from *B. bassiana* and *B. staphylinidicola*. Additionally, the genetic divergence between *B. peruviensis* and these species is higher than the minimum threshold observed in species of *Beauveria* (Table 2). In our study, *Beauveria peruviensis* showed morphological indistinctiveness to other *Beauveria* species that produce globose/subglobose/ellipsoid conidia. Additionally, *B. peruviensis* conidia is also similar in size to other *Beauveria*, especially *B. bassiana*. Previously, Rehner et al. (2011) noted that *B. bassiana* is hardly distinguishable from other species of *Beauveria*. The lack of diagnostic morphological features to delimit species in *Beauveria* was overcome by the application of molecular methods in fungal taxonomy. The segregation of *B. peruviensis* from *B. bassiana* and *B. staphylinidicola* confirmed that phylogenetic diversity and DNA-species delimitation methods discover taxa within morphologically defined species (Goldstein et al. 2000, Lu et al. 2016). Ecologically, the segregation of *B. peruviensis* from *B. bassiana* and *B. staphylinidicola* is supported by the specificity of *B. peruviensis* to the coffee borer from Amazon and the well-supported lineage in the phylogenetic analysis that might indicate the presence of a barrier in gene flow in nature (Van Valen 1976, Lu et al. 2016).

Recently, polyphasic approaches have been used to reflect the natural classification of species within many important fungal genera (Aveskamp et al. 2010, Milic et al. 2012, Lu et al. 2016). These approaches frequently incorporate morphological and phylogenetic analyses and metabolomics, but few of them use genetic distance and coalescent methods (Lu et al. 2016). The use of polyphasic analysis, including DNA-based delimitation methods, allowed the establishment of boundaries among species of morphologically conserved genera such as *Beauveria* and thus provided support for the description of new taxa (e.g., *B. peruviensis*) or validated the taxonomic uncertain of others (e.g., *B. majiangensis*). Although more recent methods avoid arbitrary cut-offs (Knowles and Carstens 2007), our results demonstrate that the congruence among this method and other methods used in a polyphasic approach (e.g., genetic distance, coalescence methods) are more likely to prove reliably supported species boundaries (Carstens et al. 2013). Among the methods applied in this study, ABGD, GMYC, BPP, and multilocus phylogeny are crucial when establishing species boundaries in *Beauveria*.

Acknowledgements

This study was supported by the National Institute of Agrarian Innovation of Peru (Project number: 002-2016-INIA-PNIA-UPMSI/IE).

References

Agrawal Y, Mual P, Shenoy BD (2014) Multi-gene genealogies reveal cryptic species *Beauveria rudraprayagi* sp. nov. from India. Mycosphere 5: 719–736. https://doi.org/10.5943/mycosphere/5/6/3

Aveskamp MM, De Gruyter J, Woudenberg JHC, Verkley GJM, Crous PW (2010) Highlights of the Didymellaceae: a polyphasic approach to characterise *Phoma* and related pleosporalean genera. Studies in Mycology 65: 1–60. https://doi.org/10.3114/sim.2010.65.01

Balsamo G (1835) Zwei neuen Arten Mucedineen, *Botrytis bassiana* und *Mucor radicans*, und uber die Entickelung der ersteren Art im Seidenwurme. Linneae 10: 609–618.

Bissett J, Widden P (1986) A new species of *Beauveria* from Scottish moorland soil. Canadian Journal of Botany 66: 361–362. https://doi.org/10.1139/b88-057

Brankovics B, Van Dam P, Rep M, de Hoog S, Van der Lee TAJ, Waalwijk C, Van Diepeningen AD (2018) Mitochondrial genomes reveal recombination in the presumed asexual *Fusarium oxysporum* species complex. BMC Genomics 201718: 735. https://doi.org/10.1186/s12864-017-4116-5

Carstens BC, Pelletier TA, Reid NM, Satler JD (2013) How to fail at species delimitation. Molecular Ecology 22: 4369–4383. https://doi.org/10.1111/mec.12413

Chen WH, Han YF, Liang ZQ, Jin DC (2017) A new araneogenous fungus in the genus *Beauveria* from Guizhou, China. Phytotaxa 302: 57–64. https://doi.org/10.11646/phytotaxa.302.1.5

Chen WH, Man L, Huang ZX, Yang GM, Han YF, Liang JD, Liang ZQ (2018) *Beauveria majiangensis*, a new entomopathogenic fungus from Guizhou, China. Phytotaxa 333: 243–250. https://doi.org/10.11646/phytotaxa.333.2.8

Clement M, Posada D, Crandall KA (2000) TCS: a computer program to estimate gene genealogies. Molecular Ecology 9: 1657–1659. https://doi.org/10.1046/j.1365-294x.2000.01020.x

Davis JI, Nixon KC (1992) Populations, genetic variation, and the delimitation of phylogenetic species. Systematic Biology 41: 421–435. https://doi.org/10.1093/sysbio/41.4.421

Degnan JH, Rosenberg NA (2009) Gene tree discordance, phylogenetic inference, and the multispecies coalescent. Trends in Ecology and Evolution 24: 332–340. https://doi.org/10.1016/j.tree.2009.01.009

De Hoog GS (1972) The genera *Beauveria*, *Isaria*, *Tritirachium*, and *Acrodontium* gen. nov. Studies in Mycology 1: 1–41.

De Hoog GS, Rao V (1975) Some new hyphomycetes. Persoonia 8: 207–212.

Drummond AJ, Suchard MA, Xie D, Rambaut A (2012) Bayesian phylogenetics with BEAUti and the BEAST 1.7. Molecular Biology and Evolution 29: 1969–1973. https://doi.org/10.1093/molbev/mss075

Faria MR, Wraight SP (2007) Mycoinsecticides and mycoacaricides: a comprehensive list with worldwide coverage and international classification of formulation types. Biological Control 43: 237–256. https://doi.org/10.1016/j.biocontrol.2007.08.001

Gerónimo-Torres JDC, Torres-de-la-Cruz M, Cruz MP, De-la-Cruz-Pérez A, Ortiz-García CF, Cappello-García S (2016) Caracterización de aislamientos nativos de *Beauveria bassiana* y su patogenicidad hacia *Hypothenemus hampei* en Tabasco, México. Revista Colombiana de Entomología. 42: 28–35. https://doi.org/10.25100/socolen.v42i1.6666

Ghikas DV, Kouvelis VN, Typas MA (2010) Phylogenetic and biogeographic implications inferred by mitochondrial intergenic region analyses and ITS1-5.8S-ITS2 of the entomopathogenic fungi *Beauveria bassiana* and *B. brongniartii*. BMC Microbiology 10: 174. https://doi.org/10.1186/1471-2180-10-174

Goldstein PZ, Desalle R, Amato G, Vogler AP (2000) Conservation genetics at the species boundary. Conservation Biology 14: 120–131. https://doi.org/10.1046/j.1523-1739.2000.98122.x

Hart MW, Sunday J (2007) Things fall apart: biological species form unconnected parsimony networks. Biology Letters 3: 509–512. https://doi.org/10.1098/rsbl.2007.0307

Huang B, Li CR, Li ZG, Fan MZ, Li ZZ (2002) Molecular identification of the teleomorph of *Beauveria bassiana*. Mycotaxon 81: 229–236.

Imoulan A, Wu HJ, Lu WL, Li Y, Li BB, Yang RH, Wang WJ, Wang XL, Kirk PM, Yao YJ (2016) *Beauveria medogensis* sp. nov., a new fungus of the entomopathogenic genus from China. Journal of Invertebrate Pathology. 139: 74–81. https://doi.org/10.1016/j.jip.2016.07.006

Kepler RM, Luangsa-ard JJ, Hywel-Jones NL, Quandt CA, Sung GH, Rehner SA, Aime MC, Henkel TW, Sanjuan T, Zare R, Chen M, Li Z, Rossman AY, Spatafora JW, Shrestha B (2017) A phylogenetically-based nomenclature for Cordycipitaceae (Hypocreales). IMA Fungus 8, 335–353. https://doi.org/10.5598/imafungus.2017.08.02.08

Knowles LL, Carstens BC (2007) Delimiting species without monophyletic gene trees. Systematic Biology 56: 887–895. https://doi.org/10.1080/10635150701701091

Lanfear R, Calcott B, Ho SYW, Guindon S (2012) PartitionFinder: combined selection of partitioning schemes and substitution models for phylogenetic analyses. Molecular Biology and Evolution 29: 1695–1701. https://doi.org/10.1093/molbev/mss020

Leaché AD, Fujita MK (2010) Bayesian species delimitation in west African forest geckos (*Hemidactylus fasciatus*). Proceedings of the Royal Society B 277: 3071–3077. https://doi.org/10.1098/rspb.2010.0662

Liu SL, Lin SM, Chen PC (2015) Phylogeny, species diversity and biogeographic patterns of the genus *Tricleocarpa* (Galaxauraceae, Rhodophyta) from the Indo-Pacific region, including *T. confertus* sp. nov. from Taiwan. European Journal of Phycology 50: 439–456. https://doi.org/10.1080/09670262.2015.1076892

Liu F, Wang M, Damm U, Crous PW, Cai L (2016) Species boundaries in plant pathogenic fungi: a Colletotrichum case study. BMC Evolutionary Biology 16: 81. https://doi.org/10.1186/s12862-016-0649-5

Lumbsch HT, Leavitt SD (2011) Goodbye morphology? A paradigm shift in the delimitation of species in lichenized fungi. Fungal Diversity 50: 59–72. https://doi.org/10.1007/s13225-011-0123-z

Luo A, Ling C, Ho SYW, Zhu CD (2018) Comparison of methods for molecular species 465 delimitation across a range of speciation scenarios. Systematic Biology 67: 830–846. https://doi.org/10.1093/sysbio/syy011

McNeill J, Barrie FF, Buck WR, Demoulin V, Greuter W, Hawksworth DL, Herendeen PS, Knapp S, Marhold K, Prado J, Prud'homme Van Reine WF, Smith GF, Wiersema JH (2012) International Code of Nomenclature for algae, fungi, and plants (Melbourne Code). [Regnum vegetabile no. 154.]Königstein: Koeltz Scientific Books.

Milic N, Kostidis S, Stavrou A, Gonou-Zagou Z, Kouvelis VN, Mikros E, Fokialakis N (2012) A polyphasic approach (metabolomics, morphological and molecular analyses) in the systematics of *Cladobotryum* species in Greece. Planta Medica 78:1137. https://doi.org/10.1055/s-0032-1320657

Millanes AM, Truong C, Westberg M, Diederich P, Wedin M (2014) Host switching promotes diversity in host-specialized mycoparasitic fungi: uncoupled evolution in the *Biatoropsis-Usnea* system. Evolution 68: 1576–1593. https://doi.org/10.1111/evo.12374

Paradis E (2018) Analysis of haplotype networks: The randomized minimum spanning tree method. Methods in Ecology and Evolution 9: 1308–1317. https://doi.org/10.1111/2041-210X.12969

Patterson N, Richter DJ, Gnerre S, Lander ES, Reich D (2006) Genetic evidence for complex speciation of humans and chimpanzees. Nature 441: 1103–1108. https://doi.org/10.1038/nature04789

Pons J, Barraclough T, Gomez-Zurita J, Cardoso A, Duran D, Hazell S, Kamoun S, Sumlin W, Vogler A (2006) Sequence-based species delimitation for the DNA taxonomy of undescribed insects. Systematic Biology 55: 595–609. https://doi.org/10.1080/10635150600852011

Puillandre N, Lambert A, Brouillet S, Achaz G (2012) ABGD, Automatic Barcode Gap Discovery for primary species delimitation. Molecular Ecology 21: 1864–1877. https://doi.org/10.1111/j.1365-294X.2011.05239.x

Quaedvlieg W, Binder M, Groenewald JZ, Summerell BA, Carnegie AJ, Burgess TI (2014) Introducing the Consolidated Species Concept to resolve species in the Teratosphaeriaceae. Persoonia 33: 1–40. https://doi.org/10.3767/003158514X681981

Rambaut A, Suchard MA, Xie D, Drummond AJ (2014) Tracer v1.6. http://beast.bio.ed.ac.uk/Tracer

Rannala B, Yang Z (2003) Bayes estimation of species divergence times and ancestral population sizes using DNA sequences from multiple loci. Genetics 164: 1645–1656.

Redaelli P, Visocchi V (1942) Agostino Bassi precursor of comparative mycopathology Mycopathologia 2: 37–42. https://doi.org/10.1007/BF00450241

Rehner SA, Buckley EP (2005) A *Beauveria* phylogeny inferred from ITS and EF1-a sequences: evidence for cryptic diversification and links to *Cordyceps* teleomorphs. Mycologia 97: 84–98. https://doi.org/10.3852/mycologia.97.1.84

Rehner SA, Posada F, Buckley EP, Infante F, Castillo A, Vega FE (2006) Phylogenetic origins of African and Neotropical *Beauveria bassiana* sl pathogens of the coffee berry borer, *Hypoth-*

enemus hampei. Journal of Invertebrate Pathology 93: 11–21. https://doi.org/10.1016/j.jip.2006.04.005

Rehner SA, Minnis AM, Sung GH, Luangsa-ard JJ, Devotto L, Humber RA (2011) Phylogeny and systematics of the anamorphic, entomopathogenic genus *Beauveria*. Mycologia 103: 1055–1073. https://doi.org/10.3852/10-302

Ronquist F, Teslenko M, Van Der Mark P, Ayres D, Darling A, Hohna S, Larget B, Liu L, Suchard MA, Huelsenbeck JP (2012) MrBayes 3.2: efficient Bayesian phylogenetic inference and model choice across a large model space. Systematic Biology 61: 539–542. https://doi.org/10.1093/sysbio/sys029

Samson RA, Evans HC (1982) Two new *Beauveria* spp. from South America. Journal of Invertebrate Pathology 39: 93–97. https://doi.org/10.1016/0022-2011(82)90162-8

Sanjuan T, Tabima J, Restrepo S, Læssøe T, Spatafora JW, Franco-Molano AE (2014) Entomopathogens of Amazonian stick insects and locusts are members of the *Beauveria* species complex (*Cordyceps sensu stricto*). Mycologia 106: 260–275. https://doi.org/10.3852/13-020

Shrestha B, Hyun MW, Oh J, Han J-G, Lee TH, Cho JY, Kang H, Kim SH, Sung GH (2014) Molecular evidence of a teleomorph-anamorph connection between *Cordyceps scarabaeicola* and *Beauveria sungii* and its implication for the systematics of *Cordyceps* sensu stricto. Mycoscience 55: 231–239. https://doi.org/10.1016/j.myc.2013.09.004

Shimazu M, Mitsuhashi W, Hashimoto H (1988) *Cordyceps brongniartii* sp. nov., the teleomorph of *Beauveria brongniartii*. Transactions of the Mycological Society of Japan 29: 323–330.

Silvestro D, Michalak I (2012) RaxmlGUI: a graphical front-end for RAxML. Organisms Diversity & Evolution 12: 335–337. https://doi.org/10.1007/s13127-011-0056-0

Stamatakis A (2014) RAxML Version 8: A tool for phylogenetic analysis and postanalysis of large phylogenies. Bioinformatics 30: 1312–1313. https://doi.org/10.1093/bioinformatics/btu033

Stewart JE, Timmer LW, Lawrence CB, Pryor BM, Peever TL (2014) Discord between morphological and phylogenetic species boundaries: incomplete lineage sorting and recombination results in fuzzy species boundaries in an asexual fungal pathogen. BMC Evolutionary Biology14: 38. https://doi.org/10.1186/1471-2148-14-38

Sung GH, Hywel-Jones NL, Sung JM, Luangsa-ard JJ, Shrestha B, Spatafora JW (2007) Phylogenetic classification of Cordyceps and the clavicipitaceous fungi. Studies in Mycology 57: 5–59. https://doi.org/10.3114/sim.2007.57.01

Tamura K, Stecher G, Peterson D, Filipski A, Kumar S (2013) MEGA6: Molecular Evolutionary Genetics Analysis Version 6.0. Molecular Biology and Evolution 30: 2725–2729. https://doi.org/10.1093/molbev/mst197

Thompson JD, Higgins DG, Gibson TJ (1994) Clustal W: improving the sensitivity of progressive multiple sequence alignment through sequence weighting, position-specific gap penalties and weight matrix choice. Nucleic Acids Research 22: 4673–4680. https://doi.org/10.1093/nar/22.22.4673

Yang Z, Rannala B (2010) Bayesian species delimitation using multilocus sequence data Proceedings of the National Academy of Sciences 107: 9264–9269. https://doi.org/10.1073/pnas.0913022107

Van Valen L (1976) Ecological species, multispecies, and oaks. Taxon 25: 233–239. https://doi.org/10.2307/1219444

Vuillemin P (1912) *Beauveria*, nouveau genre de Verticilliacées. Bulletin de la Société Botanique de France 29: 34–40. https://doi.org/10.1080/00378941.1912.10832379

Walsh PD (2000) Sample size for the diagnosis of conservation units. Conservation Biology 14: 1533–1537. https://doi.org/10.1046/j.1523-1739.2000.98149.x

Zhang DX, Zhu T, Yang Z (2011) Evaluation of a Bayesian Coalescent Method of Species Delimitation. Systematic Biology 60: 747–761. https://doi.org/10.1093/sysbio/syr071

Supplementary material 1

Tables S1, S2, Figures S1–S4

Authors: Danilo E. Bustamante, Manuel Oliva, Santos Leiva, Jani E. Mendoza, Leidy Bobadilla, Geysen Angulo, Martha S. Calderon

Data type: molecular data

Explanation note: **Table S1.** Results of the Generalized Mixed Yule-Coalescent (GMYC) analyses under the single threshold model. **Table S2.** Highest posterior probabilities of the three-gene Bayesian species delimitation analysis (BPP) by jointing species delimitation and species tree inference. **Figure S1.** Phylogenetic tree based on maximum likelihood inference of combined *Bloc* data. **Figure S2.** Phylogenetic tree based on maximum likelihood inference of combined *RPB*1 data. **Figure S3.** Phylogenetic tree based on maximum likelihood inference of combined *Tef*1 data. **Figure S4.** Bayesian inference ultrametric gene tree.

Link: https://doi.org/10.3897/mycokeys.58.35764.suppl1

MycoKeys 58: 69–82 (2019)
doi: 10.3897/mycokeys.58.36307
http://mycokeys.pensoft.net

RESEARCH ARTICLE

A peer-reviewed open-access journal
MycoKeys
Launched to accelerate biodiversity research

Clitopilus lampangensis (Agaricales, Entolomataceae), a new species from northern Thailand

Jaturong Kumla[1,2], Nakarin Suwannarach[1,2], Witchaphart Sungpalee[3], Kriangsak Sri-Ngernyuang[4], Saisamorn Lumyong[1,2,5]

1 *Department of Biology, Faculty of Science, Chiang Mai University, Chiang Mai 50200, Thailand* **2** *Center of Excellence in Microbial Diversity and Sustainable Utilization, Chiang Mai University, Chiang Mai 50200, Thailand* **3** *Faculty of Agricultural Production, Maejo University, Chiang Mai, 50290, Thailand* **4** *Faculty of Architecture and Environmental Design, Maejo University, Chiang Mai, 50290, Thailand* **5** *Academy of Science, The Royal Society of Thailand, Bangkok 10300, Thailand*

Corresponding author: *Saisamorn Lumyong* (saisamorn.l@cmu.ac.th)

Academic editor: *Kentaro Hosaka* | Received 18 May 2019 | Accepted 4 September 2019 | Published 20 September 2019

Citation: Kumla J, Suwannarach N, Sungpalee W, Sri-Ngernyuang K, Lumyong S (2019) *Clitopilus lampangensis* (Agaricales, Entolomataceae), a new species from northern Thailand. MycoKeys 58: 69–82. https://doi.org/10.3897/mycokeys.58.36307

Abstract

A new species of agaricomycetes, *Clitopilus lampangensis*, is described based on collections from northern Thailand. This species was distinguished from previously described *Clitopilus* species by its pale yellow to grayish yellow pileus with the presence of wider caulocystidia. Molecular phylogenetic analyses, based on the data of the internal transcribed spacers (ITS) and the large subunit (LSU) of the nuclear ribosomal DNA, and the second largest subunit of RNA polymerase II (*rbp2*) genes, also support the finding that *C. lampangensis* is distinct from other species within the genus *Clitopilus*. A full description, color photographs, illustrations and a phylogenetic tree showing the position of *C. lampangensis* are provided.

Keywords

Agaricomycetes, gill mushroom, morphology, phylogeny, tropics

Introduction

The genus *Clitopilus* was proposed by Kummer (1987) with *C. prunulus* (Scop.) P. Kummer as the type species. It belongs to the family Entolomataceae of the order Agaricales. This genus is saprotrophic and is widely distributed, especially in northern temperate areas (Singer 1986; Baroni and Watling 1999; Moncalvo et al. 2002; Kirk et al.

2008; Hartley et al. 2009; Crous et al. 2012; Raj and Manimohan 2018). *Clitopilus* is characterized by basidiocarps that are clitocyboid, omphalinoid or pleurotoid, mostly whitish or occasionally grayish or brownish in color, with pink or pinkish brown spore prints, ellipsoid basidiospores with longitudinal ridges that appear angular in a polar view, and hyphae lack clamp connections (Singer 1986; Noordeloos 1988). There are 30 species of *Clitopilus* worldwide (Kirk et al. 2008), although there are 201 species names recorded in the Index Fungorum (http://www.indexfungorum.org/Names/Names.asp). The taxa list in the Index Fungorum includes synonyms and misidentifications, as well as some species that are not well documented. Formerly, the genus *Clitopilus* included *Rhodocybe* (Moncalvo et al. 2002; Co-David et al. 2009; Vizzini et al. 2011a). However, molecular phylogenetic analyses have provided powerful tools for the identification of *Clitopilus*, leading to the separation of *Clitopilus* from *Rhodocybe* as well as the related genera (*Clitocella* and *Clitopilopsis*) (Cooper 2014; Kluting et al. 2014; Raj and Manimohan 2018).

Only six species, *Clitopilus apalus* (Berk. & Br.) Petch, *C. crispus* Pat. *C. doimaesalongensis* Jatuwong, Karun. & K.D. Hyde, *C. chalybescens* T.J. Baroni & Desjardin, *C. peri* (Berk. & Br.) Petch and *C. prunulus*, have been reported in Thailand (Baroni et al. 2001; Chandrasrikul et al. 2011; Kluting et al. 2014; Jatuwong et al. 2017). During an investigation of macrofungi in northern Thailand, we found a population of *Clitopilus* which we describe here as a new species based on the morphological and molecular characteristics. To confirm its taxonomic status, the phylogenetic relationship of the new species was determined by the ITS and LSU of the rDNA, and the rbp2 genes.

Materials and methods

Sample collection

Basidiocarps were collected in Mae Moh District, Lampang Province, northern Thailand in 2018. Basidiocarps were wrapped in aluminum foil and kept in plastic specimen boxes to be transported to the laboratory. Notes on the macromorphological features and photographs were obtained within 24 h of collection. The specimens were dried at 40–45 °C and deposited at the Herbarium of the Sustainable Development of Biological Resources Laboratory, Faculty of Science, Chiang Mai University (**SDBR-CMU**), and BIOTEC Bangkok Herbarium (**BBH**), Pathumthani, Thailand.

Morphological studies

Macromorphological data were recorded from fresh specimens. The recording of color names and codes followed Kornerup and Wanscher (1978). Micromorphological data were recorded from dry specimens rehydrated in 95% ethanol followed by distilled water, 3% KOH or Melzer's reagent. Anatomical features were based on at least 50

measurements of each structure as seen under a light microscope (Olympus CX51, Japan). For spore statistics, *Q* is the ratio of spore length divided by spore width and **Q** is the average *Q* of all specimens ± standard deviation.

Molecular phylogenetic studies

Genomic DNA of dry specimens (1–10 mg) was extracted using a Genomic DNA Extraction Mini-Kit (FAVORGEN, Taiwan). The ITS region of DNA was amplified by polymerase chain reactions (PCR) using ITS4 and ITS5 primers (White et al. 1990), the LSU of rDNA gene were amplified with LROR and LRO5 primers (Vilgalys and Hester 1990), and *rbp2* gene was amplified with the bRBP2-6F and bRBP2-7.1R primers (Matheny 2005). The amplification program for these three domains was performed in separated PCR reaction and consisted of an initial denaturation at 95 °C for 5 min, followed by 35 cycles of denaturation at 95 °C for 30 s, annealing at 52 °C for 30 s (ITS), 52 °C for 45 s (LSU), and 54 °C for 1 min (*rpb2*), and extension at 72 °C for 1 min on a peqSTAR thermal cycler (PEQLAB Ltd., UK). PCR products were checked on 1 % agarose gels stained with ethidium bromide under UV light. PCR products were purified using a PCR clean up Gel Extraction NucleoSpin Gel and PCR Clean-up Kit (Macherey-Nagel, Germany) following the manufacturer's protocol. The purified PCR products were directly sequenced. Sequencing reactions were performed and the sequences were automatically determined in the genetic analyzer at 1st Base company (Kembangan, Malaysia) using the PCR primers mentioned above. Sequences were used to query GenBank via BLAST (http://blast.ddbj.nig.ac.jp/top-e.html).

For phylogenetic analyses, the sequences from this study, previous studies and the GenBank database were used and provided in Table 1. The multiple sequence alignment was carried out using MUSCLE (Edgar 2004), and the combined ITS and LSU alignment, and *rpb2* alignment were deposited in TreeBASE under the study ID 24373 and 24374, respectively. Phylogenetic trees were constructed using maximum likelihood (ML) and Bayesian inference (BI) algorithms, implemented by RAxML v7.0.3 (Stamatakis 2006) and MrBayes v3.2.6 (Ronquist et al. 2012), respectively. *Rhodocybe griseoaurantia* and *R. pallidogrisea* were used as outgroup. The best-fit substitution model for BI and ML analyses were estimated by jModeltest 2.1.10 (Darriba et al. 2012) using Akaike information criterion (AIC). For ML analysis, the bootstrap (BS) replicates were set as 1000 and used to test phylogeny (Felsenstein 1985). Clades with bootstrap values (BS) of ≥ 70% were considered significantly supported (Hillis and Bull 1993). For the BI analysis, the Markov chains were run for one million generations, with six chains and random starting trees. The chains were sampled every 100 generations. Among these, the first 2,000 trees were discarded as burn-in, while the postburn-in trees were used to construct the 50% majority-rule consensus phylogram with calculated Bayesian posterior probabilities. Bayesian posterior probabilities (PP) ≥ 0.95 were considered significant support (Alfaro et al. 2003).

Table 1. Sequences used for phylogenetic analysis. The newly generated sequences are in bold.

Taxa	Voucher/strain	GenBank accession number			Refernces
		ITS	LSU	*rpb2*	
Clitopilus albidus	CAL 1320	MF926596	MF926595	MF946579	Raj and Manimohan 2018
	CORT:26394WAT	–	KR869936	KC816906	Largent and Bergemann 2016
	M536	–	AF261287	–	Moncalvo et al. 2002
Clitopilus austroprunulus	MEN2009062	KC139085	–	–	Phillips and Dinis 2012
	MEN2009001	KC139084	–	–	Phillips and Dinis 2012
Clitopilus cf. *argentinus*	MTB480412	–	–	KC816907	Kluting et al. 2014
Clitopilus chalybescens	MFUCC130808	KP938184	–	–	Jatuwong et al. 2017
	MFUCC130809	KP938185	–	–	Jatuwong et al. 2017
	SDBR-CMUUP0039	**MK773645**	**MK764940**	**MK784129**	This study
Clitopilus chrischonensis	TOHG 1994	HM623128	HM623131	–	Vizzini et al. 2011b
Clitopilus crispus	GDGM29931	JQ281489	–	–	He et al. 2012
	CORT:9982	–	–	KC816910	Kluting et al. 2014
	CORT:10027	–	–	KC816911	Kluting et al. 2014
Clitopilus cystidiatus	26	–	GQ289147	GQ289220	Co-David et al. 2009
	TOAV130	HM623129	HM623132	–	Vizzini et al. 2011b
Clitopilus doimaesalongensis	MFUCC130806	KP938183	–	–	Jatuwong et al. 2017
Clitopilus fusiformis	SAAS1038	KY385634	–	KY385632	Wang et al. 2017
	SAAS1892	KU751777	–	KY385633	Wang et al. 2017
Clitopilus giovanellae	SF14368	EF413030	EF413027	–	Moreno et al. 2007
Clitopilus hobsonii	CBS 270.36	FJ770395	–	–	Hartley et al. 2009
	CBS 445.86	FJ770385	–	–	Hartley et al. 2009
	DLL9635	–	–	KC816913	Kluting et al. 2014
	DLL9643	–	–	KC816913	Kluting et al. 2014
Clitopilus lampangensis	SDBR-CMUJK 0147	**MK764933**	**MK764935**	**MK784127**	This study
	SDBR-CMUNK 0047	**MK764934**	**MK773856**	**MK784128**	This study
Clitopilus kamaka	KA12-0364	KR673433	–	–	Kim et al. 2015
Clitopilus orientalis	CAL 1616	MG345134	MG321558	MG321559	Raj and Manimohan 2018
Clitopilus passeckeriamus	CBS299.35	MH855682	MH867198	–	Vu et al. 2019
	P78	KY962494	KY963078	–	Unpublished
Clitopilus paxilloides	CORT:5809	–	–	KC816919	Kluting et al. 2014
Clitopilus peri	CORT:10033	–	–	KC816920	Kluting et al. 2014
	CORT:10040	–	–	KC816921	Kluting et al. 2014
	CORT:10041	–	–	KC816922	Kluting et al. 2014
Clitopilus pinsitus	CBS 623.70	MH859879	MH871665	–	Vu et al. 2019
Clitopilus prunulus	Champ-15	KX449418	–	–	Pérez-Lzquierdo et al. 2017
	CBS 227.93	FJ770408	–	–	Hartley et al. 2009
	Noordeloos 2003-09-14	KR261096	–	–	Unpublished
	COPT:7003	–	–	KC816925	Kluting et al. 2014
	TB9663	–	–	GU384648	Baroni et al. 2011
	TB8229	–	–	GU384650	Baroni et al. 2011
	COPT:REH8456	–	–	KC816923	Kluting et al. 2014
Clitopilus reticulosporus	DC-2010	KC885966	HM164414	HM164416	Vu et al. 2019
Clitopilus scyphoides	CBS 127.47	MH856181	MH867707	–	Vu et al. 2019
	CBS 400.79	FJ770401	–	–	Hartley et al. 2009
Clitopilus subscyphoides	CAL 1325	MF927542	MF946580	MF946581	Raj and Manimohan 2018
Clitopilus venososulcatus	CORT:8111	–	–	KC816930	Kluting et al. 2014
Rhodocybe griseoaurantia	CAL 1324	KX083571	KX83574	KX083568	Unpublished
Rhodocybe pallidogrisea	CORT 013944	NR154437	–	KC816968	Kluting et al. 2014

Results

Phylogenetic analyses

The topology of each single-gene of ITS and LSU, and the combined ITS and LSU phylograms were found to be similar. However, differences were observed in the topology of the *rbp2* gene. Therefore, we present only the combined ITS and LSU gene phylogram (Fig. 1), and the single *rbp2* gene phylogram (Fig. 2). The combined ITS and LSU sequence dataset consisted of 34 taxa and were comprised of 1774 characters including gaps (ITS: 1–779, LSU: 780–1774). The sequence dataset of *rbp2* consisted of 27 taxa and the aligned dataset was comprised of 620 characters that included gaps. The GTR model with gamma rate heterogeneity and invariant sites (GTR+G+I) was the best-fit model used for both ML and BI analyses that were selected by AIC. The average standard deviation of the split frequencies fell to 0.011364 and 0.009837 in the BI analysis of the combined ITS and LSU, and *rbp2* sequences, respectively after one million generations. This was observed after the 50% majority consensus phylogram was constructed. The ML analysis of the combined ITS and LSU sequences was based on the parameters estimated under the GTR+I+G model, and the proportion of the invariable sites and the gamma shape parameters were 0.0250 and 0.9320, respectively. Additionally, the tree with log likelihood (-8211.7515) was built after 1000 bootstrapping replications. In the ML analysis of the *rbp2* sequence that was based on the GTR+I+G model, the proportion of the invariable sites and the gamma shape parameters were 0.5400 and 1.7960, respectively, while the tree with log likelihood (-3640.1616) was built after 1000 bootstrapping replications.

Both the combined ITS and LSU, and the *rbp2* phylograms indicated that the sequences were of a new species, *C. lampangensis*, that had formed a monophyletic clade with high BS (100 %) and PP (1.0) support (Figs 1, 2). A combined ITS and LSU phylogram revealed that the new species was a sister taxon to *C. chalybescens*. In addition, the *rbp2* phylogram indicated that the new species was a sister taxon to *C. chalybescens* and *C. peri*.

Taxonomy

Clitopilus lampangensis **J. Kumla, N. Suwannarach & S. Lumyong, sp. nov.**
MycoBank No.: 830890
Fig. 3

Diagnosis. Distinguished from other *Clitopilus* species by its pale yellow to grayish yellow pileus with the presence of caulocystidia, and from *C. chalybescens* by its wider caulocystidia, longer basidiospores, and lack of grayish blue color change on the pileus and stipe when bruised.

Etymology. '*lampangensis*', referring to Lampang Province, where the holotype was found.

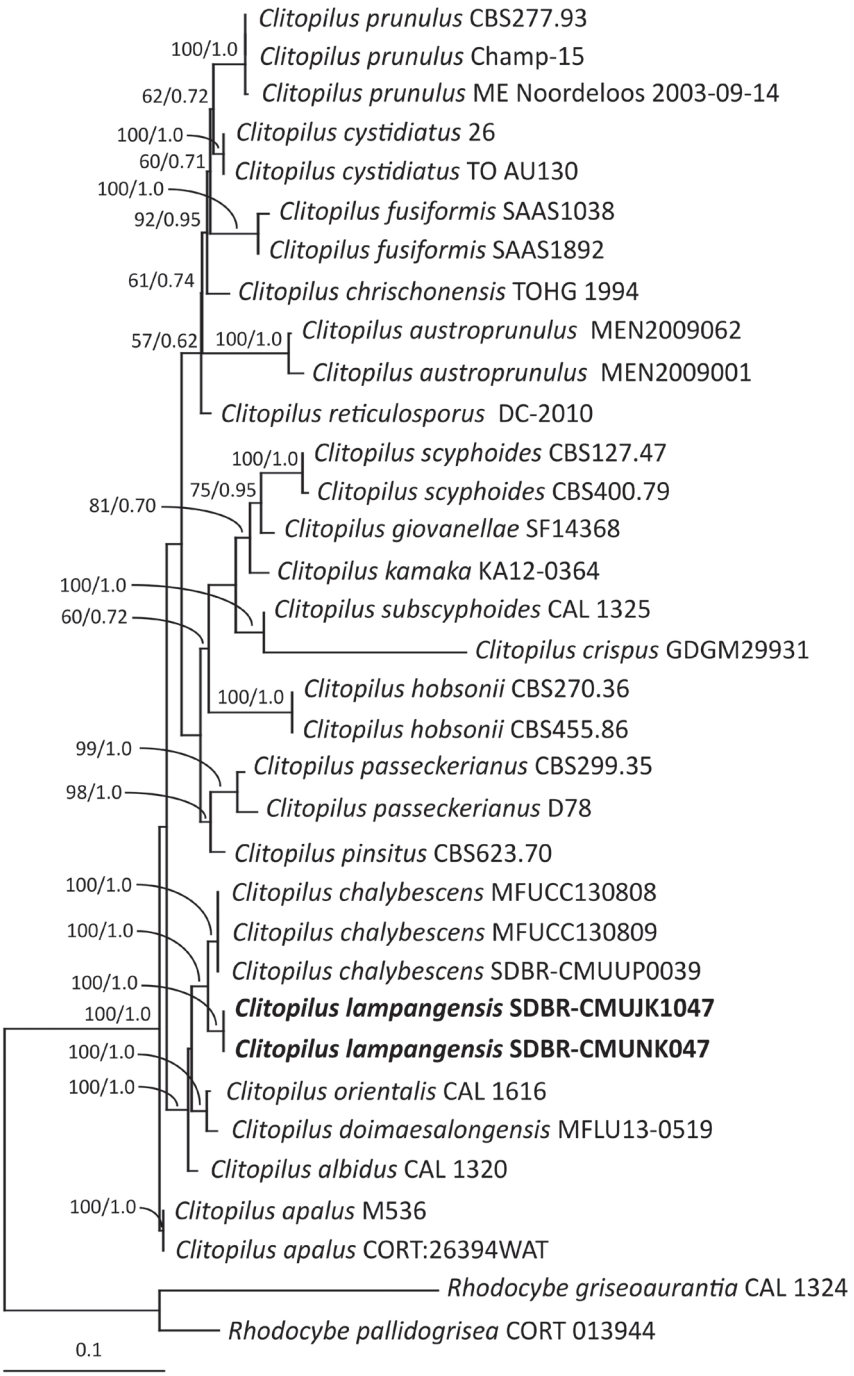

Figure 1. Phylogram derived from maximum likelihood analysis of the combined ITS and LSU region of nuclear rDNA of 34 sequences. *Rhodocybe griseoaurantia* and *R. pallidogrisea* were used as outgroup. The numbers above branches represent maximum likelihood bootstrap percentages (left) and Bayesian posterior probabilities (right). Only bootstrap values ≥ 50 % are shown, and the scale bar represents ten substitutions per nucleotide position. The fungal species obtained in this study are in bold.

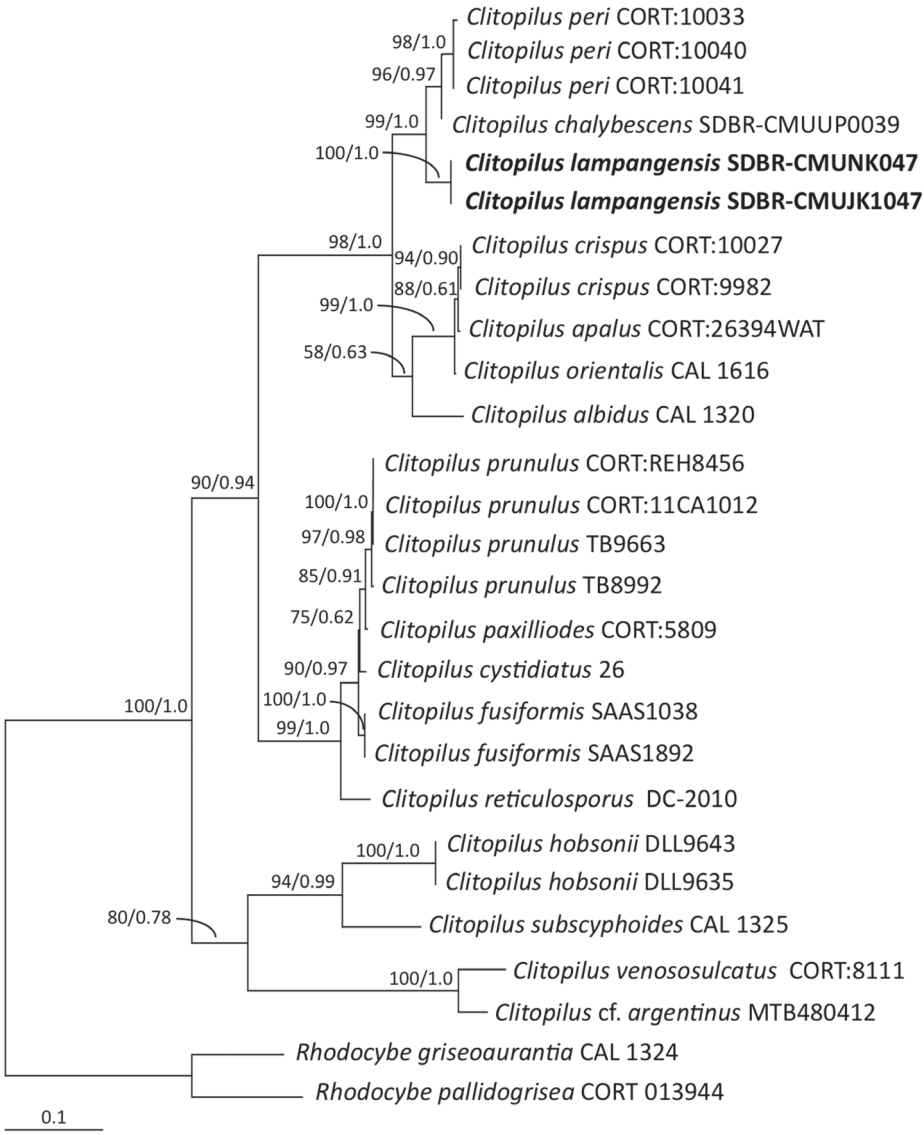

Figure 2. Phylogram derived from maximum likelihood analysis of *rpb2* gene of 27 sequences. *Rhodocybe griseoaurantia* and *R. pallidogrisea* were used as outgroup. The numbers above branches represent maximum likelihood bootstrap percentages (left) and Bayesian posterior probabilities (right). Only bootstrap values ≥ 50 % are shown, and the scale bar represents ten substitutions per nucleotide position. The fungal species obtained in this study are in bold.

Holotype. THAILAND, Lampang Province, Mae Moh District, (18°24'21"N, 99°42'26"E, elevation 380 m), on ground in a tropical deciduous forest, May, 2018, J. Kumla & N. Suwannarach, SDBR-CMUJK 0147 and BBH 43590 (isotype).

Gene sequence (from holotype). MK764933 (ITS), MK764935 (LSU) and MK784127 (*rbp2*).

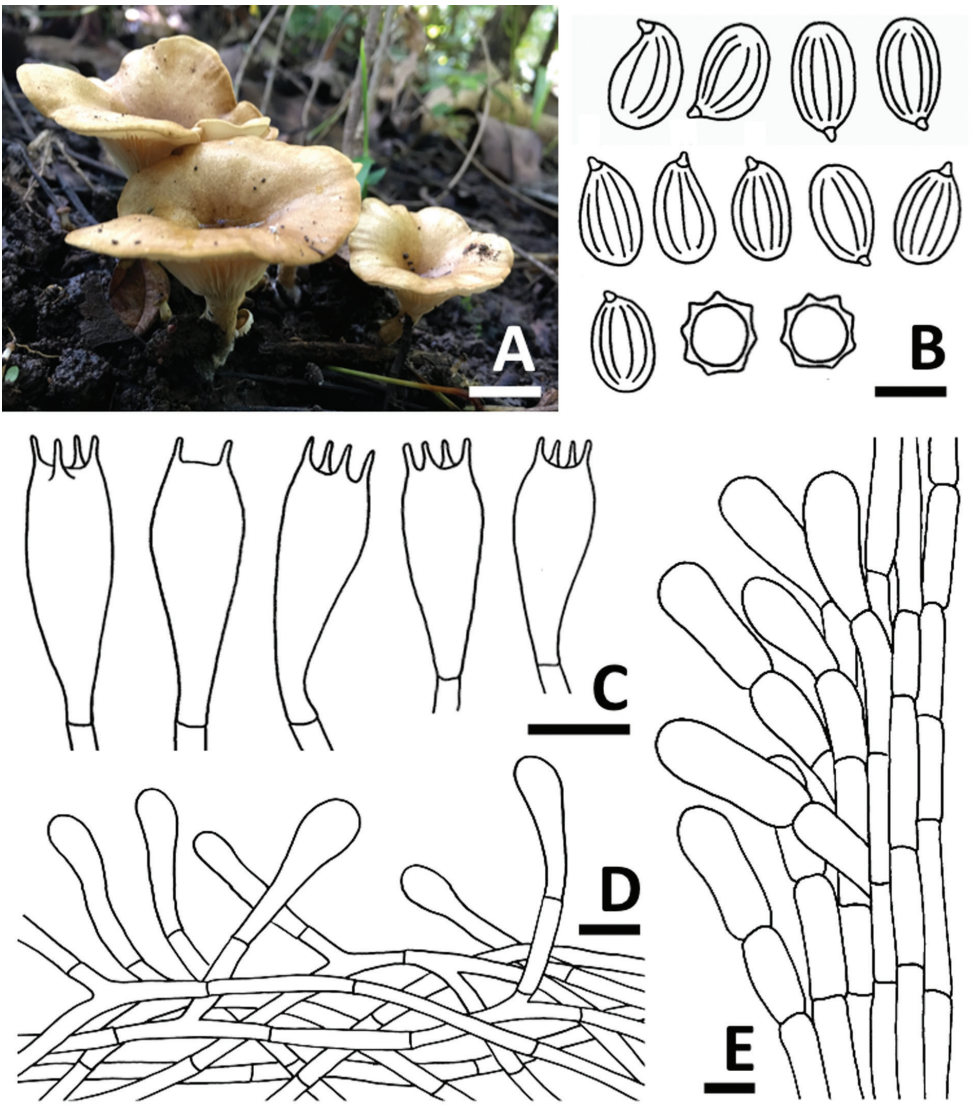

Figure 3. *Clitopilus lampangensis* SDBR-CMUJK 0147 (holotype). **A** Basidiocarps **B** Basidiospores **C** Basidia **D** Pileipellis **E** Caulocystidia. Scale bars: 10 mm (**A**), 5 µm (**B**), 10 µm (**C–E**).

Basidiocarps small, clitocyboid. Pileus 35–50 mm diam., initially convex or somewhat plano-convex with or without a central depression, becoming deeply umbilicate with age; surface pale yellow (4A3) to greyish yellow (4B5), somewhat velutinous, finely pruinose all over; margin incurved to slightly inrolled, entire or slightly wavy. Lamellae subdecurrent to decurrent, white (1A1), crowded, up to 2.5 mm wide, with lamellulae of 1–3 lengths; edge entire or slightly wavy, concolorous with the sides. Stipe 20–25 × 5–8 mm, central, solid; surface white (1A1) to yellowish white (4A2),

finely pruinose all over, densely so towards the apex; base with white cottony mycelium. Odor strong farinaceous. A pale pinkish spore print.

Basidiospores 7.0–9.0 × 3.0–5.0 µm, Q = 1.40–2.33, **Q** = 1.82 ± 0.27, ellipsoid in polar view, amygdaliform to limoniform in side view, with 6–8 prominent longitudinal ridges, colorless, thin-walled. Basidia 17.0–25.0 × 4.0–8.0 µm, clavate, colorless, thin-walled, 2- and 4-spored; sterigmata up to 4 µm long. Lamella-edge fertile. Pleurocystidia and cheilocystidia absent. Lamellar trama subregular; hyphae 2.5–4.0 µm wide, hyaline, thin-walled. Pileus trama compact, hyaline, cylindrical hyphae 5–10 µm wide. Pileipellis a cutis of loosely interwoven hyphae; 3–5 µm wide, hyaline, thin-walled, and terminal cells; subcylindric or narrowly clavate, 4–8 µm wide. Stipitipellis at stipe apex a layer of repent, hyaline, cylindrical hyphae 4–8 µm wide, thin-walled. Caulocystidia 25.5–42.5 × 8.0–15.0 µm, single or clustered, erect or repent, varying in shape from cylindrical to clavate, hyaline, slightly thick-walled. Clamp connections absent in all tissues.

Ecology and distribution. Fruiting solitary or gregarious on soil in a tropical deciduous forest. Known only from northern Thailand

Specimens examined. THAILAND, Lampang Province, Mae Moh District, (18°24'20"N, 99°42'3"E, elevation 375 m), on ground in a tropical deciduous forest, May, 2018, N. Suwannarach & J. Kumla, SDBR-CMUNK 0047, GenBank sequence MK764934 (ITS), MK773856 (LSU) and MK784128 (*rbp2*).

Discussion

The present study has identified a new species of *Clitopilus* acquired from northern Thailand based on both morphological characteristics and phylogenetic analyses. *Clitopilus lampangensis* is characterized by its clitocyboid, pale yellow to grayish yellow basidiocarps, pinkish spore-print, ellipsoid basidiospores with longitudinal ridges and hyphae lacking clamp connections. Thus, these morphological characteristics support its placement into the genus *Clitopilus* (Singer 1986; Noordeloos 1988). Based on the morphology, the pale yellow to grayish yellow pileus of *C. lampangensis* distinguishes it from the white and grayish pileus of *Clitopilus* species, with the exceptions of *C. catalonicus*, *C. djellouliae*, *C. fasciculatus*, *C. gallaecicus*, *C. giovanellae*, *C. incrustatus*, *C. luteocinnamomeus* and *C. prunulus*, (Kummer 1871; Singer 1942; Noordeloos 1984; Baroni and Halling 2000; Moreno et al. 2007; Ovrebo and Baroni 2007; Vila et al. 2008; Contu et al. 2011; Desjardin et al. 2015). The characteristics of the basidiocarps and size of the basidia, caulocystidia and basidiospores of *C. lampangensis* were compared with related *Clitopilus* species (Table 2). The presence of caulocystidia in *C. lampangensis* clearly distinguishes it from these related species. Moreover, the pileus of *C. lampangensis* (35–50 mm in diameter) are larger than *C. djellouliae* (6–18 mm in diameter; Contu et al. (2011)), *C. giovanellae* (5–15 mm in diameter; Singer (1942) and Moreno et al. (2007)) and *C. catalonicus* (up to 15 mm in diameter; Vila et al. (2008)). Prior to this study, *C. apalus*, *C. crispus*, *C. doimaesalongensis*, *C. chalybescens*, *C. peri* and *C. prunulus* had been found in Thailand

Table 2. Comparison of *Clitopilus lampangensis* with the closely related species.

Taxa	Origin	Pileus	Basidia	Caulocystidia	Basidiospores
C. lampangensis[a]	Thailand	35–50 mm in diameter, pale yellow to greyish yellow	17.0–25.0 × 4.0–8.0 µm, 2–4 streigmata	25.5–42.5 × 8.0–15.0 µm	Ellipsoid, 7.0–9.0 × 3.0–5.0 µm, 6–8 longitudinal ridges
C. chalybescens[b, c]	Thailand	15–90 mm in diameter, white, yellowish white to greyish blue	15.0–21.0 × 5.1–8.0 µm, 4 streigmata	16.0–32.0 × 5.0–7.0 µm	Ellipsoid, 5.3–7.5 × 3.6–5.0 µm, 8–10 longitudinal ridges
C. peri[d,e]	India, Sri Lanka, Thailand	8–22 mm in diameter, white	16.0–18.0 × 5.0–7.0 µm, 4 streigmata	Absent	Ellipsoid, 6.7–8.5 × 3.0–4.0 µm, 6–9 longitudinal ridges
C. prunulus[f,g]	Netherlands, Thailand, United State	25–80 mm in diameter, white, yellowish white to grayish or yellow cream	25.0–47.0 × 7.0–12.0 µm, 4 streigmata	Absent	Ellipsoid, 9.0–14.0 × 4.5–8.0 µm, 6–8 longitudinal ridges
C. fasciculatus[h]	Netherlands,	20–70 mm in diameter, pale brown	Sizes were not reported, 4 streigmata	Absent	Ellipsoid, 4.5–6.3 × 3.0–4.0 µm, 3–6 longitudinal ridges
C. gallaecicus[i]	Spain	80–90 mm in diameter, creamy, ochre to ochre-brown	20.0–35.0 × 8.5–10.5 µm, 4 streigmata	Absent	Ellipsoid, 8.0–14.5 × 4.5–7.5 µm, 3–6 longitudinal ridges
C. incrustatus[j]	Costa Rica, United State	80–90 mm in diameter, grayish brown	16.0–24.0 × 7.0–8.0 µm, 4 streigmata	Absent	Ellipsoid, 5.0–6.5 × 3.0–4.0 µm, 3–6 longitudinal ridges
C. djellouliae[k]	France	6–18 mm in diameter, light yellowish brown	22.0–32.0 × 7.5–8.5 µm, 4 streigmata	Absent	Ellipsoid, 6.0–9.0 × 4.0–6.0 µm
C. giovanellae[l,m]	Italy, Spain	5–15 mm in diameter, grayish to light brown	14.0–22.0 × 6.5–9.5 µm, 4 streigmata	Absent	Ellipsoid, 5.0–8.0 × 3.0–4.0 µm
C. luteocinnamomeus[n]	Panama	15–45 mm in diameter, ochre to light cinnamon-brown	19.0–27.0 × 6.0–7.0 µm, 4 streigmata	Absent	Subglobose to ellipsoid, 4.5–6.0 × 3.5–5.0 µm
C. catalonicus[o]	Panama	Up to 15mm in diameter, light yellowish brown	32.0–40.0 × 6.4–8.0 µm, 4 streigmata	Absent	Ellipsoid, 5.3–7.5 × 3.7–4.5 µm

[a]This study, [b]Baroni et al. (2001), [c]Jatuwong et al. (2017), [d]Pegler (1986), [e] Kluting et al. (2014), [f]Kummer (1871), [g]Desjardin et al. (2015), [h]Noordeloos (1984), [i]Blanco-Dios (2013), [j]Baroni and Halling (2000), [k]Contu et al. (2011), [l]Singer (1942), [m]Moreno et al. (2007), [n]Ovrebo and Baroni (2007) and [o]Vila et al. (2008).

(Baroni et al. 2001; Chandrasrikul et al. 2011; Kluting et al. 2014; Jatuwong et al. 2017). However, *C. apalus*, *C. crispus*, *C. peri* and *C. doimaesalongensis* differ from *C. lampangensis* by their white to chalk-white pileus and a lack of caulocystidia (Pegler 1986; Yang 2000; Jatuwong et al. 2017). The larger basidia and basidiospores, and the absence of caulocystidia in *C. prunulus* clearly differentiate it from *C. lampangensis* (Kummer 1871; Desjardin et al. 2015) (Table 2). Both *C. lampangensis* and *C. chalybescens* have caulocystidia (Baroni et al. 2001; Jatuwong et al. 2017). However, the width of the caulocystidia and the length of the basidiospores of *C. chalybescens* are narrower and shorter than in *C. lampangensis* (Table 2) (Baroni et al. 2001; Jatuwong et al. 2017).

The phylogenetic analyses of the combined ITS and LSU, and *rpb2* sequences confirmed that *C. lampangensis* formed a monophyletic clade which clearly separated it from the other *Clitopilus* species. *Clitopilus lampangensis* forms a sister taxon to *C. chalybescens* and *C. peri*. *Clitopilus peri* differs from *C. lampangensis* by its smaller white basidiocarps (8–22 mm in diameter) and the absence of caulocystidia (Pegler 1986).

Additionally, the different morphological characteristics that exist between *C. lampangensis* and *C. chalybescens* have been mentioned above.

Therefore, a combination of the morphological characteristics and the molecular analyses strongly support recognition of a new fungus species. This discovery is considered important in terms of stimulating a deeper investigation of macrofungi in Thailand, and will help researchers to better understand the distribution and ecology of *Clitopilus*.

Key to *Clitopilus* species known from Thailand

1 Pileus white to chalk-white colors **2**
– Pileus white or with other colors **5**
2 Stipe ≥ 3 mm thick **3**
– Stipe < 3 mm thick ..... ***C. peri***
3 Basidia < 8 µm wide **4**
– Basidia ≥ 8 µm wide, basidiospores 6.8–9.2 × 4.1–5.5 µm ..... ***C. doimaesalongensis***
4 Basidia up to 25 µm, basidiospores 6–8.5 × 4.5–5.5 µm ..... ***C. apalus***
– Basidia up to 30 µm, basidiospores 5.5–9 × 4–6 µm ..... ***C. cripus***
5 Pileus white to pale grayish or yellowish cream colors **6**
– Pileus pale yellow to greyish yellow colors, caulocystidia present, basidiospores 7.0–9.0 × 3.0–5.0 µm ..... ***C. lampangensis***
6 Basidia ≥ 25 µm long, caulocystidia absent, basidiospores 8.0–12.0 × 4.0–6.5 µm ..... ***C. prunulus***
– Basidia < 25 µm long, caulocystidia present, basidiospores 5.3–7.5 × 3.6–5.0 µm ..... ***C. chalybecens***

Acknowledgements

This work was supported by grants from Chiang Mai University and Center of Excellence on Biodiversity (BDC), Office of Higher Education Commission (BDC-PG3-161005), Thailand. We are grateful to staff of Mae Moh Forestry Industry Organization for their excellent field assistance, and Dr. Eric H.C. McKenzie for English proof reading.

References

Alfaro ME, Zoller S, Lutzoni F (2003) Bayes or bootstrap? A simulation study comparing the performance of Bayesian Markov Chain Monte Carlo sampling and bootstrapping in assessing phylogenetic confidence. Molecular Biology and Evolution 20: 255–266. https://doi.org/10.1093/molbev/msg028

Baroni TJ, Desjardin DE, Hywel-Jones NL (2001) *Clitopilus chalybescens*, a new species from Thailand. Fungal Diversity 6: 13–17.

Baroni TJ, Halling RE (2000) Some *Entolomataceae* (Agaricales) from Costa Rica. Brittonia 52(2): 121–135. https://doi.org/10.2307/2666502

Baroni TJ, Hofstetter V, Vilgalys R, Largent DL (2011) *Entocybe* is proposed as a new genus in the Entolomataceae (Agaricomycetes, Basidiomycota) based on morphological and molecular evidence. North America Fungi 6(12): 1–19. https://doi.org/10.2509/naf2011.006.012

Baroni TJ, Watling R (1999) Taxonomic and mycogeographic notes on some Malaysian fungi IV. Notes on *Clitopilus* and *Rhodocybe*. Mycotaxon 72: 57–72.

Blanco-Dios JB (2013) *Clitopilus gallaecicus*, a new species in section *Pleurotelloides* from Spain. Österr Z Pilzk 22: 15–20.

Chandrasrikul A, Suwanarit P, Sangwanit U, Lumyong S, Payapanon A, Sanoamuang N, Pukahuta C, Petcharat V, Sardsud U, Duengkae K, Klinhom U, Thongkantha S, Thongklam S (2011) Mushroom (Basidiomycetes) in Thailand. Office of Natural Resources and Environmental Policy and Planning, Bangkok, 482 pp.

Co-David D, Langeveld D, Noordeloos ME (2009) Molecular phylogeny and spore evolution of *Entolomataceae*. Persoonia 23: 147–176. https://doi.org/10.3767/003158509X480944

Contu M, Vizzini A, Roux P, Garcia G (2011) *Clitopilus djeloullii* spec. nov. (Agaricales, Entolomataceae) une nouvelle espéce de la Sect *Rhodocybe*. Bulletin Mycologique et Botanique Dauphine-Savoie, 200–2001: 157–164.

Cooper JA (2014) New species and combinations of some New Zealand agarics belonging to *Clitopilus*, *Lyophyllum*, *Gerhardtia*, *Clitocybe*, *Hydnangium*, *Mycena*, *Rhodocollybia* and *Gerronema*. Mycosphere 5(2): 263–288. https://doi.org/10.5943/mycosphere/5/2/2

Crous PC, Shivas RG, Wingfield MJ, Summerell BA, Rossman AY, Alves JL, Adams GC, Barreto RW, Bell A, Coutinho ML, Flory SL, Gates G, Grice KR, Hardy GESJ, Kleczewski NM, Lombard L, Longa CMO, Louis-Seize G, Macedo F, Mahoney DP, Maresi G, Martin-Sanchez PM, Marvanová L, Minnis AM, Morgado LN, Noordeloos ME, Phillips AJL, Quaedvlieg W, Ryan PG, Saiz-Jimenez C, Seifert KA, Swart WJ, Tan YP, Tanney JB, Thu PQ, Videira SIR, Walker DM, Groenewald JZ (2012) Fungal Planet description sheets: 128–153. Persoonia 29: 146–201. https://doi.org/10.3767/003158512X661589

Darriba D, Taboada GL, Doallo R, Posada D (2012) jModelTest 2: more models, new heuristics and parallel computing. Nature Methods 9(8): 772. https://doi.org/10.1038/nmeth.2109

Desjardin DE, Wood MG, Stevens FA (2015) California mushrooms: the comprehensive identification guide. Timber Press, Portland, 1–182.

Edgar RC (2004) MUSCLE: multiple sequence alignment with high accuracy and high throughput. Nucleic Acids Research 32(5): 1792–1797. https://doi.org/10.1093/nar/gkh340

Felsenstein J (1985) Confidence intervals on phylogenetics: an approach using bootstrap. Evolution 39: 783–791. https://doi.org/10.1111/j.1558-5646.1985.tb00420.x

Hillis DM, Bull JJ (1993) An empirical test of bootstrapping as a method for assessing confidence in phylogenetic analysis. Systematic Biology 42(2): 182–192. https://doi.org/10.1093/sysbio/42.2.182

Hartley AJ, de Mattos-Shipley K, Collins CM, Kilaru S, Foster GD, Bailey AM (2009) Investigating pleuromutilin-producing *Clitopilus* species and related basidiomycetes. FEMS Microbiology Letter 297(1): 24–30. https://doi.org/10.1111/j.1574-6968.2009.01656.x

He XL, Li TH, Jiang ZD, Shen YH (2012) Four new species of *Entoloma* s.l. (Agaricales) from southern China. Mycological Progress 11(4): 915–925. https://doi.org/10.1127/0029-5035/2011/0092-0425

Jatuwong K, Hyde KD, Karunarathna SC, Chamyoung S, Kakumyan P (2017) Two species of *Clitopilus* (Entolomataceae, Agaricales) from northern Thailand. Chiang Mai Journal of Science 44(1): 115–124.

Kim CS, Jo JW, Kwang YN, Sung GH, Lee SG, Kim SY, Shin CH, Han SK (2015) Mushroom flora of Ulleung-gun and a newly recorded *Bovista* species in the Republic of Korea. Mycobiology 43(3): 239–257. https://doi.org/10.5941/MYCO.2015.43.3.239

Kirk PM, Cannon PF, Minter DW, Stalpers JA (2008) Dictionary of the Fungi (10th edn). CABI Publishing, Wallingford, 640 pp.

Kluting K, Baroni TJ, Bergemann S (2014) Toward a stable classification of genera within the Entolomataceae: a phylogenetic re-evaluation of the Rhodocybe-Clitopilus clade. Mycologia 106(6): 1127–1142. https://doi.org/10.3852/13-270

Kornerup A, Wanscher JH (1978) Methuen Handbook of Colour (3rd edn). Methuen, London, 252 pp.

Kummer P (1871) De Führer in die Pizkunde, Luppe, Zerbst, 146 pp.

Largent DL, Bergemann SE (2016) *Pouzarella alissae*, a new species from northwestern California, United States. Mycotaxon 130(4): 1153–1164. https://doi.org/10.5248/130.1153

Matheny PB (2005) Improving phylogenetic inference of mushrooms with RPB1 and RPB2 nucleotide sequences (*Inocybe*, Agaricales). Molecular Phylogenetics and Evolution 35(1): 1–20. https://doi.org/10.1016/j.ympev.2004.11.014

Moncalvo JM, Vilgalys R, Redhead SA, Johnson JE, James TY, Catherine AM, Hofstetter V, Verduin SJ, Larsson E, Baroni TJ, Greg TR, Jacobsson S, Clemencon H, Miller Jr OK (2002) One hundred and seventeen clades of euagarics. Molecular Phylogenetics and Evolution 23(3): 357–400. https://doi.org/10.1016/S1055-7903(02)00027-1

Moreno G, Contu M, Orteqa A, Platas G, Peláez F (2007) Molecular phylogenetic studies show *Omphalina giovanellae* represents a new section of *Clitopilus* (Agaricomycetes). Mycological Research 111(12): 1399–1405. https://doi.org/10.1016/j.mycres.2007.09.009

Noordeloos ME (1984) Notulae ad floram agaricinam neerlandicam IV-V. *Clitopilus* and *Leucopaxillus*. Persoonia 12(2): 155–167.

Noordeloos ME (1988) *Entolomataceae*. In: Bas C, Kuyper TW, Noordeloos ME, Vellinga EC (Eds) Flora Agaricina Neerlandica 1. AA Balkema, Rotterdam, 77–182.

Ovrebo CL, Baroni TJ (2007) New taxa of *Tricholomataceae* and *Entolomataceae* (Agaricales) from central America. Fungal Diversity 27: 157–170.

Pegler DN (1986) Agaric Flora of Sri Lanka. Kew Bulletin Additional Series 12: 1–519.

Pérez-Lzquierdo L, Morin E, Maurice JP, Martin F, Rincón A, Buée M (2017) A new promising phylogenetic marker to study the diversity of fungal communities: The Glycoside Hydrolase 63 gene. Molecular Ecology Resources 17(6): e1–e11. https://doi.org/10.1111/1755-0998.12678

Phillips AJL, Dinis MFMADM (2012) Fungal planet description sheets: 128–153. Persoonia 29: 146–201. https://doi.org/10.3767/003158512X661589

Raj KNA, Manimohan P (2018) A new species and a new record of *Clitopilus* and a description of *C. orientalis* from India based on morphology and molecular phylogeny. Phytotaxa 343(1): 47–59. https://doi.org/10.11646/phytotaxa.343.1.4

Ronquist F, Teslenko M, Van der Mark P, Ayres DL, Darling A, Höhna S, Larget B, Liu L, Suchard MA, Huelsenbeck JP (2012) MrBayes 3.2: efficient Bayesian phylogenetic inference and model choice across a large model space. Systematic Biology 61(3): 539–542. https://doi.org/10.1093/sysbio/sys029

Singer R (1942) Type studies on Basidiomycetes. I. Mycologia 34(1): 61–93. https://doi.org/10.1080/00275514.1942.12020874

Singer R (1986) The Agaricales in Modern Taxonomy (4th edn). Koeltz Scientific Books, Koenigstein, 981 pp.

Stamatakis A (2006) RAxML-VI-HPC: maximum likelihood-based phylogenetic analyses with thousands of taxa and mixed models. Bioinformatics 22(21): 2688–2690. https://doi.org/10.1093/bioinformatics/btl446

Vila J, Contu M, Ortega A (2008) A new species of *Rhodocybe* (*Agaricales*, *Entolomataceae*) from Catalonia (Iberian Peninsula). Österreichische Zeitschrift für Pilzkunde 17: 75–79.

Vilgalys R, Hester M (1990) Rapid genetic identification and mapping of enzymatically amplified ribosomal DNA from several *Cryptococcus* species. Journal of Bacteriology 172(8): 4238–4246. https://doi.org/10.1128/jb.172.8.4238-4246.1990

Vizzini A, Dähncke RM, Contu M (2011a) *Clitopilus canariensis* (Basidiomycota, Entolomataceae), a new species in the *C. nitellinus*-complex (*Clitopilus* subg. *Rhodophana*) from the Canary Islands (Spain). Brittonia 63(4): 484–488. https://doi.org/10.1007/s12228-011-9187-z

Vizzini A, Musumeci E, Ercole E, Contu M (2011b) *Clitopilus chrischonensis* sp. nov. (Agaricales, Entolomataceae), a striking new fungal species from Switzerland. Nova Hedwigia 92(3–4): 425–434. https://doi.org/10.1127/0029-5035/2011/0092-0425

Vu D, Groenewald M, de Vires M, Gehrmann T, Stielow B, Eberhard U, Al-Hatmi AM, Groenewald JZ, Cardinali G, Boekhout T, Crous P, Robert V, Verkleij GJ (2019) Large-scale generation and analysis of filamentous fungal DNA barcodes boosts coverage for kingdom fungi and reveals thresholds for fungal species and higher taxon delimitation. Studies in Mycology 92: 135–154. https://doi.org/10.1016/j.simyco.2018.05.001

Wang D, Deng WQ, He XL, Peng WH, Gan BC (2017) *Clitopilus fusiformis* (Entolomataceae; Agaricales), a new species from Southwest China. Phytotaxa 321(2): 201–207. https://doi.org/10.11646/phytotaxa.321.2.5

White TJ, Bruns T, Lee S, Taylor J (1990) Amplification and direct sequencing of fungal ribosomal RNA genes for phylogenetics. In: Innis MA, Gelfand DH, Sninsky JJ, White TJ (Eds) PCR Protocols: A Guide to Methods and Applications. Academic Press, San Diego, California, 315–322. https://doi.org/10.1016/B978-0-12-372180-8.50042-1

Yang ZL (2000) Note on five common but littlr known higher basidiomycetes from tropical Yunnan, China. Mycotaxon 74(1): 45–56.

MycoKeys 58: 83–102 (2019)
doi: 10.3897/mycokeys.58.37176
http://mycokeys.pensoft.net

RESEARCH ARTICLE

A peer-reviewed open-access journal
MycoKeys
Launched to accelerate biodiversity research

Three novel insect-associated species of *Simplicillium* (Cordycipitaceae, Hypocreales) from Southwest China

Wan-Hao Chen[1], Chang Liu[2], Yan-Feng Han[3], Jian-Dong Liang[1], Wei-Yi Tian[1], Zong-Qi Liang[3]

1 *Department of Microbiology, Basic Medical School, Guizhou University of Traditional Chinese Medicine, Guiyang 550025, Guizhou, China* **2** *School of Pharmacy, Guizhou University of Traditional Chinese Medicine, Guiyang 550025, Guizhou, China* **3** *Institute of Fungus Resources, Department of Ecology, College of Life Sciences, Guizhou University, Guiyang 550025, Guizhou, China*

Corresponding author: *Yan-Feng Han* (swallow1128@126.com)

Academic editor: *Nalin Wijayawardene* | Received 12 June 2019 | Accepted 24 August 2019 | Published 25 September 2019

Citation: Chen W-H, Liu C, Han Y-F, Liang J-D, Tian W-Y, Liang Z-Q (2019) Three novel insect-associated species of *Simplicillium* (Cordycipitaceae, Hypocreales) from Southwest China. MycoKeys 58: 83–102. https://doi.org/10.3897/mycokeys.58.37176

Abstract

In this paper, we introduce three new species of *Simplicillium*, viz. *S. cicadellidae*, *S. formicidae* and *S. lepidopterorum*, which were isolated from an infected leafhopper, ant and carpenterworm, respectively. Morphological comparisons and phylogenetic analyses based on multigene datasets (LSU+RPB1+RPB2+TEF and ITS+LSU) support the establishment of the three new species. *Simplicillium cicadellidae* was distinguished from other species in morphological characteristics by having smaller phialides and ellipsoidal conidia, and lacking octahedral crystals. The reverse of colonies were yellowish (#FFBF00), especially in the middle, and radially sulcate. *Simplicillium formicidae* was morphologically distinguished from other by having longer phialides and filiform to fusoid conidia, and by lacking octahedral crystals. *Simplicillium lepidopterorum* was morphologically distinguished from other species by having smaller, ellipsoidal to fusiform conidia, and by lacking octahedral crystals. The reverse of the colony was pale white. The three new species are likely to be nourished by plant to animal (especially insect) nutrients based on the evolutionary pattern of the Hypocreales, and they are described herein as being clearly distinct from other species in *Simplicillium*.

Keywords

Commensal fungi, morphology, nutritional preference, phylogeny

Introduction

The genus *Simplicillium* W. Gams & Zare was introduced by Zare and Gams (2001) with *S. lanosoniveum* (J. F. H. Beyma) Zare & W. Gams as the type species. The genus is characterized with its complete lack of verticillate branching; mostly solitary phialides, which are discrete, aculeate and narrow and arise from aerial hyphae; conidia short-ellipsoidal to suglobose or obclavate, and adhering in globose heads or imbricate chains (Zare and Gams 2001). The members of *Simplicillium* are fungicolous and occur on various substrata (Zare and Gams 2001; Chen et al. 2008; Baiswar et al. 2014; Gauthier et al. 2014; Gomes et al. 2018). Furthermore, Zare and Gams (2001) introduced three additional species, viz., *S. lamellicola* (F. E. V. Sm.) Zare & W. Gams, *S. obclavatum* (W. Gams) Zare & W. Gams and *S. wallacei* H. C. Evans. The typical characteristics of *Simplicillium* include mostly solitary phialides, conidia adhering in globose, slimy heads or imbricate chains, and commonly present crystals in the agar (Zare and Gams 2001). Later, Zare and Gams (2008) transferred *S. wallacei* to *Lecanicillium* W. Gams & Zare based on the phylogenic analysis of internal transcribed spacer (ITS) region and this transfer was confirmed by Sung et al. (2007).

Liu and Cai (2012) reported a new species, *S. chinense* F. Liu & L. Cai, which was the first *Simplicillium* species from China. Five new *Simplicillium* species, *S. aogashimaense* Nonaka, Kaifuchi & Masuma, *S. cylindrosporum* Nonaka, Kaifuchi & Masuma, *S. minatense* Nonaka, Kaifuchi & Masuma, *S. subtropicum* Nonaka, Kaifuchi & Masuma and *S. sympodiophorum* Nonaka, Kaifuchi & Masuma were reported by Nonaka et al. (2013) from Tokyo, Japan. *Simplicillium calcicola* Z. F. Zhang, F. Liu & L. Cai, *S. coffeanum* A. A. M. Gomes & O. L. Pereira and *S. filiforme* R. M. F. Silva, R. J. V. Oliveira, Souza-Motta, J. L. Bezerra & G. A. Silva were reported by Zhang et al. (2017), Gomes et al. (2018) and Crous et al. (2018), respectively. Currently, *Simplicillium* consists of 12 species.

Kepler et al. (2017) re-evaluated the Cordycipitaceae based on the multigene dataset (SSU, LSU, TEF, RPB1 and RPB2), and indicated that *Simplicillium* species group in a clade and are the earliest diverging lineage in Cordycipitaceae. The nuclear ribosomal ITS and LSU were first used to identify cryptic diversification among *Simplicillium* species by Liu and Cai (2012) and then were widely applied in the identification of *Simplicillium* species by Nonaka et al. (2013), Zhang et al. (2017), Gomes et al. (2018) and Crous et al. (2018).

Zare and Gams (2001) noted that *Simplicillium* species were found on various substrata and fungi. Other substrata were found later, such as limstone and wood (Liu and Cai 2012; Zhang et al. 2017). Many bioactive compounds were discovered in *Simplicillium*, such as alkaloids (Fukuda et al. 2014), peptides (Liang et al. 2016; 2017; Dai et al. 2018), diketopiperazine (Yan et al. 2015), xylanases (Roy et al. 2013), anthraquinones (Huang et al. 2015), antibiotics (Takata et al. 2013; Dong et al. 2018), and especially Simpotentin, which is a new potentiator of amphotericin B activity against *Candida albicans* (C. P. Robin) Berkhout and has showed great potential ap-

plications in medicine (Uchida et al. 2019). Furthermore, the antimicrobial activities and entomopathogenicity has meant that *Simplicillium* has potential applications in biocontrol (Ward et al. 2012; Zhao et al. 2013; Le Dang et al. 2014; Lim et al. 2014; Chen et al. 2017; Skaptsov et al. 2017). However, as far as we know, there are limited reports of *Simplicillium* species isolated from infected insects.

Three infected insect specimens were found during a survey of araneogenous fungi and allies from southwestern China. Some fungal strains were isolated and purified from the three specimens. Based on polyphasic approach (morphological, ecological characteristics along with a phylogenetic analysis), they were identified as three new species, *Simplicillium cicadellidae* sp. nov., *S. formicidae* sp. nov. and *S. lepidopterorum* sp. nov.

Materials and methods

Collection and isolation

Three infected insect specimens (DL1004, GY1101 and GY2913) were collected from Dali, Rongjiang Country (26°01'58.70"N, 108°24'48.06"E) and Tongmuling (26°23'25.92"N, 106°41'3.35"E), Huaxi District, Guizhou Province, on 1 October, 9 November and 31 July, 2018, respectively. The surface of the specimens were rinsed with sterile water, followed by surface sterilization with 75% ethanol for 3–5 s. A part of the insect body was cut off and used to inoculate a piece of tissue in haemocoel on potato dextrose agar (PDA) and improved potato dextrose agar (PDA, 1% w/v peptone) (Qu et al. 2018). The strain was isolated and cultured at 22 °C for 14 d under 12 h light/12 h dark conditions following protocols described by Zou et al. (2010). Strains DL10041, DL10042, GY11011, GY11012, GY29131 and GY29132 were obtained.

Culture and identification

The strains were incubated in PDA at 25 °C for 14 d. Macroscopic and microscopic morphological characteristics of the fungi were examined using classical mycological techniques, and the growth rates were determined. The fresh hyphae were observed with an optical microscope (OM, BX35, Olympus, Japan) following pretreatment with lactophenol cotton blue solution or normal saline. The ex-type cultures and dried culture as holotype specimens were deposited in GZAC, Guizhou University, Guiyang, China.

DNA extraction, PCR amplification and nucleotide sequencing

DNA extraction was carried out in accordance with Liang et al. (2009). The extracted DNA was stored at –20 °C. The amplification of large subunit ribosomal

RNA (LSU) genes was performed using NS1-1/AB28 primers (Curran et al. 1994). Translation elongation factor 1 alpha (TEF) and DNA-directed RNA polymerase II largest subunit 2 (RPB2) were amplified using 983F/2218R and RPB2-5F/RPB2-7Cr primers according to van den Brink et al. (2012). DNA-directed RNA polymerase II largest subunit 1 (RPB1) was amplified with the primer pair CRPB1 and RPB1-Cr (Castlebury et al. 2004). The internal transcribed spacer (ITS) region was amplified using ITS4/ITS5 primers by PCR following the procedures described by White et al. (1990). PCR products were purified using the UNIQ-10 column PCR products purification kit [no. SK1141; Sangon Biotech (Shanghai) Co., Shanghai, China] in accordance with the manufacturer's protocol and sequenced at Sangon Biotech (Shanghai) Co. The resulting sequences were submitted to GenBank.

The new species *Simplicillium cicadellidae*, *S. formicidae* and *S. lepidopterorum* were registered in MycoBank with the numbers MB 831336, MB 831337 and MB 831335, respectively.

Sequence alignment and phylogenetic analyses

DNA sequences generated in this study were assembled and edited using DNASTAR Lasergene software (version 6.0). Sequences of ITS, LSU, RPB1, RPB2 and TEF were selected based on previously published data by Nonaka et al. (2013), Zhang et al. (2017), Gomes et al. (2018), Crous et al. (2018) and Mongkolsamrit et al. (2018). Multiple sequence alignments for ITS, LSU, RPB1, RPB2 and TEF were carried out using MAFFT v7.037b (Katoh and Standley 2013). Sequence editing was performed with MEGA6 (Tamura et al. 2013), and the resulting output was in Fasta file format. The concatenated LSU+RPB1+RPB2+TEF and ITS+LSU sequences were assembled by SequenceMatrix v.1.7.8 (Vaidya et al. 2011). Gene concordance was assessed with the 'hompart' command in PAUP4.0b10 (Swofford 2002).

Two different analyses have been carried out using Bayesian inference (BI) and maximum likelihood (ML) methods. Analysis 1: To check the relationship between *Simplicillium* species and its allies in Cordycipitaceae based on the combined dataset of (LSU+RPB1+RPB2+TEF). Analysis 2: To check the relationship among *Simplicillium* spp. based on the combined dataset of (ITS+LSU). For the BI analysis, two runs were executed simultaneously for 10,000,000 generations, saving trees every 500 generations, with the GTR+G nucleotide substitution model across all the partitions, in MrBayes 3.2 (Ronquist et al. 2012). After the analysis was finished, each run was examined with the program Tracer v1.5 (Drummond and Rambaut 2007) to determine burn-in and confirm that both runs had converged. For the ML analysis in RAxML (Stamatakis 2014), the GTRGAMMA model was used for all the partitions in accordance with recommendations in the RAxML manual against the use of invariant sites. The final alignment is available from TreeBASE under submission ID: 24549 (http://www.treebase.org)

Results

Phylogenetic analyses

A phylogenetic tree of *Simplicillium* in Cordycipitaceae was generated from the maximum-likelihood (ML) and Bayesian inference (BI) based on a combined data set of LSU, RPB1, RPB2 and TEF sequence data. Statistical support (≥ 50%/0.5) is shown at the nodes for ML bootstrap support/BI posterior probabilities (Fig. 1). The strain numbers are noted after each species' name. The tree is rooted with *Purpureocillium lilacinum* (Thom) Luangsa-ard, Houbraken, Hywel-Jones & Samson (CBS 284.36 and CBS 431.87). The concatenated sequences including 40 taxa and contained 2,205 characters with gaps (LSU: 447, RPB1: 518, RPB2: 560, and TEF: 680).

A phylogenetic tree of *Simplicillium* species level was generated from the maximum-likelihood (ML) and Bayesian inference (BI) analysis based on a combined data set of ITS and LSU sequence data set. Statistical support (≥ 50%/0.5) are shown at the nodes for ML bootstrap support/BI posterior probabilities. The strain numbers are noted after each species' name. The tree is rooted with *Pochonia chlamydosporia* (Goddard) Zare & W. Gams (CBS 103.65). The dataset includes 16 taxa and consists of 1,000 characters with gaps (ITS: 489 and LSU: 511).

Analysis 1: family Cordycipitaceae. The RAxML analysis of the combined dataset (LSU+RPB1+RPB2+TEF) yielded a best scoring tree (Fig. 1) with a final ML optimization likelihood value of –24,337.973328. Parameters for the GTR model of the concatenated data set was as follows: estimated base frequencies; A = 0.242689, C = 0.276532, G = 0.270879, T = 0.209901; substitution rates AC = 0.926706, AG = 2.728719, AT = 0.823168, CG = 0.803225, CT = 6.257555, GT = 1.000000; gamma distribution shape parameter α = 0.410435. The Bayesian analysis resulted in 20,001 trees after 10,000,000 generations. The first 4,000 trees, representing the burn-in phase of the analyses, were discarded, while the remaining 16,001 trees were used for calculating posterior probabilities in the majority rule consensus tree. In the phylogenetic tree (Fig. 1), *Simplicillium cicadellidae*, *S. formicidae* and *S. lepidopterorum* cluster with other *Simplicillium* species in a clade, and within the earliest diverging lineage in Cordycipitaceae.

Analysis 2: *Simplicillium* species. The RAxML analysis of the combined dataset (ITS+LSU) yielded a best scoring tree (Fig. 2) with a final ML optimization likelihood value of –4,849.039588. Parameters for the GTR model of the concatenated data set was as follows: Estimated base frequencies; A = 0.243952, C = 0.258870, G = 0.268223, T = 0.228956; substitution rates AC = 1.296760, AG = 2.678402, AT = 1.354112, CG = 1.488619, CT = 5.097242, GT = 1.000000; gamma distribution shape parameter α = 0.462419. The Bayesian analysis resulted in 20,001 trees after 10,000,000 generations. The first 4,000 trees, representing the burn-in phase of the analyses, were discarded, while the remaining 16,001 trees were used for calculating posterior probabilities in the majority rule consensus tree. In the phylogenetic tree

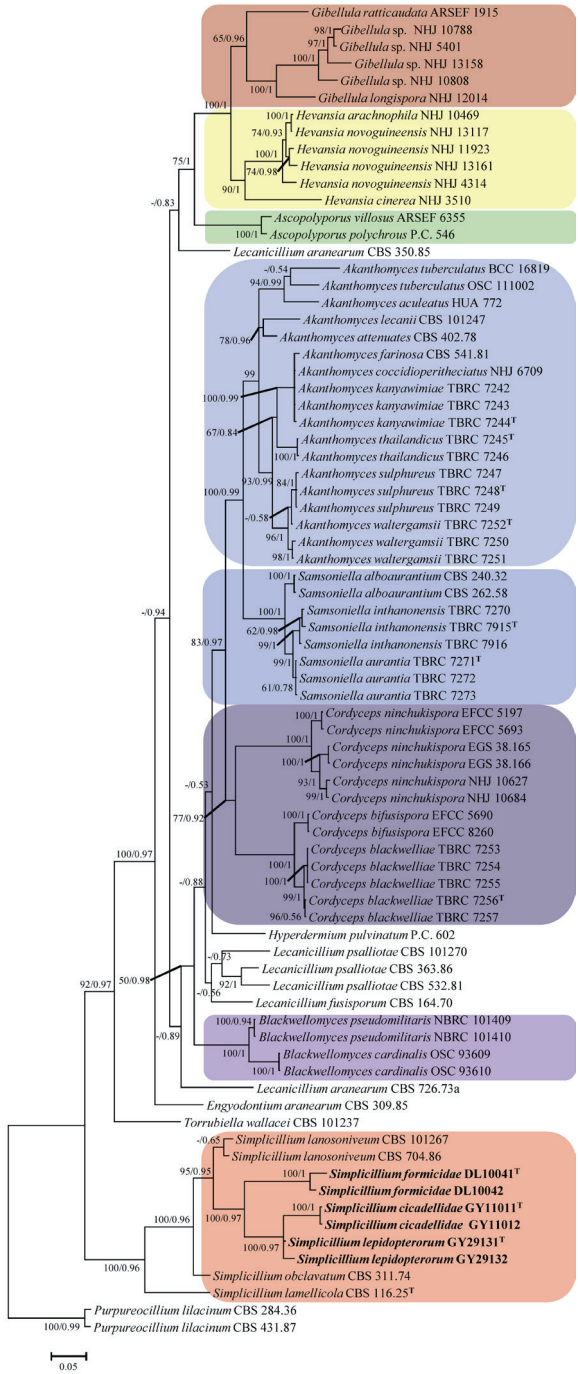

Figure 1. Phylogenetic relationships among the genus *Simplicillium* and its allies in Cordycipitaceae based on multigene dataset (LSU, RPB1, RPB2 and TEF). Statistical support values (≥ 0.5/50%) are shown at the nodes for ML bootstrap support/BI posterior probabilities. The tree is rooted with *Purpureocillium lilacinum* (CBS 284.36 and CBS 431.87). The new species are in bold face. T in the upper right corner indicates the type strains.

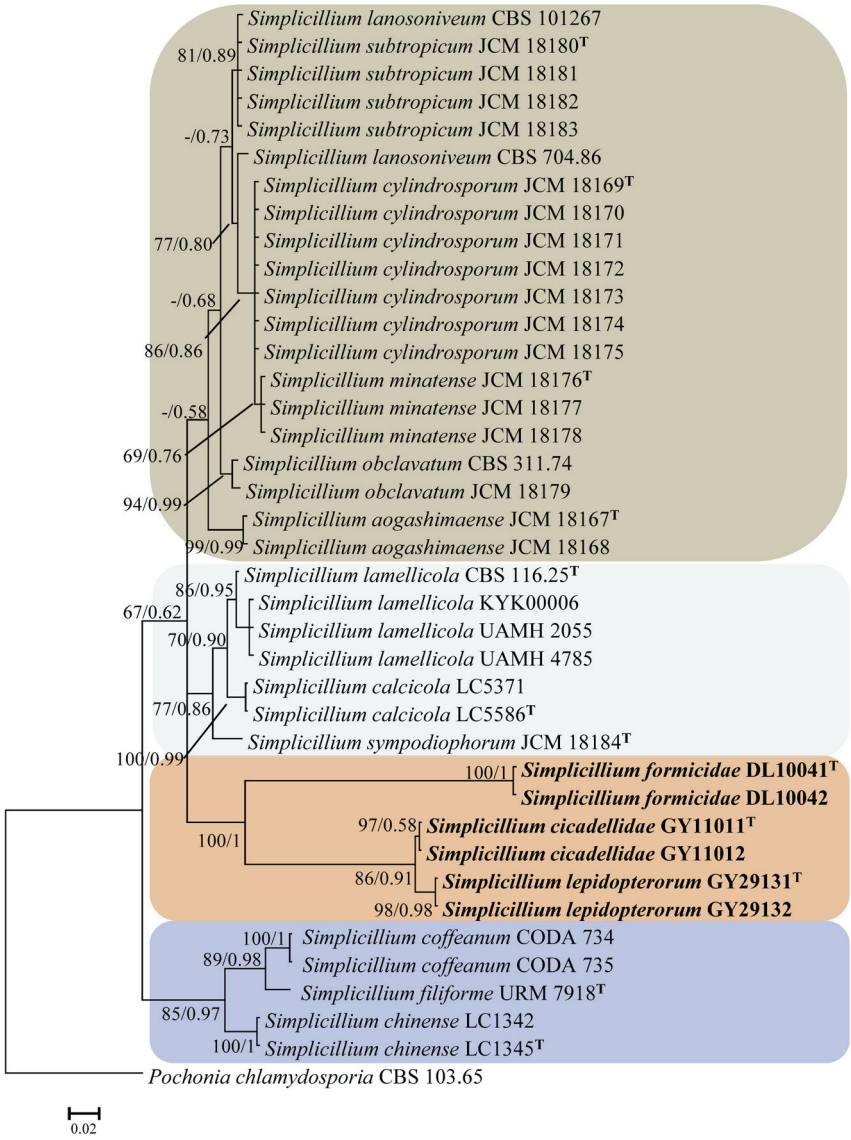

Figure 2. Phylogenetic relationships among the new taxa *S. cicadellidae*, *S. formicidae*, *S. lepidopterorum* and other *Simplicillium* species by ITS+LSU sequences. Statistical support values (≥ 0.5/50%) are shown at the nodes for ML bootstrap support/BI posterior probabilities. The tree is rooted with *Pochonia chlamydosporia* (CBS 103.65). The new species are in bold face. T in the upper right corner indicates the type strains.

(Fig. 2), *Simplicillium* species were resolved into four obvious clades. *S. cicadellidae*, *S. formicidae* and *S. lepidopterorum* were nested in a subclade and formed three independent branches, which received maximum statistical support (BI posterior probabilities 1, ML bootsrap 100%).

Table 1. Taxa included in the phylogenetic analyses

Species	Strain No.	GenBank Accession No.				
		ITS	LSU	RPB1	RPB2	TEF
Akanthomyces aculeatus	HUA 772		KC519370			KC519366
A. attenuates	CBS 402.78		AF339565	EF468888	EF468935	EF468782
A. coccidioperitheciatus	NHJ 6709		EU369042	EU369067	EU369086	EU369025
A. farinosa	CBS 541.81					JQ425686
A. kanyawimiae	TBRC 7242		MF140718	MF140784	MF140808	MF140838
	TBRC 7243		MF140717	MF140783	MF140807	MF140837
	TBRC 7244		MF140716			MF140836
A. lecanii	CBS 101247		AF339555	DQ522407	DQ522466	DQ522359
A. sulphureus	TBRC 7247		MF140720			MF140841
	TBRC 7248		MF140722	MF140787	MF140812	MF140843
	TBRC 7249		MF140721	MF140786	MF140734	MF140842
A. thailandicus	TBRC 7245				MF140809	MF140839
	TBRC 7246		MF140719		MF140810	MF140840
A. tuberculatus	BCC 16819		GQ249987			GQ250037
	OSC 111002		DQ518767	DQ522384	DQ522435	DQ522338
A. waltergamsii	TBRC 7250		MF140715			MF140835
	TBRC 7251		MF140713	MF140781	MF140805	MF140833
	TBRC 7252		MF140714	MF140782	MF140806	MF140834
Ascopolyporus polychrous	P.C. 546		DQ118737	DQ127236		DQ118745
A. villosus	ARSEF 6355		AY886544	DQ127241		DQ118750
Blackwellomyces cardinalis	OSC 93609		AY184962	DQ522370	DQ522422	DQ522325
	OSC 93610		AY184963	EF469088	EF469106	EF469059
B. pseudomilitaris	NBRC 101409		JN941393	JN992482		
	NBRC 101410		JN941394	JN992481		
Cordyceps bifusispora	EFCC 5690		EF468806	EF468854	EF468909	EF468746
	EFCC 8260		EF468807	EF468855	EF468910	EF468747
C. blackwelliae	TBRC 7253		MF140705	MF140774	MF140798	MF140825
	TBRC 7254		MF140704	MF140773	MF140797	MF140824
	TBRC 7255		MF140703	MF140772	MF140796	MF140823
	TBRC 7256		MF140702	MF140771	MF140795	MF140822
	TBRC 7257		MF140701	MF140770	MF140794	MF140821
C. ninchukispora	EFCC 5197		EF468820	EF468868		EF468760
	EFCC 5693		EF468821	EF468869		EF468762
	EGS 38.165		EF468846	EF468900		EF468795
	EGS 38.166		EF468847	EF468901		EF468794
	NHJ 10627		EF468822	EF468870		EF468763
	NHJ 10684		EF468823	EF468871		EF468761
Engyodontium aranearum	CBS 309.85		AF339526	DQ522387	DQ522439	DQ522341
Gibellula longispora	NHJ 12014			EU369055	EU369075	EU369017
G. pulchra	NHJ 10808		EU369035	EU369056	EU369076	EU369018
G. ratticaudata	ARSEF 1915		DQ518777	DQ522408	DQ522467	DQ522360
Gibellula sp.	NHJ 5401			EU369059	EU369079	
	NHJ 10788		EU369036	EU369058	EU369078	EU369019
	NHJ 13158		EU369037	EU369057	EU369077	EU369020
Hevansia arachnophila	NHJ 10469		EU369031	EU369047		EU369008
H. cinerea	NHJ 3510			EU369048	EU369070	EU369009
H. novoguineensis	NHJ 4314			EU369051	EU369071	EU369012
	NHJ 11923		EU369032	EU369052	EU369072	EU369013
	NHJ 13117			EU369049	EU369073	EU369010
	NHJ 13161			EU369050		EU369011
Hyperdermium pulvinatum	P.C. 602		AF242353	DQ127237		DQ118746
L. aranearum	CBS 726.73a		AF339537	EF468887	EF468934	EF468781
L. fusisporum	CBS 164.70**T**		AF339549	EF468889		EF468783

Species	Strain No.	GenBank Accession No.				
		ITS	LSU	RPB1	RPB2	TEF
L. psalliotae	CBS 363.86**T**		AF339559	EF468890		EF468784
	CBS 532.81		AF339560	EF469096	EF469112	EF469067
	CBS 101270		EF469081	EF469095	EF469113	EF469066
Pochonia chlamydosporia	CBS 103.65	MH858504				
Purpureocillium lilacinum	CBS 284.36		FR775484	EF468898	EF468941	EF468792
	CBS 431.87		EF468844	EF468897	EF468940	EF468791
Samsoniella alboaurantium	CBS 240.32		JF415979	JN049895	JF415999	JF416019
	CBS 262.58		MG665232			JQ425685
S. aurantia	TBRC 7271**T**		MF140728	MF140791	MF140818	MF140846
	TBRC 7272		MF140727	MF140817		MF140845
	TBRC 7273		MF140726		MF140816	MF140844
S. inthanonensis	TBRC 7915**T**		MF140725	MF140790	MF140815	MF140849
	TBRC 7916		MF140724	MF140789	MF140814	MF140848
	TBRC 7270		MF140723	MF140788	MF140813	MF140847
Simplicillium aogashimaense	JCM 18167**T**	AB604002				
	JCM 18168	AB604004				
S. calcicola	LC 5371	KU746705	KU74675			
	LC 5586**T**	KU746706	KU746752			
S. chinense	LC 1342	JQ410323	JQ410321			
	LC 1345	NR155782	JQ410322			
S. cicadellidae	**GY11011T**	MN006243	MN006249	MN022271		MN022263
	GY11012	MN006244	MN006250	MN022272		MN022264
S. coffeanum	COAD 2057**T**	MF066034	MF066032			
	COAD 2061	MF066035	MF066033			
S. cylindrosporum	JCM 18169**T**	AB603989				
	JCM 18170	AB603994				
	JCM 18171	AB603997				
	JCM 18172	AB603998				
	JCM 18173	AB603999				
	JCM 18174	AB604005				
	JCM 18175	AB604006				
S. filiforme	URM 7918	MH979338	MH979399			
S. formicidae	**DL10041T**	MN006241	MN006247	MN022269	MN022267	
	DL10042	MN006242	MN006248	MN022270	MN022268	
S. lamellicola	CBS 116.25**T**	AJ292393	AF339552	DQ522404	DQ522462	DQ522356
	UAMH 2055	AF108471				
	UAMH 4785	AF108480				
S. lamellicola[b]	KYK00006	AB378533				
S. lanosoniveum	CBS 704.86	AJ292396	AF339553	DQ522406	DQ522464	DQ522358
	CBS 101267	AJ292395	AF339554	DQ522405	DQ522463	DQ522357
S. lepidopterorum	**GY29131T**	MN006246	MN006251	MN022273		MN022265
	GY29132	MN006245	MN006252	MN022274		MN022266
S. minatense	JCM 18176**T**	AB603992				
	JCM 18177	AB603991				
	JCM 18178	AB603993				
S. obclavatum	CBS 311.74**T**	AJ292394	AF339517			EF468798
	JCM 18179	AB604000				
S. subtropicum	JCM 18180**T**	AB603990				
	JCM 18181	AB603995				
	JCM 18182	AB603996				
	JCM 18183	AB604001				
S. sympodiophorum	JCM 18184**T**	AB604003				
Torrubiella wallacei	CBS 101237**T**		AY184967	EF469102	EF469119	EF469073

T= type strains, strain and sequences generated in this study are shown in bold.

Taxonomy

Simplicillium cicadellidae **W.H. Chen, C. Liu, Y.F. Han, J.D. Liang, Z.Q. Liang sp. nov.**
MycoBank: MB 831336
Figure 3

Etymology. The epithet *cicadellidae* refers to an insect host in family Cicadellidea.

Diagnosis. Characterized by phialides always solitary and rather long and narrow, 12.9–18.3 × 0.8–1.1 μm. Conidia adhering in globose slimy heads, mostly ellipsoidal,

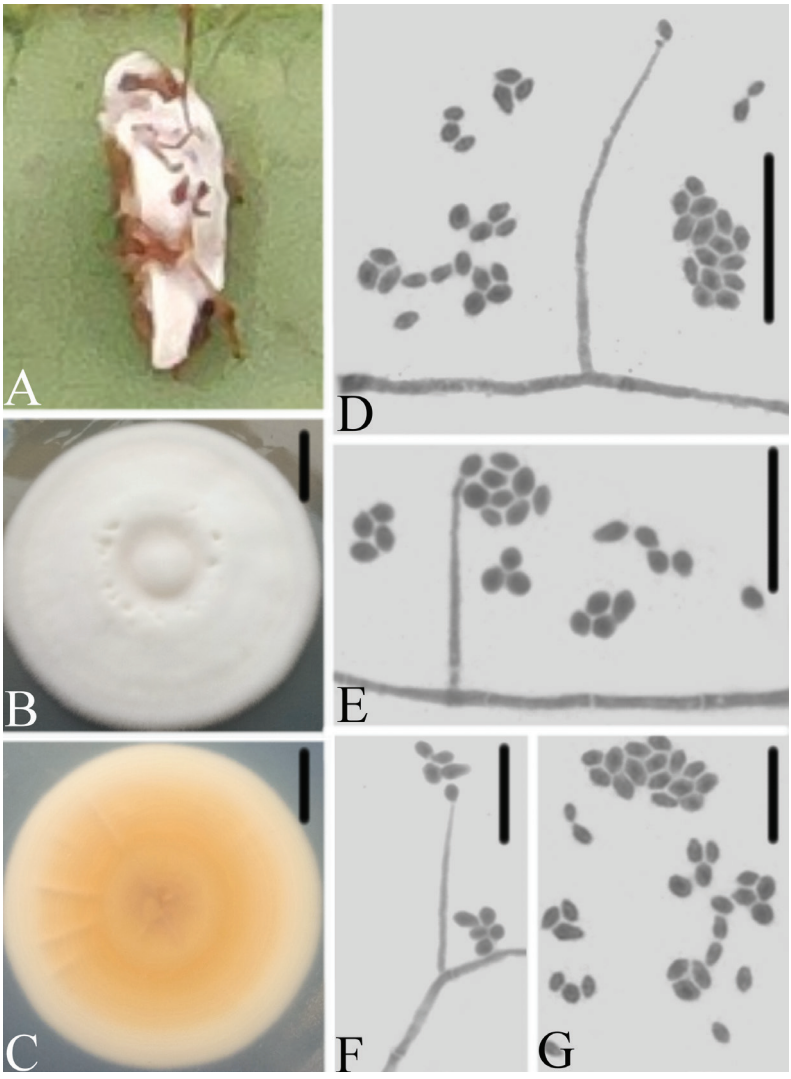

Figure 3. *Simplicillium cicadellidae* **A** infected leafhopper (Hemiptera) **B–C** culture plate, showing the front (**B**) and the reverse (**C**) of the colony, cultured on PDA medium **D–F** phialides solitary, conidia adhering ellipsoidal slimy head and conidia **G** conidia. Scale bars: 10 mm (**B, C**), 10μm (**D, E, F, G**).

1.8–2.8 × 1.4–1.8 μm. Octahedral crystals absent. Reverse of colony yellowish, especially in the middle, and radially sulcate.

Type. CHINA, Guizhou Province, Huaxi District (26°23'25.92"N, 106°41'3.35"E), 9 November 2018, Wanhao Chen, **holotype** GZAC GY1101, ex-type culture GZAC GY11011. Sequences from isolated strain GY11011 has been deposited in GenBank with accession numbers: ITS = MN006243, LSU = MN006249, RPB1 = MN022271 and TEF = MN022263.

Description. Colonies reaching 45–47 mm in diameter in 14 d on PDA; white; reverse yellowish, especially in the middle, and radially sulcate. Hyphae septate, hyaline, smooth-walled, 0.9–1.9 μm wide. Phialides arising from aerial hyphae, gradually tapering towards apex, without basal septa, always solitary and rather long and narrow, 12.9–18.3 × 0.8–1.1 μm. Conidia adhering in ellipsoidal slimy heads, mostly ellipsoidal, hyaline, smooth-walled, 1.8–2.8 × 1.4–1.8 μm. Octahedral crystals absent.

Host. Leafhopper (Hemiptera)

Distribution. Huaxi District, Guizhou Province, China

Remarks. Zare and Gams (2001) summarized the typical characteristics of *Simplicillium* as having mostly solitary phialides arising from aerial hyphae, conidia adhering in globose slimy heads or imbricate chains, crystals commonly present, fungicolous and on various other substrata. *Simplicillium cicadellidae* was easily identified as belonging to *Simplicillium* because of its solitary phialides, conidia adhering in ellipsoidal slimy heads, and lack of octahedral crystals. Comparing with the typical characteristics of 12 species (Table 2), it was easily distinguished from other species in having the phialides always solitary and rather long and narrow (12.9–18.3 × 0.8–1.1 μm), the conidia adhering in globose slimy heads, which are mostly ellipsoidal (1.8–2.8 × 1.4–1.8 μm), and the octahedral crystals absent. The reverse of colony was yellowish, especially in the middle, and radially sulcate. Based on ITS and LSU rDNA, *S. cicadellidae* is phylogenetically close to *S. formicidae* and *S. lepidopterorum*. However, *S. cicadellidae* has ellipsoidal conidia and shorter phialides (12.9–18.3 × 0.8–1.1 μm), and the reverse of colony was yellowish.

Simplicillium formicidae **W.H. Chen, C. Liu, Y.F. Han, J.D. Liang, Z.Q. Liang, sp. nov.**
MycoBank: MB 831337
Figure 4

Etymology. The epithet *formicidae* refers to an insect host in family Formicidae.

Diagnosis. Characterized by phialides always being solitary and rather long and narrow, 51–70.1 × 0.7–0.9 μm. Conidia adhering in globose slimy heads, mostly filiform to fusoid, 3.9–7.9 × 0.8–1.3 μm. Octahedral crystals absent.

Type. CHINA, Guizhou Province, Rongjiang County (26°01'58.70"N, 108°24'48.06"E), 1 October 2018, Wanhao Chen, **holotype** GZAC DL1004, ex-type culture GZAC DL10041. Sequences from isolated strain DL10041 has been deposited in GenBank with accession numbers: ITS = MN006241, LSU = MN006247, RPB1 = MN022269 and RPB2 = MN022267.

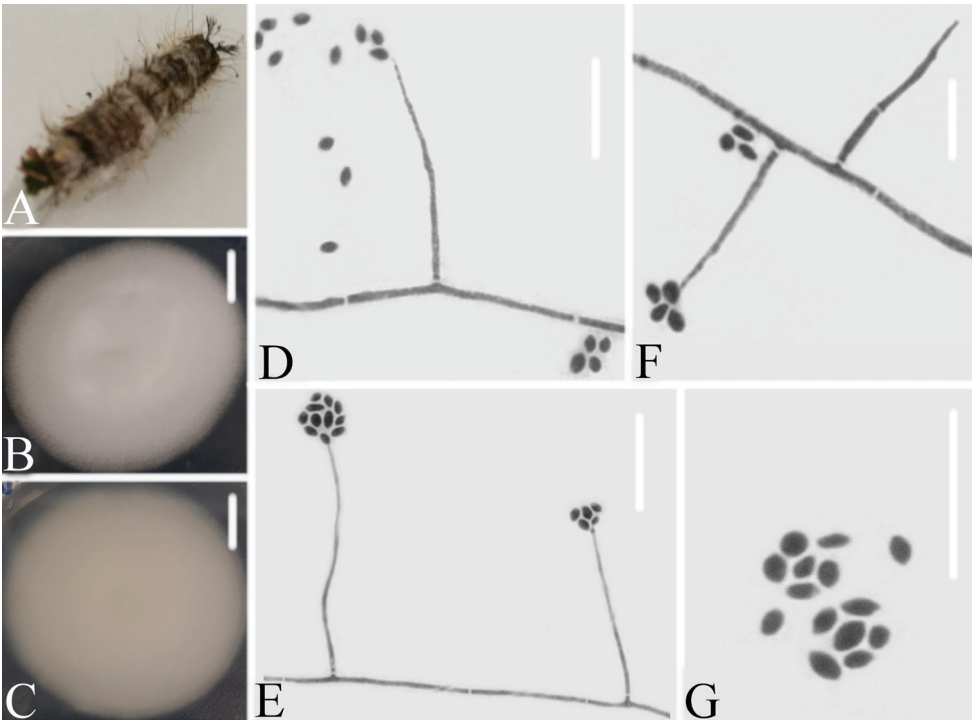

Figure 4. *Simplicillium lepidopterorum* **A** infected carpenterworm (Lepidoptera) **B, C** culture plate, showing the front (**B**) and the reverse (**C**) of the colony, cultured on PDA medium **D, E, F** phialides solitary and conidia in globose heads **D** conidia. Scale bars: 10 mm (**B, C**), 10μm (**D, E, F, G**).

Description. Colonies reaching 26–32 mm in diameter in 14 d on PDA; white; reverse pale brown to brown, and with brown secretions. Hyphae septate, hyaline, smooth-walled, 1.2–1.8 μm wide. Phialides arising from aerial hyphae, gradually tapering towards the apex, without basal septa, always solitary and rather long and narrow, 51–70.1 × 0.7–0.9 μm. Conidia adhering in globose slimy heads, mostly filiform to fusoid, hyaline, smooth-walled, 3.9–7.9 × 0.8–1.3 μm. Octahedral crystals absent.

Host. Ant (Hymenoptera)

Distribution. Rongjiang County, Guizhou Province, China

Remarks. *Simplicillium formicidae* was easily identified as belonging to *Simplicillium* because of its solitary phialides, conidia adhering in globose slimy heads, and lack of octahedral crystals. Compared with the typical characteristics of 12 species (Table 2), it was easily distinguished from those species by having the phialides always solitary and rather long and narrow (51–70.1 × 0.7–0.9 μm) and the conidia mostly filiform to fusoid (3.9–7.9 × 0.8–1.3 μm), and adhering in globose slimy heads, and in having octahedral crystals absent. Based on ITS and LSU rDNA, *S. formicidae* is phylogenetically close to *S. cicadellidae* and *S. lepidopterorum*. However, *S. formicidae* has larger filiform to fusoid conidia (3.9–7.9 × 0.8–1.3 μm).

Simplicillium lepidopterorum **W.H. Chen, C. Liu, Y.F. Han, J.D. Liang & Z.Q. Liang, sp. nov.**
MycoBank: MB 831335
Figure 5

Etymology. The epithet *lepidopterorum* refers to an insect host in order Lepidoptera.

Diagnosis. Characterized by phialides always being solitary and rather long and narrow, 15.3–26.2 × 0.7–1.4 μm, Conidia adhering in globose slimy heads, mostly ellipsoidal, 1.6–2.4 × 1.4–1.7 μm. Octahedral crystals absent. The reverse of colony was pale white.

Type. CHINA, Guizhou Province, Huaxi District (26°23'25.92"N, 106°41'3.35"E), 31 July 2018, Wanhao Chen, **holotype** GZAC GY2913, ex-type culture GZAC GY29131, sequences from isolated strain GY29131 has been deposited in GenBank with accession numbers: ITS = MN006246, LSU = MN006251, RPB1 = MN022273 and TEF = MN022265.

Description. Colonies reaching 48–51 mm in diameter in 14 d on PDA; white; reverse pale white. Hyphae septate, hyaline, smooth-walled, 1.1–2.2 μm wide. Phi-

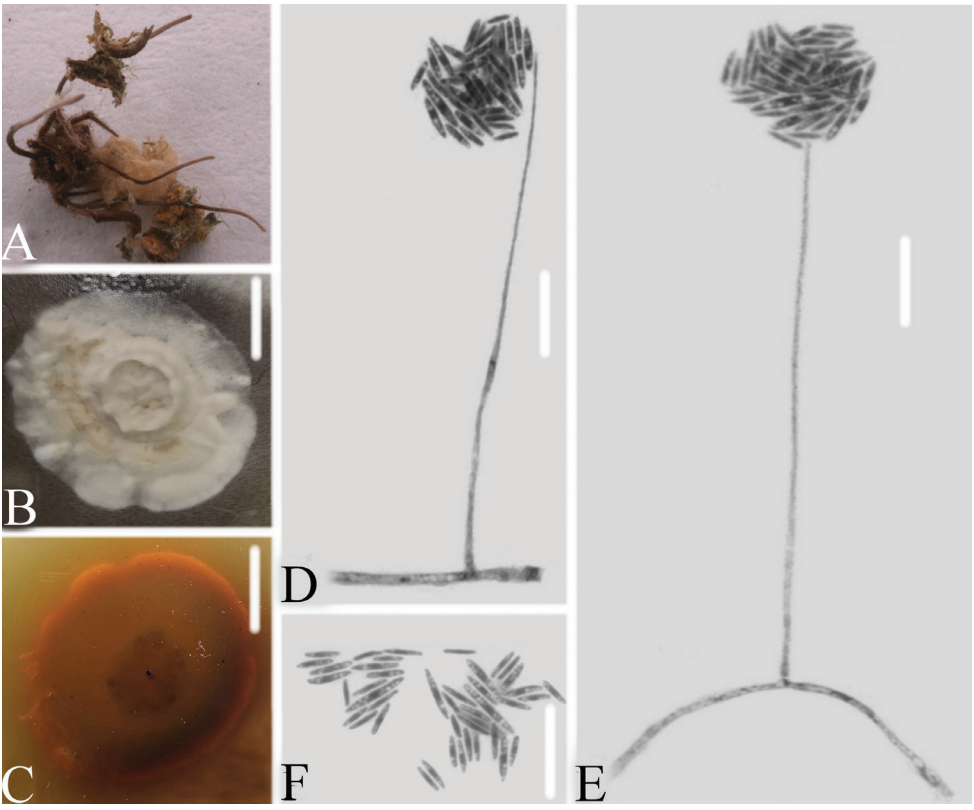

Figure 5. *Simplicillium formicidae* **A** isolated substrate an infected ant (Hymenoptera) **B–C** culture plate, showing the front (**B**) and the reverse (**C**) of the colony, cultured on PDA medium **D, E** phialides solitary, conidia adhering globose slimy head and conidia **F** conidia. Scale bars: 10 mm (**B, C**), 10μm (**D, E, F**).

Table 2. Morphological comparison of three new species with other *Simplicillium* species

Species	Morphological characteristics				Notes
	Phialide (Conidiogenous cell) (μm)	Conidia (μm)	Conidia mass	Octahedral crystals	
S. aogashimaense[a]	(19–)23–53 × 1.2–2.0	cylindrical, 4.2–6.5 × 1.2–2.0	globose heads	present	Chlamydospores present
S. calcicola[b]	14–38 × 1–2	micro-: globose, oval or ellipsoidal, 2–3.5 × 1–1.5 macro-: fusiform, 4.5–8 × 1–2		absent	
S. chinense[c]	(6.0–)15–30(–68.0) × 1.5	oval, ellipsoidal or cylindrical 3.5–5.0 × 1.0–1.5	branched or unbranched chains	present	
S. coffeanum[d]	11–40(–70) × 1.0–2.4	micro-: spindle-shaped, 5.3–8.8 × 1.0–1.6 macro-: ellipsoidal to fusiform, 2.2–3.8 × 0.8–1.5	subglobose to ellipsoidal heads	absent	
S. cylindrosporum[a]	17–32 × 1.2–2.0(–2.5)	cylindrical, 3.0–4.5(–5.0) × 1.0–2.0	globose heads	present	
S. filiforme[e]	9–18 × 1	fusoid to filiform, 7.2–12.5 × 1	zigzag chains	absent	
S. lamellicola[f]	15–50 × 0.7–1.0	micro-: spindle-shaped, 4.5–9.0 × 0.8–1.2 macro-: oval to ellipsoidal, 2.0–3.0 × 0.7–1.2	subglobose to ellipsoidal heads	present	
S. lanosoniveum[f]	15–35 × 0.7–1.5	subglobose, oval, ellipsoidal 1.5–3 × 0.7–1.3	globose heads	present	
S. minatense[a]	11–31(–47) × 1.0–1.7	globose to subglobose, sometimes ellipsoidal, 2.0–3.5 × 1.8–2.5(–2.8)	globose heads	present	
S. obclavatum[f]	30–52 × 0.8–1.2	obclavate to ellipsoidal, 2.5–3.5 × 1–2	short imbricate chains	present	
S. subtropicum[a]	(15–)20–42(–50) × 1.0–2.3	subglobose to ellipsoidal, 2.3–4.0(–4.5) × 1.5–3.3	globose heads	present	
S. sympodiophorum[a]	20–34(–47) × 0.5–1.3 denticles present	oval to ellipsoidal, 2.2–3.5 × 1.0–2.0		present	
S. cicadellidae	12.9–18.3 × 0.8–1.1	ellipsoidal, 1.8–2.8 × 1.4–1.8	ellipsoidal heads	absent	colonies reverse pale white
S. formicidae	51–70.1 × 0.7–0.9	filiform to fusoid, 3.9–7.9 × 0.8–1.3	globose heads	absent	
S. lepidopterorum	15.3–26.2 × 0.7–1.4	ellipsoidal, 1.6–2.4 × 1.4–1.7	globose heads	absent	colonies reverse yellowish

a–f: data are derived from Zare and Gams (2001), Nonaka et al. (2013), Zhang et al. (2017), Liu and Cai 2012, Gomes et al. (2018) and Crous et al. (2018), respectively.

alides arising from aerial hyphae, gradually tapering towards the apex, without basal septa, always solitary and rather long and narrow, 15.3–26.2 × 0.7–1.4 μm. Conidia adhering in globose slimy heads, ellipsoidal to fusiform, hyaline, smooth-walled, 1.6–2.4 × 1.4–1.7 μm. Octahedral crystals absent.

Host. Carpenter worm (Lepidoptera)

Distribution. Huaxi District, Guizhou Province, China

Remarks. *Simplicillium lepidopterorum* was easily identified as belonging to *Simplicillium* because of its solitary phialides, conidia adhering in globose slimy heads, and lack of octahedral crystals. Comparing with the typical characteristics of 12 species (Table 2), *S. lepidopterorum* could easily distinguished from other species by having the phialides always solitary and rather long and narrow, 15.3–26.2 × 0.7–1.4 μm. Conidia ellipsoidal (1.6–2.4 × 1.4–1.7 μm), adhering in globose slimy heads, and in

having the octahedral crystals absent. Based on ITS and LSU rDNA, *S. lepidopterorum* is phylogenetically close to *S. cicadellidae* and *S. formicidae*. However, *S. lepidopterorum* has ellipsoidal conidia, longer phialides (15.3–26.2 × 0.7–1.4 μm), and the reverse of colony was pale white.

Key

1 Conidia in globose or subglobose heads **2**
– Conidia in chains or solitary **11**
2 Macro- and microconidia present **3**
– Only one type of conidia present **4**
3 Octahedral crystals present..... ***S. lamellicola***
– Octahedral crystals absent..... ***S. coffeanum***
4 Octahedral crystals present..... **5**
– Octahedral crystals absent..... ***9***
5 Conidia cylindrical ***6***
– Conidia subglobose or ellipsoidal..... *7*
6 Chlamydospores present, conidia 4.2–6.5 × 1.2–2.0 μm... ***S. aogashimaense***
– Chlamydospores absent, conidia 3.0–4.5 (–5.0) × 1.0–2.0 μm .... ***S. cylindrosporum***
7 Conidia subglobose to ellipsoidal..... **8**
– Conidia oval or ellipsoidal to subcylindrical, 1.5–3.0 × 0.7–1.3 μm..... ..... ***S. lanosoniveum***
8 Conidia subglobose to ellipsoidal, 2.3–4.0 (–4.5) × 1.5–3.3 μm ....***S. subtropicum***
– Conidia globose to subglobose, sometimes ellipsoidal, 2.5–3.5 × 1.8–2.5 (–2.8) μm ..... ***S. minatense***
9 Conidia ellipsoidal..... **10**
– Conidia filiform to fusoid ..... ***S. formicidae***
10 The reverse of colony pale white, phialide 12.9–18.3 × 0.8–1.1 μm..... .....***S. cicadellidae***
– The reverse of colony yellowish, phialide 15.3–26.2 × 0.7–1.4 μm ....***S. lepidopterorum***
11 Denticles present in conidiogenous cell (phialide).....***S. sympodiophorum***
– Denticles absent in conidiogenous cell (phialide)..... **12**
12 Macro- and microconidia present ..... ***S. calcicola***
– Only one type of conidia present **13**
13 Conidia ellipsoidal..... **14**
– Conidia fusoid to filiform, form zigzag chains..... ***S. filiforme***
14 Conidia in branched or unbranched chains, 3.5–5.0 × 1.0–1.5 μm . ***S. chinense***
– Conidia in short imbricate chains, 2.5–3.5 × 1.0–2.0 μm..... ***S. obclavatum***

Discussion

Two types of the evolutionary correlation patterns between fungi and hosts are known, co-evolutionary patterns and the more frequent host jump events (Spatafora et al. 2007). The generation of host jumping is closely related to a common living environment (Vega et al. 2009). Nutritional sources are very important factors in determining whether a host has undergone a host jump. The nutritional model of Hypocreales fungi is from plants (including living plants and plant residues) to animals (especially insects), and finally to fungi. Plants and their residues were the initial sources of nutrition for the common ancestor of Hypocreaceae and Clavicipitaceae. The jumps from plants to animals and then to fungi indicate that the fungal nutrient requirements have changed with the environment (Spatafora et al. 2007). Prediction of the characteristics and evolutionary placement of any given member should be based on the correlation between molecular-phylogenetic genealogy and nutritional preferences (Spatafora et al. 2007; Vega et al. 2009). Additionally, host insect species are an important diagnostic feature in the identification of entomopathogenic fungi.

Among the 12 reported *Simplicillium* species, *S. aogashimaense* (soil), *S. calcicola* (calcareous rock), *S. chinense* (decaying wood), *S. cylindrosporum* (soil), *S. minatense* (soil), *S. obclavatum* (air), *S. subtropicum* (soil) and *S. sympodiophorum* (soil) were isolated from soil, marine water, rock, decaying wood and air (Zare and Gams 2001; Liu and Cai 2012; Nonaka et al. 2013; Liang et al. 2017). *Simplicillium filiforme* and *S. coffeanum* were isolated as endophytic fungi from plants (Crous et al. 2018; Gomes et al. 2018). *Simplicillium lamellicola* belongs to the hyperparasite fungi (Shin et al. 2017). *Simplicillium lanosoniveum* was reported as both an endophytic and hyperparasite fungi (Baiswar et al. 2014). It has been reported that *Simplicillium* is pathogenic to insects. Unfortunately, there are limited reports of insect-related *Simplicillium*.

The hosts of *Simplicillium cicadellidae* and *S. lepidopterorum* were larvae of Cicadidae and Lepidoptera, which feed through piercing-sucking and chewing. Moreover, *S. formicidae* was isolated from an infected ant. These three strains are likely to receive nutrients from plants (including living plants and plant residues) and animals (especially insects) based on the evolutionary pattern of Hypocreales. *Simplicillium cicadellidae*, *S. formicidae* and *S. lepidopterorum* represent three new species based on their nutritional preferences. To our knowledge, this is the first report of insect-associated *Simplicillium* species.

ITS and LSU have been widely used in the identification of *Simplicillium* (Liu and Cai 2012; Nonaka et al. 2013; Zhang et al. 2017; Sliva et al. 2018). In the present study, the combined dataset (ITS+LSU) was used to analysis of phylogenetic relationships among the new taxa and other *Simplicillium* species. Additionally, RPB1, RPB2 and TEF loci were added to analysis that the relationship among *Simplicillium* and its allies. The new species clustered with other *Simplicillium* species in a clade (Fig. 1), and this was consistent with morphological characteristics based identification. Six strains were clustered into three subclades (Fig. 2) and were distinctly different from other reported *Simplicillium* spp. Additionally, three species, *S. chinense*, *S. coffeanum* and

S. filiforme were clustered in a subclade, and these species were associated with plants. This may be because of their nutritional preferences. Therefore, *S. cicadellidae*, *S. formicidae* and *S. lepidopterorum* are based on morphological characteristics, ecological characteristics and a phylogenetic analysis.

Acknowledgements

This work was supported by the National Natural Science Foundation of China (Grant No. 31460010, 31860002), the Doctoral Fund of Guiyang University of Chinese Medicine (3043-043170023), the National first-class construction discipline in Guizhou province (Chinese medical science) (GNYL[2017]008), and Engineering Research Center of General Higher Education in Guizhou Province (Qianjiaohe(2015)337). We thank Dr. Lesley Benyon, from Liwen Bianji and Edanz Group China (http://www.liwenbianji.cn/ac), for editing the English text of a draft of this manuscript.

References

Baiswar P, Ngachan SV, Rymbai H, Chandra S (2014) *Simplicillium lanosoniveum*, a hyperparasite on *Aecidium elaeagni-latifoliae* in India. Australasian Plant Disease Notes 9(1): 144. https://doi.org/10.1007/s13314-014-0144-z

Castlebury LA, Rossman AY, Sung GH, Hyten AS, Spatafora JW (2004) Multigene phylogeny reveals new lineage for *Stachybotrys chartarum*, the indoor air fungus. Mycological Research 108: 864–872. https://doi.org/10.1017/S0953756204000607

Chen RS, Huang CC, Li JC, Tsay JG (2008) First report of *Simplicillium lanosoniveum* causing brown spot on *Salvinia auriculata* and *S. molesta* in Taiwan. Plant Disease 92(11): 1589–1589. https://doi.org/10.1094/PDIS-92-11-1589C

Chen RS, Huang CC, Li JC, Tsay JG (2017) Evaluation of characteristics of *Simplicillium lanosoniveum* on pathogenicity to aphids and in vitro antifungal potency against plant pathogenic fungi. International Journal of Environmental & Agriculture Research 3 (1): 2454–1850.

Crous PW, Luangsa-ard JJ, Wingfield MJ, Carnegie AJ, Hernández-Restrepo M, Lombard L, Roux J, Barreto RW, Baseia IG, Cano-Lira JF, Martín MP, Morezova OV, Stchigel AM, Summerell BA, Brandrud TE, Dima B, Garcia D, Giraldo A, Guarro J, Gusmão LFP, Khamsuntorn P, Noordeloos ME, Nuankaew S, Pinruan U, Rodríguez-Andrade E, Souza-Motta CM, Thangavel R, van lperen AL, Abreu VP, Accioly T, Alves JL, Andrade JP, Bahram M, Baral HO, Barbier E, Barnes CW, Bendiksen E, Bernard E, Bezerra JDP, Bezerra JL, Bizio E, Blair JE, Bulyonkova TM, Cabral TS, Caiafa MV, Cantillo T, Colmán AA, Conceição LB, Cruz S, Cunha AOB, Darveaux BA, da Silva AL, da Sliva GA, da Sliva GM, da Sliva RMF, de Oliveira RJV, Oliveira RL, De Souza JT, Dueñas M, Evans HC, Epifani F, Felipe MTC, Fernández-López J, Ferreira BW, Fugueiredo CN, Filippova NV, Flores JA, Gené J, Ghorbani G, Gibertoni TB, Glushakova AM, Healy R, Huhndorf SM, Iturrieta-González I, Javan-Nikkhah M, Juciano RF, Jurjević Ž, Kachalkin AV, Keochanpheng K,

Krisai-Greilhuber I, Li YC, Lima AA, Machado AR, Madrid H, Magalhães OMC, Marbach PAS, Melanda GCS, Miller AN, Mongkolsamrit S, Nascimento RP, Oliveira TGL, Ordoñez ME, Orzes R, Palma MA, Pearce CJ, Pereira OL, Perrone G, Peterson SW, Pham THG, Piontelli E, Pordel A, Quijada L, Raja HA, Rosas de Paz E, Ryvarden L, Saitta A, Salcede SS, Sandoval-Denis M, Santos TAB, Seifert KA, Silva BDB, Smith ME, Soares AM, Sommai S, Sousa JO, Suetrong S, Susca A, Tedersoo L, Telleria MT, Thanakitpipattana D, Valenzuela-Lopez N, Visagie CM, Zapata M, Groenewald JZ (2018) Fungal Planet description sheets: 785–867. Persoonia: Molecular Phylogeny and Evolution of Fungi 41: 1–238. https://doi.org/10.3767/persoonia.2018.41.12

Curran J, Driver F, Ballard JWO, Milner RJ (1994) Phylogeny of *Metarhizium*: analysis of ribosomal DNA sequence data. Mycological Research 98: 547–552. https://doi.org/10.1016/S0953-7562(09)80478-4

Dai Y, Lin Y, Pang X, Luo X, Salendra L, Wang JF, Zhou XF, Lu YJ, Yang B, Liu Y (2018) Peptides from the soft coral-associated fungus *Simplicillium* sp. SCSIO41209. Phytochemistry 154: 56–62. https://doi.org/10.1016/j.phytochem.2018.06.014

Dong Q, Dong R, Xing X, Li Y (2018) A new antibiotic produced by the cyanobacterium-symbiotic fungus *Simplicillium lanosoniveum*. Natural Product Research 32(11): 1348–1352. https://doi.org/10.1080/14786419.2017.1343320

Drummond A, Rambaut A (2007) BEAST: Bayesian evolutionary analysis by sampling trees. BMC Evolutionary Biology 7: 1–214. https://doi.org/10.1186/1471-2148-7-214

Fukuda T, Sudoh Y, Tsuchiya Y, Okuda T, Igarashi Y (2014) Isolation and biosynthesis of preussin B, a pyrrolidine alkaloid from *Simplicillium lanosoniveum*. Journal of Natural Products 77 (4): 813–817. https://doi.org/10.1021/np400910r

Gauthier NW, Maruthachalam K, Subbarao KV, Brown M, Xiao Y, Robertson CL, Schneider RW (2014) Mycoparasitism of *Phakopsora pachyrhizi*, the soybean rust pathogen, by *Simplicillium lanosoniveum*. Biological Control 76: 87–94. https://doi.org/10.1016/j.biocontrol.2014.05.008

Gomes AA, Pinho DB, Cardeal ZL, Menezes HC, De Queiroz MV, Pereira OL (2018) *Simplicillium coffeanum*, a new endophytic species from Brazilian coffee plants, emitting antimicrobial volatiles. Phytotaxa 333(2): 188–198. https://doi.org/10.11646/phytotaxa.333.2.2

Huang Z, Yan SZ, Chen SL (2015) Optimization on fermentation conditions of *Simplicillium obclavatum* YX016 for the production of anthraquinones. Food Science and Technology 7: 3 pp.

Katoh K, Standley DM (2013) MAFFT multiple sequence alignment software version 7: improvements in performance and usability. Molecular Biology and Evolution 30(4): 772–780. https://doi.org/10.1093/molbev/mst010

Liang JD, Han YF, Zhang JW, Du W, Liang ZQ, Li ZZ (2009) Optimal culture conditions for keratinase production by a novel thermophilic *Myceliophthora thermophila* strain GZUIFR-H49-1. Journal of Applied Microbiology 110: 871–880. https://doi.org/10.1111/j.1365-2672.2011.04949.x

Liang X, Nong XH, Huang ZH, Qi SH (2017) Antifungal and antiviral cyclic peptides from the deep-sea-derived fungus *Simplicillium obclavatum* EIODSF 020. Journal of Agricultural and Food Chemistry 65 (25): 5114–5121. https://doi.org/10.1021/acs.jafc.7b01238

Liang X, Zhang XY, Nong XH, Wang J, Huang ZH, Qi SH (2016) Eight linear peptides from the deep-sea-derived fungus *Simplicillium obclavatum* EIODSF 020. Tetrahedron 72(22): 3092–3097. https://doi.org/10.1016/j.tet.2016.04.032

Lim SY, Lee S, Kong HG, Lee J (2014) Entomopathogenicity of *Simplicillium lanosoniveum* isolated in Korea. Mycobiology 42(4): 317–321. https://doi.org/10.5941/MYCO.2014.42.4.317

Liu F, Cai L (2012) Morphological and molecular characterization of a novel species of *Simplicillium* from China. Cryptogamie, Mycologie 33(2): 137–145. https://doi.org/10.7872/crym.v33.iss2.2012.137

Mongkolsamrit S, Noisripoom W, Thanakitpipattana D, Wutikhun T, Spatafora JW, Luangsa-ard J (2018) Disentangling cryptic species with *isaria*-like morphs in Cordycipitaceae. Mycologia 110(1): 230–257.

Nonaka K, Kaifuchi S, Ōmura S, Masuma R (2013) Five new *Simplicillium* species (Cordycipitaceae) from soils in Tokyo, Japan. Mycoscience 54(1): 42–53. https://doi.org/10.1016/j.myc.2012.07.002

Qu JJ, Yu LQ, Zhang J, Han YF, Zou X (2018) A new entomopathogenic fungus, *Ophiocordyceps ponerus* sp. nov., from China. Phytotaxa 343(2): 116–126. https://doi.org/10.11646/phytotaxa.343.2.2

Ronquist F, Teslenko M, van der Mark P, Ayres DL, Darling A, Höhna S, Larget B, Liu L, Suchard MA, Huelsenbeck JP (2012) MrBayes 3.2: efficient Bayesian phylogenetic inference and model choice across a large model space. Systematic Biology 61: 539–542. https://doi.org/10.1093/sysbio/sys029

Roy S, Dutta T, Sarkar TS, Ghosh S (2013) Novel xylanases from *Simplicillium obclavatum* MTCC 9604: comparative analysis of production, purification and characterization of enzyme from submerged and solid state fermentation. SpringerPlus 2(1): 382. https://doi.org/10.1186/2193-1801-2-382

Shin TS, Yu NH, Lee J, Choi GJ, Kim JC, Shin CS (2017) Development of a biofungicide using a mycoparasitic fungus *Simplicillium lamellicola* BCP and its control efficacy against gray mold diseases of tomato and ginseng. The Plant Pathology Journal 33(3): 337. https://doi.org/10.5423/PPJ.FT.04.2017.0087

Skaptsov M, Smirnov S, Kutsev M, Uvarova O, Sinitsyna T, Shmakov A, Matsyura A (2017) Pathogenicity of *Simplicillium lanosoniveum* to *Coccus hesperidum*. Ukrainian Journal of Ecology 7 (4): 689–691. https://doi.org/10.15421/2017_1801

Spatafora JW, Sung GH, Sung JM, Hywel-Jones NL, White JF (2007) Phylogenetic evidence for an animal pathogen origin of ergot and the grass endophytes. Molecular Ecology 16: 1701–1711. https://doi.org/10.1111/j.1365-294X.2007.03225.x

Stamatakis A (2014) RAxML version 8: a tool for phylogenetic analysis and post-analysis of large phylogenies. Bioinformatics 30: 1312–1313. https://doi.org/10.1093/bioinformatics/btu033

Sung GH, Hywel-Jones NL, Sung JM, Luangsa-ard JJ, Shrestha B, Spatafora JW (2007) Phylogenetic classification of *Cordyceps* and the clavicipitaceous fungi. Studies in Mycology 57: 1–64. https://doi.org/10.3114/sim.2007.57.01

Swofford DL (2002) PAUP* 4.0b10: phylogenetic analysis using parsimony (*and other methods). Sinauer, Sunderland.

Takata K, Iwatsuki M, Yamamoto T, Shirahata T, Nonaka K, Masuma R, Hayakawa Y, Hanaki H, Kobayashi Y, Petersson GA, Ōmura S, Shiomi K (2013) Aogacillins A and B produced by *Simplicillium* sp. FKI-5985: new circumventors of arbekacin resistance in MRSA. Organic Letters 15(18): 4678–4681. https://doi.org/10.1021/ol401975z

Tamura K, Stecher G, Peterson D, Filipski A, Kumar S (2013) MEGA6: molecular evolutionary genetics analysis version 6.0. Molecular Biology and Evolution 30: 2725–2729. https://doi.org/10.1093/molbev/mst197

Uchida R, Kondo A, Yagi A, Nonaka K, Masuma R, Kobayashi K, Tomoda H (2019) Simpotentin, a new potentiator of amphotericin B activity against *Candida albicans*, produced by *Simplicillium minatense* FKI-4981. The Journal of Antibiotics 72(3): 134 pp. https://doi.org/10.1038/s41429-018-0128-x

Vaidya G, Lohman DJ, Meier R (2011) SequenceMatrix: concatenation software for the fast assembly of multi-gene datasets with character set and codon information. Cladistics 27(2): 171–180. https://doi.org/10.1111/j.1096-0031.2010.00329.x

van den Brink J, Samson RA, Hagen F, Boekhout T, de Vries RP (2012) Phylogeny of the industrial relevant, thermophilic genera *Myceliophthora* and *Corynascus*. Fungal Diversity 52: 197–207. https://doi.org/10.1007/s13225-011-0107-z

Ward NA, Robertson CL, Chanda AK, Schneider RW (2012) Effects of *Simplicillium lanosoniveum* on *Phakopsora pachyrhizi*, the soybean rust pathogen, and its use as a biological control agent. Phytopathology 102(8): 749–760. https://doi.org/10.1094/PHYTO-01-11-0031

White TJ, Bruns T, Lee S, Taylor J (1990) Amplification and direct sequencing of fungal ribosomal RNA genes for phylogenetics. In: Innis MA, Gelfand DH, Sninsky JJ, White TJ (Eds) PCR protocols: a guide to methods and applications. Academic Press, New York. 315–322. https://doi.org/10.1016/B978-0-12-372180-8.50042-1

Yan B, Fang ST, Li WZ, Liu SJ, Wang JH, Xia CH (2015) A new minor diketopiperazine from the sponge-derived fungus *Simplicillium* sp. YZ-11. Natural Product Research 29 (21): 2013–2017. https://doi.org/10.1080/14786419.2015.1027890

Zare R, Gams W (2001) A revision of *Verticillium* section *Prostrata*. IV. The genera *Lecanicillium* and *Simplicillium* gen. nov. Nova Hedwigia 73: 1–50.

Zare R, Gams W (2008) A revision of the *Verticillium fungicola* species complex and its affinity with the genus *Lecanicillium*. Mycological Research 112 (7): 811–824. https://doi.org/10.1016/j.mycres.2008.01.019

Zhang ZF, Liu F, Zhou X, Liu XZ, Liu SJ, Cai L (2017) Culturable mycobiota from Karst caves in China, with descriptions of 20 new species. Persoonia: Molecular Phylogeny and Evolution of Fungi 39: 1 pp. https://doi.org/10.3767/persoonia.2017.39.01

Zhao D, Liu B, Li LY, Zhu XF, Wang YY, Wang JQ, Duan YX, Chen LJ (2013) *Simplicillium chinense*: a biological control agent against plant parasitic nematodes. Biocontrol Science and Technology 23 (8): 980–986. https://doi.org/10.1080/09583157.2013.809514

Zou X, Liu AY, Liang ZQ, Han YF, Yang M (2010) *Hirsutella liboensis*, a new entomopathogenic species affecting Cossidae (Lepidoptera) in China. Mycotaxon 111 (1): 39–44. https://doi.org/10.5248/111.39

MycoKeys 58: 103–127 (2019)
doi: 10.3897/mycokeys.58.35324
http://mycokeys.pensoft.net

RESEARCH ARTICLE

A peer-reviewed open-access journal
MycoKeys
Launched to accelerate biodiversity research

Behind the veil – exploring the diversity in *Phallus indusiatus* s.l. (Phallomycetidae, Basidiomycota)

Tiara S. Cabral[1], Bianca D.B. Silva[2], María P. Martín[3], Charles R. Clement[1], Kentaro Hosaka[4], Iuri G. Baseia[5]

1 *Instituto Nacional de Pesquisas da Amazônia, Manaus, Amazonas, Brazil* **2** *Universidade Federal da Bahia, Salvador, Bahia, Brazil* **3** *Real Jardín Botánico-CSIC, Madrid, Spain* **4** *National Museum of Nature and Science, Tsukuba, Ibaraki, Japan* **5** *Universidade Federal do Rio Grande do Norte, Natal, Rio Grande do Norte, Brazil*

Corresponding author: *Tiara S. Cabral* (ttiara@gmail.com)

Academic editor: *Bryn Dentinger* | Received 23 April 2019 | Accepted 5 August 2019 | Published 2 October 2019

Citation: Cabral TS, Silva BDB, Martín MP, Clement CR, Hosaka K, Baseia IG (2019) Behind the veil – exploring the diversity in *Phallus indusiatus* s.l. (Phallomycetidae, Basidiomycota). MycoKeys 58: 103–127. https://doi.org/10.3897/mycokeys.58.35324

Abstract

Studies have demonstrated that many cosmopolitan species actually consist of divergent clades that present high levels of morphological stasis throughout their evolutionary histories. *Phallus indusiatus* s.l. has been described as a circum-tropical species. However, this distribution may actually reflect the lack of taxonomic resolution due to the small number of diagnostic morphological characters, which leads to the identification of new records as populations of *P. indusiatus*. Here, we examine the diversity of *P. indusiatus*-like species in Brazilian Amazonia. We show a clear congruence between detailed morphological data and ITS, nuc-LSU and *atp*6 based phylogenetic analyses and three new species are described within the Brazilian indusiate clade. These results highlight the importance of more detailed investigation, with the inclusion of molecular information, in Neotropical fungi.

Keywords

Amazonia, *atp*6, ITS, Neotropics, nuc-LSU, Phallales

Introduction

The worldwide distribution of fungal species hypotheses has been questioned by modern molecular analyses. Studies have demonstrated that many cosmopolitan species actually consist of divergent clades that present high levels of morphological stasis

throughout their evolutionary histories (Mueller et al. 2001, Bickford et al. 2007, Geml et al. 2008, Davis et al. 2014). *Phallus indusiatus* Vent. – also known as the "veiled lady" mushroom – has been described as a circum-tropical species, with records for South and Central America (Dennis 1960, Saénz and Nassar 1982, Leite et al. 2007, Cheype 2010), Mexico (Guzmán et al. 1990), Africa (Dissing and Lange 1962, Dring 1964, Demoulin and Dring 1975, Dring and Rose 1977, Desjardin and Perry 2015), Asia (Dennis 1953, Liu 1984, Hosaka 2010) and Australia (Smith 2005). For some groups of fungi, spore dispersal mechanisms may support the idea of transoceanic dispersal connecting geographically isolated populations (Halling et al. 2008, Hosaka et al. 2008). However, the current distribution of *P. indusiatus* may actually reflect the lack of taxonomic resolution due to the small number of diagnostic morphological characters, which leads to the identification of new records as populations of *P. indusiatus*. The insect-dependent mechanism of spore dispersal may also have played an important role in determining the current distribution of *P. indusiatus*.

As in phalloid fungi in general, few morphological characters are available to delimit species in *Phallus*. In addition, most of the widely used diagnostic characters – such as colour and sizes – show high plasticity, another factor that may lead to misidentifications and mask the real diversity within the genus (Kreisel 1996, Calonge 2005). As a consequence of these taxonomic uncertainties, a great number of synonyms are reported for several species of this clade. *Phallus indusiatus* is an emblematic example, where at least nineteen synonyms and several distinct forms have been described (Lloyd 1909, Liu 1984, Guzmán et al. 1990, Kreisel 1996, Calonge 2005, Das et al. 2007, Cheype 2010).

Due to lack of resolution when using morphological characters to identify *Phallus* species, we believe that several specimens that have been identified as *P. indusiatus* might actually consist of independently evolving entities. In fact, some new species with minimal, yet noticeable morphological differences from *P. indusiatus*, have been proposed. For instance, *P. serrata* H.L. Li, L. Ye, P.E. Mortimer, J.C. Xu & K.D. Hyde, described for China, differs by the meshes of the indusium with serrate edges (Li et al. 2014); *P. echinovolvatus* (M. Zang, D.R. Zheng and Z.X. Hu) Kreisel has a whitish volva with mycelioid projections on the surface (Zang et al. 1988); and *P. flavidus* Kreisel & Hausknecht, described for the Seychelles, has yellowish pigments on the receptacle and indusium (Kreisel and Hausknecht 2009). Some of these species were described with the support of molecular analyses, which reinforces the importance of this kind of analysis to resolve these taxonomic uncertainties. At least three species resembling *P. indusiatus* were described for Brazil: *Phallus moelleri* Lloyd, *Dictyophora callichroa* Möller and *Dictyophora phalloidea* Desv. In the original descriptions, they present some inherent characteristics that distinguish them from *P. indusiatus*, such as the above-ground development of the volva in *D. phalloidea* and the orange receptacle and pinkish receptacle apex in *D. callichroa* (Möller 1895). Lloyd (1909) described *P. moelleri* based on a Brazilian species and synonymised *D. callichroa* with it. All three species are now considered synonyms of *P. indusiatus* by some authors and Index Fungorum (Lloyd 1909, Fischer 1928, Saénz and Nassar 1982, Calonge 2005, Kreisel and Hausknecht 2009).

Phallus indusiatus was described by Étienne Pierre Ventenat in 1798, based on a specimen from Suriname. In 1809, Desvaux created a new genus, *Dictyophora* Desv.,

mainly characterised by the presence of an indusium, a skirt-like structure that expands from the receptacle towards the ground. Ventenat's species was transferred to *Dictyophora* and named *D. indusiata* (Vent.) Desv. Kreisel (1996) considered that the importance of an indusium for the taxonomy of the genus was overestimated, hence he downgraded *Dictyophora* to a section of *Phallus*. More recently, with the introduction of molecular data to the systematics and taxonomy of fungi, studies have shown that the indusium is a recurrent character, which independently emerged several times during the evolution of the group (Hosaka et al. 2006, Cabral et al. 2012, Marincowitz et al. 2015, Trierveiler-Pereira et al. 2017). Today, *P. indusiatus* Vent. is the valid name for Ventenat's species. *Phallus indusiatus* is widespread in Brazil, with records from four of the six Brazilian biomes (Magnago et al. 2013), but information concerning its diversity and distribution is still incomplete.

In this study, we examined the diversity of *P. indusiatus*-like species in Brazilian Amazonia. We show a clear congruence between detailed morphological data and DNA-based phylogenetic analyses and three new species are described within the Brazilian indusiate clade. These results highlight the importance of more detailed investigation, with the inclusion of molecular information, in Neotropical fungi.

Material and methods

Morphological data

Specimens of *Phallus* sp. with white indusium were collected during the rainy seasons of 2013 to 2015 in various areas of the Amazon Rainforest domain (Figure 1). We included in the analyses four additional specimens attributed to *P. indusiatus* borrowed from the Herbarium of the Instituto de Botânica (São Paulo) and the Universidade Federal de Rio Grande do Norte-Fungos, which were collected in various areas of the Atlantic Rainforest domain. Other *Phallus* species were included in the molecular analysis to increase taxon coverage, both from GenBank and newly sequenced specimens from the Paleartic-Oriental region (Suppl. material 1: Table S1). Species were morphologically described based on fresh and dried material. Macroscopic characters were described based on field notes and photographs, while microscopic details were obtained by mounting slides with fragments from different layers and structures of dried basidiome in 5% potassium hydroxide (KOH) and/or stained with Congo red dye. We followed the specific literature for species identification (Lloyd 1909, Kreisel 1996, Calonge 2005, Kreisel and Hausknecht 2009) and colours were described following Küppers (1979).

DNA extraction, amplification and sequencing

DNA extraction followed Hosaka (2009). The nuclear ribosomal ITS and nuc-LSU regions, as well as mitochondrial *atp6* region, were amplified using previously described

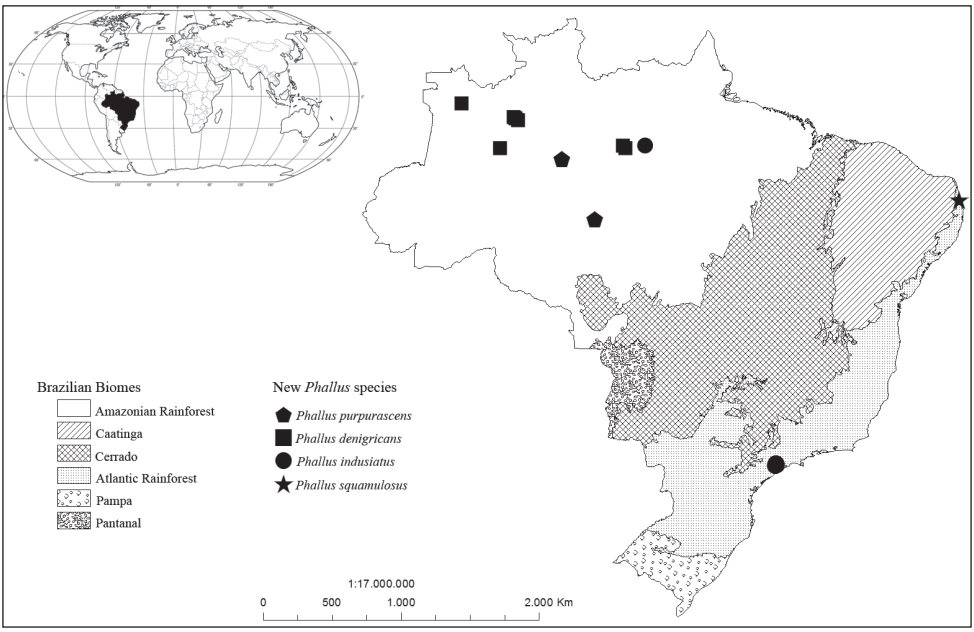

Figure 1. Currently known distributions of the *Phallus* species described in this study. Highlighted areas are the Brazilian Biomes (IBGE 2012): Amazonian Rainforest, Cerrado, Caatinga, Atlantic Rainforest, Pantanal and Pampa.

primers and protocols (Vilgalys and Hester 1990, White et al. 1990, Kretzer and Bruns 1999). DNA fragments were visualised in 1% agarose gel stained with GelRed™ (Biotium) under UV light. The fragments were purified using Ilustra ExoProStar (GE Healthcare) and then sequenced using the Big Dye Terminator Cycle Sequencing Kit (Applied Biosystems) with the same primer pairs. After sequencing, some ITS electropherograms presented double peaks; in order to resolve these, the ITS PCR fragments were cloned following Marincowitz et al. (2015). All ribotypes were included in the phylogenetic analyses.

Molecular phylogenetic analyses

We submitted each sequence to a BLAST search to identify the closest relatives and to check for possible contamination. The closest sequences resulting from the BLAST search and sequences with genus names of *Phallus* or *Dictyophora* were retrieved from GenBank and added to the dataset. All sequences were aligned and manually edited with Geneious R6.1 (Biomatters Ltd.). Two analyses were run, one for the ITS dataset (ITS) and the other with ITS, nuc-LSU and *atp*6 concatenated matrix (CONC). The ITS final aligned matrix contained 618 positions, while the concatenated matrix contained 1896 positions (571 for ITS, 794 for nuc-LSU and 529 for *atp*6). These two

matrices were analysed separately. Based on a previous phylogeny (Trierveiler-Pereira et al. 2014), species of the genus *Mutinus* were chosen as outgroups. Maximum Parsimony (MP) analyses were performed with PAUP* (Swofford 2003) using heuristic searches with the TBR branch-swapping algorithm; the initial tree was obtained by stepwise addition of random additional sequences repeated 100 times and 1000 replicates as bootstrap (bs) settings. For Bayesian analysis (BA), the substitution model of evolution was chosen with MrModelTest (Nylander 2004). The analyses were run in MrBayes 3.2.6, as follows: two parallel runs were executed with four incrementally-heated simultaneous MCMC simulations over 5 million generations, with trees sampled every 1000 generations. The consensus trees were reconstructed with the remaining trees after the burn-in stage, which was defined based on the average standard deviation of split frequency values. The confidence values were estimated with posterior probabilities (pp). Trees were visualised and edited in FigTree version 1.4.2. All data are available in TreeBASE under ID 21524.

Results

A total of 19 recently collected specimens of *Phallus* spp. with white indusium were studied, 15 of which were collected in Brazilian Amazonia, while four other specimens were collected from the Brazilian Atlantic Rainforest (SP and UFRN-Fungos herbaria) (Figure 1). Additionally, we obtained sequences from 21 *Phallus* specimens from Japan, Russia, Vietnam and Thailand. The collection localities, herbarium vouchers and GenBank accession numbers can be found in the Suppl. material 1: Table S1, as well as in species descriptions.

Phylogenetic analyses

We obtained 95 sequences, amongst which 54 were ITS, 19 were nuc-LSU and 22 were *atp*6 (Suppl. material 1: Table S1). The ITS final aligned matrix contained 618 positions, while the concatenated matrix contained 1896 positions (571 for ITS, 795 for nuc-LSU and 530 for *atp6*). Maximum Parsimony and Bayesian analyses with both matrices (ITS and CONC) resulted in trees with the same intraspecific relationships, but with different topologies (Figures 2, 3; MP trees in Suppl. material 2: Figures S1, S2). For Maximum Parsimony analysis, of the 618 positions from the ITS matrix, 382 were informative and resulted in a most parsimonious tree with 2006 steps (CI = 0.458, RI = 0.859, RC = 0.394), while of the 1896 positions from the CONC matrix, 502 were informative and resulted in a most parsimonious tree with 1097 steps (CI = 0.547, RI = 0.709, RC = 0.388). In all of the phylogenetic trees obtained in this study, the Brazilian specimens of *Phallus* grouped together (ITS: pp = 1, bs = 94%; CONC: pp = 1, bs = 100%). This clade can be divided into six groups, which correspond to the four morphospecies identified and described here (coloured clades on Figures 2,

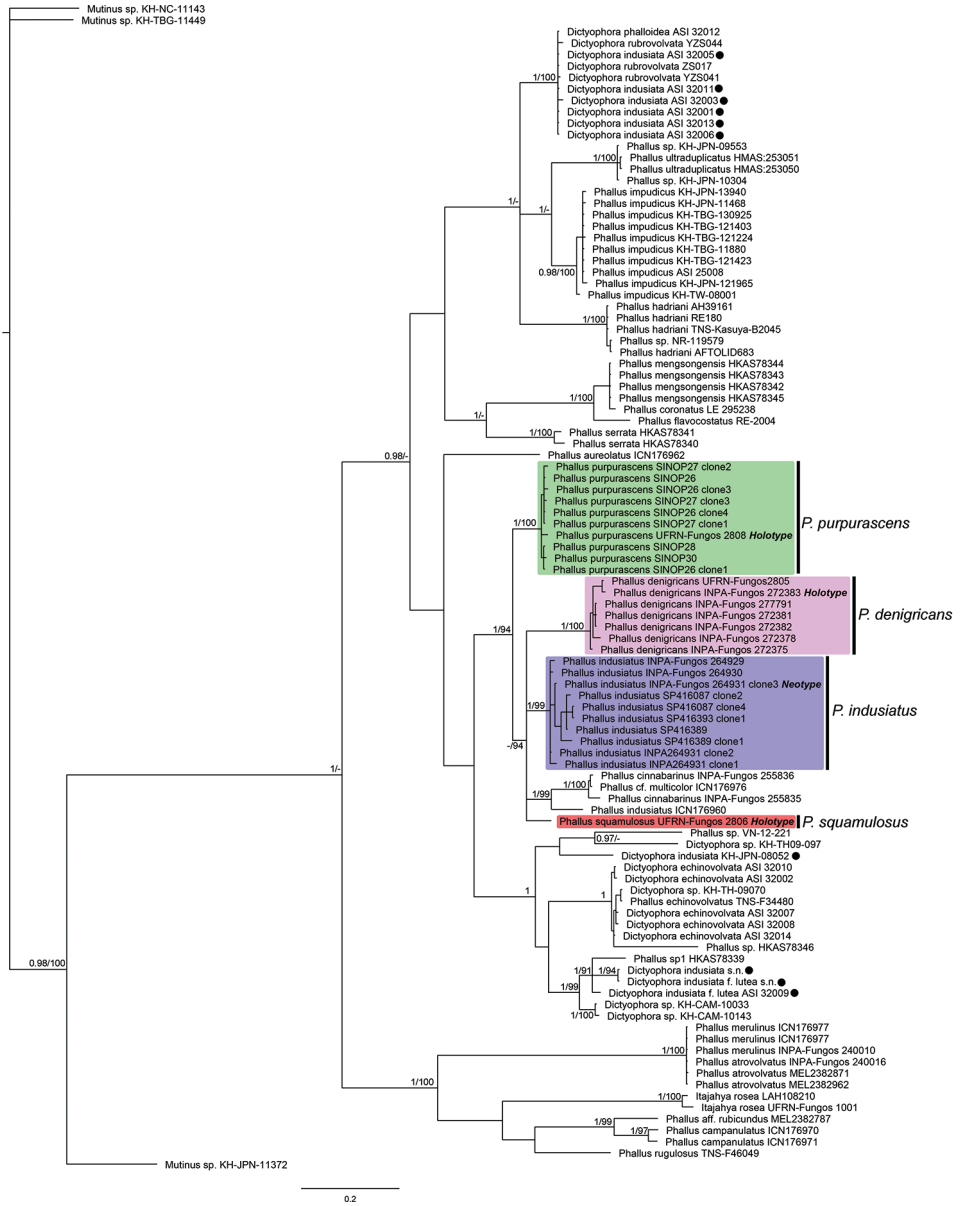

Figure 2. Phylogenetic tree obtained by Bayesian analysis with ITS. Brazilian clades corresponding to the new species and *P. indusiatus* are indicated (the holotype of each species is in bold). Posterior probabilities and bootstrap values are on the nodes (pp/bs), values of pp < 0.95 and bs < 90 are not shown. The black dots indicate specimens under *Phallus indusiatus* deposited in Genbank and downloaded for this study.

3), *Phallus cinnabarinus* (W.S. Lee) Kreisel found in Amazonia (Cabral et al. 2015) and one specimen from southern Brazil (*P. indusiatus* ICN 176960), for which we do not have morphological information. Sequences under the name *P. indusiatus* (and

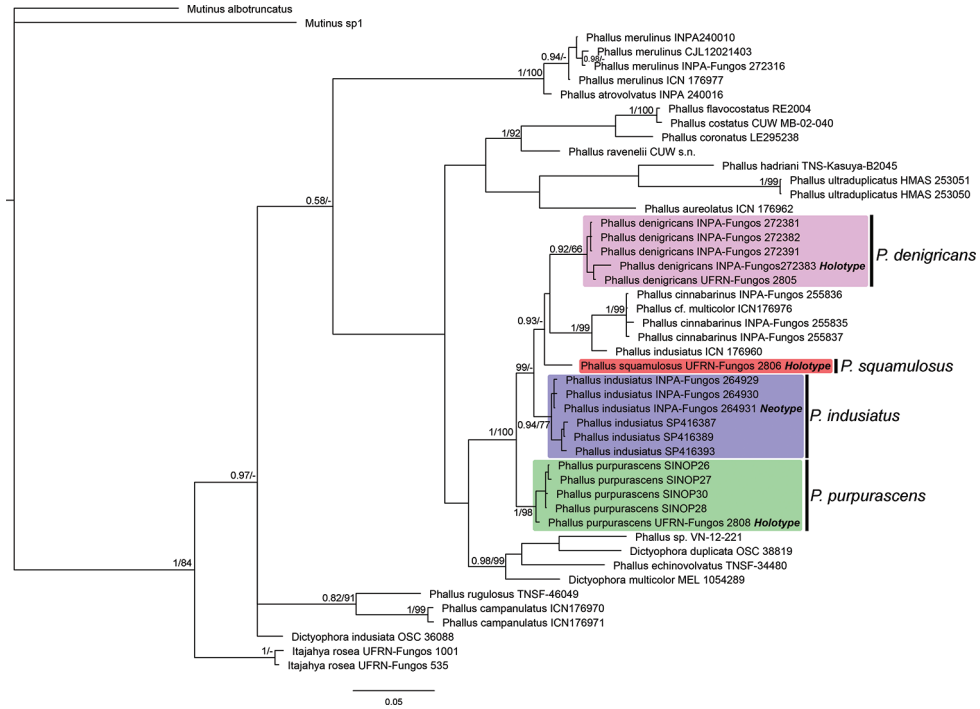

Figure 3. Phylogenetic tree obtained by Bayesian analysis with concatenated data (ITS, nuc-LSU and *atp6*). Brazilian clades corresponding to the new species and *P. indusiatus* are indicated (the holotype of each species is in bold). Posterior probabilities and bootstrap values are on the nodes (pp/bs), values of pp < 0.95 and bs < 90 are not shown (except for *P. denigricans* clade).

D. indusiata) retrieved from GenBank, all from Asia (China and Japan), as well as those collected by us in this study, form a paraphyletic clade with intercontinental disjunct distributions. Based on morphological similarities and the geographical proximity to the type locality (Suriname) of the Amazonian specimens collected and supported by the molecular data, one Brazilian clade (blue on Figures 2, 3) corresponds to *P. indusiatus* sensu stricto.

Taxonomy

Phallus denigricans **T.S.Cabral, B.D.B.Silva & Baseia, sp. nov.**
MycoBank No: 824632
Figure 4

Diagnosis. This species is characterised by the campanulate receptacle slightly constricted at the base, pale yellow, reticulated, with a prominent apical pore, epigeous development of basidiome, volva varying from white to dark brown and spores up to 4.6 × 2.5 µm.

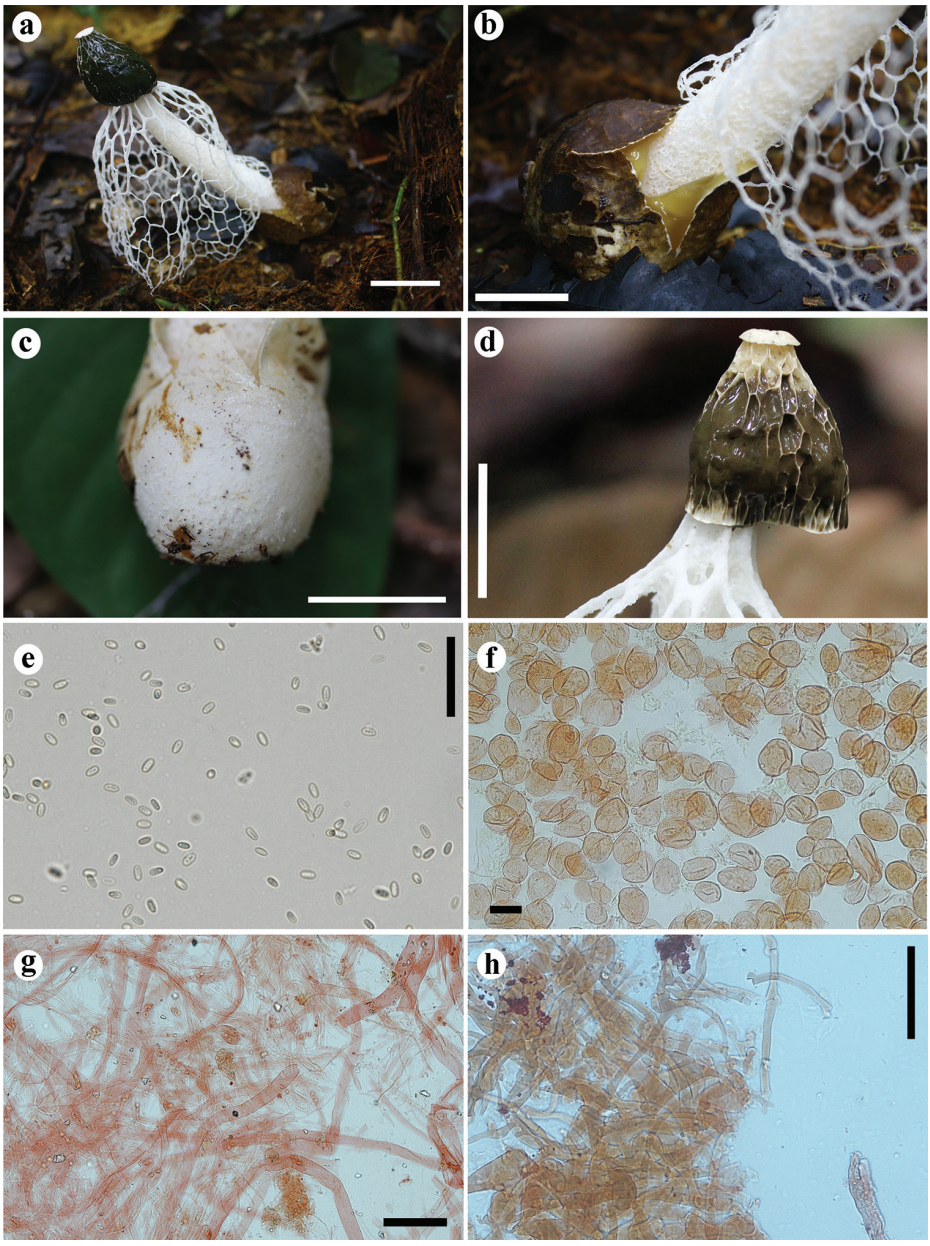

Figure 4. *Phallus denigricans* UFRN-Fungos 2805, holotype. **A** Basidiome **B** blackish and smooth volva in detail **C** white volva with projections **D** receptacle with a prominent pore **E** spores **F** pseudoparenchymatous hyphae of pseudostipe **G** hyphae from rhizomorphs **H** hyphae from volva. Scale bars: 20 mm (**A–D**), 20 µm (**E**), 40 µm (**F–H**).

Holotype. BRAZIL. Amazonas: São Gabriel da Cachoeira, Itacoatiara Mirim Community (0.304167S, 66.8403W), 1 April 2013, Komura DL (INPA-Fungos 272383). GenBank accessions: MG678486 (ITS), MG678455 (nuc-LSU), MG678541 (*atp*6).

Immature basidiomes not observed. Fresh expanded basidiome 98 mm high. Receptacle [25] 26 × 19 [25] mm, campanulate, but slightly constricted at the base, with a prominent apical pore, deeply reticulated surface. Pseudostipe [81] 54 × 10 [22] mm, cylindrical, spongy, white ($N_{00}A_{00}M_{00}$); pseudoparenchymatous, composed of globose to elongate-ovoid cells, [20.5] 18.5–65.5 [60.8] × [17.5] 19–52.5 [51.2] µm, hyaline. Indusium poorly developed, extending to 2/3 of pseudostipe, white ($N_{00}A_{00}M_{00}$), 53 mm in length, attached to the apex of the pseudostipe, polygonal to irregular meshes up to 13 × 8 mm. Volva epigeous, white ($N_{00}A_{00}M_{00}$) in some specimens to dark brown ($N_{60}A_{60}M_{50}$) in others, with smooth surface or sometimes with small hyphae projections on surface; formed by filamentous hyphae, septate, branched, hyaline, clamp connections present, [2.5] 1.8–5 [3.5] µm diameter, with inflated ends up to 15.5 µm diameter. Rhizomorphs composed of at least two types of hyphae: filamentous thin-walled hyphae, with clamp connections; and thicker hyphae (7–16 µm) that seem to communicate with each other by pores on the inflated tips. Crystals in globose cells were found distributed amongst the hyphae of volva and rhizomorphs of some of the white volva species, measuring 8.2–11.5 × 6.8–10.6 µm. Gleba olive brown ($N_{99}A_{50}M_{10}$), mucilaginous. Basidiospores elongated, smooth, 3.6–4.6 × 2.2–2.5 µm, hyaline in 5% KOH.

Habitat and distribution. On soil, in a fragment of upland old-growth forest. So far restricted to the Brazilian Atlantic and Amazon forests, found in the municipalities of Barcelos, Parintins, São Gabriel da Cachoeira and Maraã (State of Amazonas, Brazil); and Natal (State of Rio Grande do Norte).

Etymology. with reference to the volva becoming blackish.

Other specimens examined (paratypes). Brazil. Amazonas: Maraã, Reserva de Desenvolvimento Sustentável do Amanã, Ubim Community (2.50500S, 64.66039W), 15 February 2014, Cabral TS (UFRN-Fungos 2805). Barcelos, Bacabal Community (0.49004S, 62.93089W), 7 April 2015, Cabral TS (INPA-Fungos 277791). Parintins, Açaí Community (2.62665S, 56.54041W), 5 March 2015, Cabral TS (INPA-Fungos 272375); 6 March 2015 (INPA-Fungos 272378); Barcelos, Bacabal Community (0.49004S, 62.93089W), 7 April 2015, Cabral TS (INPA-Fungos 272381, INPA-Fungos 272382). Rio Grande do Norte: Natal (6.305093S, 35.361112W), 10 September 2005, Barbosa MMB (UFRN-Fungos 417).

Notes. *Phallus flavidus* Kreisel & Hauskn. could be comparable with *P. denigricans* by the conical receptacle and the indusium size; however, *P. flavidus* has smaller spores (up to 3.6 × 1.8 µm), the surface of the volva is light grey with an orange flush and the indusium is cream to yellow (Kreisel and Hausknecht 2009). *Phallus impudicus* var. *obliteratus* (Malençon) Kreisel has a reticulate white receptacle and a rudimentary white indusium; *Phallus denigricans* also has a poorly-developed indusium, but it is very different from *P. impudicus* var. *obliteratus*, where the indusium is hidden under the receptacle (Calonge 2005, Kreisel and Hausknecht 2009). *Phallus callichrous* (Möller) Lloyd is a species described from Brazil, with white indusium and differs from *P. denigricans* by having an orange to pink receptacle and reddish-violet rhizomorphs. Recently, another indusiate species was described for Brazil, *Phallus aureolatus*, but it differs from *P. denigricans* mainly by the strongly developed pore and the merulioid

surface of the receptacle (Trierveiler-Pereira et al. 2017), in addition to its different phylogenetic placement (Figures 2, 3). *Phallus echinovolvatus* (M. Zang, D.R. Zheng & Z.X. Hu) Kreisel is another white-indusiate species, characterised mainly by the volva covered with echinulate hyphae projections; in *P. denigricans*, hyphae projections on the volva surface can also be found in some specimens, but they are smaller than in *P. echinovolvatus* (Zang et al. 1988). In *P. indusiatus*, the receptacle is campanulate, the immature basidiome is hypogeous, so that the volva is buried under the ground when the basidiome is fully developed, the indusium is completely developed reaching the ground and the volva and rhizomorphs have pinkish pigments (Ventenat 1798). On the other hand, in *P. denigricans* the campanulate receptacle is constricted at the base, the basidiome has a completely epigeous development, the indusium is poorly-developed reaching only 2/3 of the basidiome and the rhizomorphs and volva are white to brownish.

It is not rare to find *Phallus* specimens with a blackish volva; recently, a new species was described, *P. fuscoechinovolvatus* (Song et al. 2018), but it is quite different from *P. denigricans* mainly by the strongly echinulated volva. *Phallus merulinus* (Berk.) Cooke and *P. atrovolvatus* Kreisel & Calonge are very similar, differing by the volva colour – that is black in *P. atrovolvatus* and white in *P. merulinus* – and the habitat (Calonge 2005). In our ITS phylogenetic analyses (Figure 3), specimens identified as *P. atrovolvatus* and *P. merulinus* grouped together in the same clade, indicating a possible identity between these two species. However, no type material was analysed here, which prevents a reliable determination of the species boundaries between *P. atrovolvatus* and *P. merulinus*. Similarly, in *P. denigricans*, we found specimens with white and pale white to brownish volva all grouping in the same clade in phylogenetic trees (Figures 2, 3). This suggests that the volva colour might change due to the soil properties or with the maturity of the basidiome. Therefore, this specific characteristic – pale or darker volva – should be carefully analysed before it can be used as a diagnostic character in *Phallus* species.

In both the Bayesian and Maximum Parsimony phylogenetic trees (Figures 2, 3 and Suppl. material 2: Figures S1, S2, specimens of *P. denigricans* grouped in a clade with high support values (ITS tree: pp = 1, bs = 100%), in concordance with morphological data.

Phallus purpurascens **T.S.Cabral, B.D.B.Silva & Baseia, sp. nov.**
MycoBank No: 824633
Figure 5

Diagnosis. This species is characterised by its large basidiome (up to 200 mm), the indusium reaching 2/3 of the basidiome, the purplish volva and rhizomorphs and the thimble-like and strongly reticulated receptacle.

Holotype. BRAZIL. Amazonas: Manaus (3.0615S, 60.0111W), 27 February 2014, Cabral TS (UFRN-Fungos 2808). GenBank accessions: MG678487 (ITS), MG678456 (nuc-LSU), MG678542 (*atp*6).

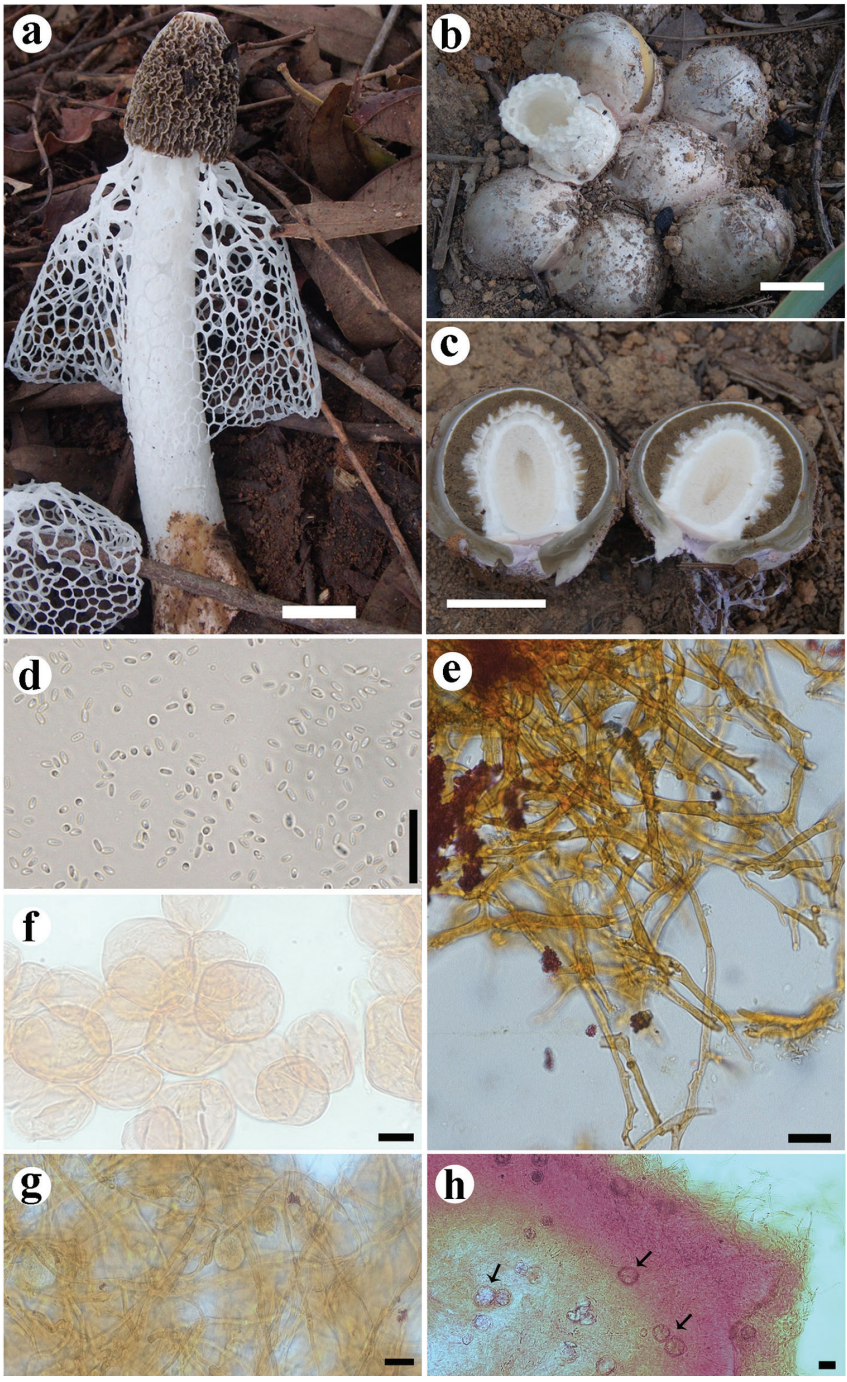

Figure 5. *Phallus purpurascens* SINOP27, paratype. **A** Fresh basidiome **B** gregarious immature basidiome, with purplish pigments on surface **C** longitudinal section of an immature basidiome, showing the purplish volva and rhizomorphs. *Phallus purpurascens* UFRN-Fungos 2808, holotype. **D** Spores **E** rhizomorphs hyphae **F** pseudoparenchymatous hyphae from pseudostipe **G** hyphae from volva **H** crystals in globose cells found on volva. Scale bars: 20 mm (**A–C**), 20 µm (**C–H**).

Immature basidiomes whitish ($N_{60}A_{60}M_{50}$) with purplish pigments ($A_{10}M_{10}C_{10}$), globose to subglobose, up to 56 × 43 mm, growing gregariously. Fresh expanded basidiome up to 200 mm high. Receptacle up to 45 × 29 mm, thimble-like, flat at the apex with an apical pore; strongly reticulated surface, shallow reticulations up to 3.2 × 1.7 mm, white ($N_{00}A_{00}M_{00}$). Pseudostipe up to 122 × 21 mm, cylindrical, spongy, white ($N_{00}A_{00}M_{00}$); pseudoparenchymatous, composed of globose to elongate-ovoid cells, 37–65.5 × 22.5–48 µm, hyaline. Indusium well-developed, extending up to 2/3 of the pseudostipe, white ($N_{00}A_{00}M_{00}$), up to 100 mm in length, attached to the apex of the pseudostipe; polygonal meshes up to 10 × 5 mm. Volva semi-hypogeous, white ($N_{00}A_{00}M_{00}$) becoming purplish ($A_{10}M_{10}C_{10}$) when exposed, with a smooth surface; formed by filamentous hyphae, septate, branched, hyaline, clamp connections present, 3.1–6.6 µm diameter; with crystal deposits in globose cells widely distributed amongst the hyphae, 17.5–38 × 20.5–35.7 µm. Rhizomorphs composed of at least two types of hyphae: filamentous thin-walled hyphae, with clamp connections; and thicker hyphae (3–6.5 µm) that seem to communicate with each other by pores on the inflated tips. Gleba olive-brown ($N_{99}A_{50}M_{10}$), mucilaginous. Basidiospores cylindrical, smooth, 4.4–5 × 2.5–3.4 µm, hyaline in 5% KOH.

Habitat and distribution. on soil, in a fragment of upland secondary forest. It was found in the municipalities of Manaus (State of Amazonas, Brazil) and Sinop (State of Mato Grosso, Brazil).

Etymology. with reference to the volva becoming purple.

Other specimens examined (paratypes). Mato Grosso: Sinop, Parque Florestal de Sinop (11.8359S, 55.5008W), 7 November 2013, Cabral TS (SINOP26, SINOP27, SINOP28, SINOP30).

Notes. This species is the most distinctive amongst our collections, mainly due to its large basidiome, the purplish volva and rhizomorphs and the strongly reticulated receptacle. *Phallus rubrovolvatus* (M. Zang, D.G. Ji & X.X. Liu) Kreisel is one of the largest white-indusiate species (up to 330 mm); it differs from *P. purpurascens* by the deep red volva, the fragile indusium, by larger reticulations on the receptacle and smaller spores (3.7–4 × 2–2.5 µm) (Liu 1984, Calonge 2005). Additionally, in the phylogenetic analysis (Figures 2, 3), *P. rubrovolvatus* does not group with *P. purpurascens*, which confirms their separate identities. *Phallus callichrous* has an orange to pink receptacle, reddish-violet rhizomorphs and orange receptacle with pink margin (Möller 1895, Kreisel and Hausknecht 2009), which differ from the white receptacle, purplish volva and rhizomorphs of *P. purpurascens*; unfortunately, there is little information available for this Brazilian species (Calonge 2005). *Phallus multicolor* (Berk. & Broome) Cooke is similar to *P. purpurascens* in the purplish volva and rhizomorphs, but it differs by the cream to orange indusium and the light yellow pseudostipe (Lloyd 1909, Calonge 2005, Kreisel and Hausknecht 2009). *Phallus indusiatus* differs from *P. purpurascens* by the smaller basidiome, the hypogeous development of the immature basidiome and smaller spores (up to 4.1 × 2.2 µm), the well-developed indusium reaching the ground and the campanulate receptacle with wider reticulations (Ventenat 1798). The phylogenetic analyses show specimens of *P. purpurascens* grouping in a clade with high

support values (ITS tree: pp = 1, bs = 100%; CONC tree: pp = 1, bs = 98%), confirming its distinct identity.

Phallus purpurascens was found in a fragment of secondary forest, in an extremely threatened area of the Amazonian forest domain in the State of Mato Grosso, Brazil. This state was the second most deforested in Brazil in 2018 (INPE 2018), meaning that species in this area may be suffering the consequences of habitat fragmentation, which is one of the main causes of decline in fungal species (Courtecuisse 2008). Thus, this new species record shows the urgency of cataloguing fungal biodiversity of threatened areas, such as Neotropical forests.

Phallus squamulosus **T.S.Cabral, B.D.B.Silva & Baseia, sp. nov.**
MycoBank No: 824634
Figure 6

Diagnosis. This species is characterised by its immature basidiome and volva with a squamous surface, white receptacle with shallow reticulations and a wide pore.

Holotype. BRAZIL. Rio Grande do Norte: Baía Formosa, Reserva Particular do Patrimônio Natural Mata Estrela (6.383307S, 35.000365W), 27 February 2014, Silva BDB (UFRN-Fungos 2806). GenBank accessions: MG678497 (ITS), MG678547 (*atp*6).

Immature basidiomes whitish ($N_{60}A_{60}M_{50}$), up to 39 × 34 mm, ovoid, with squamous surface. Fresh expanded basidiome up to 95 mm high. Receptacle 20 × 28 mm, campanulate to thimble-like, with a wide apical pore; and a strongly but shallow reticulated surface, reticulations 1.6–2 × 0.8–1.2 mm. Pseudostipe 60 × 12 mm, cylindrical, spongy, white ($N_{00}A_{00}M_{00}$); pseudoparenchymatous, composed of globose to elongate-ovoid cells, 18–71 × 10.5–35 µm, hyaline. Indusium well-developed, extending to 2/3 of pseudostipe, white ($N_{00}A_{00}M_{00}$), 44 mm in length, attached to the apex of the pseudostipe; polygonal to rounded meshes up to 6 × 3 mm. Volva epigeous, whitish ($N_{00}A_{00}M_{00}$) to pale yellow ($N_{00}C_{00}A_{30}$), with squamous surface; formed by filamentous hyphae, septate, branched, hyaline, clamp connections present, 2.5–4.5 µm diameter. Rhizomorphs whitish ($N_{00}A_{00}M_{00}$), composed of filamentous thin-walled hyphae, with clamp connections; with crystal deposits in globose cells distributed amongst the hyphae, 15–17.9 × 14–17 µm. Gleba olive-brown ($N_{99}A_{50}M_{10}$), mucilaginous. Basidiospores elongated, smooth, 3.5–4.4 × 1.8–2.2 µm, hyaline in 5% KOH.

Habitat and distribution. found growing on sandy soil, in a fragment of ombrophilous forest in the Atlantic Rainforest domain.

Etymology. with reference to the volva covered with small scales.

Notes. Only one specimen of this species has been found to date in the northern Atlantic Rainforest domain, but it is quite distinct from other species found in this study. We could not find white-indusiate species records with squamous exoperidium in the available literature. However, *P. duplicatus*, described in Martín and Tabarés (1994), presents an immature basidiome with fine scales on the exoperidium, but this character is not found in other described *P. duplicatus* (Lloyd 1909, Liu 1984,

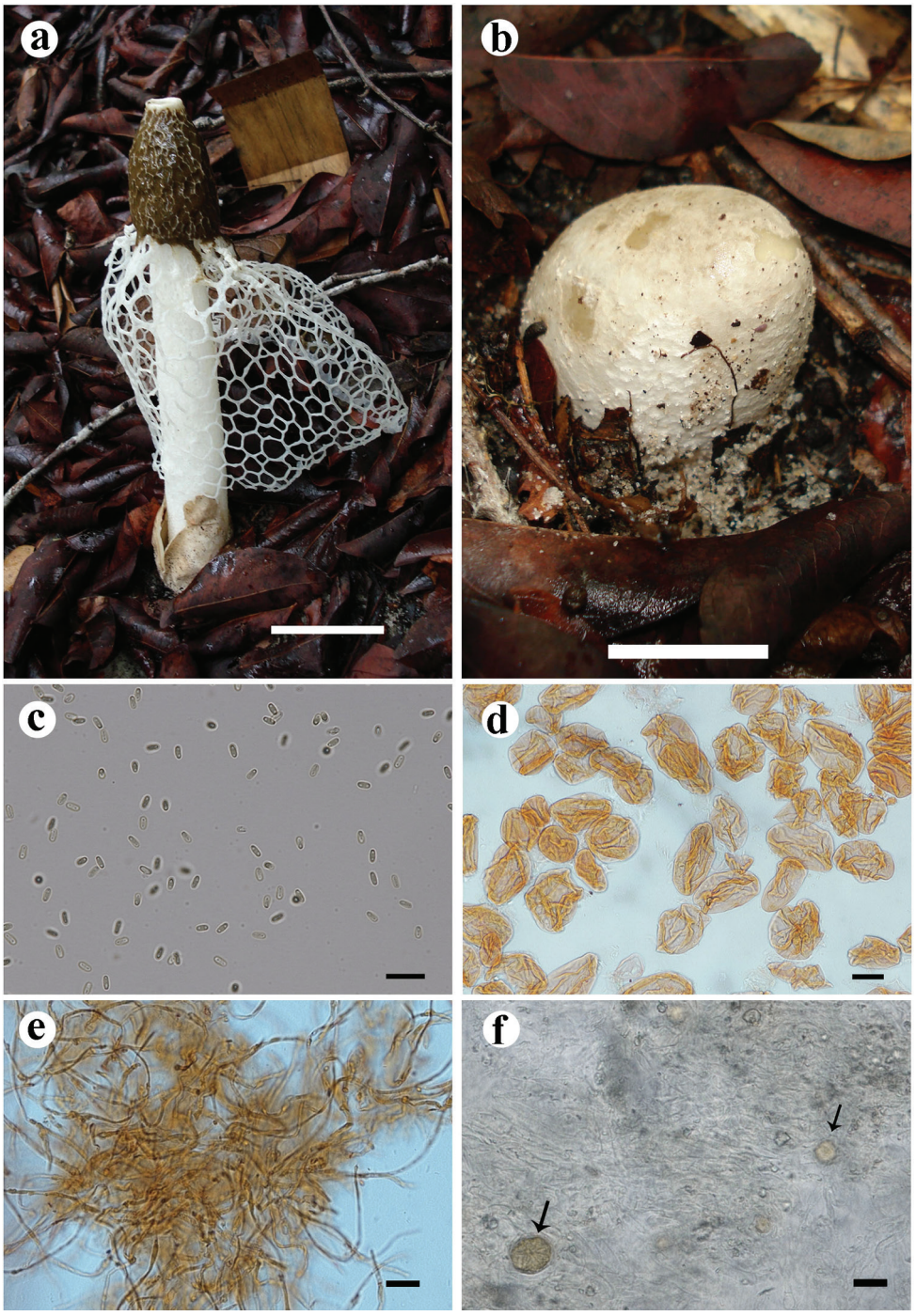

Figure 6. *Phallus squamulosus* UFRN-Fungos 2806, holotype. **A** Fresh basidiome **B** immature basidiome with squamous surface **C** spores **D** pseudoparenchymatous hyphae from pseudostipe **E** hyphae from volva **F** hyphae from rhizomorphs and crystals deposits on globose cells. Scale bars: 20 mm (**A, B**), 20 μm (**C–F**).

Kreisel and Hausknecht 2009, Kibby and McNeil 2012). Nevertheless, the material described by Martín and Tabarés (1994) differs from *P. squamulosus* mainly by having a conic-campanulate receptacle with crenulate disc on the apex. *Phallus denigricans* presents small hyphae projections on immature exoperidium surfaces of some specimens, but these projections are arranged differently in *P. squamulosus*, where they appear as scales. *Phallus indusiatus* is different from *P. squamulosus* by the campanulate receptacle with a smaller pore and deeper reticulations, the indusium extending to the ground and the immature basidiome that is hypogeous with a smooth surface and pinkish pigments.

***Phallus indusiatus* Vent., Mém. Inst. Natl. Sci., Sci. Math. 1: 520, 1798**
MycoBank No: 245788
Figure 7

≡ *Dictyophora indusiata* (Vent.) Desv., J. Bot., Paris 2: 92 (1809)
≡ *Hymenophallus indusiatus* (Vent.) Nees, Syst. Pilze (Würzburg): 251 (1816)
= *Dictyophora indusiata* f. *rosea* (Ces.) Kobayasi, J. Jap. Bot. 40: 180 (1965)
= *Dictyophora indusiata* f. *callichroa* (Möller) Kobayasi, Trans. Mycol. Soc. Japan 6: 6 (1965)
= *Hymenophallus roseus* Ces., Atti Accad. Sci. fis. mat. Napoli 8(8): 12 (1879)
= *Hymenophallus duplicatus* (Bosc) Nees, Syst. Pilze (Würzburg): 251 (1816)
= *Phallus duplicatus* Bosc, Mag. Gesell. naturf. Freunde, Berlin 5: 86 (1811)
= *Dictyophora duplicata* (Bosc) E. Fisch., in Berlese, De Toni & Fischer, Syll. fung. (Abellini) 7(1): 6 (1888)
= *Dictyophora rosea* (Ces.) E. Fisch., in Saccardo, Syll. fung. (Abellini) 7(1): 6 (1888)
= *Dictyophora phalloidea* var. *rosea* (Ces.) Lloyd, Synopsis of the known phalloids 7: 20 (1909)
= *Dictyophora phalloidea* var. *callichroa* (Möller) Lloyd, Synopsis of the known phalloids 7: 20 (1909)
= *Dictyophora callichroa* Möller, Bot. Mitt. Trop. 7: 129, 148 (1895)
≡ *Phallus callichrous* (Möller) Lloyd, Mycol. Writ. 7: 6 (1907)
= *Phallus indusiatus* var. *rochesterensis* (Lloyd) Lloyd, Synopsis of the known phalloids 7: 81 (1909)
= *Phallus rochesterensis* Lloyd, Synopsis of the known phalloids 7: 20 (1909)
= *Dictyophora phalloidea* var. *rochesterensis* (Lloyd) Sacc. & Trotter, Syll. fung. (Abellini) 21: 460 (1912)
= *Dictyophora indusiata* f. *aurantiaca* Kobayasi, Nov. fl. jap. 2: 83 (1938)
= *Phallus indusiatus* f. *citrinus* K. Das, S.K. Singh & Calonge, Boln Soc. Micol. Madrid 31: 136 (2007)

Neotype. (designated here): BRAZIL. Pará: Belterra, Floresta Nacional do Tapajós, Jamaraqua Community (2.812667S, 55.033083W), 25 March 2014, Cabral TS

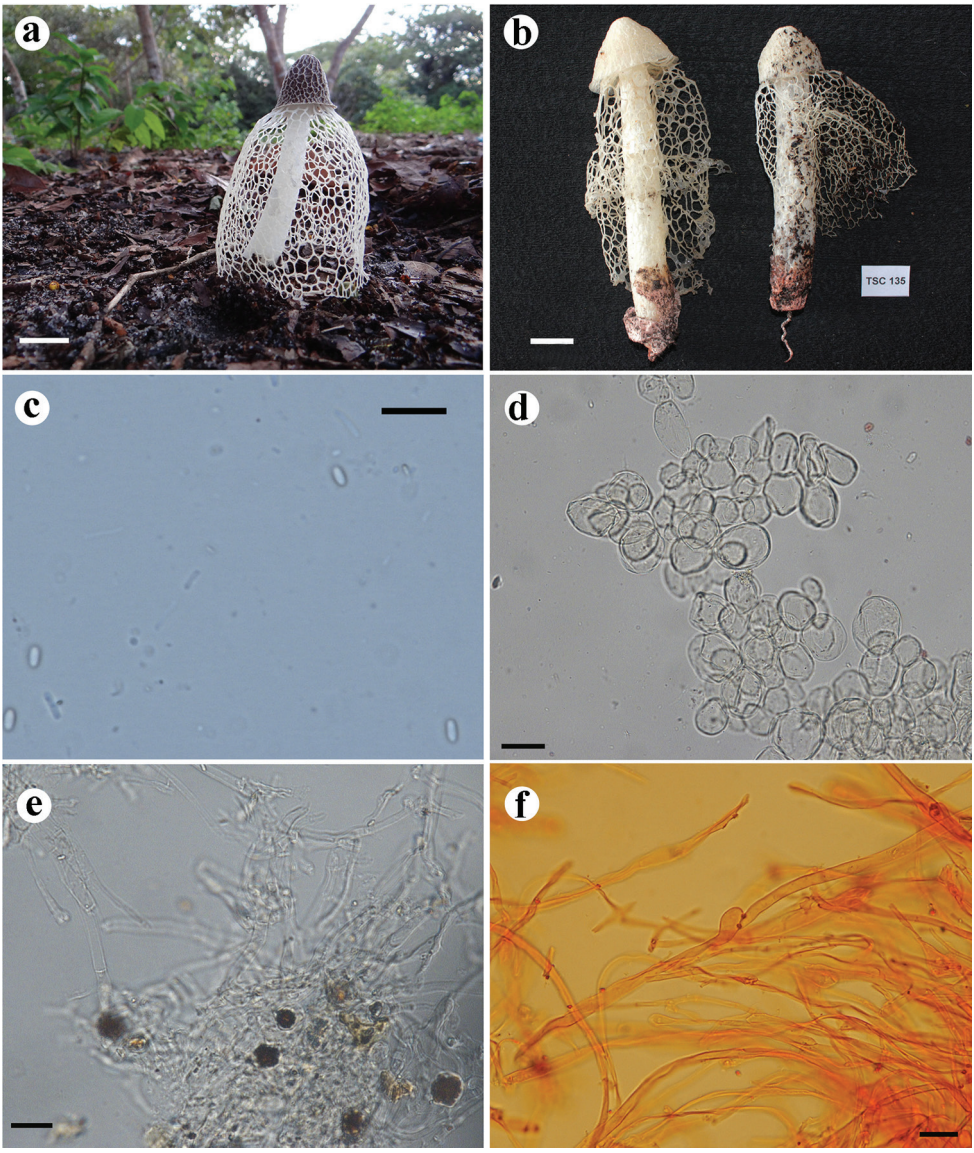

Figure 7. *Phallus indusiatus.* Fresh basidiome of **A** INPA-Fungos 264931 (neotype), and **B** INPA-Fungos 264929, showing the volva with pinkish pigments **C** spores **D** pseudoparenchymatous hyphae from pseudostipe **E** hyphae from volva and crystals deposits on globose cells **F** hyphae from rhizomorphs. Scale bars: 20 mm (**A, B**); 10 μm (**C**); 40 μm (**D**); 20 μm (**E, F**).

(INPA-Fungos 264931). GenBank accessions: MG678500, MG678501, MG678502 (ITS); MG678463 (nuc-LSU); MG678550 (*atp6*).

Immature basidiomes not observed. Fresh expanded basidiome 120 mm high. Receptacle 25 × 25 mm, campanulate, with an apical pore, reticulated surface. Pseudostipe 67 × 12 mm, cylindrical, spongy, white ($N_{00}A_{00}M_{00}$); pseudoparenchymatous, composed of globose to elongate-ovoid cells, 29.5–56.8 × 17.2–44 μm, hyaline. In-

dusium in full development extending to the ground, white ($N_{00}A_{00}M_{00}$), 74 mm in length, attached to the apex of the pseudostipe; polygonal to rounded meshes up to 7 × 4 mm, composed of pseudoparenchymatous cells, 31–53.8 × 23.8–41 µm. Volva hypogeous, white ($N_{00}A_{00}M_{0}$), with pinkish pigments ($N_{00}M_{10}C_{00}$); outer layer papery, composed of filamentous hyphae, 3.22–6.5 µm, yellowish, septate, with clamp connections; crystal deposits in globose cells distributed amongst the hyphae, 11.5–13.8 × 19.6–22.7 µm. Rhizomorphs composed of filamentous thin-walled hyphae, with clamp connections. Gleba olive-brown ($N_{99}A_{50}M_{10}$), mucilaginous. Basidiospores elongated, smooth, 3.6–4.1 × 1.5–2.2 µm, hyaline in 5% KOH.

Habitat and Distribution. found on sandy soil, in dense old-growth forest. It has a questionable circum-tropical distribution, with records for South and Central America, Mexico, Africa, Asia and Australia, but we believe that the distribution is restricted to South America.

Other specimens examined. BRAZIL. Pará: Belterra, Floresta Nacional do Tapajós, Jamaraqua Community (2.812667S, 55.033083W), 25 March 2014, Cabral TS (INPA-Fungos 264929, INPA-Fungos 264930); São Paulo, Parque Estadual das Fontes do Ipiranga (23.54S, 46.63W), January 2011, Oliveira, J.J.S. (SP416389); March 2011, Ventura, P.O. (SP416393); Capelari, M. (SP416087).

Notes. According to Ventenat's original description, *P. indusiatus* is characterised by the hypogeous volva, the campanulate and reticulated receptacle and by the indusium reaching the ground. The indusium is white, but it can become reddish as it matures. Ventenat does not give information on the colour of the volva and rhizomorphs, but some authors state that the volva can be light pinkish and rhizomorphs can be pinkish to violet (Calonge 2005, Kreisel and Hausknecht 2009). Our collection presents the same characteristics of the original description and those in the key for indusiate species presented by Kreisel and Hausknecht (2009a); in addition, some of the specimens are from the State of Pará, which is geographically close (about 970 km in a straight line) and with the same forest domain as the type locality (Suriname). Therefore, we believe that the specimens that are nested in the same clade in the phylogenetic trees (Figures 2, 3), all collected in the Brazilian Amazonian and Atlantic rainforests, correspond to *P. indusiatus* sensu stricto. Since Ventenat's original description does not designate a type specimen and, consequentially, it is not possible to find the original material in herbarium for comparison, we designated here a neotype for *Phallus indusiatus*, in accordance with the provisions of the International Code of Nomenclature for algae, fungi and plants (ICN) (Article 9.8) (Turland et al. 2017).

Discussion

Molecular and morphological analyses, as well as geographical distributions, support the description of three new species within the *Phallus indusiatus*-like specimens from Brazil, with partially overlapping distributions. Our results suggest that a great number of species might be hidden within the circum-tropical *P. indusiatus* species concept, since the sequence data obtained from GenBank are clearly polyphyletic with different

relationships with other *Phallus* species (Figures 2, 3). In a similar way, several studies have unveiled cryptic fungal diversity hidden within species complexes, especially after the integration of phenotypic, single-DNA and next-generation sequencing (NGS) data (Geml et al. 2006, Jargeat et al. 2010, Kasuya et al. 2012, Kõljalg et al. 2013, Sousa et al. 2017, Accioly et al. 2019). For instance, Geml et al. (2008) revealed that at least eight phylogenetic species are found in the worldwide distribution of *Amanita muscaria* (L.) Lam, with strong intercontinental genetic disjunctions and intracontinental phylogeographic structure. Sousa et al. (2017) revealed four species within the pepper pot *Myriostoma* (Phallomycetidae, Basidiomycota), which has always been considered a monotypic worldwide genus. Long-distance dispersal and cosmopolitanism seems not to be the rule in fungal geographical distribution and, for this reason, there are few species with truly worldwide distributions (Salgado-Salazar et al. 2013). Peay et al. (2016) affirm that climate, environment and dispersal play important roles in shaping fungal communities, where endemism is the most common result in continental and global-scale studies, instead of cosmopolitanism. This becomes clear when analysing the *P. indusiatus* s.l. distribution. As in all gasteroid fungi – basidiomycetes that produce spores inside the fruiting body – this species has a passive mechanism of spore dispersal (statismospory) (Wilson et al. 2011). Phalloid fungi have developed a peculiar spore dispersal mechanism that depends mainly on insects as vectors for dispersal and this factor, together with environmental conditions, should limit *P. indusiatus* s.l. geographical distributions, generating the species mosaic observed here.

Regarding the Brazilian indusiate clade, we suggest that species within this group are, in fact, divergent entities that maintained the general ancestral phenotype (*P. indusiatus* s.l.) throughout their evolutionary history, due to high levels of morphological stasis. This would explain the high frequency of taxonomic uncertainties, which generates a great number of synonyms of *P. indusiatus*. The maintenance of a conserved morphology due to low rates of phenotypic variation has been widely discussed in evolution (Davis et al. 2014). Two main mechanisms have been proposed to explain the small levels of morphological change through time: genetic and developmental constraints may restrict the appearance of phenotypic variation; or there is strong stabilising selection for a phenotype (Lee and Frost 2002, Geml et al. 2008, Davis et al. 2014). In our hypothesis, because the different species in *P. indusiatus* occupy similar niches and, therefore, they are in similar environmental conditions, they are likely to experience similar selective pressures. A similar pattern was found by Mueller et al. (2001) in two disjunct and paraphyletic populations of *Suillus spraguei* (Berk. & M.A. Curtis) Kuntze, that presented no noticeable morphological differences, probably as a result of stabilising selection. For the future, this could be tested for other *Phallus indusiatus*-like species from other continents and alternative methodologies should be applied, such as ancestral state reconstruction.

When studying phalloid species, it is noticeable that macro-characters are more variable than micro-characters. For instance, spores are often cylindrical to bacilloid and smooth throughout the order (except for Gastrosporiaceae), probably as an adaptation for dispersal, since they are dispersed through the gut and do not adhere on the bodies of insects (Tuno 1998, Oliveira and Morato 2000). The presence of rounded crystals in

Table 1. Morphological differences between the new *Phallus* species described here and *Phallus indusiatus.*

	Phallus denigricans	***Phallus purpurascens***	***Phallus squamulosus***	***Phallus indusiatus***
Basidiome development	Epigeous	Partially epigeous	Epigeous	Initially hypogeous
Receptacle	Constricted at the base, pale yellow, prominent apical pore	Conical, thimble-like, flat at the apex, white, strongly reticulated, with an apical pore	Campanulate to thimble-like, with a wide apical pore, strongly reticulated surface	Campanulate, white, reticulated, with an apical pore
Indusium	Extending to 2/3 of pseudostipe, poorly developed	Extending to 2/3 of pseudostipe, well developed	Extending to 2/3 of pseudostipe, well developed	Fully developed, extending to the ground
Volva	White to blackish, smooth surface or with projections, epigeous	White, becoming purplish, smooth surface, semi-hypogeous	Whitish to pale yellow, squamous surface, epigeous	White, pinkish pigments, hypogeous
Crystal deposits	Found on both volva and rhizomorphs of white volva specimens	Found on volva	Found on rhizomorphs	Found on volva
Basidiospores	Elongated, 3.6–4.6 × 2.2–2.5 µm	Cylindrical, 4.4–5 × 2.5–3.4 µm	Elongated, 3.5–4.4 × 1.8–2.2 µm	Elongated, 3.6–4.1 × 1.5–2.2 µm

globose cells amongst hyphae of the volva and rhizomorphs was reported for Phallales species (Iofisidou and Agerer 2002), but it is not a commonly used character in species descriptions. Probably these crystals consist of calcium oxalate, as found in other Phallomycetidae species, such as *Gastrosporium simplex* Mattir. and *Geastrum* Pers. (Iofisidou and Agerer 2002, Zamora et al. 2013), but further studies about function and composition in *Phallus* are needed. These crystals are present in most of the species described here, although on different parts: only on the volva of *P. purpurascens*, only on rhizomorphs of *P. squamulosus* and on both volva and rhizomorphs in *P. denigricans*. Further studies are needed in order to evaluate the taxonomic value of the presence of crystals in phalloid fungi. For instance, the presence, shape and the arrangement of oxalate crystals were found to be important characters to delimit species in *Geastrum* (Zamora et al. 2013).

On the other hand, macro-characters, such as the shape, surface and colour of the main structures (receptacle, pseudostipe, indusium, volva and rhizomorphs), are important characters for infrageneric classification (Kreisel 1996). In this study, the phylogenetic clades of *P. indusiatus*-like species were differentiated, based on these features (Table 1), confirming their importance as diagnostic characters. Given that these diagnostic characters are lost once phalloid specimens are dehydrated, it is extremely important that newly described species and new records should be well illustrated with coloured photographs of fresh material. In addition, we believe that molecular data are indispensable for delimiting and describing species in *Phallus*.

Acknowledgements

The authors wish to thank the Brazilian funding agencies Conselho Nacional de Desenvolvimento Científico e Tecnológico (CNPq 473422/2012-3, 160321/2013-1 and 458210/2014-5) and Fundação de Amparo a Pesquisa do Estado do Amazonas (FAPEAM 3137/2012) for grant awards and Coordenação de Aperfeiçoamento de Pessoal de Nível Superior (CAPES 7296/14-2) and Ministério da Ciência, Tecnolo-

gia, Inovação e Comunicação (303851/2015-5) for scholarships. We thank Dr. Doriane Picanço Rodrigues for coordination of the Laboratory of Applied Evolution at the Federal University of Amazonas, where part of the molecular data was obtained. We are grateful to Ricardo Braga Neto and Dirce Leimi Komura for collecting support.

References

Accioly T, Sousa JO, Moreau P-A, Lécuru C, Silva BDB, Roy M, Gardes M, Baseia IG, Martín MP (2019) Hidden fungal diversity from the Neotropics: *Geastrum hirsutum*, *G. schweinitzii* (Basidiomycota, Geastrales) and their allies. PloS One 14: e0211388. https://doi.org/10.1371/journal.pone.0211388

Bickford D, Lohman DJ, Sodhi NS, Ng PKL, Meier R, Winker K, Ingram KK, Das I (2007) Cryptic species as a window on diversity and conservation. Trends in Ecology & Evolution 22: 148–155. https://doi.org/10.1016/j.tree.2006.11.004

Cabral TS, Marinho P, Goto BT, Baseia IG (2012) *Abrachium*, a new genus in the *Clathraceae*, and *Itajahya* reassessed. Mycotaxon 119: 419–429. https://doi.org/10.5248/119.419

Cabral TS, Clement CR, Baseia IG (2015) Amazonian phalloids: New records for Brazil and South America. Mycotaxon 130: 315–320. https://doi.org/10.5248/130.315

Calonge FD (2005) A tentative key to identify the species of *Phallus*. Boletin de La Sociedad Micologica de Madrid 29: 9–18.

Cheype J (2010) Phallaceae et Clathrus récoltés en Guyane Française. Bulletin Mycologique et Botanique Dauphiné-Savoie 197: 51–66.

Courtecuisse R (2008) Current trends and perspectives for the global conservation of fungi. In: Moore D, Nauta MM, Evans SE, Rotheroe M (Eds) Fungal Conservation: Issues and Solutions. Cambridge University Press, New York, 7–18. https://doi.org/10.1017/CBO9780511565168.003

Das K, Singhi SK, Calonge FD (2007) Gasteromycetes of western Ghats, India: I. a new form of *Phallus indusiatus*. Boletin de La Sociedad Micologica de Madrid 31: 135–138.

Davis CC, Schaefer H, Xi Z, Baum DA, Donoghue MJ, Harmon LJ (2014) Long-term morphological stasis maintained by a plant-pollinator mutualism. Proceedings of the National Academy of Sciences of the United States of America 111: 5914–5919. https://doi.org/10.1073/pnas.1403157111

Demoulin V, Dring DM (1975) Gasteromycetes of Kivu (Zaire), Rwanda and Burundi. Bulletin Du Jardin Botanique National de Belgique 45: 339–372. https://doi.org/10.2307/3667488

Dennis RWG (1953) Some West Indian Gasteromycetes. Kew Bulletin 8: 307–328. https://doi.org/10.2307/4115517

Dennis RWG (1960) Fungi venezuelani: III. Kew Bulletin 14: 418–458. https://doi.org/10.2307/4114758

Desjardin DE, Perry B (2015) Clavarioid fungi and Gasteromycetes from Republic of São Tomé and Príncipe, West Africa. Mycosphere 6: 515–531. https://doi.org/10.5943/mycosphere/6/5/2

Dissing H, Lange M (1962) Gasteromycetes of Congo. Bulletin Du Jardin Botanique de l'État a Bruxelles 32: 325–416. https://doi.org/10.2307/3667249

Dring DM (1964) Gasteromycetes of West Tropical Africa. Mycological Papers 15: 1–60.

Dring DM, Rose AC (1977) Additions to West African phalloid fungi. Kew Bulletin 31: 741–751. https://doi.org/10.2307/4119427

Fischer VE (1928) Untersuchungen über Phalloideen aus Surinam. Gebr. Fretz AG, 39 pp.

Geml J, Laursen Ga, O'neill K, Nusbaum HC, Taylor DL (2006) Beringian origins and cryptic speciation events in the fly agaric (*Amanita muscaria*). Molecular Ecology 15: 225–239. https://doi.org/10.1111/j.1365-294X.2005.02799.x

Geml J, Tulloss RE, Laursen GA, Sazanova NA, Taylor DL (2008) Evidence for strong inter- and intracontinental phylogeographic structure in *Amanita muscaria*, a wind-dispersed ectomycorrhizal basidiomycete. Molecular Phylogenetics and Evolution 48: 694–701. https://doi.org/10.1016/j.ympev.2008.04.029

Guzmán G, Montoya L, Bandala VM (1990) Las especies y formas de *Dictyophora* (Fungi, Basidiomycetes, Phallales) en México y observaciones sobre su distribución en América latina. Acta Botánica Mexicana 9: 1–11. https://doi.org/10.21829/abm9.1990.587

Halling RE, Osmundson TW, Neves M-A (2008) Pacific boletes: implications for biogeographic relationships. Mycological Research 112: 437–447. https://doi.org/10.1016/j.mycres.2007.11.021

Hosaka K (2009) Phylogeography of the genus *Pisolithus* revisited with some additional taxa from New Caledonia and Japan. Bulletin of the National Museum of Nature and Science 35: 151–167.

Hosaka K (2010) Preliminary list of Phallales (Phallomycetidae, Basidiomycota) in Taiwan. Memoirs of the National Science Museum 46: 57–64.

Hosaka K, Bates ST, Beever RE, Castellano MA, Colgan W, Domínguez LS, Nouhra ER, Geml J, Giachini AJ, Kenney SR, Simpson NB, Spatafora JW, Trappe JM (2006) Molecular phylogenetics of the gomphoid-phalloid fungi with an establishment of the new subclass Phallomycetidae and two new orders. Mycologia 98: 949–959. https://doi.org/10.3852/mycologia.98.6.949

Hosaka K, Castellano MA, Spatafora JW (2008) Biogeography of Hysterangiales (Phallomycetidae, Basidiomycota). Mycological Research 112: 448–62. https://doi.org/10.1016/j.mycres.2007.06.004

IBGE (2012) Manual Técnico da Vegetação Brasileira. 271 pp.

INPE (2018) Projeto de Monitoramento do Desmatamento na Amazônia Legal por Satélite.

Iofisidou P, Agerer R (2002) Die Rhizomorphen von *Gastrosporium simplex* und einige Gedanken zur systematischen Stellung der Gastrosporiaceae (Hymenomycetes, Basidiomycota). Feddes Repertorium 113: 11–23. https://doi.org/10.1002/1522-239X(200205)113:1/2%3C11::AID-FEDR11%3E3.0.CO;2-B

Jargeat P, Martos F, Carriconde F, Gryta H, Moreau P-A, Gardes M (2010) Phylogenetic species delimitation in ectomycorrhizal fungi and implications for barcoding: the case of the *Tricholoma scalpturatum* complex (Basidiomycota). Molecular Ecology 19: 5216–5230. https://doi.org/10.1111/j.1365-294X.2010.04863.x

Kasuya T, Hosaka K, Uno K, Kakishima M (2012) Phylogenetic placement of *Geastrum melanocephalum* and polyphyly of *Geastrum triplex*. Mycoscience 53: 411–426. https://doi.org/10.1007/S10267-012-0186-Z

Kibby G, McNeil D (2012) *Phallus duplicatus* new to Britain. Field Mycology 13: 86–89. https://doi.org/10.1016/j.fldmyc.2012.06.009

Kõljalg U, Nilsson RH, Abarenkov K, Tedersoo L, Taylor AFS, Bahram M, Bates ST, Bruns TD, Bengtsson-Palme J, Callaghan TM, Douglas B, Drenkhan T, Eberhardt U, Dueñas M, Grebenc T, Griffith GW, Hartmann M, Kirk PM, Kohout P, Larsson E, Lindahl BD, Lücking R, Martín MP, Matheny PB, Nguyen NH, Niskanen T, Oja J, Peay KG, Peintner U et al. (2013) Towards a unified paradigm for sequence-based identification of fungi. Molecular Ecology 22: 5271–5277. https://doi.org/10.1111/mec.12481

Kreisel H (1996) A preliminary survey of the genus *Phallus* sensu lato. Czech Mycology 48: 273–281.

Kreisel H, Hausknecht A (2009) The gasteral Basidiomycetes of Mascarenes and Seychelles 3. Some recent records. Österr Z Pilzk 18: 149–159.

Kretzer AM, Bruns TD (1999) Use of atp6 in fungal phylogenetics: an example from the Boletales. Molecular Phylogenetics and Evolution 13: 483–492. https://doi.org/10.1006/mpev.1999.0680

Küppers H (1979) Atlas de los colores. Editorial Blume, Barcelona, 161 pp.

Lee CE, Frost BW (2002) Morphological stasis in the *Eurytemora affinis* species complex (Copepoda: Temoridae). Hydrobiologia 480: 111–128. https://doi.org/10.1023/A:1021293203512

Leite AG, Silva BDB da, Araújo RS, Baseia IG (2007) Espécies raras de *Phallales* (Agaricomycetidae, Basidiomycetes) no Nordeste do Brasil. Acta Botanica Brasilica 21: 119–124. https://doi.org/10.1590/S0102-33062007000100011

Li H, Mortimer PE, Karunarathna SC, Xu J, Hyde KD (2014) New species of *Phallus* from a subtropical forest in Xishuangbanna, China. Phytotaxa 163: 91–103. https://doi.org/10.11646/phytotaxa.163.2.3

Liu B (1984) The Gasteromycetes of China. J. Cramer, 235 pp.

Lloyd CG (1909) Synopsis of the known phalloids. Bulletin of the Lloyd Library 13: 1–96.

Magnago AC, Trierveiler-Pereira L, Neves M-A (2013) *Phallales* (Agaricomycetes, Fungi) from the tropical Atlantic Forest of Brazil. Journal of the Torrey Botanical Society 140: 236–244. https://doi.org/10.3159/TORREY-D-12-00054.1

Marincowitz S, Coetzee MPA, Wilken PM, Wingfield BD, Wingfield MJ (2015) Phylogenetic placement of *Itajahya*: An unusual *Jacaranda* fungal associate. IMA Fungus 6: 257–262. https://doi.org/10.5598/imafungus.2015.06.02.01

Martín MP, Tabarés M (1994) Notas sobre Gasteromycetes II: *Phallus duplicatus* Bosc. Revista Catalana de Micologia 16–17: 87–98.

Möller A (1895) Brasilische Pilzblumen. G. Fischer, Jena, 152 pp. https://doi.org/10.5962/bhl.title.2748

Mueller GM, Wu Q-X, Huang Y-Q, Gou S-Y, Aldana-Gomez R, Vilgalys R (2001) Assessing biogeographic relationships between North American and Chinese macrofungi. Journal of Biogeography 28: 271–281. https://doi.org/10.1046/j.1365-2699.2001.00540.x

Nylander JAA (2004) MrModeltest v2. Program distributed by the author.

Oliveira ML, Morato EF (2000) Stingless bees (Hymenoptera, Meliponini) feeding on stinkhorn spores (Fungi, Phallales): robbery or dispersal? Revista Brasileira de Zoologia 17: 881–884. https://doi.org/10.1590/S0101-81752000000300025

Peay KG, Kennedy PG, Talbot JM (2016) Dimensions of biodiversity in the Earth mycobiome. Nature Reviews Microbiology 14: 434–447. https://doi.org/10.1038/nrmicro.2016.59

Saénz JA, Nassar M (1982) Hongos de Costa Rica: Familias Phallaceae y Clathraceae. Revista de Biología Tropical 30: 41–52.

Salgado-Salazar C, Rossman AY, Chaverri P (2013) Not as Ubiquitous as We Thought: Taxonomic Crypsis, Hidden Diversity and Cryptic Speciation in the Cosmopolitan Fungus *Thelonectria discophora* (Nectriaceae, Hypocreales, Ascomycota). PLoS ONE 8: e76737. https://doi.org/10.1371/journal.pone.0076737

Smith KN (2005) A Field Guide to the Fungi of Australia. UNSW Press, Sidney, 200 pp.

Song B, Li T, Li T, Huang Q, Deng W (2018) *Phallus fuscoechinovolvatus* (Phallaceae, Basidiomycota), a new species with a dark spinose volva from southern China. Phytotaxa 334: 19–27. https://doi.org/10.11646/phytotaxa.334.1.3

Sousa JO, Suz LM, García MA, Alfredo DS, Conrado LM, Marinho P, Ainsworth AM, Baseia IG, Martín MP (2017) More than one fungus in the pepper pot: Integrative taxonomy unmasks hidden species within *Myriostoma coliforme* (Geastraceae, Basidiomycota). PloS ONE 12: e0177873. https://doi.org/10.1371/journal.pone.0177873

Swofford DL (2003) PAUP*. Phylogenetic Analysis Using Parsimony (*and Other Methods). Version 4.0 b.10.

Trierveiler-Pereira L, Meijer AAR, Reck MA, Kentaro H, Silveira RMB da (2017) *Phallus aureolatus* (Phallaceae, Agaricomycetes), a new species from the Brazilian Atlantic Forest. Phytotaxa 327: 223–236. https://doi.org/10.11646/phytotaxa.327.3.2

Trierveiler-Pereira L, Silveira R, Hosaka K (2014) Multigene phylogeny of the Phallales (Phallomycetidae, Agaricomycetes) focusing on some previously unrepresented genera. Mycologia 106: 904–911. https://doi.org/10.3852/13-188

Tuno N (1998) Spore dispersal of *Dictyophora* fungi (Phallaceae) by fies. Ecological Research 13: 7–15. https://doi.org/10.1046/j.1440-1703.1998.00241.x

Turland NJ, Wiersema JH, Barrie FR, Greuter W, Hawksworth DL, Herendeen PS, Knapp S, Kusber WS, Li DZ, Marhold K, May TW, McNeill J, Monro AM, Prado J, Price MJ, Smith GF (2017) International Code of Nomenclature for algae, fungi, and plants (Shenzhen Code) adopted by the Nineteenth International Botanical Congress Shenzhen, China, July 2017. Koeltz Botanical Books, Glashütten. https://doi.org/10.12705/Code.2018

Ventenat EP (1798) Dissertation sur le genre *Phallus*. Mémoires de L'institut National Des Sciences et Arts 1: 503–523.

Vilgalys R, Hester M (1990) Rapid genetic identification and mapping of enzymatically amplified ribosomal DNA from several cryptococcus species. Journal of Bacteriology 172: 4238–4246. https://doi.org/10.1128/jb.172.8.4238-4246.1990

White TJ, Bruns TD, Lee S, Taylor J (1990) Amplification and direct sequencing of fungal ribosomal RNA genes for phylogenetics. In: Innis MA, Sninsky DH, White TJ (Eds) PCR Protocols: A Guide to Methods and Applications. Academic Press Inc, New York, 315–322. https://doi.org/10.1016/B978-0-12-372180-8.50042-1

Wilson AW, Binder M, Hibbett DS (2011) Effects of gasteroid fruiting body morphology on diversification rates in three independent clades of fungi estimated using binary state speciation and extinction analysis. Evolution 65: 1305–1322. https://doi.org/10.1111/j.1558-5646.2010.01214.x

Zamora JC, Calonge FD, Martin MP (2013) New sources of taxonomic information for earthstars (*Geastrum*, Geastraceae, Basidiomycota): Phenoloxidases and rhizomorph crystals. Phytotaxa 132: 1–20. https://doi.org/10.11646/phytotaxa.132.1.1

Zang M, Zheng D, Hu Z (1988) A new species of the genus *Dictyophora* from China. Mycotaxon 33: 145–148.

Supplementary material 1

Table S1

Authors: Tiara S. Cabral, Bianca D.B. Silva, María P. Martín, Charles R. Clement, Kentaro Hosaka, Iuri G. Baseia

Data type: species data

Link: https://doi.org/10.3897/mycokeys.58.35324.suppl1

Supplementary material 2

Figure S1

Authors: Tiara S. Cabral, Bianca D.B. Silva, María P. Martín, Charles R. Clement, Kentaro Hosaka, Iuri G. Baseia

Data type: phylogenetic tree

Link: https://doi.org/10.3897/mycokeys.58.35324.suppl2

Supplementary material 3

Figure S2

Authors: Tiara S. Cabral, Bianca D.B. Silva, María P. Martín, Charles R. Clement, Kentaro Hosaka, Iuri G. Baseia

Data type: phylogenetic tree

Link: https://doi.org/10.3897/mycokeys.58.35324.suppl3

MycoKeys 58: 129–129 (2019)
doi: 10.3897/mycokeys.58.38856
http://mycokeys.pensoft.net

CORRIGENDA

A peer-reviewed open-access journal
MycoKeys
Launched to accelerate biodiversity research

Corrigendum: Sicoli G, Passalacqua NG, De Giuseppe AB, Palermo AM, Pellegrino G (2019) A new species of *Psathyrella* (Psathyrellaceae, Agaricales) from Italy. MycoKeys 52: 89–102. https://doi.org/10.3897/mycokeys.52.31415

Giovanni Sicoli[1], Nicodemo G. Passalacqua[2], Antonio B. De Giuseppe[2], Anna Maria Palermo[1], Giuseppe Pellegrino[1]

1 *Department of Biology, Ecology and Earth Science, The University of Calabria, 87036 Arcavàcata di Rende, Cosenza, Italy* **2** *Museum of Natural History of Calabria and Botanical Garden, The University of Calabria, 87036 Arcavàcata di Rende, Cosenza, Italy*

Corresponding author: *Giovanni Sicoli* (giovanni.sicoli@unical.it)

Academic editor: *Bryn Dentinger* | Received 9 August 2019 | Accepted 9 August 2019 | Published 2 October 2019

Citation: Sicoli G, Passalacqua NG, De Giuseppe AB, Palermo AM, Pellegrino G (2019) Corrigenda: Sicoli G, Passalacqua NG, De Giuseppe AB, Palermo AM, Pellegrino G (2019) A new species of *Psathyrella* (Psathyrellaceae, Agaricales) from Italy. MycoKeys 52: 89–102. https://doi.org/10.3897/mycokeys.52.31415. MycoKeys 58: 129–129. https://doi.org/10.3897/mycokeys.58.38856

Two morphological features of the new *Psathyrella* species, described in the paper, need to be emended: the presence of pleurocystidia and the spore length range.

Figure 3 (G, H and I) showed pyriform cells on the cap cuticle, not pleurocystidia. This mistake originated from a wrong labelling of the photo folder. Conversely to what is stated in Table 1 and on pages 93 and 100, pleurocystidia were not observed. Coherently with the DNA analysis, this correction addresses the discussion on page 99 to the certain inclusion of our fungus in the Section *Spintrigerae* (Fr.) Konr. & Maubl. and in the "*candolleana*" clade.

Due to a transcription error, the spore length range was 7.2–8.8 µm instead of 7.2–11.8 µm.

Missing reference (cited in the Introduction as Lansdown et al. 2018):

Lansdown RV, Juffe Bignoli D, Beentje HJ (2017) *Cladium mariscus*. The IUCN Red List of Threatened Species 2017: e.T164157A65910896. https://www.iucnredlist.org/species/164157/65910896